



Universitat Autònoma de Barcelona

**ADVERTIMENT.** L'accés als continguts d'aquesta tesi queda condicionat a l'acceptació de les condicions d'ús establertes per la següent llicència Creative Commons:  [http://cat.creativecommons.org/?page\\_id=184](http://cat.creativecommons.org/?page_id=184)

**ADVERTENCIA.** El acceso a los contenidos de esta tesis queda condicionado a la aceptación de las condiciones de uso establecidas por la siguiente licencia Creative Commons:  <http://es.creativecommons.org/blog/licencias/>

**WARNING.** The access to the contents of this doctoral thesis it is limited to the acceptance of the use conditions set by the following Creative Commons license:  <https://creativecommons.org/licenses/?lang=en>



**Universitat Autònoma de Barcelona**

DOCTORAL THESIS

**SIGNIFICANT ROLES OF ITGB3 IN THE  
TUMOUR MICROENVIRONMENT: EMT DRIVER  
IN HYPOXIC CONDITIONS AND CENTRAL AXIS  
IN INTERCELLULAR COMMUNICATION**

PRESENTED BY:

**PEDRO FUENTES VARELA**

THIS THESIS HAS BEEN CONDUCTED IN THE TRANSLATIONAL MOLECULAR  
PATHOLOGY GROUP AT VALL D'HEBRON RESEARCH INSTITUTE (VHIR)

DIRECTED BY:

SANTIAGO RAMÓN Y CAJAL AGÜERAS, MD, PhD AND MARTA SESÉ FAUSTINO, PhD

ACADEMIC TUTOR:

SANTIAGO RAMÓN Y CAJAL AGÜERAS, MD, PhD

THESIS SUBMITTED TO OBTAIN THE DEGREE OF DOCTOR OF PHILOSOPHY  
PhD PROGRAM IN MEDICAL SCHOOL, DEPARTMENT OF MORPHOLOGICAL  
SCIENCES:

DOCTORATE IN SURGERY AND MORPHOLOGICAL SCIENCES

LINES OF RESEARCH: ANATOMICAL PATHOLOGY

UNIVERSITAT AUTÒNOMA DE BARCELONA

BARCELONA 2020



SANTIAGO RAMÓN Y CAJAL AGÜERAS, Doctor en Medicina, jefe del servicio de Anatomía patológica del Hospital Vall d'Hebron y jefe del laboratorio de Patología molecular traslacional del VHIR y MARTA SESÉ FAUSTINO, Doctora en Biología,

HACEN CONSTAR,

que la tesis *Significant roles of ITGB3 in the tumour microenvironment: EMT driver in hypoxic conditions and central axis in intercellular communication* presentada por PEDRO FUENTES VARELA para optar al grado de Doctor, se ha realizado bajo su dirección, y al considerarla concluida, autorizan su presentación para ser juzgada por el tribunal correspondiente.

Y para que conste a los efectos firman la presente.

Barcelona, septiembre de 2020

Dr. Prof. Santiago Ramón y Cajal  
(Director de la tesis)

Dra. Marta Sesé Faustino  
(Directora de la tesis)

Pedro Fuentes Varela  
(Doctorando)





“It is the province of knowledge to speak, and it is the privilege of wisdom to listen.”

(Oliver Wendell Holmes,1872)



**LIST OF CONTENTS**

ABBREVIATIONS.....	VII
ACKNOWLEDGEMENTS.....	IX
PROLOGUE.....	XV
INTRODUCTION .....	1
1. Breast Cancer: Subtypes. Diagnosis Treatments.....	3
1.1. Triple Negative Breast Cancer .....	5
2. Protein synthesis control and cancer .....	6
2.1. Canonical initiation of mRNA translation.....	7
2.2. Non-Canonical initiation of mRNA translation.....	8
2.2.1. Internal Ribosome Entry Sites (IRES).....	9
2.2.2. Cap-independent translation element (CITE).....	10
2.2.3. Translation Initiator of Short 5'UTR (TISU) .....	10
2.2.4. Others: miRNAs, lncRNAs.....	11
2.3. Polysome profiling.....	12
3. Hypoxic stress.....	13
3.1. Adaptation mechanisms to hypoxic stress: transcriptional and post-transcriptional events.....	15
3.1.1. Transcriptional changes.....	15
3.1.2. Translational changes: Adaptive protein synthesis in hypoxia.....	16
4. Metastasis.....	19
4.1. Epithelial-Mesenchymal Transition (EMT) .....	20
4.1.1. EMT in cancer.....	20
4.1.2. TGF- $\beta$ Pathway.....	21
4.2. Intercellular communication .....	23
4.2.1. Extracellular vesicles-dependent intercellular communication .....	23
4.2.2. Extracellular vesicle biology .....	24
4.2.3. Exosomes uptake .....	25
4.2.4. Exosome biogenesis.....	27
4.2.5. Exosome heterogeneity.....	28
5. Integrins.....	29
5.1. Integrin structure and family .....	30
5.2. The role of integrins: multidirectional integrin signalling .....	31
5.3. Integrins and cancer .....	34
5.4. ITGB3 .....	37
HYPOTHESIS AND OBJECTIVES.....	43
RESULTS.....	47
Summary .....	49
CHAPTER 1.....	51
Manuscript.....	53
UNPUBLISHED DATA .....	87
CHAPTER 2.....	95
Manuscript.....	97
DISCUSSION .....	129
CONCLUSIONS.....	149
REFERENCES.....	153

## LIST OF FIGURES

### INTRODUCTION FIGURES

<b>Figure Intro. 1.</b> Median survival time (months) of different distant metastatic diseases stratified by molecular subtypes.....	5
<b>Figure Intro. 2</b> RNA elements .....	7
<b>Figure Intro. 3.</b> Canonical and Non-Canonical translational pathways.....	12
<b>Figure Intro. 4.</b> Polysome profiling representation.....	13
<b>Figure Intro. 5.</b> Tumor-associated blood vasculature .....	14
<b>Figure Intro. 6.</b> Mechanisms of hypoxic adaptations .....	19
<b>Figure Intro. 7.</b> Metastatic cascade.....	20
<b>Figure Intro. 8.</b> TGF- $\beta$ SMAD-dependent and -independent-signaling.....	22
<b>Figure Intro. 9.</b> Identity and the heterogeneity of EVs and exosomes.....	25
<b>Figure Intro. 10.</b> Biogenesis of exosomes .....	28
<b>Figure Intro. 11.</b> Exosome internalization and biogenesis.....	29
<b>Figure Intro. 12.</b> Integrin families .....	31
<b>Figure Intro. 13.</b> Multidirectional integrin signaling .....	33
<b>Figure Intro. 14.</b> Integrin-dependent functions relevant to cancer.....	36
<b>Figure Intro. 15.</b> Integrin Beta 3 gene location, transcript and protein structure, based on the version GRCh38.p13 of the Human genome.....	38

### RESULTS FIGURES

#### Chapter 1

<b>Figure 1.</b> Overview of the polysomal RNA-Seq screen after hypoxia and mTOR inhibition .....	58
<b>Figure 2.</b> Transcriptional and translational changes in non-tumoural and malignant cells under hypoxic and mTOR inhibition conditions.....	59
<b>Figure 3.</b> Transcriptome analysis of MCF10A and MDA.MB.231 cells after hypoxia and hypoxia + PP242.....	60
<b>Figure 4.</b> Increased translational efficiency (Te) is accompanied by increased protein .....	62
<b>Figure 5.</b> ITGB3 is translationally activated under hypoxic conditions and is important for breast cancer survival and migration.....	63
<b>Figure 6.</b> Survival and lung metastasis after intravenous inoculation with ITGB3-depleted-MDA.MB.231 human breast cancer cells.....	64
<b>Figure 7.</b> ITGB3 depletion blocks TGF- $\beta$ pathway activation more efficiently in hypoxia than in normoxia .....	66
<b>Figure 8.</b> eIF4E is essential for enhanced protein synthesis of ITGB3 under low-oxygen conditions.....	67
<b>Supplementary Figure 1.</b> Venn diagrams showing the distribution of transcriptionally deregulated genes in H, HPP and NPP in MDA.MB.231 (A) and MCF10A (B) cell lines.....	76
<b>Supplementary Figure 2.</b> Analysis of transcriptionally downregulated genes under hypoxic and hypoxic + PP242 conditions .....	77
<b>Supplementary Figure 3.</b> Analysis of transcriptionally deregulated genes when cells are treated with PP242 .....	78

<b>Supplementary Figure 4.</b> Translationally downregulated transcripts upon PP242 treatment.....	79
<b>Supplementary Figure 5.</b> Increased translational efficiency (Te) of ITGB3 is accompanied by increased protein in other breast cancer cell lines.....	80
<b>Supplementary Figure 6.</b> Validation of the screening by qRT-PCR and NanoString in MDA.MB.231 cells.....	81
<b>Supplementary Figure 7.</b> Validation of the screening by qRT-PCR and NanoString in MCF10A cells .....	82
<b>Supplementary Figure 8.</b> Screening by siRNA of candidate translationally activated genes in hypoxia with PP242.....	83
<b>Supplementary Figure 9.</b> Migration assay of MDA-MB-231 and MCF10A cells with ITGB3 silencing and treated with TGB- $\beta$ .....	84
<b>Supplementary Figure 10.</b> eIF4E is essential for protein synthesis activation of ITGB3 under low-oxygen conditions.....	85

## Chapter 2

<b>Figure 1.</b> ITGB3 is required for EV-induced colony formation in MDA.MB.231 cells .....	101
<b>Figure 2.</b> Endocytic uptake of vesicles in MDA.MB.231 cells depends on ITGB3, HSPGs and Dynamin activity .....	103
<b>Figure 3.</b> Interaction of EVs with the cell surface is a highly dynamic process.....	104
<b>Figure 4.</b> Characterization of EVs isolated from MDA.MB.231 shCON and MDA.MB.231 shITGB3 cells .....	105
<b>Figure 5.</b> Alterations in the proteome of shITGB3-derived EVs.....	106
<b>Figure 6.</b> EV-induced activation of FAK is required for ITGB3-dependent EV uptake .....	108
<b>Supplementary Figure 1.</b> shITGB3 MDA.MB.231 cells are capable of homing in the lung .....	114
<b>Supplementary Figure 2.</b> Phenotype confirmation using a different ITGB3-targeting shRNA.....	114
<b>Supplementary Figure 3.</b> Microvesicles are not able to sustain the clonogenic growth capacity .....	115
<b>Supplementary Figure 4.</b> Phenotype confirmation using a different ITGB3-targeting shRNA.....	116
<b>Supplementary Figure 5.</b> Phenotype confirmation using a different breast cancer cell line .....	116
<b>Supplementary Figure 6.</b> Co-localization between EVs and ITGB3 at cellular membrane .....	117
<b>Supplementary Figure 7.</b> EV uptake is an energy-dependent process .....	117
<b>Supplementary Figure 8.</b> Dynamin regulates ITGB3 localization.....	118
<b>Supplementary Figure 9.</b> Extracellular vesicles co-localizes with ITGB3 in endocytic-pathway structures.....	119
<b>Supplementary Figure 10.</b> Characterization of EVs isolated from MDA.MB.231 shCON and MDA.MB.231 shITGB3 cells .....	120
<b>Supplementary Figure 11.</b> Heat map representation showing the difference in the abundance of proteins with a described role in endocytosis (A) and exosome biogenesis (B) and Gene ontology enrichment analysis (C).....	121

**Supplementary Figure 12.** Phenotype confirmation using a different breast cancer cell line ..... 122

**Supplementary Figure 13.** IMR90 cells displayed an increased migratory capacity when co-cultured with MDA.MB.231 cells, but not when co-cultured with shITGB3 cells ..... 122

**Supplementary Figure 14.** Only FAK activity was stimulated by EV treatment among all tested signalling pathways reported to be downstream of ITGB3..... 123

**Supplementary Figure 15.** Representative FACS gating strategy and histogram intensity from which the bar charts for EVs internalization in A) Figure 1C, and B) Figure 1D were generated. 124

**Supplementary Figure 16.** FACS gating strategy and histogram intensity from which the bar charts for EVs internalization in A-E) Figure 2, and F-H) Figure 3A-B were generated ..... 125

**Supplementary Figure 17.** FACS gating strategy and histogram intensity from which the bar charts for EVs internalization in A-B) Figure 6B, and C) Figure 6D were generated.. 126

**Supplementary Figure 18.** FACS gating strategy and histogram intensity from which the bar charts for EVs internalization in A-D) Supplementary Figure 4, E) Supplementary Figure 5, and F-G) Supplementary Figure 7 were generated..... 127

**UNPUBLISHED FIGURES**

**Unpublished Figure 1.** ITGB3 depletion affects growth rate in breast cancer cell spheroids .....90

**Unpublished Figure 2.** The lack of ITGB3 affects mammosphere formation, but similarly in Normoxia and Hypoxia in MCF7 cell line..... 92

**DISCUSSION FIGURES**

**Figure Dis. 1.** Schematic of ITGB3-TGF- $\beta$  signaling pathway. .... 139

**Figure Dis. 2.** Model for the proposed role of ITGB3 in EV uptake..... 144

## LIST OF TABLES

### INTRODUCTION TABLES

<b>Table Intro. 1.</b> Prevalence, Prognosis, and Therapeutic Options for the three Breast Cancer Subtypes .....	4
<b>Table Intro. 2</b> Integrin expression in metastatic tumour cells compared to primary tumour cells.....	35
<b>Table Intro. 3.</b> Integrins in cancer progression.....	37

### DISCUSSION TABLES

<b>Table Dis. 1.</b> Summary of ITGB3 inhibitors currently being tested or soon to be tested in clinical trials.....	146
--	-----





**ABBREVIATIONS**

<b>2D:</b> two-dimensional	<b>eIF4F<sup>H</sup>:</b> hypoxia-specific eIF4F complex	<b>MET:</b> mesenchymal-epithelial transition
<b>3D:</b> three-dimensional	<b>eIF4G:</b> eukaryotic translation initiation factor 4G	<b>MIF:</b> macrophage migration inhibitory factor
<b>4E-BP1:</b> 4E-binding protein 1	<b>EMT:</b> epithelial to mesenchymal transition	<b>miRNA:</b> micro RNA
<b>4-ET:</b> eukaryotic translation initiation factor 4E transporter	<b>ER:</b> estrogen receptors	<b>MNK1/2:</b> MAP kinase-interacting serine/threonine-protein kinase 1
<b>AA:</b> aminoacid	<b>ERK:</b> extracellular signal regulated kinase	<b>mTORC1/2:</b> mechanistic target of rapamycin complex 1/2
<b>AKT:</b> serine-threonine protein kinase AKT	<b>EV:</b> extracellular vesicle	<b>MVB:</b> multivesicular bodies
<b>ALDH:</b> aldehyde dehydrogenase	<b>FA:</b> focal adhesion	<b>NCBP1:</b> nuclear cap binding protein subunit 1
<b>AMP:</b> adenosine monophosphate	<b>FAK:</b> FA kinase	<b>ODDs:</b> oxygen-dependent degradation domains
<b>ARNT:</b> aryl hydrocarbon receptor nuclear translocator	<b>FC:</b> fold change	<b>ORF:</b> open reading frame
<b>ATF4:</b> activation transcription factor 4	<b>FDR:</b> false discovery rate	<b>p-70S6K:</b> phosphorylated ribosomal protein S6 kinase
<b>ATP:</b> adenosine triphosphate	<b>GDP:</b> guanosine-5'-diphosphate	<b>PABP:</b> poly(A)-binding protein
<b>BCSC:</b> breast cancer stem cell	<b>GO:</b> gene ontology	<b>PAS:</b> PER-ARNT-SIM domain
<b>BrCa:</b> breast cancer	<b>GSK3:</b> glycogen synthase kinase 3	<b>PDGF:</b> platelet-derived growth factor
<b>CA9:</b> carbonic anhydrase 9	<b>GTP:</b> guanosine-5'-triphosphate	<b>PERK:</b> endoplasmic reticulum resident kinase
<b>CAF:</b> cancer-associated fibroblast	<b>HER2:</b> human epidermal growth factor receptor 2	<b>PHDs:</b> prolyl hydroxylase domain proteins
<b>CITE:</b> cap-independent translation element	<b>HGFR:</b> hepatocyte growth factor receptor	<b>PKD1:</b> PKC-related kinase
<b>ECM:</b> extracellular matrix	<b>HIF-1:</b> hypoxia induced factor 1	<b>PR:</b> progesterone receptors
<b>EE:</b> early endosome	<b>HOXB3:</b> homeobox B3	<b>RBPs:</b> RNA-binding proteins
<b>eEF2:</b> eukaryotic elongation factor 2	<b>HRE:</b> hypoxia response element	<b>REDD1:</b> regulated in development and DNA damage responses 1
<b>eEF2K:</b> eukaryotic elongation factor 2 kinase	<b>HS:</b> heparan sulfate	<b>RG4s:</b> RNA G-quadruplex structures
<b>EGF:</b> epithelial growth factor	<b>HSPG:</b> heparan sulfate proteoglycans	
<b>EGFR:</b> EGF receptor	<b>ILK:</b> integrin-linked kinase	
<b>eIF4A:</b> eukaryotic translation initiation factor 4A	<b>ILV:</b> intraluminal vesicles	
<b>eIF4E:</b> eukaryotic translation initiation factor 4E	<b>IRES:</b> internal ribosome entry sites	
<b>eIF4F:</b> eukaryotic translation initiation factor 4F	<b>IRF9:</b> interferon regulatory factor 9	
	<b>ITAFs:</b> IRES transacting factors	
	<b>ITGB3:</b> integrin beta 3	
	<b>lncRNA:</b> long non-coding RNA	
	<b>MAPK:</b> mitogen-activated protein kinase	

## Abbreviations

**RGD:** arginine-glycine-aspartate

**shRNA:** short hairpin RNA

**SRC:** proto-oncogene tyrosine-protein kinase SRC

**TGF- $\beta$ :** transforming growth factor beta

**TGF- $\beta$ R:** transforming growth factor beta receptor

**TISU:** translation initiator of short 5'UTR

**TNBC:** triple negative breast cancer

**TSC1/2:** tuberous sclerosis complex 1/2

**UORFs:** upstream open reading frames

**UPR:** unfolded protein response

**UTR:** untranslated region

**VEGF:** vascular endothelial growth factor

**VEGFR:** vascular endothelial growth factor receptor

**VHL:** Von Hippel-Lindau protein

**$\alpha$ V $\beta$ 3:** integrin alpha V beta 3

**$\alpha$ IIb $\beta$ 3:** integrin alpha IIb beta 3

## **ACKNOWLEDGEMENTS**



Llega el momento de dar las gracias, ya que todo esto no ha sido solo fruto de mi trabajo.

De manera especial quisiera mostrar mi gratitud al Dr. Santiago Ramón y Cajal, jefe del grupo de Patología molecular traslacional y director/tutor de esta tesis, por confiar en mí y darme la oportunidad de empezar este camino. También quiero agradecer todas las facilidades y ayudas que me ha prestado durante todo este tiempo y que me han dado la oportunidad de asistir a congresos y cursos, tanto en ámbito nacional como internacional, así como la posibilidad de poder hacer una estancia en el extranjero. Muchas gracias Santiago.

Després a la “jefa”, Dra. Marta Sesé, co-directora de tesis. Moltes gràcies per ajudar-me durant aquests 5 anys i haver estat sempre que ho he necessitat. Gràcies de tot cor per haver confiat sempre en mi, i per haver-me recolzat en tot moment. Sabia que si necessitava qualsevol cosa et podia trucar, i això és bàsic durant aquest període. Tot i que la situació professional ha canviat des de l'inici fins al final de la tesis, sense cap mena de dubte crec que em fet un gran equip. Moltes gràcies jefa.

De la misma manera, aunque no haya formado parte de manera oficial de esta tesis, el Dr. Stefan Hümmmer es sin duda parte esencial de ella. In fact, the second part is both yours and mine. Your support during this period has been essential. Especially this last year that has been quite hard, after so many revisions. It was exhausting, but in the end, it was worth it. I hope with all my heart that you are doing great, both personally and professionally, without any doubt, you deserve it. Let me tell you that you have become essential for the Translational Molecular Pathology group. Have no doubt, this thesis is also yours. *Vielen Dank*.

Dr. Héctor Peinado, jefe del grupo de Microambiente y Metástasis del CNIO. La segunda parte de esta tesis sin tu ayuda no habría sido posible. Gracias por abrirme las puertas de tu laboratorio.

Thank you to the people of Tumour and Vascular Biology Laboratory of Professor Alan McIntyre in Nottingham. Thank you for your warm hospitality and for opening to me the doors of your laboratory. Moreover, especially, to Leonardo da Motta, for your support with the project and for making me comfortable both in the laboratory and in the city. Likewise, thanks to Hannah Bolland for your willingness helping me in the lab during all the time that I spent there.

No me quiero dejar al Dr. Antonio Gentilella, “Antoni”. Desde el principio viste algo en mí. Desde que empecé como técnico en Idibell, sin casi nada de experiencia, me arropaste

## *Acknowledgements*

y me enseñaste casi todo. Tú fuiste el primero, antes que yo mismo, en creer que podía hacer la tesis y en empujarme a ello. Aunque lo intentamos, al final no pudimos hacerla juntos, pero, aun así, siéntete parte de esto. *Gràzie assàje*.

Gracias también a todos los integrantes que han ido pasando y/o siguen por el grupo de Patología molecular traslacional, en especial a Marta Emperador, que con su trabajo de máster y su posterior ayuda con el microscopio confocal, ha sido importantísima en la segunda parte de la tesis.

Y qué decir de los demás. Empezando por Sara. Desde el primer momento conectamos ¡¡menos en el fútbol!! Cuando te fuiste a Madrid dejaste un vacío importante no solo en el pasillo, diría que en el VHIR. Igualmente, nos alegramos muchísimo de que por fin pudieras estar cerca de Álvaro y más cerca de los tuyos. ¡Por suerte, luego tuvimos unas semanas trabajando juntos en el CNIO! Muchas gracias por ayudarme ese tiempo. Uno de los primeros resultados y de los que nos abrieron las puertas de la nueva historia ¡fue allí contigo! Gracias Sara.

Yoelsis y María José. Después de Kim ¡seguramente seréis las personas con las que más tiempo he pasado durante los últimos 5 años! Ratos en la oficina, cafés, cervezas, mojitas, *calçotadas*, sala de cultivos, fines de semana por el labo, etc. Cómo me alegra haberme encontrado con vosotros y haber hecho todo este camino juntos.

Pedro ¡eres un crack! La segunda parte de esta tesis deberías firmarla tú también. Mientras yo estaba fuera tú mantuviste y avanzaste con el proyecto, y luego seguiste trabajando mano a mano conmigo (además de hacer 1000 cosas más en el laboratorio). Siempre dispuesto a todo, sin una mala cara o mal gesto, aunque a veces me lo mereciera por pesado. Como decía Stefan cuando te estaba buscando: ¿Dónde está tu hermano mayor? ¡Cuánta razón! Fue una mierda cuando te fuiste del laboratorio, pero cómo me alegro de que te vaya todo tan bien. Tú, Vero y la pequeña Carolina sois una familia espectacular. Kim y yo nos llevamos a unos amigos a los que visitar cuando bajamos para Málaga.

A mi familia, mis padres y mi hermana, porque si he llegado hasta aquí ha sido gracias a vuestra educación y vuestro apoyo. Siempre hemos sido uno.

Por último, esta tesis no tendría ningún sentido sin ti Kim. Tesis y nosotros van de la mano. Me has apoyado en cada uno de los pasos, incluso me has empujado en algunos de ellos, como cuando quería irme fuera un tiempo. Siempre has estado ahí, y como me conoces como nadie, muchas veces “simplemente” estando ahí. Gracias por tu paciencia y comprensión, que falta te ha hecho y te hace (spoiler: te va a seguir haciendo falta). Esto es tuyo. No sé qué va a ser de nosotros de aquí en adelante, qué haremos, dónde, cuándo,

cómo...pero lo que es seguro es que seguirá siendo como hasta ahora, tu i jo, la meva companya, uno al lado del otro. Por cierto, aún no te has librado, ahora viene el practicar la defensa...

Y como bien sabes, el léxico y la expresión tanto escrita como oral no son mi fuerte, todo cuadra y se entiende en mi cabeza, pero a la hora de sacarlo fuera, algo pasa siempre. Por eso creo que la mejor manera de decirte gracias y el porqué es así...

per... *l'olor a cafè pels matins quan em llevo amb tu...*

porque.... *no me sonrojo si te digo que te quiero ...*

porque...*se me ponen si me besas, rojitas las orejas...*

porque...*si tuviera que decir que es, tu eres eso...*

perquè...*no vull veure't, vull mirar-te, no vull imaginar-te, vull sentir-te, vull compartir tot allò que sents, no vull tenir-te a tu, vull tenir amb tu el temps....*

porque...*por ti, por mí, por volverte a ver, por fin sentir que lo puedo hacer... ¿por qué? Por como lo hicimos, por el día aquel que nos conocimos....*

porque...*quiero decirte 'te quiero' como si un niño pequeño no lo hubiese hecho jamás...*

porque...*me quedo un ratito a mirar tus ojitos que huelen como a primavera y voy a celebrarlo...*

porque...*yo no creo en la iglesia, pero creo en tu mirada...*

porque...*duerme conmigo, si eres piedra da igual, yo seré pedregoso camino...*

porque...*llévame a envejecer a aquella playa, con tu sombrero y tu botella de cerveza verde viendo los barcos que se alejan y se pierden...*

y porque...*la felicidad es la mayor recompensa...*





## **PROLOGUE**



La tesis está compuesta por dos artículos, publicados a fecha 12 de diciembre de 2017 y 26 de agosto de 2020. Ambos artículos han sido admitidos para formar parte de dicha tesis en su formato de compendio de artículos por la Comisión Académica del Programa de Doctorado de Cirugía y Ciencias Morfológicas, en la línea de investigación de Anatomía Patológica, con fecha 28 de julio de 2020.

El trabajo aquí presentado está dividido en diferentes apartados; el primero de ellos consta de una introducción conjunta donde se presentan los antecedentes y conocimientos previos en los cuales se basan las hipótesis y los objetivos expuestos seguidamente.

A continuación, el apartado de resultados está dividido en dos grandes capítulos donde despliegan los artículos que forman la tesis. En el primer capítulo se presenta un estudio con el que se pretendía identificar factores que a través de su regulación traduccional, bajo condiciones de estrés hipóxico y de bloqueo de la vía canónica de la síntesis proteica, fueran capaces de conferir resistencia a dichas condiciones. Para ello se llevó a cabo un RNA-Seq de ARN polisómico en condiciones de: 1) normoxia, 2) hipoxia (0,5% de oxígeno), 24h., 3) normoxia + PP242 e 4) hipoxia + PP242, un conocido inhibidor de mTORC1/mTORC2. La Integrina Beta 3 (ITGB3) fue uno de los candidatos obtenidos. Posteriores estudios demostraron que su inhibición, y de manera más categórica en hipoxia, no solo aumentó la apoptosis y redujo la supervivencia y la migración celular, si no que ITGB3 era requerida para la activación sostenida de la vía de TGF- $\beta$ . Todo ello sumado a que la inhibición de ITGB3 redujo significativamente la metástasis pulmonar y mejoró la supervivencia general en ratones.

Cabe destacar, que en el primer capítulo se ha añadido un sub-apartado de datos no publicados. Estos resultados se obtuvieron durante mi estancia de tres meses en el laboratorio del Profesor Alan McIntyre en la Universidad de Nottingham, Inglaterra. Durante dicha estancia, el artículo fue aceptado por la revista y por este motivo los resultados obtenidos no fueron añadidos a la publicación.

El capítulo II está centrado en el rol de ITGB3 en la comunicación intercelular a través de vesículas extracelulares y como la desregulación de este proceso podría explicar la disminución en la aparición de metástasis en células con la integrina inhibida descrita en el capítulo I. En este estudio, hemos definido un rol esencial y hasta ahora desconocido de ITGB3 en la absorción de vesículas. El mecanismo funcional, basado en la interacción de ITGB3 con glucoproteínas heparán sulfatadas (HSPG) y en el proceso de reciclaje de las integrinas, también ha sido descrito. La combinación de ambos mecanismos permite la captura de vesículas extracelulares y su internalización mediada por endocitosis. Además,

en el complejo de internalización juegan un papel importante otras proteínas como la GTPasa dinamina y la quinasa de adhesiones focales (FAK). Ambas proteínas son clave para llevar a cabo la endocitosis y la posterior entrada de las vesículas extracelulares a la ruta endocítica a través de los endosomas. Consecuentemente, podemos afirmar que ITGB3 tiene un papel central en la comunicación intracelular a través de vesículas extracelulares, mecanismo que se presupone crítico durante la metástasis tumoral.

Tras el apartado de resultados, se continúa con una discusión conjunta de ambos capítulos donde además de discutir sobre los resultados obtenidos, se debaten las posibles aplicaciones traslaciones, mayoritariamente con un enfoque terapéutico, de dichos estudios. Para acabar, se exponen las conclusiones más relevantes extraídas de dicha tesis.

The thesis is made up of two articles dated December 12, 2017 and August 26, 2020. Both articles have been admitted to form part of the said thesis in its compendium format of articles by the Academic Commission of the Doctorate Program of Surgery and Morphological Sciences, in the research line of Pathological Anatomy, dated July 28<sup>th</sup>, 2020.

The work presented here is divided into different sections. The first of them consists of a joint introduction where the background and prior knowledge on which the hypotheses and the objectives set forth below are based are presented.

Next, the results section is divided into two large chapters where the publications that make up this thesis are displayed. The first chapter refers to the first article already published which aimed to identify factors that through their translational regulation under hypoxic stress conditions and the blockage of the canonical pathway of protein synthesis, were able to confer survival resistance to these conditions. For this, RNA-Seq of polysomal RNA was carried out under conditions of 1) normoxia, 2) hypoxia (0.5% oxygen), 24h., 3) normoxia + PP242, and 4) hypoxia + PP242, a known mTORC1 / mTORC2 inhibitor. Integrin Beta 3 (ITGB3) was one of the obtained candidates. Subsequent studies demonstrated that its inhibition, and more categorically in hypoxia, not only increased apoptosis and reduced survival and cell migration, but that ITGB3 was required for sustained activation of the TGF- $\beta$  pathway. All of this added to the fact that ITGB3 inhibition significantly reduced lung metastasis and improved overall survival in mice.

It should be noted that in the first chapter a sub-section of unpublished data has been added. These results were obtained during my three-month stay in Professor Alan McIntyre's laboratory at the University of Nottingham, England. During this stay, the article was accepted by the journal, and for this reason, the obtained results were not added to the publication.

Chapter II focuses on the role of ITGB3 in extracellular vesicle-based intercellular communication and how this could explain the decrease in the formation of metastasis in cells with ITGB3 inhibition, described in Chapter I. In this study, we have described an essential and far unknown role of ITGB3 in the absorption of vesicles. The functional requirement is based on the interaction of ITGB3 with Heparan Sulfated Glycoproteins (HSPG) and with the recycling process of the integrins. The combination of both mechanisms allows the capture of extracellular vesicles and their internalization mediated by endocytosis. Also, other proteins such as the GTPase Dynamin and Focal Adhesion Kinase (FAK) play an important role in the internalization complex. Both proteins are key for carrying out endocytosis and the subsequent entry of extracellular vesicles into the

endosomes of the endocytic pathway. Thus, ITGB3 has a central role in intracellular communication via extracellular vesicles, proposed to be critical for cancer metastasis.

After the results section, a combined discussion of both chapters is presented, where, in addition to discussing the obtained results, we discuss the possible translational applications, mostly with a therapeutic approach. To finish, the most relevant conclusions drawn are exposed.

La tesi està composta per dos articles publicats amb data de 12 de desembre de 2017 i 26 d'agost de 2020. Tots dos articles han estat admesos per formar part d'aquesta tesi en el seu format de compendi d'articles per la Comissió Acadèmica de el Programa de Doctorat de Cirurgia i Ciències Morfològiques, en la línia d'investigació d'Anatomia Patològica, amb data de 28 de juliol de 2020.

El treball aquí presentat està dividit en diferents apartats; el primer d'ells consta d'una introducció conjunta on es presenten els antecedents i coneixements previs en els quals es basen les hipòtesis i els objectius exposats tot seguit.

A continuació, l'apartat de resultats està dividit en dos grans capítols on es presenten els articles que formen la tesi. En el primer capítol es presenta un estudi amb el qual es pretenia identificar factors que a través de la seva regulació traduccional, sota condicions d'estrès hipòxic i de bloqueig de la via canònica de la síntesi proteica, fossin capaços de conferir resistència a aquestes condicions. Per a això es va dur a terme un RNA-Seq d'ARN polisòmic en condicions de: 1) normòxia, 2) hipòxia (0,5% d'oxigen), 24h., 3) normòxia + PP242 i 4) hipòxia + PP242, un conegut inhibidor de mTORC1 / mTORC2. La Integrina Beta 3 (ITGB3) va ser un dels candidats obtinguts. Posteriors estudis van demostrar que la seva inhibició, i de manera més categòrica en hipòxia, no només va augmentar l'apoptosi i va reduir la supervivència i la migració cel·lular, sinó que ITGB3 era requerida per a l'activació sostinguda de la via de TGF- $\beta$ . Tot això sumat al fet que la inhibició de ITGB3 va reduir significativament la metàstasi pulmonar i va millorar la supervivència general en ratolins.

Cal destacar, que en el primer capítol s'ha afegit un sub-apartat de dades no publicades. Aquests resultats es van obtenir durant la meua estada de tres mesos al laboratori del Professor Alan McIntyre a la Universitat de Nottingham, Anglaterra. Durant aquesta estada, l'article va ser acceptat per la revista i per aquest motiu els resultats obtinguts no van ser afegits a la publicació.

El capítol II està centrat en el paper de ITGB3 en la comunicació intercel·lular a través de vesícules extracel·lulars i com la desregulació d'aquesta podria explicar la disminució en l'aparició de metàstasis en cèl·lules amb la integrina inhibida descrita en el capítol I. En aquest estudi, hem definit un paper essencial i fins ara desconegut de ITGB3 en l'absorció de vesícules. El mecanisme funcional, basat en la interacció de ITGB3 amb glucoproteïnes heparan sulfatades (HSPG) i en el procés de reciclatge de les integrines, també ha sigut descrit. La combinació d'ambdós mecanismes permet la captura de vesícules



extracel·lulars i la seva internalització mitjançada per endocitosi. A més, en el complex d'internalització són molt importants altres proteïnes com la GTPasa dinamina i la quinasa d'adhesions focals (FAK). Les dues proteïnes són clau per dur a terme l'endocitosi i la posterior entrada de les vesícules extracel·lulars a la ruta endocítica a través dels endosomes. Conseqüentment, podem afirmar que ITGB3 té un paper central en la comunicació intracel·lular a través de vesícules extracel·lulars, mecanisme que es pressuposa crític durant la metàstasi tumoral.

Després de l'apartat de resultats, es continua amb una discussió conjunta dels dos capítols on a més de discutir sobre els resultats obtinguts, es debaten les possibles aplicacions translacionals, majoritàriament amb un enfocament terapèutic. Per acabar, s'exposen les conclusions més rellevants extretes d'aquesta tesi.

# **INTRODUCTION**



## **1. Breast Cancer: Subtypes. Diagnosis. Treatments**

Breast Cancer (BrCa) is the most diagnosed cancer and the leading cause of cancer-related deaths in women worldwide, despite advances in conventional and targeted therapies<sup>1</sup>. Its incidence continues to rise while mortality is falling, partially due to early diagnosis and improved therapies. Nevertheless, around 20-30% of patients develop metastatic disease, and it is currently estimated that 40% of all BrCa cases relapse, of which about 60-70% presents distant metastases<sup>2</sup>. Although scientific advancements over the last few decades have dramatically improved BrCa survival, when tumour localizes to secondary organs, the success rate of these patients drops dramatically.

BrCa is an heterogeneous complex of diseases, with a great spectrum of subtypes with distinct biological features that lead to different response patterns and clinical outcomes. Traditional classification systems take into account biological characteristics, such as tumour size, lymph node invasion, histological grade, patient's age, Estrogen Receptors (ER), Progesterone Receptors (PR) and Human Epidermal Growth Factor receptor 2 (HER2) status, are usually used for patient prognosis and management<sup>3,4</sup>. Accumulating evidence has suggested that BrCas with different histopathological and biological features exhibit distinct behaviours that lead to different treatment responses (Table Intro. 1)<sup>5</sup>.

Local therapy for non-metastatic BrCa involves surgical removal and sampling or subtraction of axillary lymph nodes, with consideration of post-operative radiation. Systemic therapy might be pre-operative (neoadjuvant), post-operative (adjuvant), or both. BrCa subtype guides the standard systemic administered therapy (Table Intro. 1), which consists of endocrine therapy for all Hormone Receptor (HR<sup>+</sup>) tumours (with some patients needing chemotherapy as well), trastuzumab-based HER2-directed antibody therapy plus chemotherapy for all HER2<sup>+</sup> tumours (with endocrine therapy as well, if simultaneous HR<sup>+</sup>), and chemotherapy alone for Triple Negative Breast Cancer (TNBC)<sup>6,7</sup>. For metastatic BrCa, therapeutic goals are prolonging life and symptom palliation as currently, it remains incurable in virtually all affected patients. The same basic categories of systemic therapy are used in metastatic BrCa. Local therapy modalities (surgery and radiation) are only used for palliation in metastatic disease.

**Table Intro. 1.** Prevalence, prognosis, and therapeutic options for the three BrC Subtypes

	<b>Hormone Receptor (HR) (ER<sup>+</sup> or PR<sup>+</sup>)</b>	<b>HER2<sup>+</sup> (HR<sup>+</sup> or HR<sup>-</sup>)</b>	<b>TNBC</b>
<b>Pathological definition</b>	≥1% of tumour cells stain positive for ER or PR proteins	Tumour cells stain strongly for HER2 protein or HER2 gene is amplified in tumour cells. Approximately half of HER2 <sup>+</sup> tumours are also HR <sup>+</sup>	Tumour does not meet any pathologic criteria for positivity of ER, PR, or HER2.
<b>Molecular pathogenesis</b>	ERα (steroid hormone receptor) activates oncogenic growth pathways	The oncogene HER2, encoding HER2 receptor tyrosine kinase from the epidermal growth factor receptor family, is overactive	Unknown (likely various)
<b>Percentage of BrCa, %</b>	70	15-20	15
<b>Prognosis</b>			
Stage I (5-y BrCa-specific survival),%	≥99	≥94	≥85
Metastatic (median overall survival)	4-5 years	5 years	10-13 months
<b>Typical systemic therapies for non-metastatic disease (agents, route, and duration)</b>	Endocrine therapy (all patients): Tamoxifen, letrozole, anastrozole, or exemestane Oral therapy 5-10 years Chemotherapy (some patients): Adriamycin/cyclophosphamide (AC) Adriamycin/cyclophosphamide/paclitaxel (AC-T) Docetaxel/cyclophosphamide (TC) Intravenous therapy 12-20 weeks	Chemotherapy plus HER2-targeted therapy (all patients): Paclitaxel/trastuzumab (TH) Adriamycin/cyclophosphamide/paclitaxel/trastuzumab ± pertuzumab (AC-TH±P) Docetaxel/carboplatin/trastuzumab ± pertuzumab (TCH±P) Intravenous therapy 12-20 weeks of chemotherapy; 1 year of HER2-targeted therapy Adriamycin/cyclophosphamide (AC) Endocrine therapy (if also HR <sup>+</sup> ) Tamoxifen, letrozole, anastrozole, or exemestane Oral therapy 5-10 years	Chemotherapy (all patients): AC AC-T TC Intravenous therapy 12-20 weeks
<b>Outcome</b>	Intermediate	Poor	Poor

Adapted table from Adrienne G. Waks *et al.*, 2019<sup>6</sup> and Funmilola A. Fisusi *et al.*, 2019<sup>7</sup>.

### 1.1. Triple Negative Breast Cancer

TNBC is a highly aggressive tumour subtype with a high risk of recurrence, metastasis, chemotherapy resistance and acquired capacity to survive and grow under nutrient-deprived and hypoxic (low-oxygen) conditions. All of these features involve an inherently aggressive clinical behaviour compared to other BrCa subtypes<sup>8</sup>.

Histologically, TNBC are known to be ductal type, with a high mitotic rate, increased lymphocytic infiltrate and large tumour size. Regarding clinical features, TNBC patients usually present early visceral metastases and lymph node invasion at the time of diagnosis, involving an adverse prognosis at that moment. This metastasis rate has been observed to be four times more likely to occur than in patients with non-TNBC subtypes. Further, researchers have observed that the median survival of TNBC patients with specific metastatic status is lower than the other subtypes involving a worse prognosis (Figure Intro. 1)<sup>9</sup>.

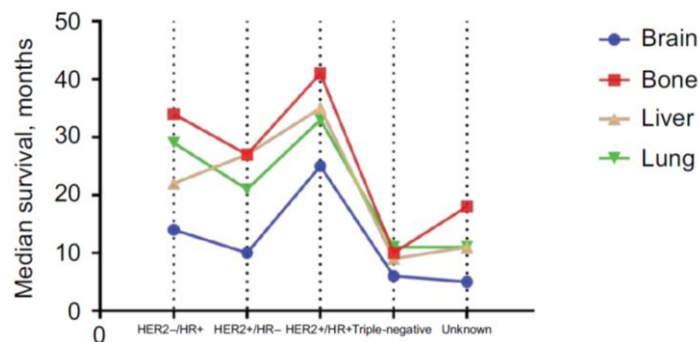


**Figure Intro. 1.** Median survival time (months) of different distant metastatic diseases stratified by molecular subtypes. (Xiao *et al.*, 2018<sup>9</sup>).

Another important factor to take into account is the tumour heterogeneity. As described by Lehmann *et al.*<sup>10</sup>, the gene expression analysis of 587 TNBCs showed six different TNBC subtypes having unique gene expression profiles. These data were further confirmed by the identification of TNBC cell line models representative of all subtypes and the subsequent prediction of driver signalling pathways pharmacologically targetable.

The combination of these histopathological and clinical features makes this type of tumour difficult in terms of therapy, being the chemotherapy the main therapeutic approach alone or in combination with surgery and radiation therapy. Taxane-based agents are the most commonly used, followed by taxol derivatives and anthracycline chemotherapy, used as a conventional route in the case of failure with taxanes. It is important to note that since the first application of taxanes, used in adjuvant therapy for

over 20 years<sup>6,7,11</sup>, relatively few new agents have been proposed for the treatment of patients with TNBC.

TNBC malignancy and resistance-related features can be explained, at least in part, by the inherited capacity of these cells to respond to cellular stress by mimicking a hypoxia gene signature associated with poor prognosis<sup>12-14</sup>. Under hypoxic conditions, TNBC cells can grow, survive, induce metabolic reprogramming and apoptosis, and alter cell adhesion and motility to facilitate metastasis and resistance to chemotherapy. TNBC is inherently hypoxic due to poor vascularization, as shown by overexpression of hypoxia-inducible factor 1- $\alpha$  (HIF-1 $\alpha$ )<sup>15</sup>, and a median partial oxygen pressure of 10 mmHg compared to 65 mmHg found in healthy breast tissue. Chen *et al.*<sup>16</sup> identified a molecular signature in TNBC that correlated with the activation of the XBP1 branch of the unfolded protein response (UPR) pathway and to hypoxia response. In addition, Dales *et al.*<sup>17</sup> established a significant relationship between clinicopathological characteristics and patient metastasis-free survival, studying the prognostic value of different HIF-1 $\alpha$  transcripts expression levels in BrCa. They showed that mRNA expression of a *HIF-1 $\alpha$ TAG* splice variant reflects a stage of BrCa progression associated with a worse prognosis<sup>17</sup>. Further, a recent meta-analysis with a total of 31 eligible studies including 5177 patients, done by Zhao *et al.*<sup>18</sup>, concluded that HIF-1 $\alpha$  might serve as an independent prognostic biomarker and a promising therapeutic target for BrCa<sup>18</sup>. So, based on that TNBC frequently shows morphologic evidence of hypoxia (central fibrosis and necrosis)<sup>19</sup>, augmented expression of HIF-1 $\alpha$  might be considered a hallmark of TNBC tumours.

All this data reflect a scenario where there are still many significant clinical and scientific challenges in terms of TNBC diagnosis, and treatment, as well as in the discovery of resistance mechanisms to current therapies<sup>20-23</sup>. Therefore, it is particularly challenging to find pharmacological targets that result in a longer metastasis-free disease and increase the overall survival rates in these patients<sup>23-25</sup>.

## **2. Protein synthesis control and cancer**

In the latest years, the significance of regulating mRNA translation for gene expression and cell phenotype control has been strongly established. This process is highly regulated and finely sensitive to several forms of cellular stress as well as to growth factors and other cell signalling processes. mRNA translation regulation relevance is that cell proliferation and growth are proportional to the rate of protein synthesis. Therefore, control of translation has been recognized critical in regulating many other physiological processes in

the cell including: growth stimulation, cell cycle progression, differentiation, stress response, and oncogenic signalling in cancer<sup>26-29</sup>.

From a structural perspective, mRNA can be thought of as a scaffold molecule that recruits a variety of players (Figure Intro. 2). Each mRNA can be roughly divided into five portions, which bind specific sets of RNA-binding proteins (RBPs) and others RNAs (like miRNA and lncRNAs), and thus have distinct roles in mRNA organization: the 5' cap, the 5' untranslated region (UTR), the open reading frame (ORF), the 3'UTR, and the 3' poly(A) tail. It is interesting to note the potential role of these RBPs, including mRNA stability, capping, translation initiation, and mRNA cleavage, among others.

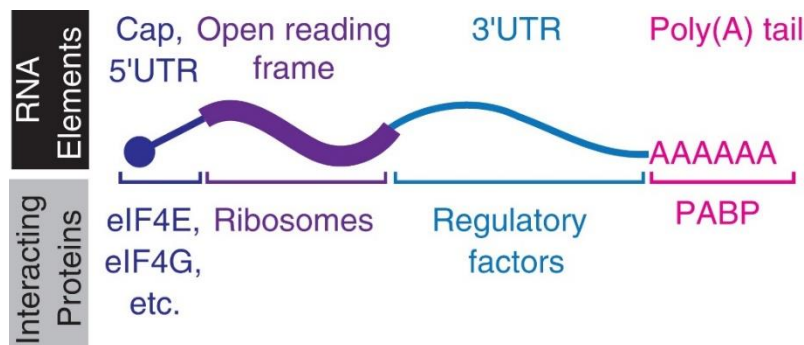


**Figure Intro. 2** RNA elements. (Olivia S. Rissland 2016<sup>47</sup>)

## 2.1. Canonical initiation of mRNA translation

Regulation of eukaryotic protein synthesis occurs mainly at the level of translation initiation. Most mRNAs recruit ribosomes through the m<sup>7</sup>G-cap structure, the 5' CAP, localized in the 5'UTR end of the mRNA, by the eukaryotic initiation factor 4F (eIF4F) complex, comprising eIF4E, eIF4A, and eIF4G. Then, binding of the 43S preinitiation complex, consisting of a 40S ribosomal subunit, eIF1A, eIF3, and eIF2-GTP, binds to the initiator tRNA and allows scanning downstream to the initiating AUG. Successful translation initiation is only achieved when eIF2 $\alpha$  binds GTP and tRNA, thereby forming the ternary complex. Formation of this complex is dependent on the exchange factor eIF2B, which exchanges the GDP bound to eIF2 $\alpha$  for GTP. The complex formation can be inhibited by the phosphorylation of eIF2 $\alpha$  at Ser-51 by an active eIF2 $\alpha$  kinase<sup>30,31</sup>.

The mTOR pathway plays an evolutionarily conserved role in coordinating cell growth and cell proliferation and it is probably the central protein kinase for the regulation of translation. mTOR is a highly conserved Ser/Thr kinase in all eukaryotes that controls cell growth, metabolism, survival, and proliferation in response to growth factors, nutrients, energy, and environmental conditions. mTOR forms two multi-protein complexes, mTOR complex 1 (mTORC1) and mTOR complex 2 (mTORC2). mTOR-containing complexes have different sensitivities to rapamycin as well as to different upstream and downstream



partners<sup>32</sup>. mTORC1 is the primary effector for the nutrient-sensitive functions of mTOR, whereas mTORC2 has been implicated in cytoskeletal reorganization, cell survival and metabolism<sup>33</sup>. The best-described upstream regulators of mTORC1 are growth factors, energy status, oxygen, nutrients, and amino acids.

Cellular stresses such as low energy, low oxygen levels or DNA damage, break down the activation of mTORC1. In response to these cellular stresses, ATP generation drops substantially and AMP levels increase leading to the activation of the AMP-activated protein kinase (AMPK). AMPK stops mTOR signalling by phosphorylation of raptor and TSC2. Additionally, Wnt signalling has been also shown to regulate the mTORC1 pathway by increasing mTORC1 signalling through the inhibition of Glycogen Synthase Kinase 3 (GSK3), a kinase that phosphorylates TSC2<sup>32</sup>.

mTOR downstream events are also crucial regulators of protein synthesis. Activated mTORC1 directly phosphorylates two translation regulators, the eukaryotic initiation factor 4E-binding protein 1 (4E-BP1) and ribosomal protein S6 kinase 1 (S6K1). mTOR stimulates mRNA translation by phosphorylation and inactivation of the eIF4E repressor 4E-BP1, and through phosphorylation and activation of S6K. In a stress situation, the binding of 4E-BP1 to eIF4E impedes the assembly of the translation initiation complex eIF4F. In a nutrient-rich environment, mTORC1 is activated and consequently phosphorylates 4E-BP1, which results in the release of eIF4E, enabling it to participate in the formation of the translation initiation complex involved in the cap-dependent translation<sup>32,34</sup>.

## **2.2. Non-Canonical initiation of mRNA translation**

The eukaryotic translation initiation relies not only on the cap-dependent mechanism of mRNA binding to the ribosome but also on poorly studied cap-independent ways of recruiting mRNAs to ribosomes. The latter mode plays an important role in cell differentiation and cellular response to abnormal conditions, such as oxygen-reduced conditions, when mRNAs cannot be translated through the cap-dependent mechanism<sup>35</sup>. The switch usually occurs secondary to the dephosphorylation of 4E-BP1 and the consequent inhibition of cap-dependent translation and enhanced translation of those mRNA which can utilize the cap-independent translation pathway. The most commonly accepted way to explain cap-independent translation of cellular mRNAs is the presence of internal ribosome entry sites (IRESs). However, alternative mechanisms may exist, as some of the cap-independent translation processes cannot be explained by the regulation of IRES and new concepts such as CITEs, TISU, and miRNA translational control have emerged<sup>36,37</sup>.

### 2.2.1. Internal Ribosome Entry Sites (IRES)

In the situations where mRNAs cannot be translated through canonical cap-dependent mechanisms, the cap-independent translation driven by IRESs can attend as an alternative machine for protein production. These elements were originally discovered in the viruses of the *Picornaviridae* family such as poliovirus and encephalomyocarditis virus. A large number of IRES were later identified in pathogenic viruses, including human immunodeficiency virus, hepatitis C virus (HCV), and foot and mouth disease virus. Though these viral IRESs contain different sequences, many of them have analogous secondary structures and initiate translation through similar mechanisms<sup>35</sup>. An IRES is a structured RNA element that facilitates 5' end-independent translation using subsets of translation initiation factors, in other words, RNA elements that recruit ribosomes to the internal region of mRNAs to initiate the translation<sup>35,36</sup>. Indeed, most suggested cellular IRESs reside in mRNAs that rely on internal initiation for sustained translation in conditions of stress, mitosis or apoptosis<sup>38</sup>.

Several cellular IRESs are thought to be activated through a structural change in their RNA motifs following a change in cellular conditions. It is proposed that cellular IRESs can be mainly classified into three groups based on which factors or mRNA elements interact with the IRES structure: assisting IRES-trans-acting factors (ITAFs), which remodel IRES structures; upstream open reading frames (uORFs), which sequester ribosomes and affect IRES structures; or RNA G-quadruplex structures (RG4s), as part of IRES structures<sup>38</sup>. A well-known IRES-dependent translation example is the case of the transcription factor c-Myc. Translation of c-Myc is activated following the induction of apoptosis in response to genotoxic stress and in a mTOR independent manner<sup>39,40</sup>.

IRES-ITAF interactions might contribute to the stabilization of unstable IRES structures or to the induction of a conformational change that allows the recruitment and precise placing of the ribosome. Thus, different IRESs require sequential or combinatorial binding by ITAFs to induce the structural changes that serve to recruit ribosome subunits in a cap-independent manner.

An uORF is an ORF located in the 5'UTR of an mRNA. uORFs translation can regulate eukaryotic gene expression, through the inhibition of downstream expression of the primary ORF<sup>35,38</sup>. In this context, the suppression forced by uORFs on the initiation of translation of the main ORF is relieved, thus letting the production of specific proteins in response to stress. The mode of action of each uORF seems dictated by its initiation codon context, secondary structure and coding capacities. Moreover, the overall regulation of a

given mRNA will depend on the precise combination and organization of uORFs in its 5'terminal area<sup>41</sup>.

In addition to secondary mRNA structures, specific RNA modifications may have a strong impact on alternative translation mechanisms. For instance, RG4s, an extremely stable RNA structure formed in G-rich regions by the stacking of at least two G-tetrads that forms a square-shaped structure, localize in 5'UTR structures, contributing to the regulation of IRES-mediated translation and to the direct recruitment of the 40S ribosomal subunit. These structures can also suppress translation and stimulate ribosomal frameshifting<sup>42</sup>.

In summary, structured cellular IRES in 5'UTR engages diverse strategies to overcome translation silencing in response to environmental changes (Figure Intro. 3).

### **2.2.2. Cap-independent translation element (CITE)**

In the last times, an alternative cap-independent mechanism has been proposed: the concept of cap-independent translation enhancers (CITEs) for mammalian mRNAs. CITEs are elements in the mRNA that attract key initiation factors, thereby promoting the assembly of translation initiation complexes. Unlike IRESs, CITEs can be located both within 5' and 3' UTRs, and bind mRNA recruiting translational components. Another difference by scanning the sequence is that they need free 5' ends of mRNAs and localize the initiation codon<sup>37</sup> (Figure Intro. 3).

Originally, CITEs were discovered two decades ago in UTRs of mRNAs from some plant viruses, where they were observed to provide high levels of translation of naturally uncapped virus mRNAs. Ilya M. Terenin *et al.*<sup>43</sup> showed that inserting a CITE element from a virus stimulates the direct binding of eIF4G to 5'UTR of cap-dependent mRNAs and dramatically reduces their requirement for the 5'-terminal m<sup>7</sup>G-cap, therefore, increasing the resistance to translation inhibition by the inactivation of eIF4F. Thus, it was showed that contained CITEs in the 5'UTR that directly or indirectly bind key components of the translational machinery can be more or less resistant to stress<sup>37,43</sup>. Not many cellular CITEs have been described so far, but the DAP5 protein, an homologous for eIF4G, has been shown to mediate the cap-independent translation of a number of C-mRNAs, including the p53-, BCL2-, and CDK1- CITE-mRNA, among others<sup>37</sup>.

### **2.2.3. Translation Initiator of Short 5'UTR (TISU)**

Translation in eukaryotes classically starts at the 5' end of the mRNA, with the 5' CAP and the UTR as the entry point for the ribosome. However, some uncommon mRNAs completely lack 5'UTR, for example, mammalian mitochondrial mRNAs, which are known

to be leaderless. In some humans, it has been described the presence of mRNAs with an extremely short 5' UTR, which undergo scanning-free initiation, a mechanism identified as translation initiator of short 5'UTR (TISU)<sup>38</sup>. The TISU element comprises an invariable AUG in the middle of its sequence as the start codon of TISU mRNAs. Since the position of the TISU element is downstream and very close to the m<sup>7</sup>G cap, TISU mRNAs have an abnormally short 5' UTR, with a median length of 12 nt<sup>44</sup> (Figure Intro. 3). Simplifying, these mRNAs are dependent on the m<sup>7</sup>G cap but avoid scanning for the initiation of translation. These special mechanisms direct protein synthesis of mRNAs with either an extremely short or a highly complex 5' UTR and are advantageous under specific physiological settings.

This TISU element is highly prevalent among genes with “housekeeping” functions such as protein synthesis, mitochondrial activities, and energy metabolism. A recent study discovered that TISU confers translational resistance to global inhibition of translation in response to energy stress but not to other stresses<sup>44,45</sup>.

#### **2.2.4. Others: miRNAs, lncRNAs**

Even though the 5'UTR plays a central role in the translation process, it is important to remark that the 3'UTR is also involved in the regulation of translation. It is very clear that small micro RNAs (miRNAs) (~22 nucleotides length) contribute to the regulation of protein synthesis by two different mechanisms, mRNA destabilization or translational repression. miRNAs seem to control translational suppression by targeting the 3'UTR of the mRNA, leading to the destabilization and following degradation of the mRNA target<sup>46-49</sup>.

Repression of translation by miRNAs can occur through inhibition of translation initiation or elongation, and may also lead to changes in the status of the mRNA 3' poly(A) tail. Actually, the poly(A)-binding protein (PABP) interacts with the cap through eIF4G and eIF4B, triggering to the circularization of the mRNA. Furthermore, circularization of mRNA brings the 3'UTR binding regulators, such as micro-RNAs, next to the 5'UTR, giving them the capability to modulate the translation initiation step<sup>41</sup>. New reports have proposed that in addition to the canonical binding of miRNAs to the 3'UTR of mRNAs, they might bind also to the 5'UTR region and ORF. Binding to sites located in coding regions and in 5'UTRs seem to produce less robust inhibition than those in 3'UTR and, surprisingly, determine translational activation, and not repression of miRNA targeted mRNAs (Figure Intro. 3). This situation has been described under growth arrest circumstances<sup>49</sup>.

On the other hand, other non-coding mRNAs such as lncRNAs have been postulated as translational modulators. Through homologous base-pairing with mRNA transcripts and interactions with ribosomal proteins and/or RNAs, lncRNAs are able to target mRNAs to the ribosomes. Containing complementary target sequences, lncRNAs also serve as miRNA decoys to prevent interactions of miRNAs with protein-coding transcripts (Figure Intro. 3).

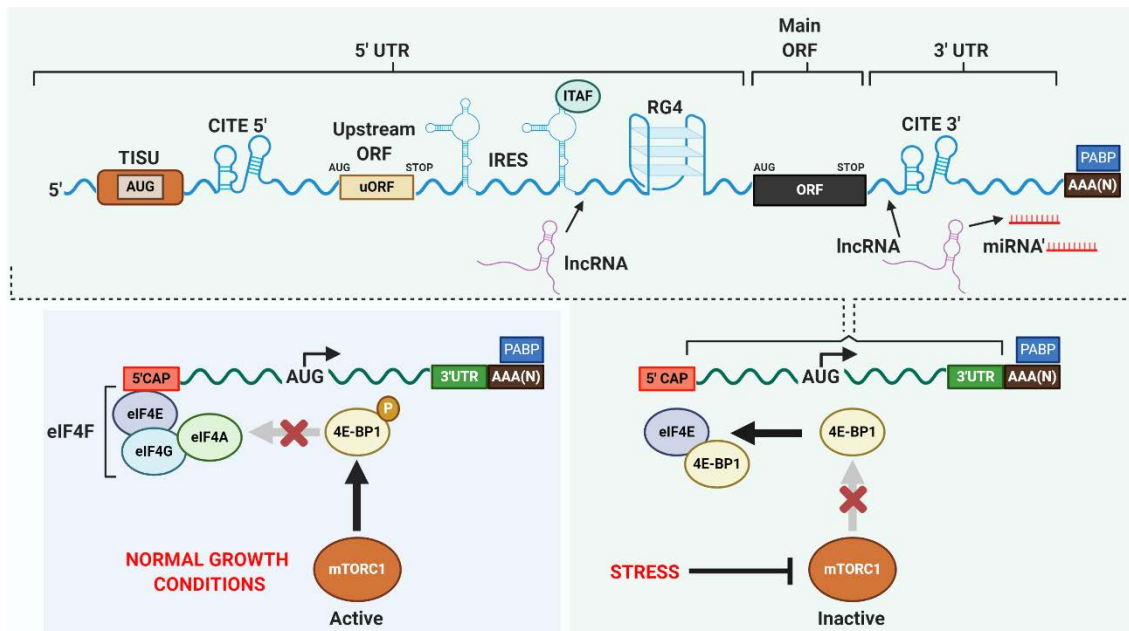


**Figure Intro. 3.** Canonical and Non-Canonical translational pathways. In a nutrient-rich environment, mTORC1 is activated and consequently phosphorylates 4E-BP1, which results in its release from eIF4E, enabling it to participate in the formation of the translation initiation complex involve in the canonical protein synthesis pathway. Stress conditions triggers inhibition of mTORC1 with the consequent dephosphorylating of 4E-BP1. Binding of 4E-BP1 to eIF4E impedes the assembly of the translation initiation complex eIF4F leading to the inhibition of the canonical protein synthesis pathway.

### 2.3. Polysome profiling

Polysome profiling provides a key methodology for the development of translation-related studies. The overall aim of the polysome profiling technique is to study and quantify the translation state of specific mRNAs under different cellular conditions. The principle of the technique is to capture mRNA translation by “freezing” actively-translating ribosomes on different transcripts and separate the resultant polyribosomes by ultracentrifugation on a sucrose gradient, thus allowing for a distinction between highly translated transcripts (bound by several ribosomes) and poorly translated ones (bound by one or two ribosomes). First, cells are lysed and loaded on top of a sucrose gradient. After ultracentrifugation, the gradient is monitored at A254 (absorbance) using a flow cell coupled to a spectrophotometer and then fractionated into equal sections: untranslated mRNAs (top fractions) are separated from polysome-associated mRNAs (bottom fractions) (Figure Intro. 4). Finally, fractions can be then processed for further characterization by traditional biochemical and molecular biology methods. Importantly, combining polysome profiling

with high throughput genomic approaches allows for a large scale analysis of translational regulation<sup>50,51</sup>. For the development of the technique, it is important to use chemicals that blocks the release of ribosome-translating mRNA. Both, cycloheximide, that binds to the 60S ribosomal subunit and blocks the release of deacetylated tRNA from the ribosome E site<sup>52</sup>, inhibiting ribosome translocation and stall ribosomes on translating mRNAs, or emetine, which also blocks translation elongation<sup>53</sup>, can be used<sup>50,51</sup>.

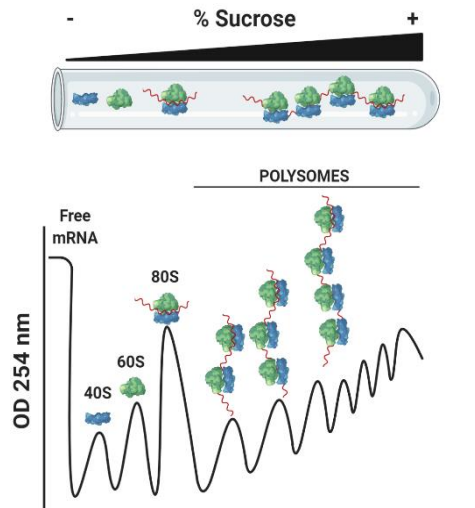


**Figure Intro. 4.** Polysome profiling representation.

### 3. Hypoxic stress

In healthy tissues, the oxygen supply fits the cellular requirements (normoxia). Hypoxia takes place when oxygen source and consumption are not balanced, and normal cellular functions cannot be maintained. The microenvironment of solid tumours is considerably different from normal tissue in terms of oxygenation, making the occurrence of hypoxic tissue areas a frequent feature of solid tumours. These areas are heterogeneously distributed within the tumour mass (Figure Intro. 5). It has been described that this lack of efficient oxygenation within the tumour centre gives rise to a higher malignancy, including the occurrence of metastasis secondary to induction of hypoxia-related factors, a phenomenon associated with poor patient outcome in several types of cancer<sup>54,55</sup>.

High cancer cells proliferation rate results in a huge increase of O<sub>2</sub> consumption and promotes abnormal cell growth patterns. Hypoxic areas, at the same time, induces the formation of new vasculature, but it is usually insufficient and defective. This neovasculature shows severe structural and functional abnormalities; they are often occluded and leaky, resulting in perfusion-limited areas within the tumour that causes variations in oxygen supply and nutrients (Figure Intro. 5). As a result, the area within 70-

100  $\mu\text{m}$  away from the blood vessel is relatively oxygenated, but  $\text{O}_2$  diffusion is dramatically compromised beyond 100-150  $\mu\text{m}$  distance to the blood vessel, leading to chronic hypoxia<sup>56-58</sup>.

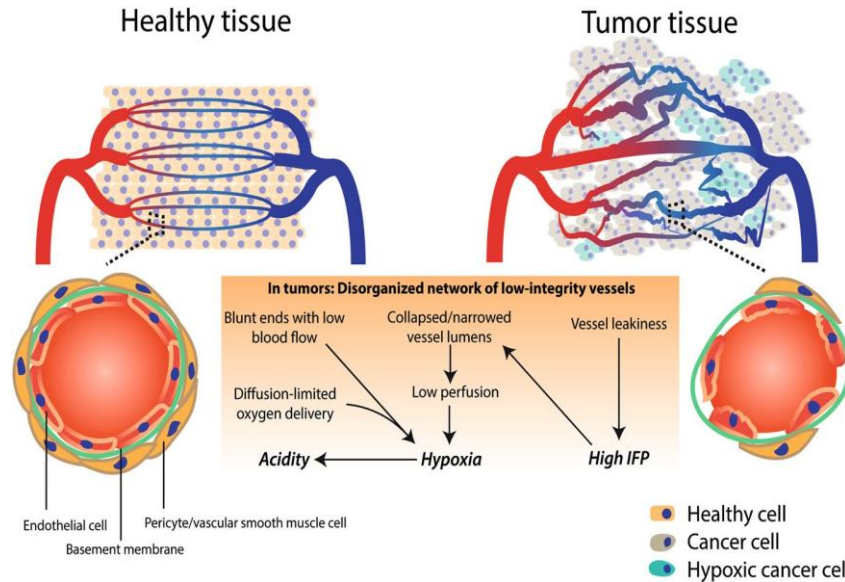


**Figure Intro. 5.** Tumor-associated blood vasculature. (Marco B. Schaaf *et al.*, 2018<sup>249</sup>)

From a biological point of view, several features have been described in cells exposed to a hypoxic environment. It has been shown that intermittent hypoxia makes tumour and endothelial cells more resistant to apoptosis and radiotherapy. Moreover, cancer cells exposed to hypoxia are more aggressive and increase their ability in tumour initiation and metastasis. It has been also described that hypoxia may increase oxidative stress in tumours, what correlates with the effect known as re-oxygenation injury, that is consequence of the fluctuating levels of oxygen, and results in an increase of free radicals, tissue damage and activation of stress-response genes<sup>57,58</sup>.

Generally, most solid tumours preserve hypoxic areas throughout disease progression, selecting for aggressive malignant cells that can survive the ischemic stresses of the adverse tumour microenvironment. This results in a clonal selection of hypoxia-resistant cancer cells, as well as DNA damage, resistance to chemotherapy and radiotherapy, and an increased likelihood of metastasis. Beyond HIFs dependent-response, reactions to decreased  $\text{O}_2$  levels involve changes in the epigenome, non-coding RNAs, the metabolome, signalling pathways, and biochemical reactions to ensure cell survival during hypoxic stress<sup>59</sup>.

In addition to this, in the absence of oxygen, the DNA damage produced by the free radicals is reduced restoring the DNA to its original form and allowing cell survival<sup>60</sup>. The survival of these cancer cells permits the tumour to proliferate and metastasize as the

disease progresses. Also, different sub-populations of cancer cells which are able to resist conventional radiotherapy, are capable of metastasizing to distant sites and possess stem-cell like features, has been identified. This subset is known as cancer stem cells (CSCs)<sup>61</sup>.

The existence of Breast Cancer Stem Cells (BCSCs) has been well documented since their first identification and isolation in BrCa by Al-Hajj *et al.*<sup>62</sup>. The subset of BCSCs were identified by FACS as a population of cells with a CD22<sup>-</sup>/CD44<sup>+</sup> expression profile, that were able to recapitulate the primary breast tumour in immunodeficient mice when as few as 100 of the CD22<sup>-</sup>/CD44<sup>+</sup> cells were xenografted. Subsequently, there have been numerous investigations that have further defined the BCSC population based on their expression of markers, including the positive expression of CD133, epithelial surface antigen (ESA), and aldehyde dehydrogenase (ALDH) 1<sup>63,64</sup>.

Cancer is caused by the accumulation of multiple and consecutive genetic alterations together with the evolving crosstalk with the surrounding microenvironment<sup>65</sup>. In the past, the influence of microenvironment has been mostly ignored by cancer biologists, that is why, they routinely used two-dimensional (2D) cultures for studying the mechanisms involved in this disease. The development of three-dimensional (3D) cultures that incorporate multiple physical, mechanical, and chemical cues from the extracellular matrix (ECM) is crucial to get closer to the real situation and continue moving forward. They re-establish tumour architecture shape, principally cores that contain quiescent and hypoxic cells. Remarkably, it has been demonstrated that they exhibit higher anticancer drug resistance as compared to classical 2D cultures, as well as a better mimicking of the *in vivo* situation<sup>66,67</sup>. However, this model presents important limitations, since cells grow as independent cellular aggregates and show reduced interactions with extracellular milieu.

### **3.1. Adaptation mechanisms to hypoxic stress: transcriptional and post-transcriptional events**

#### **3.1.1. Transcriptional changes**

Hypoxia transcriptionally induces a robust set of genes controlled by HIFs. The vast majority of oxygen-sensitive genes are in fact direct HIF targets<sup>68</sup>. Specifically, cellular responses and adaptation to hypoxia are mediated partially through the activation of the HIF-1 signalling pathway. HIF transcription factors are heterodimers that comprise two subunits, a hypoxia inducible-expressed HIF-1 $\alpha$ , and a constitutively-expressed HIF-1 $\beta$  subunit, also known as aryl hydrocarbon receptor nuclear translocator (ARNT), which belongs to the PER-ARNT-SIM (PAS) subfamily of the basic helix-loop-helix (bHLH) family of transcription factors<sup>69,70</sup>. Their structures are similar and both contain the following



domains: a N-terminus bHLH domain, a central region with a PAS domain and a C-terminus. Regarding its functionality, the bHLH domain mediates DNA-binding, PAS and bHLH domains mediate heterodimerization and the C-terminal regions are responsible for the recruitment of transcriptional co-regulatory proteins<sup>71</sup>.

Under normal oxygen conditions, HIF-1 $\alpha$  is continuously synthesized and rapidly degraded by the ubiquitin-proteasome system. For its degradation, HIF-1 $\alpha$  is hydroxylated by prolyl hydroxylases (PHDs) on two proline amino acid residues (P402 and P564) located in the oxygen-dependent degradation domains (ODDDs)<sup>72</sup>. The prolyl hydroxylation results in an increase of the affinity of von Hippel-Lindau tumour suppressor protein (VHL) for HIF-1 $\alpha$ , promoting its ubiquitination by VHL and its subsequent proteasomal degradation. Additionally, there is one more hydroxylation in one C-terminal asparagine residue (N803) in the transactivation domain by the asparaginyl hydroxylase termed factor inhibiting HIF-1 (FIH-1). FIH-1 hydroxylation avoids the recruitment of p300/CBP (CREB binding protein) and the subsequent transactivation of HIF target genes. Under hypoxic conditions, the activity of PHDs and FIH-1 is reduced, as a consequence of their requirement of molecular O<sub>2</sub> as a co-substrate. HIF-1 $\alpha$  is stabilized, accumulated, and it translocated to the nucleus, where it dimerizes with HIF-1 $\beta$  and associates with co-activators, such p300/CBP<sup>73</sup>. HIF binds to target genes, specifically to the hypoxia response elements (HREs) located in their promoters. Under these conditions, HIF is able to modulate the transcription of many hypoxia-responding genes, involved in several biological functions including angiogenesis (e.g. vascular endothelial growth factor (VEGF)), pH regulation (e.g. carbonic anhydrase 9 (CA9)), and cellular metabolism (e.g. lactate dehydrogenase-A (ALDH))<sup>74,75</sup>.

### **3.1.2. Translational changes: Adaptive protein synthesis in hypoxia**

Although the transcriptional components of the response to hypoxia have been studied reasonably well, changes in protein synthesis rates under low oxygen have been less well characterized. It might be said that the main goal of the negative regulation of translation is to suppress costly energy processes, such as "unnecessary" protein synthesis, and also to prevent the accumulation of stress-induced unfolded and/or misfolded proteins.

Exposure to hypoxia involves a fast and continued inhibition of mRNA translation, basically by direct inhibition of the initiation step. The rate of protein synthesis is reduced by 60-70% within 1 hour of hypoxic exposure, and quickly returns to state levels after O<sub>2</sub> reintroduction. During longer hypoxia exposures where mRNA translation remains significantly repressed for up to 24 hours, the maximal inhibition occurs in approximately 2 hours followed by a small recovery after 4 hours<sup>76</sup>.

Under physiological conditions, eukaryotic initiation factor 2 (eIF2) promotes translation initiation in its un-phosphorylated form; but in the context of O<sub>2</sub> depletion, the endoplasmic reticulum (ER) resident kinase PERK phosphorylates eIF2 $\alpha$  with the consequent suppression of mRNA translation initiation, involving an effect in global protein synthesis that limits the detrimental effects of proteotoxicity. In addition, hypoxia negatively regulates mTOR. There are two possible independent mechanisms to do so: first, hypoxia inhibits mTOR by an increase in AMP, which leads to the activation of AMPK<sup>77</sup>; and second, HIF-induced gene DNA damage response 1 (REDD1) activates the TSC complex, resulting in mTOR inhibition and involving a more direct link between HIF and mTOR<sup>78,79</sup>. Both cases end up in direct phosphorylation of TSC2/1 complex and subsequent mTOR inhibition and thus, effects on mTOR targets result in the regulation of translation in cancer cells<sup>80</sup>. This mTOR inhibition, maintains eIF4E bound to 4E-BPs, resulting in the inhibition of eIF4F assembly and decreased global translation rates. Interestingly, prolonged hypoxic exposure activates an alternative eIF2 $\alpha$  mTORC1-independent pathway, which maintains translation repression, where eIF4F complex breakdown results in eIF4E becoming sequestered in the nucleus by its transporter 4-ET<sup>59</sup>.

During hypoxia events, not only translational inhibition occurs, in parallel, translation of certain transcripts that encode proteins vital for survival in hypoxic environments is enlarged, in order to allow adaptation of cells to this stressful situation. Consequently, hypoxic control of mRNA translation undoubtedly influences individual gene expression and contribute to the hypoxic phenotype. The phosphorylation of eIF2 $\alpha$  by PERK, not only results in translational attenuation, but it specifically promotes the translation of the activation transcription factor 4 (ATF4), a significant mediator of the unfolded protein response; and it plays an important role regulating other genes including CHP and GADD34, particularly important for preventing oxidative stress and apoptosis, respectively<sup>81,82</sup>.

Importantly, there are some mRNAs that need to overcome the translation repression induced by hypoxia, obviously including those encoding mediators of hypoxia such as HIF-responsive genes, whose mRNA contains reverse hypoxia response elements (rHREs). Low oxygen levels stimulate the formation of a complex including HIF2 $\alpha$ . HIF2 $\alpha$ , apart from its function as a transcription factor, is a component of a cap-dependent translation initiation complex. This complex is composed by RNA binding motif protein 4 (RBM4) and eIF4E2 (eIF4E homolog) and assembles at these rHREs to promote translation initiation. Hypoxia also promotes formation of hypoxia-specific eIF4F complex (eIF4F<sup>H</sup>) that binds rHREs. O<sub>2</sub> levels influence in the composition of the eIF4F complex, switching from eIF4E-eIF4A-eIF4G to eIF4E2-eIF4A-eIF4G3, which selectively recruits, with higher efficiency, mRNAs

## *Introduction*

regulated by HIF to the ribosome for translation, independently of the overall cellular transcription competency<sup>59,75</sup>.

Another mechanism for selective hypoxia-responsive mRNA translation involves direct binding at IRES encoded in the 5'UTR of some specific mRNAs such as VEGF, eIF4G and MYC<sup>83-85</sup>.

In addition to these translational methods of HIF $\alpha$  regulation, non-coding RNAs also play an important role in mediating cellular response to hypoxia. Some of the most well-known non-coding RNAs in hypoxia are micro-RNA-429 (miRNA-429) and micro-RNA-210 (miRNA-210). These two miRNAs have been demonstrated to directly bind to the 3' UTR of the HIF1 $\alpha$  gene, in the end reducing the expression of HIF1 $\alpha$ . At the same time, these miRNAs are also target genes of HIF1 $\alpha$ , generating a negative feedback loop of HIF1 $\alpha$  expression in hypoxia. HIFs can be also regulated by hypoxia-responsive long non-coding RNA (HRL). HRLs have a notable impact in hypoxic cancers as they have been associated with increased tumorigenesis, ionizing radiation therapy resistance and metastasis. HRLs are transcriptional targets of HIFs and unlike miRNAs, create a positive feedback by stabilizing them<sup>86</sup>.

In summary, hypoxia induces elevated levels of 4E-BP1 resulting in the inhibition of canonical mRNA translation. Collectively, it results in an adaptive tumour cell response, thereby promoting a switch to the non-canonical protein synthesis pathway by several routes and mechanisms. That is why focus on the research of those fine-tuning translationally activated factors upon hypoxia conditions, can be the key to break down the malignant effects that hypoxia triggers during tumorigenesis.

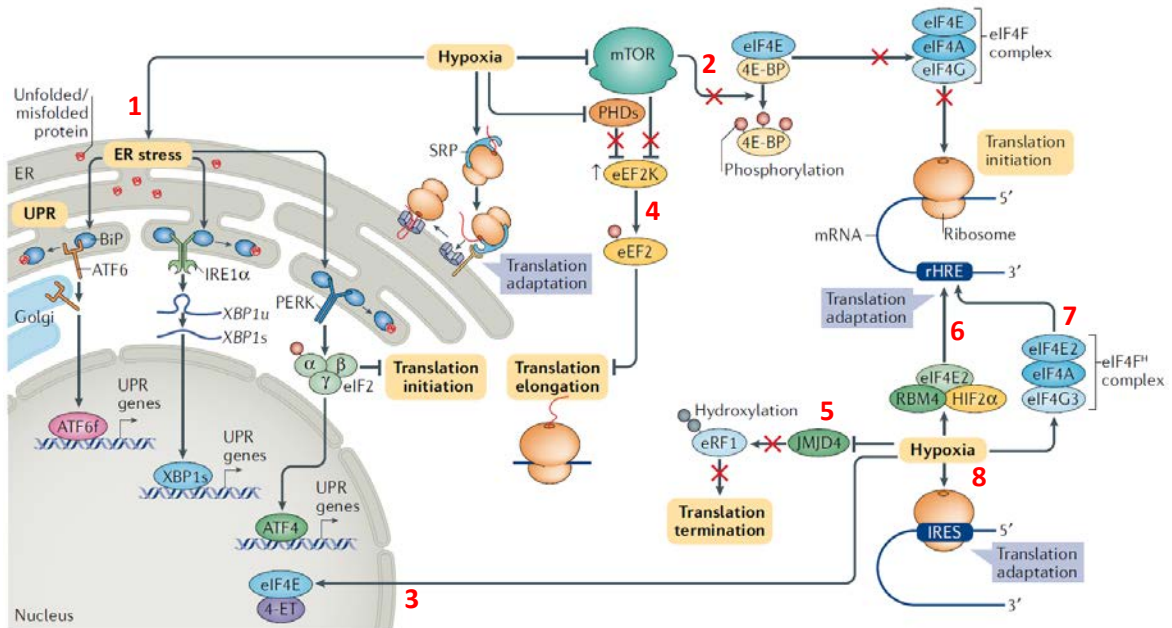


**Figure Intro. 6.** Mechanisms of hypoxic adaptations. Hypoxia can induce (1) ER stress with the consequent inhibition of eIF2 $\alpha$  by PERK, and in parallel the activation of ATF6, to initiate responses to restore ER homeostasis. Upon activation, PERK phosphorylates eIF2 $\alpha$  to decrease general peptide translation and promote the expression of transcription factor ATF4. Activation of the UPR alleviates the burden of misfolded and/or unfolded proteins, while translation inhibition decreases energy expenditure. (2) Hypoxia also negatively regulates mTORC1 activity resulting in a negative regulation of translation initiation by controlling the formation of the mRNA cap-binding eIF4F complex. (3) In addition, hypoxia also promotes nuclear sequestration of eIF4E by its transporter, 4-ET. (4) Elongation of mRNA translation is also controlled during hypoxia by modulating the activity of eEF2K, an inhibitor of eEF2. (5) Translation termination is negatively regulated by hypoxia due to decreased hydroxylation of eRF1 by JMJD4. (6) Some mRNAs overcome the translation repression induced by hypoxia, including those encoding mediators of hypoxia. Hypoxia-responsive mRNAs contain rHREs. Low oxygen stimulates the formation of a complex including HIF2 $\alpha$ , RBM4 and eIF4E2 that assembles at these rHREs to promote translation initiation. (7) Hypoxia also leads to the formation of eIF4F<sup>H</sup> that binds rHREs. (8) Selective hypoxia responsive mRNA translation can also occur by direct binding of ribosomes to IRES sequences of certain mRNAs. (Pearl Lee *et al.*, 2020<sup>59</sup>).

#### 4. Metastasis

Metastasis is a multistep process, illustrated in Figure Intro. 7, which consists in several steps that all need to be completed successfully to form a metastatic tumour. Cancer cells have developed the ability to disseminate from the primary tumour, being able to travel through the blood and lymphatic system to distant sites in the body where they can form new colonies<sup>87,88</sup>. First of all, cancer cells need to cross the basal membrane in order to invade the adjacent stroma, a process called localized invasion. During the following step, intravasation occurs and cancer cells enter into the blood and lymphatic vessels. Once in the circulation, tumour cells can adhere to larger blood vessels and extravasate into nearby tissues through paracellular or transcellular migration, giving place to the formation of micro metastases in the target tissue when the tissue microenvironment is favorable<sup>89</sup>.

Finally, colonizer cancer cells may begin to proliferate and form a secondary tumour, a process known as colonization<sup>87,90,91</sup>.

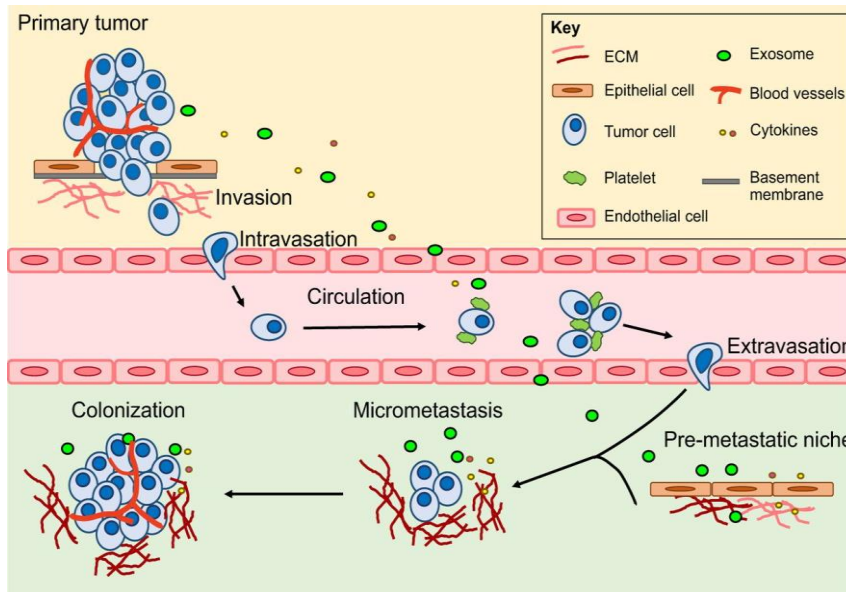


**Figure Intro. 7.** Metastatic cascade. Metastasis is a multistep process. (Laura Gómez-Cuadrado *et al.*, 2017<sup>89</sup>)

#### 4.1. Epithelial-Mesenchymal Transition (EMT)

Epithelial-Mesenchymal Transition (EMT) is the process by which an epithelial cell shifts to a more mesenchymal phenotype<sup>92,93</sup>. A wide range of cellular events occurs during this process, which includes increased resistance to apoptosis, loss of apico-basal polarity, dissociation of cell adhesion junctions (cell-cell and cell-basal membrane junctions) and an important architectural reorganization of the cytoskeleton. These events are associated with the synchronized upregulation of mesenchymal markers and downregulation of epithelial markers. At the phenotype level, this acquisition of mesenchymal properties basically leads to an increase in cell motility<sup>94</sup>. Because of cellular plasticity, EMT can be recapitulated to the reverse of this process, Mesenchymal-Epithelial Transition (MET), which is associated with a loss of this migratory capacity, apico-basal polarization and expression of the junctional complexes that are hallmarks of epithelial tissues<sup>95</sup>.

##### 4.1.1. EMT in cancer

It is thought that EMT is activated in cancer cells in order to allow its dissociation from the primary tumour and its intravasation in the blood vessels (Figure Intro. 7). However, the impact of EMT on cancer progression and patient survival is still far from being fully understood. Although many *in vitro* models have been used to detect EMT, the lack of evidence of EMT in clinical cancer samples has questioned its relevance during cancer progression<sup>95</sup>. It is important to keep in mind that EMT is considered a transient and non-homogeneous event and a tumour specimen represents only one particular instant,

highlighting the need to view EMT as a spectrum of intermediate states. This, added to the difficulty to distinguish cancer cells with mesenchymal properties from other mesenchymal cells within the tumour stroma, has been a subject of controversy. Paying attention to the invasive front, cancer cells, which spread from the tumour mass to the adjacent stroma, can be detected expressing both epithelial or mesenchymal markers<sup>96,97</sup>. By contrast, the main tumour bulk remains largely epithelial. So, the most likely situation *in vivo* is an EMT gradient from full (invasive front) to partial or even absent (tumour mass), reflecting the intrinsic heterogeneity of tumour cells and tumour microenvironment when compared with the relative homogeneity of cell culture models<sup>95</sup>. Importantly, this spectrum of intermediate states is also observed when the cells arrive to destination, just after cell extravasation, where there is usually a reversion to the epithelial phenotype, recovering epithelial phenotype through undergoing MET<sup>94</sup>.

#### 4.1.2. TGF- $\beta$ Pathway

It is broadly documented that Transforming Growth Factor Beta (TGF- $\beta$ ) plays central roles in carcinogenesis<sup>98,99</sup>. Interestingly, it plays a dual role during this process acting as a tumour suppressor and as a tumour promoter. As a tumour suppressor, in normal epithelial cells, it inhibits tumorigenesis by inducing growth arrest and apoptosis. It also regulates cell differentiation, senescence, adhesion, and motility<sup>99</sup>. As a tumour promoter, since tumour cells are known to be resistant to TGF- $\beta$  anti-mitogenic effects, it leads to tumour cell migration and stimulates EMT, increasing the expression of mesenchymal markers, such as N-Cadherin and vimentin, and reducing the expression of epithelial markers, such as E-Cadherin. Immunostaining analyses have demonstrated a correlation between TGF- $\beta$  expression and metastasis in breast, colon and prostate cancer. Moreover, the intensity of TGF- $\beta$  staining in invading lymph node metastases has been observed to be higher in breast and colon cancer metastasis than in the primary tumours<sup>100,101</sup>.

TGF- $\beta$  ligands bind to TGF- $\beta$ RII dimers, which in turn recruit a dimer of TGF- $\beta$ RI forming an hetero-tetrameric complex. Then, the receptor rotates in such a way that their cytoplasmic region is oriented towards a catalytically favourable conformation. TGF- $\beta$ RII trans-phosphorylates the serine residues of TGF- $\beta$ RI, resulting in its activation and the subsequent binding, phosphorylation and stimulation of the latent transcription factors SMAD2 and SMAD3. TGF- $\beta$ RIII also contributes to this process as a co-receptor that increases the binding of ligands to TGF- $\beta$ RII<sup>98,99</sup>. Once activated, SMAD proteins shuttle to the nucleus forming a complex with SMAD4, a binding partner common to all SMAD isoforms<sup>98,99</sup>. This SMAD-dependent pathway is also known as Canonical TGF- $\beta$  pathway (Figure Intro. 8).

Although SMAD proteins are fundamental for TGF- $\beta$  driven cellular responses, there are numerous signalling processes stimulated by TGF- $\beta$  that occur independently of them, they are known as non-canonical TGF- $\beta$  signalling and complement SMAD-dependent actions. Factors such as tumour necrosis factor (TNF), receptor associated factor 4 (TRAF4), TRAF6, TGF- $\beta$ -activated kinase 1 (TAK1), p38 mitogen-activated protein kinase (p38 MAPK), p42/p44 MAPK, RHO, phosphoinositide 3-kinase PI3K/AKT, extracellular signal regulated kinase (ERK), JUN N-terminal kinase (JNK), or nuclear factor-kB (NF-kB) act by supporting or mitigating TGF- $\beta$  downstream cellular responses.

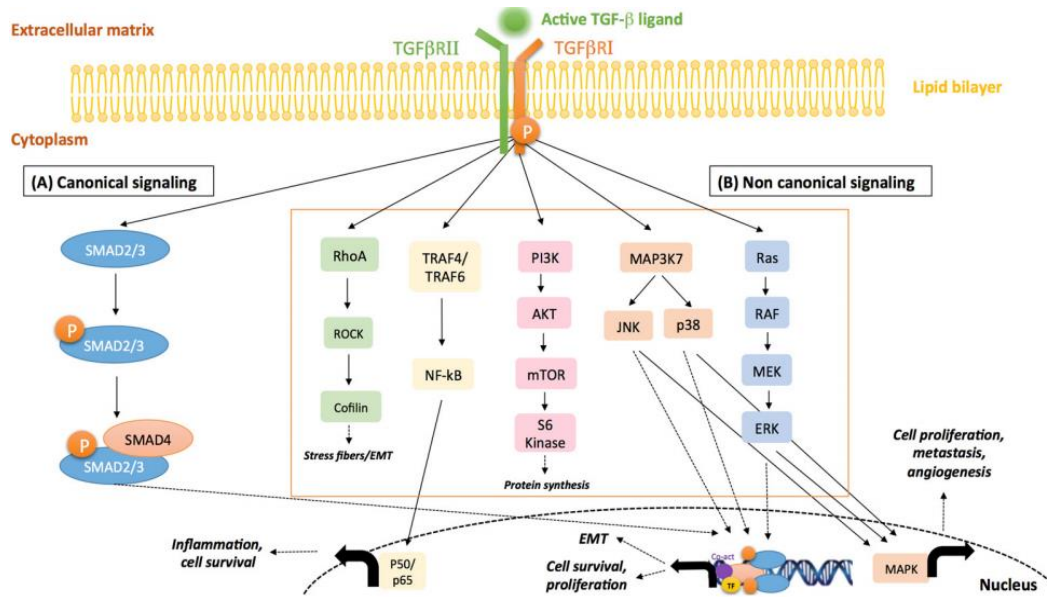


**Figure Intro. 8.** TGF- $\beta$  SMAD-dependent and -independent signaling. (Constanza Brunella *et al.*, 2017<sup>250</sup>)

Cells under EMT not only lose apical-basal cell polarity, but also gain spindle-shaped, fibroblast-like morphology distinctive for mesenchymal cells. These phenotypic changes are the result of molecular changes, basically based in the loss of E-Cadherin expression together with other components of epithelial cell junctions. As a substitute, they generate a mesenchymal-like cell cytoskeleton and acquire motility and invasive properties. All the orchestra is driven by a set of transcription factors including the zinc-finger proteins SNAIL and SLUG, the bHLH factor TWIST, the zinc-finger/homeodomain proteins ZEB-1 and -2, and the fork head factor FOXC3<sup>98</sup>.

Cell junction complexes are also regulated by TGF- $\beta$  and thus can be regulated by SMAD-dependent and SMAD-independent events. SMAD-mediated expression of HMGA2 induces expression of SNAIL-1/2 and TWIST. TGF- $\beta$  also upregulates integrin-linked kinase (ILK), increasing cellular motility. Moreover, expression of integrins (e.g.,  $\alpha 5$ ,  $\alpha v$ ,  $\beta 1$ ,  $\beta 3$ ,  $\beta 5$ ), which bind the ECM, is also enhanced by TGF- $\beta$ . As a result of this binding, there is an induction of TGF- $\beta$  production that leads to a feed-forward loop between tumour cells and ECM<sup>102</sup>. Cooperatively, these phenotypic and morphologic changes collaborate to convert

steady multicellular epithelial tissue into highly mobile, independent cells ready for invasion and metastasis.

## **4.2. Intercellular communication**

Intercellular communication between cancer cells and other nearby cells within the tumour microenvironment plays a major and well-established role in tumour development. Tumours are not isolated entities, they contain infiltrates of stromal cells, normal cells from the tissue of origin, and vascular and immune cells, all of them embedded in an ECM containing various connective tissue structures, as well as growth factors, cytokines and chemokines, extracellular vesicles (EVs), metabolites and nutrients, electrolytes, oxygen, etc. All these molecules can either promote or inhibit tumorigenesis, depending on the situation of the tumour microenvironment and their effect on cell activation status<sup>103-105</sup>. At early stages of tumorigenesis, the microenvironment displays anti-tumour activity in order to control tumour growth. As the tumour keeps on developing, the leading role of the microenvironment shifts over to be tumour promotive, providing mitogenic growth factors, trophic factors or blocking growth inhibitory signals. These heterotypic interactions may occur through direct contact between cells or paracrine signal exchange of intracellular material<sup>106,107</sup>, signals that can be mediated by soluble factors and/or EVs. Although studies have been mainly focused on soluble factors, showing how chemokines and cytokines produced in the tumour are mostly responsible for changes in cancer and stromal cells, accumulated pieces of evidence point towards the contribution of another mode of cell communication involving EVs in cancer progression<sup>104</sup>.

### **4.2.1. Extracellular vesicles-dependent intercellular communication**

EVs have become important players in intercellular communication within the tumour microenvironment, metastasis and drug resistance. They can influence either local sites, close to their place of production, or they can be directed to distant sites<sup>108-110</sup>. EVs can transport biomolecules, modulate changes in signalling pathways, regulate maturation and differentiation, and induce genetic changes in cells. It is known that EVs have the same topology than the cell they are originated from.

Following the idea that they are present in biological fluids, added to their relative stability and their resistance to proteolytic and nuclease activity, together with their ability to carry out the transfer of a variety of molecules, tumour-derived EVs are perfect actors to take into account in the liquid biopsy field. Current research has focused on their characterization in different cancer types and their potential for multicomponent analyses<sup>111,112</sup>.



Cancer-associated fibroblasts (CAFs) are known to be another important central point in EVs-related cancer progression. On the one hand, it has been described how EVs promote activation and reprogramming of fibroblast toward the phenotype of CAF, triggering the support of tumour growth and the establishment of a favourable tumour microenvironment. On the other hand, EVs secreted by CAFs can increase cell motility and invasiveness promoting EMT activation in surrounding cancer cells<sup>113-116</sup>.

In recent studies, tumour-derived EVs have been demonstrated to play an important role in pre-conditioning future metastatic sites. EVs derived from metastatic melanoma cell lines were found to localize *in vivo* at the site of future metastasis and to educate the site towards a pro-metastatic phenotype via the upregulation of hepatocyte growth factor receptor (HGFR) also known as MET<sup>108</sup>. Similarly, it was shown that EVs containing Macrophage Migration Inhibitory Factor (MIF) primes the liver for metastasis and may be a prognostic marker for the development of Pancreas Ductal Adenocarcinoma (PDAC) liver metastasis<sup>109</sup>.

Finally, concerning evasion of immune recognition by cancer cells, several studies have confirmed tumour derived-EVs to be immunosuppressive and to induce apoptosis of T cells by delivery of FasL and TNF-related apoptosis-inducing ligand (TRAIL)<sup>116-118</sup>.

#### **4.2.2. Extracellular vesicle biology**

EVs are an heterogeneous group of secreted membranous vesicles including apoptotic bodies, microvesicles, ectosomes, and exosomes<sup>119</sup>, although it is worthy to note that the classification of EVs is continuously growing as a consequence of the novelty in the field<sup>120</sup>. Ectosomes are vesicles generated by the direct outward budding of the plasma membrane, which produces microvesicles, microparticles, and large vesicles in the size range of ~50 nm to 1µm in diameter. By contrast, exosomes have endosomal origin and comprise a size range of ~40 to 160 nm in diameter (~100 nm on average)<sup>121</sup>. However, the mechanisms underlying their biosynthesis, release from donor cells, and uptake into target cells remain poorly understood. Exosomes are of particular interest in EVs-biology because their formation implicates a complex intracellular regulatory process that likely determines their composition, and possibly their functions, once secreted into the extracellular space<sup>121</sup>. Once released from the donor cell, these vesicles induce cell signalling, either by interacting with target cell-surface proteins or by being internalized into the receiving cell<sup>119,122</sup>. Exosomes are a highly heterogeneous population that is known to have distinct abilities to induce complex biological responses. This complexity is based on the basis of their size, content (cargo), functional impact on recipient cells, and cell of origin (source). Distinct

combinations of these features give rise to differences among exosomes highlighting the heterogeneity of this population of EVs (Figure Intro. 9)<sup>121</sup>.

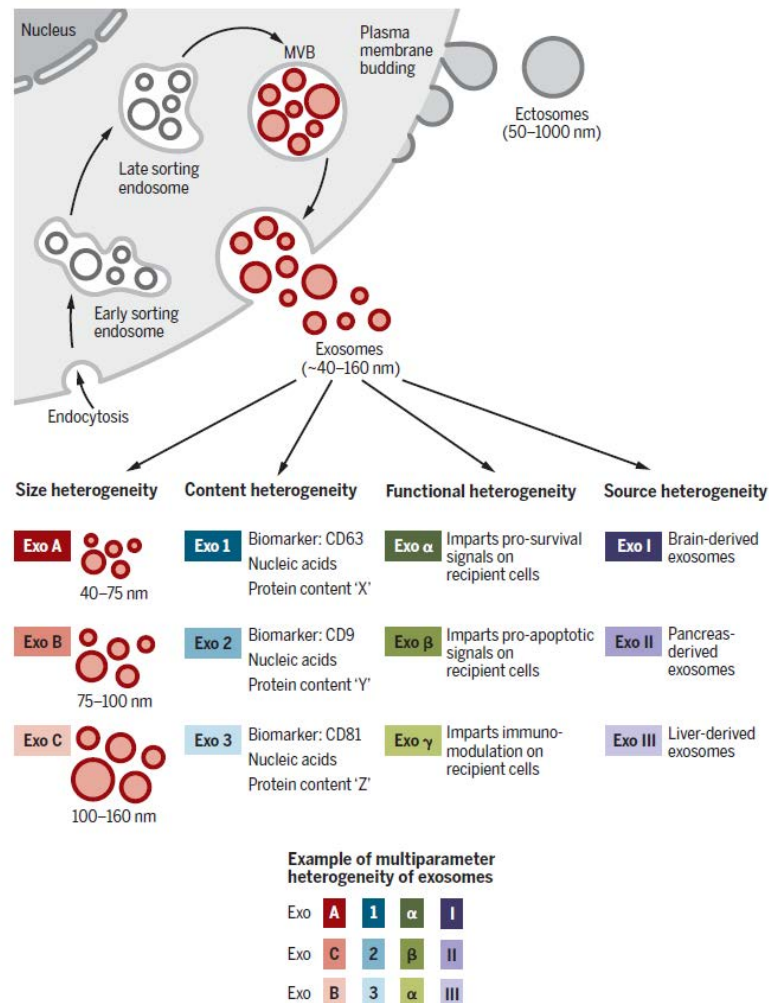


**Figure Intro. 9.** Identity and the heterogeneity of EVs and exosomes. (Adapted from Kalluri *et al.*, 2020<sup>121</sup>)

#### 4.2.3. Exosomes uptake

The questions surrounding the function of exosomes are mostly focused on understanding the destiny of their components and the phenotypic and molecular changes that they induce on receiving cells. Many and largely distinct mechanisms and pathways associated with exosome uptake have been described<sup>119,123</sup> and the putative specificity of exosomes for certain cell types, add complexity to the function of exosomes and its relevance in intercellular communication<sup>121</sup>.

To enable communication, it is essential for the exosomes to dock on the plasma membrane and engage with surface receptors, which in turn activate other molecules on the surface and trigger rapid downstream signalling, uptake, or fusion with the recipient cell membrane. The uptake is currently the less understood step in vesicle-based

intercellular communication, and proposed mechanisms range from passive membrane fusion to active uptake via: 1) general mechanisms: macropinocytosis, phagocytosis, lipid raft-dependent, and 2) alternative mechanisms: caveolin-/clathrin-dependent or independent endocytosis pathways<sup>124-129</sup>. All these mechanisms are still incompletely understood but everything seems to indicate that both, the particle size and cell type, play a crucial role in determining specific exosomes behaviours. Because of the low size of the caveolae, its endocytosed material tends to be minor than 60 nm, while clathrin-involved mechanisms are able to internalize particles up to 120 nm. This size restriction in terms of uptake may point out functional differences depending on exosome size<sup>128</sup>. Moreover, it is still unknown whether a different mode of exosome uptake by recipient cells results in distinct localization, degradation, and/or functional outcomes of the exosomal constituents.

Previous to internalization, it is essential for the EV to recognize and dock with the cellular membrane. Heparan Sulfate Proteoglycans (HSPG) are plasmatic membrane receptors binding a variety of ligands through their Heparan Sulfate (HS) chains. These receptors participate in many different activities in cells and tissues including ligand-receptor clustering and signalling, endocytosis and trafficking of cytoplasmic vesicles, cytoskeletal dynamics, cell adhesion and motility, basement membrane organization, chemotactic gradient formation, and cell-cell cross talk. Many studies have described HSPGs as "co-endocytosis receptors," which internalize structures by transferring ligands to other receptors or by forming a complex that takes the ligand into the cell. HSPGs can be directly tied to exosomes, facilitating extracellular interactions. It is important to note that the location of HSPG is essential to its impact on exosomes uptake. It has been shown that the treatment of different cancer cell lines with both heparin, a highly-sulfated glucosaminoglycan that mimics heparin sulfate, or with heparinase, an enzyme that specifically acts on HSPG proteins, effectively regulates exosomes uptake, rather than the direct treatment of exosomes<sup>130-132</sup>. HSPGs receptors inhibition do not completely abolish exosomes uptake, indicating it is not the only functioning mechanism involved in this process<sup>128</sup>. Interestingly, very similar mechanisms have been described for virus endocytosis<sup>133,134</sup>, which begins when viral membrane glycoproteins bind to glycoprotein attachment factors, such as HSPGs, on the target cell surface, supporting the hypothesis that this mechanism may be also occurring in EVs, with virus-comparable size.

After the uptake, several studies have proposed that exosomal cargo can be transferred to recipient cells; however, the fate of exosomes and their cargo in recipient cells leftovers incompletely understood. Tracking of fluorescent purified exosomes revealed that exosomes that enter cells through filopodia are transferred to endocytic vesicles and to

the endoplasmic reticulum and then targeted to lysosomes for degradation in fibroblasts. Other studies exhibited how labelled fibroblast-derived exosomes co-localize with mitochondria in BrCa cells. What looks clearer is that exosomes or exosome subpopulations may not be trafficked in the same way in all cell types. Further studies could offer a critical understanding of the fate of exosomes and how this ultimately influences acceptor cell behavior<sup>121,135</sup>.

#### **4.2.4. Exosome biogenesis**

Biogenesis is the main source of differences among vesicle subtypes, while microvesicles and ectosomes bud from the plasma membrane, exosome formation begins on early endosomes (EE). EE formation occurs after the invagination of the plasma membrane and it is followed by the formation of intracellular multivesicular bodies (MVBs) through the invagination of the endosomal membrane and formation of intraluminal vesicles (ILVs)<sup>136,137</sup>, which later will give rise to exosomes. Ultimately, exosomes are released by the fusion of ILVs with the plasma membrane<sup>107,123,138</sup>. The first invagination of the plasma membrane forms a structure that includes cell surface proteins and molecules associated with the extracellular medium (Figure Intro.10). This leads to the *de novo* formation of an early-sorting endosome (ESE). In some cases, it may directly merge with a pre-existing ESE, with material originated from the endoplasmic reticulum (ER), trans-Golgi network (TGN), and mitochondria. ESEs can mature into late sorting endosomes (LSEs) and eventually generate MVBs through the second invagination of the endosomal limiting membrane in the LSEs. It is at that point, when proteins that were originally from the cell surface could be distinctly distributed among the ILVs contained in the MVB, which will give rise to exosomes. Then, the MVB can either fuse with lysosomes or autophagosomes to be degraded or can be fused with the luminal side of the plasma membrane in order to release the contained ILVs as exosomes (Figure Intro. 10)<sup>121,138</sup>. Several proteins are known to be involved in exosome biogenesis, including RAB GTPases, ESCRT proteins, syntenin-1, ALIX, syndecan-1, TSG101, as well as others that are also used as markers for exosomes (tetraspanins, phospholipids, flotillin, SNARE, integrins, and ceramides). Loss- and gain-of-function assays involving RAB and ESCRT proteins have provided evidence about the regulation of exosomes biogenesis, highlighting the crucial role of these proteins in this process, specifically during the formation of ILVs<sup>121,136,139,140</sup>.

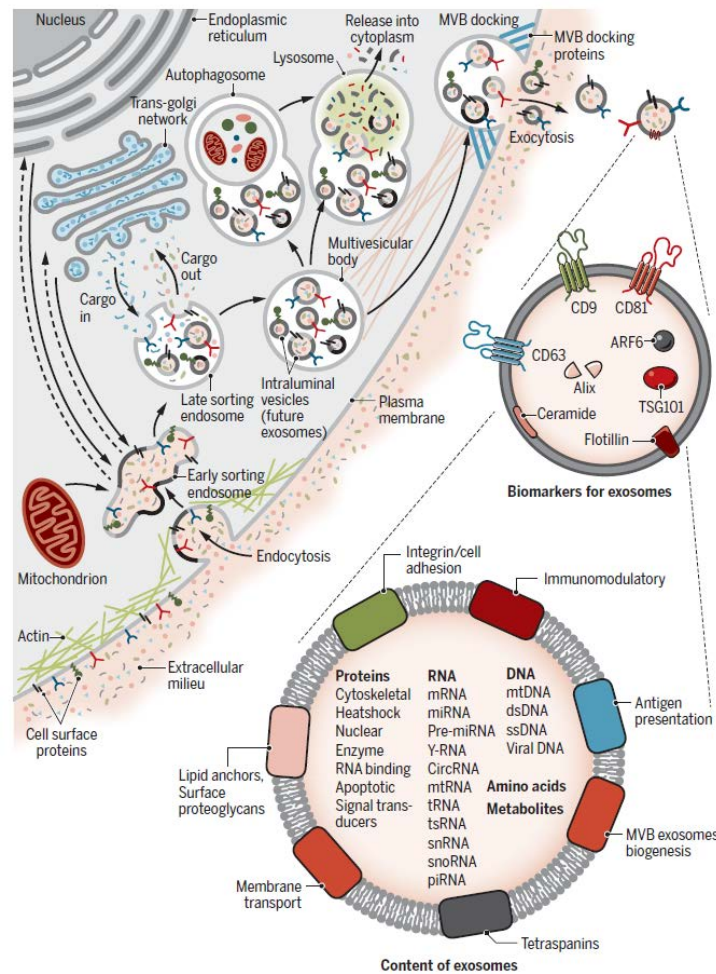


**Figure Intro. 10.** Biogenesis of exosomes. (Adapted from Kalluri *et al.*, 2020<sup>121</sup>)

#### 4.2.5. Exosome heterogeneity

The heterogeneity of exosomes is a reflection of their size, content, functional impact on recipient cells, and cellular origin (Figure Intro. 9). In addition to this, it is lately raising the idea that exosome uptake and secretion pathway as well as exosome biogenesis may be interconnected, resulting in net production of a mixed population composed of both endogenously produced and recycled exosomes (Figure Intro. 11).

Exosomes can directly enter cells by different mechanisms, as explained above (Figure Intro. 11; red) and in parallel, they can also be generated *de novo* by the cells through the endocytic pathway (Figure Intro. 11; blue), meaning exosomes are continuously being generated and taken up by cells. Those that are taken up may get degraded by lysosomes or fuse with pre-existing ESEs, which already contains *de novo* exosomes previously generated. It is more than likely that they can be secreted as a mixture of the *de novo* generated and internalized exosomes (Figure Intro. 11; red and blue), however, it is still unknown if the release of both, endogenously generated or acquired exosomes, occurs at the same time or separately. Computing the rate of exosome production is challenging as a result of the



dynamic of the process, derived from the *de novo* production and uptake of external exosomes by any given cell type<sup>121</sup>.

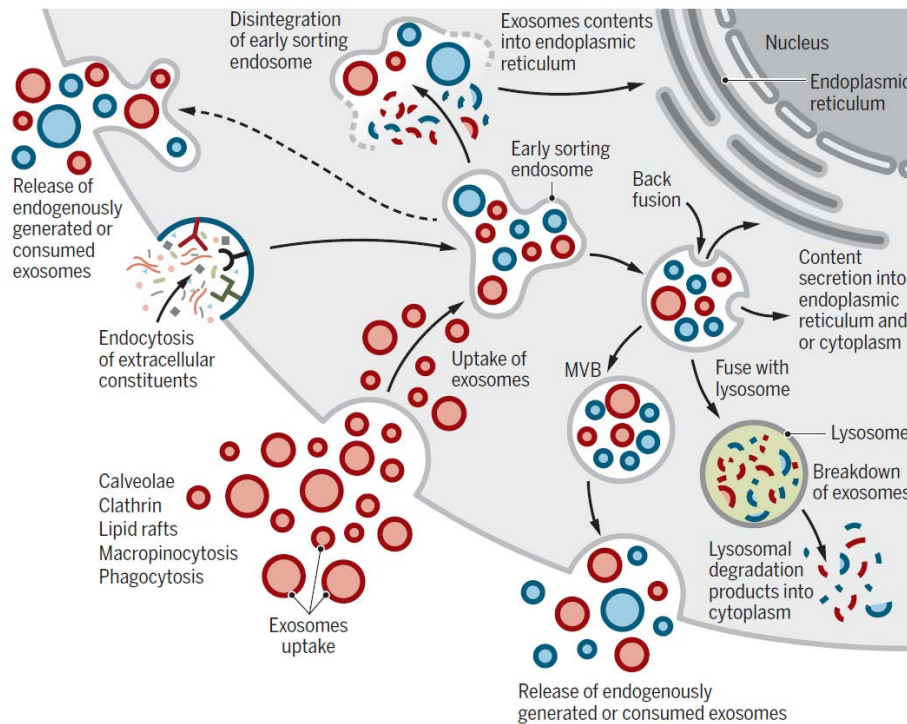


**Figure Intro. 11.** Exosome internalization and biogenesis may be interconnected: Heterogeneity of exosomes. (Adapted from Kalluri *et al.*, 2020<sup>121</sup>)

## 5. Integrins

Integrins, the main cell adhesion receptors for ECM components, constitute a family of transmembrane proteins that form a bidirectional hub transmitting signals between cells and their environment<sup>141</sup>. Until twenty-four different transmembrane heterodimers can be generated, in a stable non-covalent manner, from a combination of  $18\alpha$  and  $8\beta$  integrin subunits within the endoplasmic reticulum, which following post-translational modification in the Golgi apparatus are able to perform their numerous functions. The extracellular domain of these resultant integrins shows a strong affinity for ECM proteins, including fibronectin, vitronectin, collagen, and laminin. After binding to ECM and consequent integrin's clustering, these integrins also trigger signal transduction pathways through their intracellular domain. It results in a cascade activation that regulates a wide variety of processes including cell growth, survival, cell division, and migration. Due to the huge range of mechanisms where integrins are involved with, dysregulated integrin-mediated adhesion and signalling is a precursor in of pathogenesis in many human diseases, including bleeding disorders, cardiovascular diseases and cancer.

## 5.1. Integrin structure and family

Integrins act as heterodimers, consisting of an  $\alpha$  and a  $\beta$  subunit. Each subunit has a large (700-1000 aas)  $\text{NH}_2$ -terminal extracellular domain, a single membrane-spanning domain, and a generally short and unstructured cytoplasmic domain (13-70 aas), as well as flexible linkers between them. Unlike the remarkable homology between the  $\beta$  cytoplasmic tails, with the exception of  $\beta_4$ , there is a huge divergence regarding  $\alpha$  cytoplasmic tails, excepting for a conserved GFFKR motif next to the transmembrane region, a crucial point for association with the  $\beta$  tail<sup>142,143</sup>.

It is important to remark the great specificity of these subunits ( $\alpha$  and  $\beta$ ) in the binding to cytoskeleton and signalling proteins. Specifically, NPxY motif, found in the vast majority of  $\beta$  tails, contains a potentially binding site to a wide variety of cytoskeletal and signalling proteins that contain a PTB-domain. Phosphorylation of tyrosine residues in the NPxY motif may denote a manner of regulation of integrin interaction at the cytoplasmic face what allows the recruitment of proteins that bind cytoskeleton filaments. This way, cytoplasmic tails intercede in the essential integrin-mediator role between ECM and the intracellular space.

There are four different types of integrins categorized according to which cell surface, ECM or inflammatory ligands they bind: 1) laminin receptors, 2) leukocyte-specific receptors, 3) collagen receptors, and 4) RGD receptors, which recognize the sequence Arginine-Glycine-Aspartate (RGD) found in several ECM proteins such as fibronectin, collagen, vitronectin, osteoponin, and thrombospondin (Figure Intro. 12)<sup>144</sup>.

Integrins  $\beta_1$  and  $\alpha_v$  are the major subgroups. The first one can associate with all  $\alpha$  subunits with the exception of  $\alpha_D$ ,  $\alpha_M$ ,  $\alpha_X$ ,  $\alpha_L$ ,  $\alpha_{IIb}$ , and  $\alpha_E$ . In the case of  $\alpha_v$  subunit, it can interact with at least five distinct  $\beta$  subunits including  $\beta_1$ ,  $\beta_3$ ,  $\beta_5$ ,  $\beta_6$  and  $\beta_8$ , whereas the integrin  $\beta_3$  subunit can exclusively form heterodimers with  $\alpha_v$  and  $\alpha_{IIb}$  subunits.

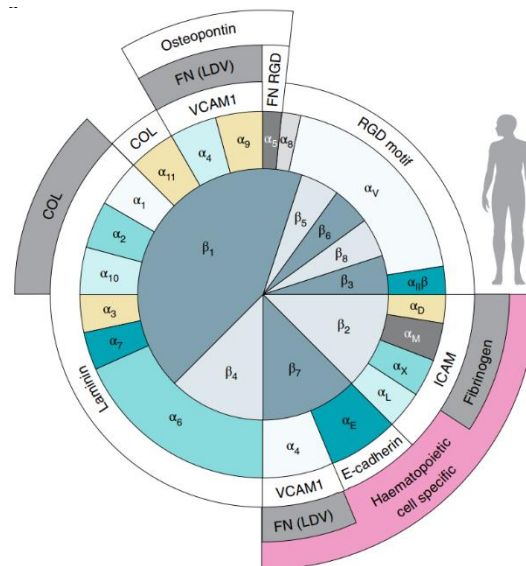


**Figure Intro. 12.** Integrin families. Reported pairing between integrin  $\alpha$ -subunits and  $\beta$ -subunits and the ECM ligand (or ligands) for each heterodimer (Adapted from Paulina Moreno-Layseca *et al.*, 2019<sup>144</sup>)

## 5.2. The role of integrins: multidirectional integrin signalling

A great variety of mechanisms have been reported as regulators of integrin function, including conformational changes, protein-protein interactions and trafficking. Integrin's function mainly depends on two general factors, 1) a gentle balance between active and inactive receptors on the cell surface, and 2) spatiotemporal control of integrin activation. Tight regulation of this last one is key for efficient adhesion and cell motility since it is a highly dynamic process undergoing constant cycles of assembly and disassembly.

Integrins-dependent signalling is characterized by its bi-directionality. Integrins processing includes the switch from inactive or close conformation, presenting low affinity for ECM ligands, to a fully extended or open form, where the integrin is active and capable of promoting downstream signalling and cellular responses following ligand engagement. Through "inside-out" signals, an intracellular signal promotes the binding of proteins such as talin and kindlin to the  $\beta$  tail, what results in the switch of the receptor into an extended conformation with a high affinity for ECM ligands, eliciting the receptor-like role of the integrins. Then, additional junctions between the ECM and integrin, in turn, generates "outside-in" signals that recruit protein complexes, consisting of scaffolding/adaptors molecules, kinases, and phosphatases that regulate cell behaviour. This outside-in signal is heterodimer-dependent and context-dependent, but typically involves recruitment and autophosphorylation of FAK with subsequent recruitment and activation of SRC. Other processes secondly involved are RAS-MAPK and PI3K-AKT signalling pathways (Figure Intro.13), as well as the regulation of small GTPases of the RHO family<sup>145-149</sup>.



On the other hand, spatiotemporal control is related to the trafficking of integrins, the mechanism by which cells regulate integrin-cell surface availability and distribution<sup>148,150</sup>. Integrins both active and inactive forms, are constantly endocytosed from the plasma membrane. Cycles of endocytosis and re-exocytosis (recycling) can control the availability of integrins. Almost all of the surface pools of integrins are cleared within a time period of around 30 minutes. The degradative turnover of integrins is slow (the half-life of surface-labelled integrins is 12-24 hours), and hence the majority of internalized integrins are recycled.

Multiple distinct mechanisms are used by the cells for integrin-endocytosis from the cell surface, including micropinocytosis, clathrin-dependent and clathrin-independent routes. In all cases, integrins are transmitted to early endosomes. EEs are key organelles for the targeting of integrins to different recycling or degradation pathways, which is extremely dependent on the integrin heterodimer and cell type, as well as on the stimuli and the ECM composition. Independently of the route used by the cell, there are some common actors in both pathways that are able to act as regulators; including RAB and ARF family of small GTPases, implicated in each step of this process, FAK, Disabled-2 (DAB-2), Adaptor-complex 2 (AP2) and the GTPase Dynamin (DYN), involved in vesicle scission<sup>151,152</sup>. These last ones have been suggested to be related to endocytosis of ligand-bound active integrins during focal adhesion (FA) assembly and disassembly, crucial steps in integrin endocytosis.

There is clear evidence that efficient kinetic, in terms of integrin trafficking, result crucial for the cell. This is way, kinetics regulation is known to be commonly altered in cancer, resulting in changes in the usual cell surface/endosomal pool ratios of the receptor. Furthermore, endocytosed integrins are not only important in terms of kinetics, they are also able to transmit intracytoplasmic “inside-in” signals either using the endosomes as a platform for integrin-mediated signalling<sup>153,154</sup> or by enhancing the signalling of co-traffic growth factor receptors<sup>148,155</sup>.

Regarding FAK signalling, regulation depending on integrins is not only secondary to their recruitment to FA areas after integrin-clustering (outside-in) (Figure Intro.13). There is a subtle regulation network of FAK signalling secondary to integrin trafficking. Alanko, J *et al.*<sup>153</sup> showed that integrin-containing endosomes have the capacity to recruit and activate FAK on endomembranes<sup>153</sup>. This mechanism is a clear example of the functionality of integrins in subcellular locations other than plasma membrane adhesion sites. Another interesting point is how integrin endocytosis can be fine-tweaked by extracellular-initiated signals, mechanism sustained by the presence of extracellular molecules in endocytic vesicles together with the endocytosed integrin, confirming co-

endocytosis. A clear example of this phenomenon has been described in fibroblasts; the binding of syndecan-4 to ECM molecule fibronectin triggers a signalling cascade that results in integrin endocytosis mediated by caveolin and DYN<sup>156</sup>. Thus, interactions and signals at the cell surface can be vital for triggering integrin endocytosis.

In summary, integrins's activity extremely depends on the recruitment of proteins to both cytoplasmic tails (inside-out) and extracellular domains (outside-in), to regulate their ligand binding affinity and establish a connection to the actin cytoskeleton, initiating intracellular signalling and even regulating their intracellular trafficking. Moreover, active integrins and integrin-dependent signalling complexes, alongside with ECM ligands, membrane receptors or kinase proteins found within endosomes, can trigger “inside-in” signalling, which is strongly dependent on integrin endocytosis (Figure Intro. 13)<sup>145</sup>.

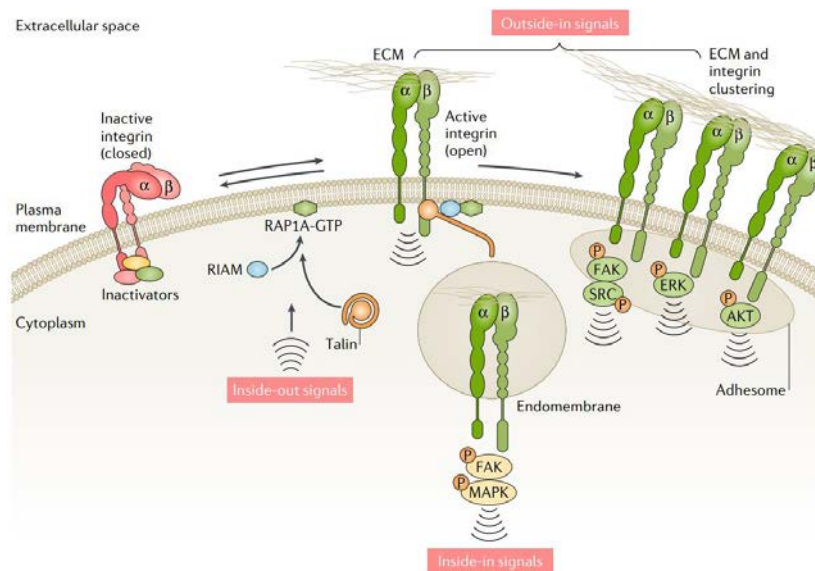


**Figure Intro. 13.** Multidirectional integrin signaling. (Adapted from Hellyeh Hamidi *et al.*, 2018<sup>145</sup>)

From a phenotypic point of view, all these mechanisms are translated in plenty of integrin-related processes. Much of the literature has associated this family to several mechanisms such as migration, invasion, cell survival, and adhesion. It is important to note that many other processes have been also associated with integrins, including viruses entrance, stemness, and epithelial plasticity.

Integrins play a crucial role in cell biology by directly promoting proliferation or indirectly, by interacting with growth factor receptors. Due to their ability to interact with the ECM, integrins can either enhance cell survival or initiate apoptosis. In a cell in which most of the integrins are ligated with their ligands, a pro-survival pathway is maintained<sup>157-160</sup>. Moreover, integrins have a clear role in motility as a mediator of the stability between adhesion molecules and cytoskeleton. It is very likely indeed that deregulation of migration can lead to the development of pathologies such as cancer, specifically, metastatic cancer.

Migrating cells are characterized by a polarized morphology. At the cell front, a structure called lamellipodium containing an actin network is related to stationary focal complexes, while at the rear, F-actin stress fibres are connected with inward sliding focal contacts. During migration, integrins are essentially stabilizing the lamellipodium through the building of a bridge between the actin cytoskeleton and the ECM or neighbouring cells. By anchoring the actin cytoskeleton to the ECM in cell-matrix adhesions, integrins are also required for the generation of propulsive forces. It is important to note that different integrins stimulate distinct ways of motility and cells may alter their motile behaviour by expressing different isoforms.

In summary, actin polymerization in the direction of the attractant at the leading edge pushes the cell membrane forward and free integrins at the cell surface form new contacts with proteins in the matrix. On the other side, rear, old contacts with the ECM are broken, integrins are internalized and trafficked to the sites where new contacts with the matrix are formed, and actin is retracted towards the leading edge.

Although the classical integrin functions are related to cell survival, cell migration, and cell adhesion, in the last times, it has been shown the contribution of integrins to several and striking mechanisms. Up to 20 different viruses, as well as other pathogens, have been found to use integrins as a cellular receptor. As it has been explained above, integrins can be internalized through several mechanisms, making this fact an interesting strategy for viruses entrance into the cell following the same routes than those described for integrin trafficking<sup>133,134</sup>. Another example of a non-classical integrin function is the role in stemness. Recent studies have revealed that integrin signalling drives multiple stem cell functions, including tumour initiation and epithelial plasticity<sup>149</sup>. Integrins have been proposed as markers of both normal progenitor and stem cell populations as well as markers of cancer stem cells.

### **5.3. Integrins and cancer**

An extensive variety of integrins contribute to tumour progression, but because of integrin regulation, ECM composition, concomitant signalling from growth factor receptors, and pleiotropic functions together with their contribution to cancer may differ across different cancer types, stages and treatment, it is significantly complicated to associate a specific cancer-related phenotype to a given integrin. Despite the above, some crucial factors influencing cancer progression has been recognized in particular metastasis.

Each cell type displays a specific range of integrins and this range changes according to the cellular or environmental input. In cancer, changes in the components of the ECM, in

response to growth factors or due to intracellular alterations such as activation of oncogenes, impact in this integrin's variety (Table Intro. 2). Moreover, several studies have suggested that integrins on tumour cells are not only altered quantitatively but qualitatively, by changes at phosphorylation and/or glycosylation level, what disturbs the properties of the cytoskeletal and extracellular ligand-binding capabilities. The contribution of these alterations may influence both transformation and tumour progression.

**Table Intro. 2** Integrin expression in metastatic tumour cells compared to primary tumour cells.

Cancer Type	$\alpha 1\beta 1$	$\alpha 2\beta 1$	$\alpha 3\beta 1$	$\alpha 6\beta 1$	$\alpha 5\beta 1$	$\alpha V\beta 3$	$\alpha 4\beta 1$
<b>Breast</b>	Up	Down			Up	Up	
<b>Skin</b>		Up	Up	Up		Down	
<b>Ovary</b>						Up	Up
<b>Colon</b>		Down			Up	Up	
<b>Kidney</b>							
<b>Lung</b>		Down			Up		
<b>Melanoma</b>	Up	Up		Up	Up	Up	
<b>Prostate</b>						Up	
<b>Pancreatic</b>						Up	
<b>Cervical</b>						Up	
<b>Glioblastoma</b>						Up	

Adapted table from Antti Arjonen. (2013). Integrins on the move (Doctoral Thesis). University of Turku. Turku, Finland<sup>161</sup>.

An additional level of regulation is related to the ratio of the receptors between the cell surface and endosomal pools. Cancer cells frequently present altered integrin endocytosis and recycling back to the plasma membrane. Recent studies have shed new light on the controversial ligation-dependent effects. There are evidence about how un-ligated integrins can positively or negatively influence tumour cell survival, thereby affecting tumour growth and metastasis<sup>162</sup>. The establishment of more defined mechanisms by which integrins affect tumour cell survival both in the ligated and un-ligated states could be a crucial determinant of the efficacy of integrin antagonists in cancer.

Integrins role in cancer does not finish in tumour cells themselves; they are also relevant on the surface of tumour-associated host cells. The tumour microenvironment is full of several host cell types, including endothelial cells, perivascular cells, fibroblasts, and inflammatory cells, contributing to tumour progression by modulating angiogenesis, lymphangiogenesis, desmoplasia, and inflammation. In line with this, and probably contributing to communication among all of these cell types, it has been demonstrated the role of integrins in cell-to-cell communication, not only acting as a co-receptor for growth factors or oncogenes but also as an important player for EVs biology. Specifically, integrins present in EVs have a functional role in priming the metastatic niche<sup>109,110</sup>. EVs released by cancer cells may support metastasis by contributing to the development of organ-specific

(pre)-metastatic niches through their capacity to transfer metabolites, proteins, and RNA to distant tissues. Extraordinarily, enrichment of integrins on the surface of cancer-derived EVs contributes to organ-specific targeting<sup>163</sup>. For example,  $\alpha 6 \beta 1$  and  $\alpha 6 \beta 4$  present in EVs surface secreted by cancer cells, have the ability to promote the cell tumour homing in the lung, while  $\alpha \nu \beta 5$  integrin-EVs, home preferentially to the liver<sup>108,110,163</sup>. Once there, EVs contribute to the creation of a pre-metastatic niche by inducing the expression of specific ECM proteins and pro-inflammatory factors, which allow the recruitment of inflammatory cells.

In summary, integrins show an extraordinary biological role in the link of cells to counter-receptors on other cells and ligands in the ECM, what leads to changes in tumour cell behaviour and microenvironment status by the triggering of a variety of signal transduction pathways<sup>164</sup>. Integrin activation can also regulate ECM assembly and the polarity of migrating cells, in that way interceding tumour metastasis and non-tumour cell infiltration<sup>165</sup>. In consequence, microenvironmental influences on cell behaviour might be determined by the pattern of integrin expression on the cell surface<sup>80</sup>. Thus, integrins could be interpreted as the hub family of proteins that connects tumour cells and their surrounding microenvironment<sup>164</sup>.

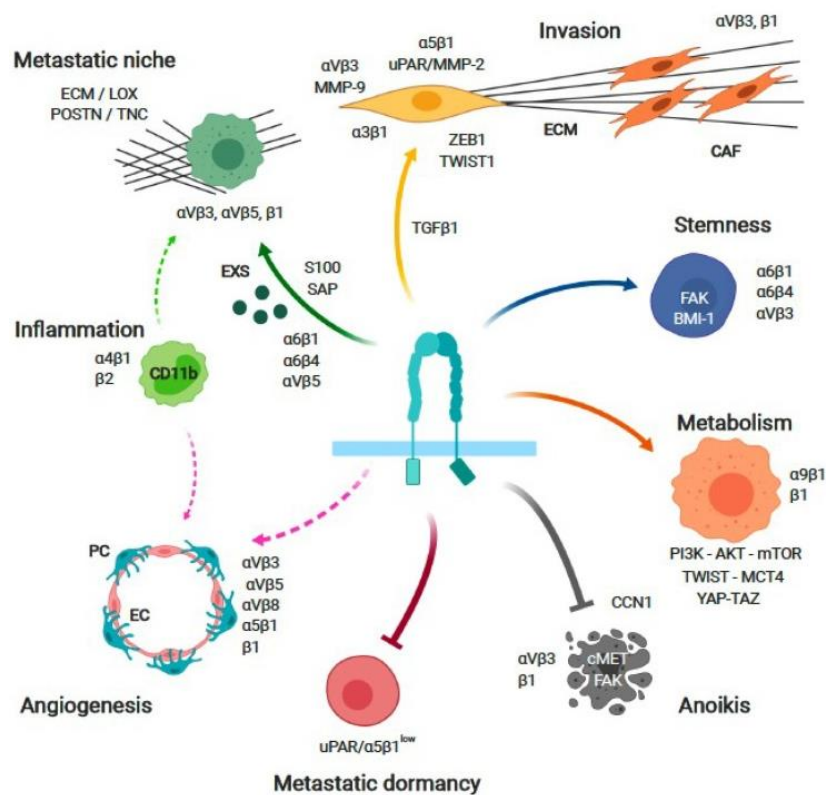


**Figure Intro. 14.** Integrin-dependent functions relevant to cancer. (Adapted from Begoña Alday-Parejo *et al.*, 2019<sup>163</sup>)

A great variety of integrins contribute to tumour progression. In one hand, those integrins usually expressed by epithelial cells, the main source of many solid tumours, which includes  $\alpha6\beta4$ ,  $\alpha6\beta1$ ,  $\alpha\nu\beta5$ ,  $\alpha2\beta1$  and  $\alpha3\beta1$ ; on the other hand, those integrins typically expressed at low or undetectable levels in most adult epithelia but that have been observed to be highly altered in some tumours, including  $\alpha\nu\beta3$ ,  $\alpha5\beta1$ , and  $\alpha\nu\beta6$ <sup>162</sup>. There is an abundant collection of literature supporting these integrin expression pattern alterations in a wide range of cancer types (Table Intro. 3).

**Table Intro. 3.** Integrins in cancer progression.

Tumour type	Integrins expressed	Associated phenotypes
<b>Melanoma</b>	$\alpha\nu\beta3$ and $\alpha5\beta1$	Vertical growth phase and lymph node metastasis
<b>Breast</b>	$\alpha6\beta4$ , $\alpha\nu\beta3$ , $\alpha\nu\beta5$ and $\alpha\nu\beta6$	Increased tumour size and grade, and decreased survival ( $\alpha6\beta4$ ). Increased bone metastasis ( $\alpha\nu\beta3$ ) and increased invasiveness of breast cancer cells ( $\alpha\nu\beta5$ ). Associated with very poor survival and increased metastases to distant sites ( $\alpha\nu\beta6$ )
<b>Prostate</b>	$\alpha\nu\beta3$ and $\alpha\nu\beta5$	Increased bone metastasis ( $\alpha\nu\beta3$ ) and correlated significantly with the Gleason pattern ( $\alpha\nu\beta5$ )
<b>Pancreatic</b>	$\alpha\nu\beta3$	Lymph node metastasis
<b>Ovarian</b>	$\alpha4\beta1$ and $\alpha\nu\beta3$	Increased peritoneal metastasis ( $\alpha4\beta1$ ) and tumour proliferation ( $\alpha\nu\beta3$ )
<b>Cervical</b>	$\alpha\nu\beta3$ and $\alpha\nu\beta6$	Decreased patient survival
<b>Glioblastoma</b>	$\alpha\nu\beta3$ and $\alpha\nu\beta5$	Expressed at the tumour-normal tissue margin. Possible role in invasion. Associated with a poor prognosis/decreased survival
<b>Non-small-cell lung carcinoma</b>	$\alpha5\beta1$	Decreased survival in patients with lymph node-negative tumours
<b>HNSCC</b>	$\alpha\nu\beta5$	Lymphatic metastasis and angiogenesis
<b>Colon</b>	$\alpha\nu\beta6$ and $\alpha\nu\beta3$	Reduced patient survival. Significantly associated with T stage and TNM stage ( $\alpha\nu\beta6$ ) and correlated with poor differentiation and lymph node invasion ( $\alpha\nu\beta3$ )

Adapted table from Jay S. Desgrosellier *et al.*, 2010<sup>166</sup> and H.T.A and Ahmedah (2015). Correlation between the expression of integrins and their role in cancer progression (Doctoral Thesis). Bradford, West Yorkshire, England. University of Bradford, England<sup>167</sup>.

#### 5.4. ITGB3

Integrin Beta 3, also known as CD61, GP3A or GPIIIa, is a protein that in humans is encoded by the ITGB3 gene, localizes on chromosome 17 (GRCh38:17:47253827:47313743:1), and is one of the most broadly studied members of the integrin family. It contains 15 exons and spans 59.89 kb (Figure Intro. 15). Three isoforms produced by alternative splicing have been described and two more potential isoforms have been computationally mapped. Isoform beta-3A (P05106-1), isoform beta-3B (P05106-2) and isoform beta-3C (P05106-3) are tissue-specific, being isoform beta-3A expressed in osteoblast cells, and isoform beta-3C in prostate and testis. The beta-3A isoform is the canonical sequence. After mRNA processing and translation, the integrin undergoes a series of O- and N-glycosylations and post-translational modifications in the endoplasmic

reticulum and the Golgi apparatus. The primary structure of Integrin Beta 3 consists of a sequence of 788 amino acids and has a molecular weight of 87.058 KDa. For the secondary structure, about 13% of the chains are in the form of alpha helix and 29% in the beta lamina form. Another smaller part of the sequence (about 8%) is occupied by turns that change the direction within the sheets. The rest of the polypeptide chain corresponds to intrinsically disordered regions, which are very common in signalling proteins, such as integrins. Given that Integrin Beta 3 is a transmembrane protein, three parts can be distinguished: extracellular (the largest by far, consisting of about 692 amino acids), transmembrane (23 amino acids) and cytoplasmic (47 amino acids). Transmembrane amino acids share the characteristic of hydrophobicity, which is essential to cross the membrane. Thus, it can be seen that valines, leucines, isoleucines, glycines and alanines predominate. In the extracellular part different regions and domains responsible for Integrin Beta 3 functionality can be distinguished<sup>143,168-170</sup>.

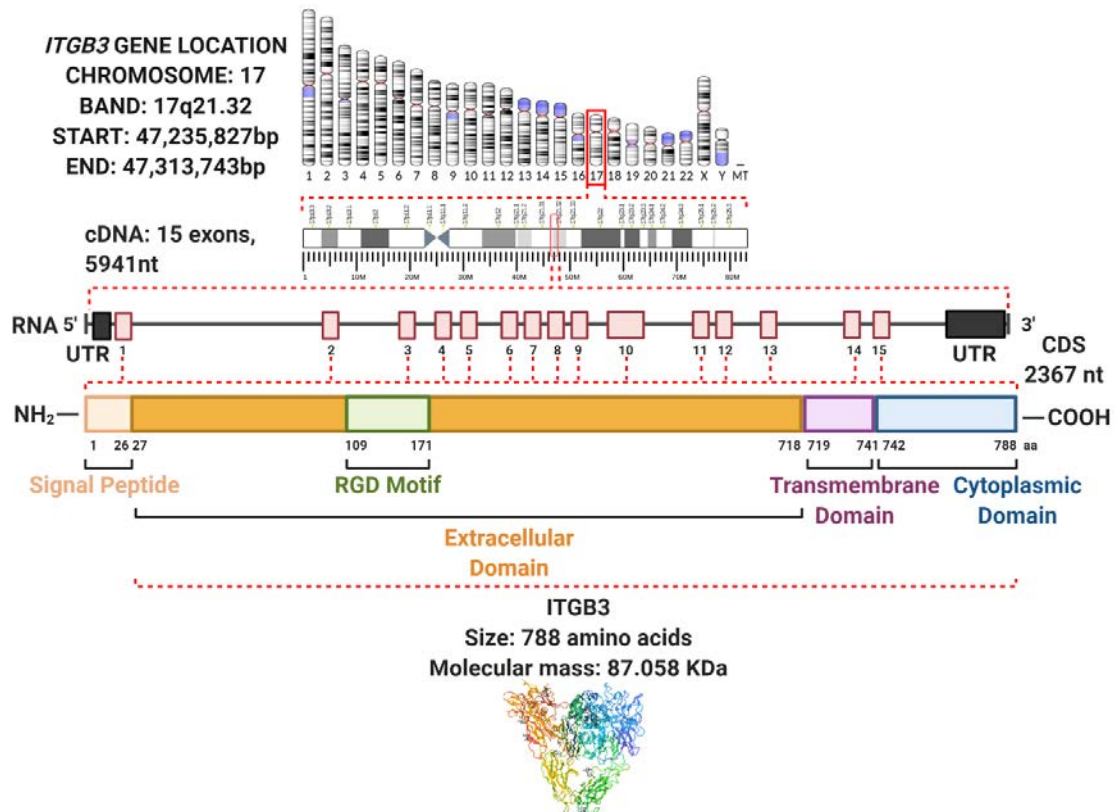


**Figure Intro. 15.** Integrin Beta 3 gene location, transcript and protein structure, based on the version GRCh38.p13 of the Human genome.

As an heterodimer, ITGB3 is constituted by two main forms,  $\alpha$ IIb $\beta$ 3 and  $\alpha$ v $\beta$ 3, both of which can selectively discriminate ligands containing an RGD tripeptide active site, like vitronectin and fibronectin<sup>142,164</sup>.  $\alpha$ IIb $\beta$ 3 integrin is highly expressed in platelets, where it is associated with the pathogenesis of Glanzmann thrombasthenia<sup>171</sup> and its role in platelet tumorigenesis has been suggested<sup>164,172,173</sup>. Besides, although  $\alpha$ v $\beta$ 3 integrin is expressed at low levels on resting epithelial cells,  $\alpha$ v $\beta$ 3 overexpression has been observed in angiogenic



endothelial cells, as well as tumour cells, promoting invasion and migration in numerous malignant tumours<sup>174-178</sup>. Furthermore, ITGB3 is considered a robust prognostic factor concerning poor survival in non-small cell lung cancer, BrCa, cervical cancer, pancreatic ductal adenocarcinomas, T-cell acute lymphoblastic leukaemia and gliomas<sup>164,179-182</sup>.

$\alpha\beta3$ , together with  $\alpha\beta5$ , is probably the most prominent integrin involved in tumorigenesis. This is supported by a great variety of mechanisms that  $\alpha\beta3$  is somehow involved with. It has diverse central roles in malignant tumour progression and the reprogramming of the tumour microenvironment, which is reflected in the alteration of several biological processes such as metabolic reprogramming<sup>183,184</sup>, EMT<sup>185</sup>, endothelial to mesenchymal transition (EMT)<sup>186</sup>, stemness regulation, drug-resistant acquisition<sup>187,188</sup>, angiogenesis<sup>189,190</sup>, and stromal and immune microenvironment re-education<sup>164,191-195</sup>.

In ovarian cancer, it has been shown that together with  $\alpha\beta1$ ,  $\alpha\beta3$  enhances proliferation via ILK and blockage of  $\alpha\upsilon$  was observed to be sufficient to arrest cell cycle<sup>196</sup>. This regulation of cell proliferation has been supported *in vitro*, where TGF- $\beta$ 1 increased levels of  $\alpha\beta3$ , as well as FGFR (Fibroblast Growth Factor Receptor) under expression of  $\beta3$  subunit context<sup>185</sup>. In BrCa cells,  $\beta3$  integrin, together with SRC, facilitates TGF- $\beta$  mediated induction of EMT<sup>197</sup>. As in this context  $\alpha\beta3$  expression depends on TGF- $\beta$  induction, its expression was shown to be sufficient and necessary to activate SLUG, a well-known EMT-inductor<sup>198</sup>.

A similar example of crosstalk between  $\alpha\beta3$  and oncogenes has also been described in vascular endothelial cells. Recruitment of SRC by VEGFR2 triggers  $\alpha\beta3$ -SRC crosstalk resulting in conformational changes and phosphorylation modifications that promote an increase of  $\beta3$ -VEGFR2 complex formation<sup>162</sup>. SRC kinase phosphorylates two tyrosine residues in the cytoplasmic domain of  $\beta3$  integrin (Y747 and Y759) which are necessary for the interaction between the two receptors,  $\beta3$  integrin and VEGFR2<sup>199</sup>. This may be the explanation for the increased levels of VEGFR2 in ITGB3-/- mice that leads to an increase in angiogenesis. Another scenario where ITGB3 is influenced by VEGF results from a feedback loop where VEGF regulates the activation state of the integrin and on the other way around, activation of ITGB3 can increase tumour cell secretion of VEGF, resulting in increased tumour growth<sup>162,200</sup>.

Recent studies have linked anchorage-independent tumour cell survival *in vitro* and metastasis *in vivo* to the  $\alpha\beta3$ -dependent resistance to integrin-mediated death. To note, although in non-anchored cells, clustering of most integrins on the plasma membrane with the ECM is lost, un-ligated  $\alpha\beta3$  is still able to work as a signal-transmitter, due to its unique



ability to maintain receptor clustering<sup>201</sup>. Un-ligated  $\alpha v\beta 3$ , through recruitment and activation of SRC, provokes a switch to a FAK-independent survival pathway to confer anoikis resistance to cancer cells<sup>201</sup>. Another described anchorage-independent clustering depending on  $\alpha v\beta 3$  is mediated by galectin 3 and gives rise to membrane-proximal KRAS clustering, allowing numerous oncogenic functions of activated KRAS<sup>145</sup>.

In the case of ITGB3 regulation by endocytosis, several studies have related its trafficking with tumorigenesis. RAB34, a small GTPase that it is overexpressed in aggressive BrCa, can bind to the cytoplasmic tail of ITGB3, regulating its trafficking in a SRC-dependent manner. EGF stimulation recruits RAB34 to the plasma membrane and promotes its SRC-mediated tyrosine-phosphorylation, which induces  $\beta 3$ -integrin internalization and delivery to recycling compartments. This process protects  $\beta 3$ -integrin from degradation and stimulates cancer cell migration and invasion.<sup>202</sup>.

Another example of the role of  $\beta 3$ -trafficking in tumorigenesis is in cooperation with syndecan-4. The tyrosine phosphorylation status of syndecan-4, which depends on SRC, can be switched, monitoring differential recycling of  $\alpha v\beta 3$ - and  $\alpha 5\beta 1$ -integrins. This results in a fine-tuned balanced availability of these two receptors at the plasma membrane that determines FA half-life and cell migration behaviour. Non-phosphorylatable syndecan-4 mutants stimulate recycling of  $\alpha 5\beta 1$ , as well as  $\alpha v\beta 3$  recycling suppression, leading to a fast adhesion turnover and as a consequence, reduced cell migration<sup>203,204</sup>. It has been also demonstrated that after treatment with platelet-derived growth factor (PDGF),  $\alpha v\beta 3$  is trafficked via short-loop recycling to the cell surface in a RAB4-dependent manner what promotes the formation of new adhesions at the leading edge. This mechanism needs direct interaction between integrin  $\alpha v\beta 3$  and PKC-related kinase (PKD1). Recycling through this route stimulates the creation of  $\alpha v\beta 3$ -integrin-containing cell-matrix adhesions at the leading edge to maintain directionally persistent migration of fibroblasts and cancer cells<sup>205-207</sup>.

Another unexpected process, within tumorigenesis, in which ITGB3 has been involved in recent times, is cancer cells stemness. Mammary progenitor cell populations have been shown to express high levels of CD61 (ITGB3), which is only marginally expressed in normal mammary epithelia. Employing three different mouse models of mammary tumorigenesis, they found that in two of them (MMTV-Wnt-1 and p53<sup>+/-</sup>), CD61<sup>+</sup> recognized a subpopulation that was highly enriched for tumorigenic capability relative to the CD61<sup>-</sup> subgroup<sup>63</sup>. Their data provide additional evidence that breast cancers can develop according to a CSC model of mammary tumorigenesis and highlight the importance of the progenitor marker CD61 in defining a cellular hierarchy within some tumours.

Furthermore, there are several *in vivo* studies that support the implication of ITGB3 in cancer progression, especially in metastasis. These studies show both, promotion of bone metastasis through overexpression of  $\alpha\beta3$ , and inhibition of metastasis upon  $\alpha\beta3$  knockdown<sup>208</sup>. Additional studies using a constitutively activated mutant of  $\alpha\beta3$  ( $\alpha\beta3^{D723R}$ ) showed an increase in lung metastatic activity compared with cells expressing  $\alpha\beta3^{WT}$  or  $\alpha\beta3$  knockdown<sup>209</sup>. In the same manner, it was demonstrated that MYC blocks BrCa metastasis to the lung by suppressing transcriptional  $\alpha\beta3$  expression. This phenotype was rescued by exogenous expression of  $\beta3$  integrin in those cells that did not express it<sup>210</sup>. Finally, Parvani *et al.*<sup>211</sup> showed that TGF- $\beta$ -pre-stimulated MDA.MB.231 mouse tumours treated intravenously with si $\beta3$ -nanoparticles (nanoparticles containing integrin  $\beta3$  siRNA) did not present metastasis and did not show relapse after primary tumour resection neither 4 weeks after release from the treatment, in comparison to untreated mice<sup>211</sup>.

Collectively, there is widespread evidence that ITGB3 is able to regulate cell behaviour in a variety of cell types and it is involved in tumorigenic processes. Understanding the multiple roles of ITGB3 will help us to understand the biology behind tumour progression and to develop strategies considering ITGB3 as a potential target for the treatment of cancer, likely in combination with conventional cytotoxic therapies.



## **HYPOTHESIS AND OBJECTIVES**



The overall aim of this thesis was to identify novel factors conferring resistance to cellular stress in breast cancer. Hypoxic stress confers malignancy, aggressiveness and metastasis features acquisition in cancer cells. A lot has been characterized about transcriptional changes occurring in cancer cells submitted to hypoxia, however, less is known about protein synthesis activation in a microenvironment where mRNA translation is heavily downregulated. Therefore, a screening designed to discover novel factors actively translated in oxygen-depleted conditions could reveal factors responsible for the hypoxic stress resistance that may facilitate malignancy and metastasis in breast cancer. An exhaustive study of the function and mechanisms of action of identified factors in the screen would allow us to define new promising targetable proteins.

After having carried out the RNA-Seq screening for translationally activated proteins in hypoxia plus mTOR inhibition, the candidate ITGB3 protein has been subjected to further analysis. Therefore, the objectives of this doctoral thesis have been divided into two main chapters as follows:

Chapter I:

I.1-To identify and characterize new proteins upregulated at the translational level (protein synthesis) in low oxygen conditions, through setting up an RNA-Seq screening to determine factors present in polysomes after hypoxic stress and mTOR inhibition.

I.2- To establish translationally activated candidate mRNAs under hypoxia and hypoxia plus mTOR inhibition through a bioinformatics analysis. The altered factors will be analysed through RT-PCR and WB to validate the screening.

I.3-To study the differential protein expression response to hypoxic stress in tumour cells versus non-tumour cells.

I.4-To elucidate the potential mechanism of action of one of the identified candidates, ITGB3, through the analysis of its role in malignant phenotypes such as survival, migration, growth rate in spheroids and mammospheres capacity formation.

I.5-To categorize the translational machinery behind ITGB3 protein synthesis.

I.6- *In vitro* and *in vivo* functional validation of the newly identified factors in the progression of breast cancer.

The formation of metastasis requires complex interactions; 1) between cancer cell subpopulations, 2) between cancer cells and non-malignant cells surrounding the primary tumour and 3) between cancer cells and the tissue where metastasis is formed. During the

last years, tumour-derived extracellular vesicles have been described as one of the key factors orchestrating this interplay in intercellular communication. Also, some specific integrins contribute particularly to metastasis by developing a role in this mechanism.

Because integrins are crucial for the role of extracellular vesicles in cancer progression and particularly in metastasis, together with our previous findings that ITGB3 is required for lung metastasis in MDA.MB.231 cells, we pretended to delineate the role of ITGB3 in extracellular vesicles-mediated intercellular communication in breast cancer cell lines.

This was achieved through the following objectives:

In Chapter II:

II.1- To study the role of ITGB3 in the homing step of lung metastasis. Both, control and shITGB3 cells, fluorescently labelled, will be injected into the tail of the mouse and the next day the fluorescence intensity in the lungs of the mice will be analysed by Flow Cytometer.

II.2- To study the role of ITGB3 in intercellular communication by analysing the growth capacity of cells with ITGB3 inhibited versus control cells. For this, previously conditioned medium from both control and shITGB3 cells will be used and compared with cells without the conditioned medium.

II.3- To elucidate the role of extracellular vesicles in intracellular communication through the study of cell growth capacity using conditioned medium previously depleted of extracellular vesicles.

II.4- To analyse the mechanism involved in the uptake of extracellular vesicles in cells. Control cells and shITGB3 will be treated with fluorescently-labelled vesicles and then, using Flow Cytometer, the intensity of fluorescence in the acceptor cells will be analysed. Also, known proteins involved in different types of uptake will be inhibited to know the exact mechanism as well as the involved players.

II.5- To characterize the secretome of the extracellular vesicles of both control cells and cells with ITGB3 inhibited. The vesicles will be characterized by Nanosight and cryo-electron microscopy and their proteome will be determined by LC-MS/MS and Western blot.

## **RESULTS**





## **Summary**

The results section is divided into two different chapters. Chapter I contains the paper I and some unpublished data. We performed a polysomal RNA-Seq screen in non-malignant breast epithelial (MCF10A) and TNBC (MDA.MB.231) cells exposed to normoxic or hypoxic conditions and/or treated with an mTOR pathway inhibitor. Analysis of both the transcriptome and the translome identified mRNA transcripts translationally activated or repressed by hypoxia in an mTOR-dependent or -independent manner. Integrin Beta 3 (ITGB3) was translationally activated in hypoxia and its knockdown increased apoptosis and reduced survival, spheroid growth, mammosphere formation and migration, particularly under hypoxic conditions. Moreover, ITGB3 was required for sustained TGF- $\beta$  pathway activation and the induction of Snail and associated epithelial-mesenchymal transition markers. ITGB3 downregulation significantly reduced lung metastasis and improved overall survival in mice. Collectively, these data suggested that ITGB3 was translationally activated in hypoxia and regulated malignant features, including epithelial-mesenchymal transition and cell migration, through the TGF- $\beta$  pathway, revealing a novel angle for the treatment of therapy-resistant hypoxic tumours.

In the follow-up Paper II, and after having been previously described that ITGB3 plays an important role in BrCa metastasis, we have uncovered essential and far unknown roles of ITGB3 in vesicle uptake. The functional requirement for ITGB3 derives from its interactions with HSPGs and the process of integrin recycling, allowing the capture of extracellular vesicles and their endocytosis-mediated internalization. Key for the function of ITGB3 is the interaction and activation of FAK, which is required for endocytosis of these vesicles. Thus, ITGB3 has a central role in intracellular communication via extracellular vesicles, proposed to be critical for cancer metastasis.

Altogether, these studies further demonstrate the important role of ITGB3 in adaptive mechanisms to tumour microenvironment and stress at different levels and pave the way for the evaluation of novel, potential therapeutic strategies.



## **CHAPTER 1**



## Manuscript

Sesé M\*, **Fuentes P\***, Esteve-Codina A, Béjar E, McGrail K, Thomas G, Aasen T, Ramón y Cajal S. Hypoxia-mediated translational activation of ITGB3 in breast cancer cells enhances TGF- $\beta$  signalling and malignant features *in vitro* and *in vivo*. *Oncotarget*. 2017; 8:114856-114876.

\*These authors contributed equally to this work

## Summary

**Introduction:** Breast cancer is the most prevalent malignancy in women and new therapeutic approaches are needed. Control of protein synthesis plays an essential role in cell growth and is particularly implicated in tumour progression, resistance to therapy and cellular stress. In particular, hypoxic cancer cells attain invasive and metastatic properties, as well as chemotherapy resistance, which together constitutes the lethal cancer phenotype; but the regulation and role of protein synthesis in this setting is poorly understood. In this study, we have utilized polysome profiling to separate and quantify mRNAs bound to ribosomes, the ones that are actively translating, by a sucrose gradient fractionation.

**Objectives:** Identify new factors that confer resistance to cellular stress that can be inhibited and become possible therapeutic targets. To face that, we characterized new factors that confer resistance to hypoxic stress and mTORC1 / 2 inhibition, after performing *in vitro* screening through RNA-Seq for translationally active mRNAs (bound to polysomes) in both, non-malignant (MCF10A) and tumorigenic (MDA.MB.231) cells. Finally, phenotypes of malignancy will be assessed *in vitro* and *in vivo* for loss/gain of function of identified factors.

**Methodology:** Both, non-malignant breast epithelial cells (MCF10A) and breast cancer cells (MDA.MB.231) were exposed to hypoxic conditions (0.5 % O<sub>2</sub> for 24h) and treated with or without an inhibitor of cap-dependent translation (2.5mM of PP242 for 3h). We performed RNA-Seq polysomal profiling to compare the levels of total and polysomal (actively translating) mRNA. Polysomal mRNA was obtained by 10-50% sucrose gradient sedimentation. Then, mRNA populations of each sample were converted to cDNA libraries using the TruSeq protocol and then sequenced using a HiSeq 2000 machine. Paired-end reads were mapped against the reference human genome (GRCh38) with STAR v2.5.1b (ENCODE parameters for long RNA) and GENCODE v24 annotation. Gene quantification was performed using RSEM v1.2.28 with default parameters. Only protein-coding genes were kept for the analysis. Normalization of the count matrix was done with the TMM method of the edgeR package.

Translationally activated candidate targets such as ITGB3 with a translational efficiency (Te) >1.5 were selected and tested by siRNA- and shRNA-mediated knockdown in MDA.MB.231 and MCF10A cells followed by the analysis of expression by WB, proliferation, survival, migration, apoptosis in the presence or absence of hypoxia, mammospheres and spheroid formation, as well as the study of the molecular mechanism behind. MDA.MB.231 cells with knockdown of ITGB3 were used in the study of lung metastasis *in vivo*.

**Results:** Through an RNA-Seq polysome profiling under hypoxic conditions, we have identified the Integrin Beta 3 translationally activated. After further phenotypic studies, we show that Integrin Beta 3 is activated at protein synthesis level in hypoxia and hypoxia + mTOR inhibitor conditions, and that is important to allow cells to migrate in these particular environments. In particular, knockdown of ITGB3 in breast cancer cells increases apoptosis and reduces survival, cancer stem cell formation and migration *in vitro* and in mice, where we observe a significant reduction of lung metastasis.

**Conclusions:** We propose a new mechanism to analyse translational control in cells and we show that the Integrin Beta 3 is controlled at the protein synthesis level in hypoxia. ITGB3 regulates malignant features, including epithelial-mesenchymal transition and its knockdown, increases apoptosis and reduces survival and migration in breast cancer cells through the regulation of Snail in a TGF- $\beta$  pathway-dependent manner, especially under hypoxic conditions. This mechanism is translated into a significant reduction of lung metastasis and improved overall survival in mice, revealing a novel angle for the treatment of therapy-resistant hypoxic tumours.

## Hypoxia-mediated translational activation of ITGB3 in breast cancer cells enhances TGF- $\beta$ signaling and malignant features *in vitro* and *in vivo*

Marta Sesé<sup>1,2,\*</sup>, Pedro Fuentes<sup>1,2,\*</sup>, Anna Esteve-Codina<sup>3</sup>, Eva Béjar<sup>1,2</sup>, Kimberley McGrail<sup>4</sup>, George Thomas<sup>5,6,7</sup>, Trond Aasen<sup>1,2</sup> and Santiago Ramón y Cajal<sup>1,2</sup>

<sup>1</sup>Translational Molecular Pathology, Vall d'Hebron Research Institute, Universitat Autònoma de Barcelona, Barcelona, Spain

<sup>2</sup>Spanish Biomedical Research Network Centre in Oncology, CIBERONC, Barcelona, Spain

<sup>3</sup>CNAG-CRG, Centre for Genomic Regulation, Barcelona Institute of Science and Technology, Universitat Pompeu Fabra, Barcelona, Spain

<sup>4</sup>Biomedical Research in Melanoma-Animal Models and Cancer Laboratory, Oncology Program, Vall d'Hebron Research Institute, VHIR-Vall d'Hebron Hospital, Barcelona-UAB, Barcelona, Spain

<sup>5</sup>Division of Hematology/Oncology, Department of Internal Medicine, University of Cincinnati Medical School, Cincinnati, OH, USA

<sup>6</sup>Metabolism and Cancer Group, Molecular Mechanisms And Experimental Therapy In Oncology Program, Bellvitge Biomedical Research Institute, IDIBELL, Barcelona, Spain

<sup>7</sup>Physiological Sciences Department, Faculty of Medicine and Health Science, University of Barcelona, Barcelona, Spain

\*These authors contributed equally to this work

**Correspondence to:** Marta Sesé, email: [marta.sese@vhir.org](mailto:marta.sese@vhir.org)

Santiago Ramón y Cajal, email: [sramon@vhebron.net](mailto:sramon@vhebron.net)

**Keywords:** hypoxia; polysomes; breast cancer; migration; integrin beta 3

**Received:** July 05, 2017

**Accepted:** November 14, 2017

**Published:** December 12, 2017

**Copyright:** Sesé et al. This is an open-access article distributed under the terms of the Creative Commons Attribution License 3.0 (CC BY 3.0), which permits unrestricted use, distribution, and reproduction in any medium, provided the original author and source are credited.

### ABSTRACT

Breast cancer is the most prevalent malignancy in women and there is an urgent need for new therapeutic drugs targeting aggressive and metastatic subtypes, such as hormone-refractory triple-negative breast cancer (TNBC). Control of protein synthesis is vital to cell growth and tumour progression and permits increased resistance to therapy and cellular stress. Hypoxic cancer cells attain invasive and metastatic properties and chemotherapy resistance, but the regulation and role of protein synthesis in this setting is poorly understood. We performed a polysomal RNA-Seq screen in non-malignant breast epithelial (MCF10A) and TNBC (MDA-MB-231) cells exposed to normoxic or hypoxic conditions and/ or treated with an mTOR pathway inhibitor. Analysis of both the transcriptome and the translome identified mRNA transcripts translationally activated or repressed by hypoxia in an mTOR-dependent or -independent manner. Integrin beta 3 (ITGB3) was translationally activated in hypoxia and its knockdown increased apoptosis and reduced survival and migration, particularly under hypoxic conditions. Moreover, ITGB3 was required for sustained TGF- $\beta$  pathway activation and for the induction of Snail and associated epithelial-mesenchymal transition markers. ITGB3 downregulation significantly reduced lung metastasis and improved overall survival in mice. Collectively, these data suggest that ITGB3 is translationally activated in hypoxia and regulates malignant features, including epithelial-mesenchymal transition and cell migration, through the TGF- $\beta$  pathway, revealing a novel angle for the treatment of therapy-resistant hypoxic tumours.



## INTRODUCTION

Breast cancer is the most common malignancy and the second leading cause of cancer-related death in adult women [1]. Despite significant advances in the characterization of breast cancer subtypes and the development of new therapeutic approaches, advanced and aggressive forms of breast cancer continue to have a poor prognosis [2]. Triple-negative breast cancer (TNBC) is an important subtype of breast cancer defined by the loss of estrogen receptor, progesterone receptor and human epidermal growth factor receptor type 2 (HER2), all of which are clinically important therapeutic targets because the major therapeutic strategies in breast cancer are hormone therapy and/or HER2 antibodies [3]. TNBC is a highly aggressive tumour subtype with high risk of recurrence, metastasis, chemotherapy resistance and acquired capacity to survive and grow under nutrient-deprived and hypoxic (low-oxygen) conditions. TNBC also appears to adopt a unique response to cell stress by mimicking a hypoxia gene signature associated with poor prognosis [4]. Under hypoxic conditions, TNBC cells can grow, survive, induce metabolic reprogramming and apoptosis and alter cell adhesion and motility to facilitate metastasis and resistance to chemotherapy [5, 6]. Most of these phenotypes involve several transcriptional changes mainly related to the stabilization of the master transcription factor HIF1 $\alpha$  [7, 8]. However, little is known about mRNA regulation at the translational level under low-oxygen conditions [9, 10], although prolonged exposure to hypoxia inhibits translation via repression of the mTOR (mechanistic target of rapamycin) signalling pathway more efficiently at 0.3%–0.5% O<sub>2</sub> compared to 1% of O<sub>2</sub> concentration [10, 11]. Little is known about translational regulated targets in low oxygen conditions, in particular those subsets of mRNAs that are still capable to be translated that may favour cell migration and survival of TNBC cells under this stress.

Tumours display a high rate of protein synthesis [12] and several studies have shown that control of mRNA translation is critical not only for survival under hypoxic conditions, but also for cancer initiation, progression, migration and invasion [13, 14]. Translation is mostly controlled at initiation, when eukaryotic translation initiation factors (eIFs) are recruited to the 5'-m<sup>7</sup>G cap structure of mRNA, forming the eIF4F complex that recruits the eukaryotic small 40S ribosomal subunit. This step is mainly regulated by the mTOR signalling pathway [15–17]. mTOR forms two distinct complexes, mTOR complex 1 (mTORC1) and mTOR complex 2 (mTORC2) [18]. mTORC1 is composed of mTOR, regulatory-associated protein of mTOR (Raptor), mammalian LST8/G-protein  $\beta$ -subunit-like protein (mLST8/G $\beta$ L) and the PRAS40 and DEPTOR partners [19] and is a master regulator of protein synthesis that couples nutrient sensing to cell growth and cancer cell survival. The major regulators of protein synthesis downstream

of mTORC1 are 4E-BP1 and p70S6K1/2 [19–21]. Upon phosphorylation by mTORC1, 4E-BP1 releases eIF4E, which can then recruit eIF4A and eIF4G to form the eIF4F complex [22, 23]. This global downregulation of protein synthesis under low-oxygen conditions coincides with a simultaneous enhanced translation of certain mRNAs that encode proteins involved in adaptation to cellular stress. Activation of the eIF4F initiation complex is compromised under hypoxic conditions [9, 24] in favour of an eIF4F<sup>H</sup> complex composed of eIF4E2, eIF4A and eIF4G3 [25]. HIF2 $\alpha$  is induced by hypoxia and binds to a specific element in the 3'UTR (untranslated region) of some mRNA transcripts, allowing their selective translation initiation via recruitment of eIF4E2 [25–27]. Transcripts activated through this mechanism include the epidermal growth factor receptor (EGFR) and the insulin growth factor receptor (IGFR1) [26].

Another proposed mechanism to ensure protein synthesis when cap-dependent translation is inhibited is IRES (internal ribosome entry site)-mediated translation [28–30]. The presence of potential IRES elements in the 5'UTR of certain mRNAs such as HIF1 $\alpha$ , VEGF and c-MYC enables activation of their translation through a cap-independent pathway in hypoxia.

Finally, a third mechanism is the observation that, in hypoxia, uORF (upstream ORF)-mediated translation is enhanced due to an increase in eIF2 $\alpha$  phosphorylation by PERK. Transcripts containing uORFs in their 5'UTR include genes related to proliferation and cell survival under stress conditions such as ATF4, CHOP and GADD34 [31].

Polysome profiling is a standardized technique to capture mRNA translation by immobilizing actively translating mRNAs on ribosomes and separate the resulting polyribosomes by ultracentrifugation on a sucrose gradient, thus allowing for an analysis of translated mRNAs compared to total mRNA [32]. The combined use of polysomal fractionation with microarray analysis or of ribosome profiling with high-throughput RNA sequencing (RNA-Seq) has identified specific transcripts actively translated under low-oxygen conditions in tumour cells [24, 25, 33–35]. These approaches have already revealed the ability of an mTORC1 inhibitor to block cap-dependent translation in the translome of both fibroblasts and PC-3 cells [36, 37]. Nevertheless, the mechanisms underlying this selective translation are poorly understood, as well as how it affects the behaviour and survival of cancer cells exposed to hypoxia.

ITGB3 is an integrin that forms heterodimers with alpha chains, either ITGAV or ITGAIIB. These adhesion molecules are receptors for fibronectin, vitronectin, collagen and laminin and facilitate attachment between the cell cytoskeleton and the extracellular matrix [38]. Most integrins induce transmembrane signalling through activation of focal adhesion kinase (FAK) and Src family kinases that in turn activate downstream effectors such as small GTPases. Functional inhibition of ITGB3 suppresses neovascularisation, tumour growth and metastasis, suggesting that  $\alpha$ v $\beta$ 3 integrin may be a critical modulator

of pathological angiogenesis [39–44]. ITGB3 is expressed in a subpopulation of breast cancer stem cells and is associated with poor outcome [45, 46].

In this study, we used sucrose gradient fractionation and polysome profiling to separate and quantify actively translating mRNAs bound to ribosomes. We sequenced total and polysomal mRNAs and examined the effects of hypoxia alone and hypoxia combined with mTOR inhibition to avoid standard cap-dependent translation on the translome of the non-malignant MCF10A epithelial breast cell line and the triple-negative MDA-MB-231 breast cancer cell line. Our screen identified translational regulation of a number of genes under highly inhibitory and stressful situations, including ITGB3, which was upregulated at the protein synthesis level in hypoxia. Increased ITGB3 facilitates the migratory and invasive capabilities of breast cancer cells through induction of Snail and epithelial-mesenchymal transition (EMT) via the TGF- $\beta$  pathway, an effect particularly evident under hypoxic conditions. Moreover, ITGB3 silencing with shRNA reduced tumourigenesis *in vitro* and *in vivo*, suggesting that ITGB3 is a candidate therapeutic target for most aggressive breast tumours able to survive under low-oxygen conditions.

## RESULTS

### Combination of hypoxia and mTOR inhibitor treatment identifies a unique subset of genes regulated at both transcriptional and translational levels

We aimed to analyse differential transcription and translation efficiencies under hypoxic conditions by comparing non-tumourigenic cells (MCF10A) to malignant TNBC cells (MDA-MB-231). We conducted a polysomal RNA-Seq screen after exposing cells to 24 hours of hypoxia (0.5% O<sub>2</sub>) or normoxia (21% O<sub>2</sub>), with or without 3-hour treatment with the mTORC1 and -2 inhibitor PP242 (Figure 1A). PP242 treatment was used to discriminate between mRNAs that were still bound to polysomes after mTORC1/-2 inhibition under low-oxygen conditions in order to identify transcripts supposedly translated in a cap-independent manner. As expected, HIF1 $\alpha$  accumulated in cells exposed to hypoxia, and its induction was slightly diminished in cells co-treated with PP242 [47], which dephosphorylated 4E-BP1 (Figure 1B) and thereby inhibited cap-dependent translation. Under all four conditions, total mRNA was isolated and fractionated using a sucrose gradient to separate monosomes and oligosomes (free mRNA, F) from the actively translated mRNAs bound to polysomes (polysomal mRNA, P) (Figure 1B). A systematic analysis of the total (T) and polysome-bound (P) mRNA of each sample was carried out by high-throughput RNA-Seq and analysed bioinformatically to obtain differential gene expression with regards to both the transcriptome and translome in the two cell lines.

Principal component analysis (PCA) of the raw data clearly separated MCF10A and MDA-MB-231 samples in accordance with the highly different transcriptomes of the two cell types (Figure 1C). The within-cell type variability upon treatment, which is reflected by principal component 2 (PC2), appeared to be higher for the MCF10A samples than the tumour samples (Figure 1C), meaning that non-tumourigenic MCF10A cells were more affected by hypoxia or PP242 than tumoural MDA-MB-231 cells. Independent PCAs were performed for each cell type dataset to inspect in greater detail the clustering within each cell type. In tumour cells, PC1 mainly reflected variance attributable to differences between the total mRNA and polysome-bound mRNA and PC2 differentiated normoxic and hypoxic conditions. In non-tumoural cells, the pattern was the reverse (Figure 1D). However, in both cases, PC3 explained the drug effect (PP242 vs non-PP242) (data not shown). These results confirmed that there was variability between cell lines and within treatments.

Following bioinformatic analysis of the differential gene expression in both total (T) and polysome-bound (P) mRNA, the fold change expression (log<sub>2</sub>FC) levels were calculated by comparing all conditions with the control condition of normoxia and plotting the correlation between log<sub>2</sub>FC\_P and log<sub>2</sub>FC\_T for each treatment. There was a close correlation between differentially expressed genes in total mRNA versus genes differentially expressed in polysomes, meaning that major transcriptional changes were also reflected at the level of translation (blue colour in Figure 2). We classified the genes into four groups: (1) transcriptionally upregulated or downregulated (blue colour in Figure 2); (2) transcriptionally upregulated or downregulated but no changes in translation (green colour in Figure 2); (3) translationally upregulated or downregulated (red colour in Figure 2); and (4) non-significant changes (black colour in Figure 2). Notably, the translation of some genes was specifically activated or inactivated by the different treatments (red colour in Figure 2). In general, we observed the most significant activation and inhibition, both transcriptionally and translationally, upon double hypoxia + PP242 treatment. Normoxia + PP242 treatment alone did not affect transcription, but potently inhibited translation, as expected. Moreover, in all conditions, MCF10A cell lines were more affected at the level of both transcription and translation than MDA-MB-231 cells, supporting the findings of our PCA analysis (Figure 1C). These findings mean that MCF10A cells have to enact major changes to survive under low-oxygen conditions (Figure 2).

### Transcriptional changes are more extensive in the non-tumourigenic cell line in both hypoxia and combined hypoxia + PP242

Next, we analysed the transcriptional differences between the two cell lines upon hypoxia (H) and hypoxia

+ PP242 (HPP) treatment. We detected 236 upregulated and 17 downregulated genes in MCF10A cells and 61 upregulated and 9 downregulated genes in MDA-MB-231 cells at the transcriptional level in hypoxia; 23 of these genes were the same in the two cell lines (Supplementary Figure 1). By analysing the function of genes upregulated in the intersection between the two cell lines, we found

that most of the Gene Ontology (GO) categories were related to response to hypoxia and glycolysis and oxidation-reduction processes, as expected (Figure 3A). The MDA-MB-231 cell line did not show any significant GO-enriched category (perhaps because fewer genes were applied to the analysis), whereas the genes upregulated in MCF10A cells were associated with nucleosome assembly,

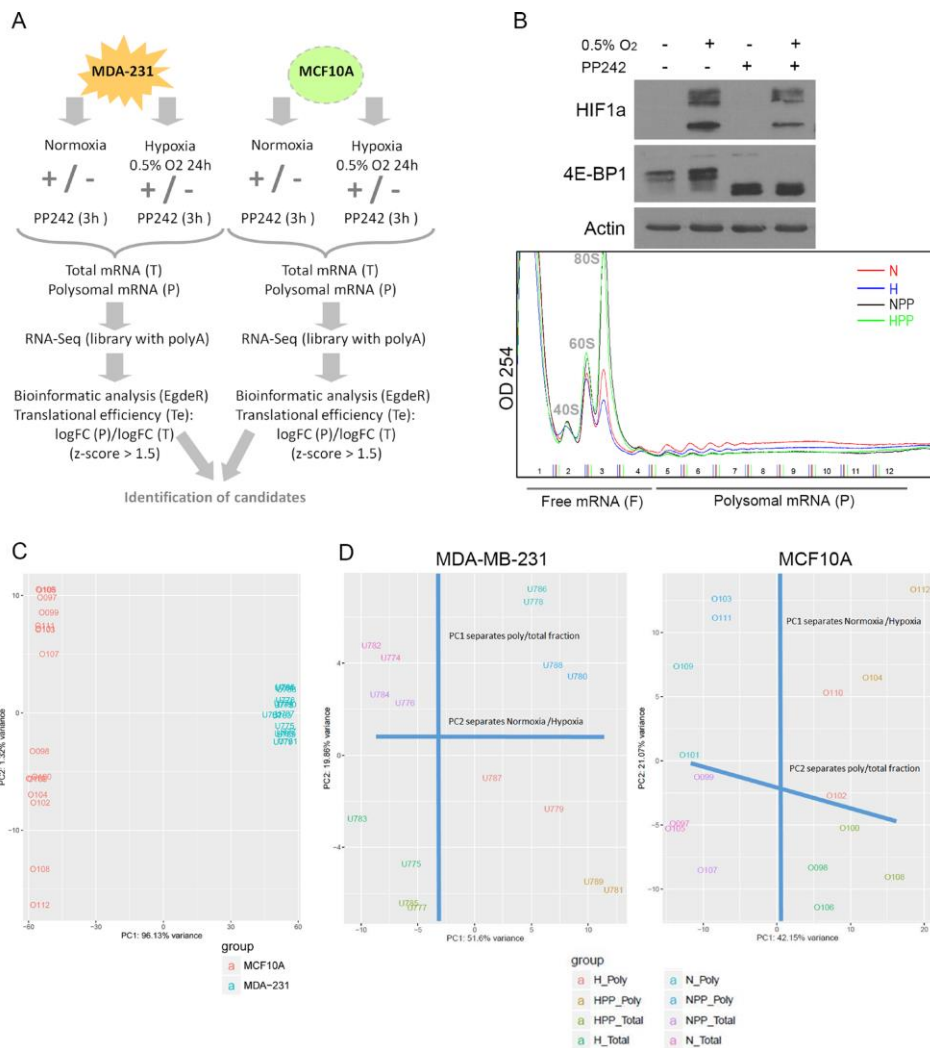


**Figure 1: Overview of the polysomal RNA-Seq screen after hypoxia and mTOR inhibition. (A)** Schematic workflow of the experiment. **(B)** Above: Immunoblot of HIF1α and 4E-BP1 under normoxic (N), hypoxic (H), PP242 (PP) and hypoxic + PP242 (HPP) conditions. Below: Polysome profiles of MCF10A cells in all conditions. **(C)** PCA plot of all samples of the dataset to emphasize the variation between replicates, treatments and cell lines. The first component (PC1) explained 96% of the total variance while PC2 explained 32%. **(D)** PCA plot of MDA-MB-231 (left) and MCF10A (right) samples showing that one PC separates total from polysomal mRNA and the other separates normoxic from hypoxic conditions.

apoptosis, angiogenesis and proliferation. This difference may suggest that changes induced by hypoxia in genes associated with malignant features are more extensive in the non-tumourigenic cell line than in the tumourigenic TNBC cell line.

Transcriptional changes were more evident when cells were treated with combined hypoxia + PP242, especially in MCF10A cells, which showed more up- and downregulated transcripts than MDA-MB-231 cells (Supplementary Figure 1). In particular, 631 mRNAs were upregulated in MCF10A cells upon HPP treatment, compared with only 130 genes in MDA-MB-231 cells, with 74 genes common to the two cell lines. Again, GO analysis indicated that the genes in the intersection were devoted to the response to hypoxia, nucleosome assembly and glycolysis categories. In cancer cells, angiogenesis and the Notch signalling and p53 pathways were upregulated. In MCF10A cells, cell adhesion, cell–cell signalling, apoptosis, growth, proliferation and cell cycle categories were upregulated, indicating a more organized change in

the non-tumourigenic cell line towards a full EMT program (Figure 3B). On the other hand, genes transcriptionally downregulated under H and HPP conditions were mainly related to cell proliferation and cell cycle in the two cell lines (Supplementary Figure 2A). In terms of GO categories and pathways downregulated in HPP, minor changes were observed in MDA-MB-231 cells. However, in MCF10A cells, several signalling pathways were downregulated, such as the Wnt pathway, the Hippo pathway, the TGF- $\beta$  pathway and pathways related to the cell cycle (Supplementary Figure 2B). As expected, no significant transcriptional changes were observed in cells treated with PP242 alone (Supplementary Figure 3). Genes transcriptionally deregulated in each condition are listed in Supplementary Table 1.

Although many of the genes transcriptionally upregulated upon hypoxia + PP242 treatment are important for cell survival, we focused our attention on genes activated at the protein synthesis level, a less understood and studied feature.

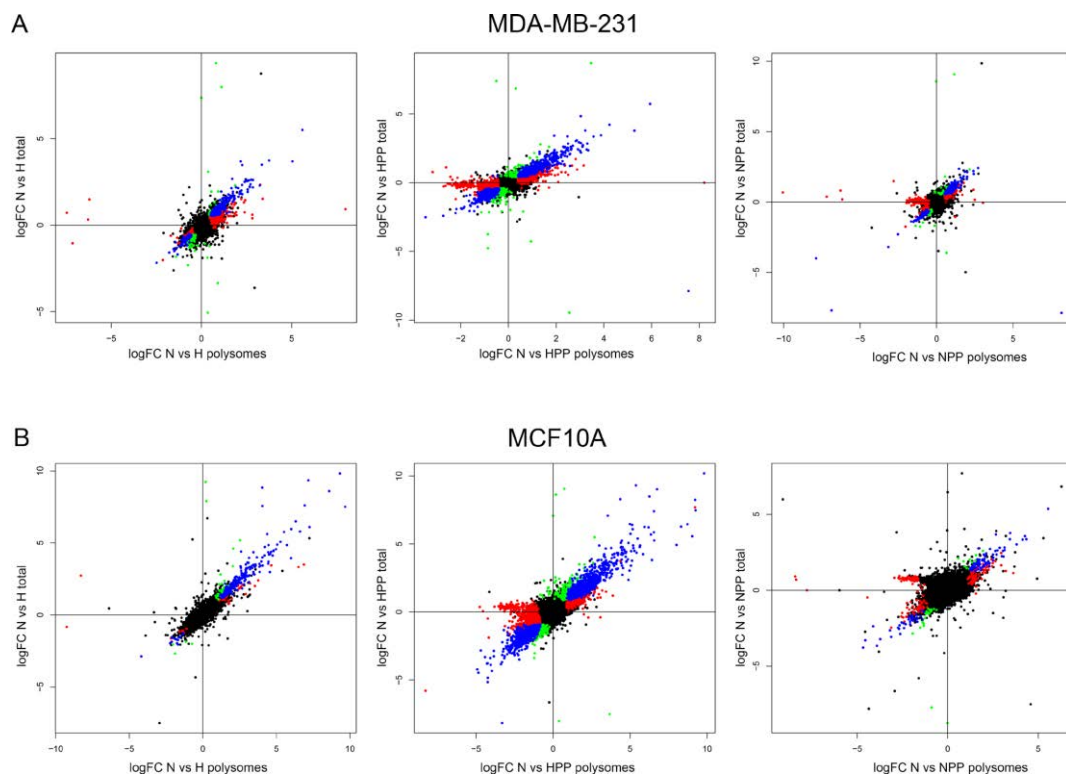


**Figure 2: Transcriptional and translational changes in non-tumoural and malignant cells under hypoxic and mTOR inhibition conditions.** (A and B) Correlation between transcript expression in total mRNA versus mRNA in polysomal fractions under the different conditions in (A) MCF10A and (B) MDA-MB-231 cell lines. Classification of the transcripts as (I) deregulated at the transcriptional level (blue), (II) translationally activated or inhibited (red) and (III) not significantly regulated (black). Overall, the results show that more genes are regulated transcriptionally and translationally in non-tumoural cells than in tumoural cells.

**The MCF10A and MDA-MB-231 translome in hypoxia and hypoxia + PP242**

We analysed the translational efficiency (Te) to identify translationally activated (z-score > 1.5) or inactivated (z-score < 1.5) genes under H, HPP and NPP conditions (Supplementary Table 1). In hypoxia, 82 and 43 genes were upregulated and 12 and 22 genes were downregulated at the translational level in MDA-MB-231 and MCF10A cells, respectively (Figure 4A, Supplementary Figure 4B, Supplementary Table 1). This

suggests that a limited number of genes are significantly regulated at the level of translation under hypoxic conditions. Curiously, more genes were regulated at the translational level in the tumour cell line (MDA-MB-231) than in non-tumoural cells (MCF10A), which is the opposite of what was occurring in terms of transcriptional changes. With hypoxia + PP242 treatment, we detected 87 and 99 genes translationally upregulated and 224 and 450 translationally inactivated in MDA-MB-231 and MCF10A cells, respectively (Figure 4A, Supplementary Figure 4B, Supplementary Table 1). However, as expected, mRNAs

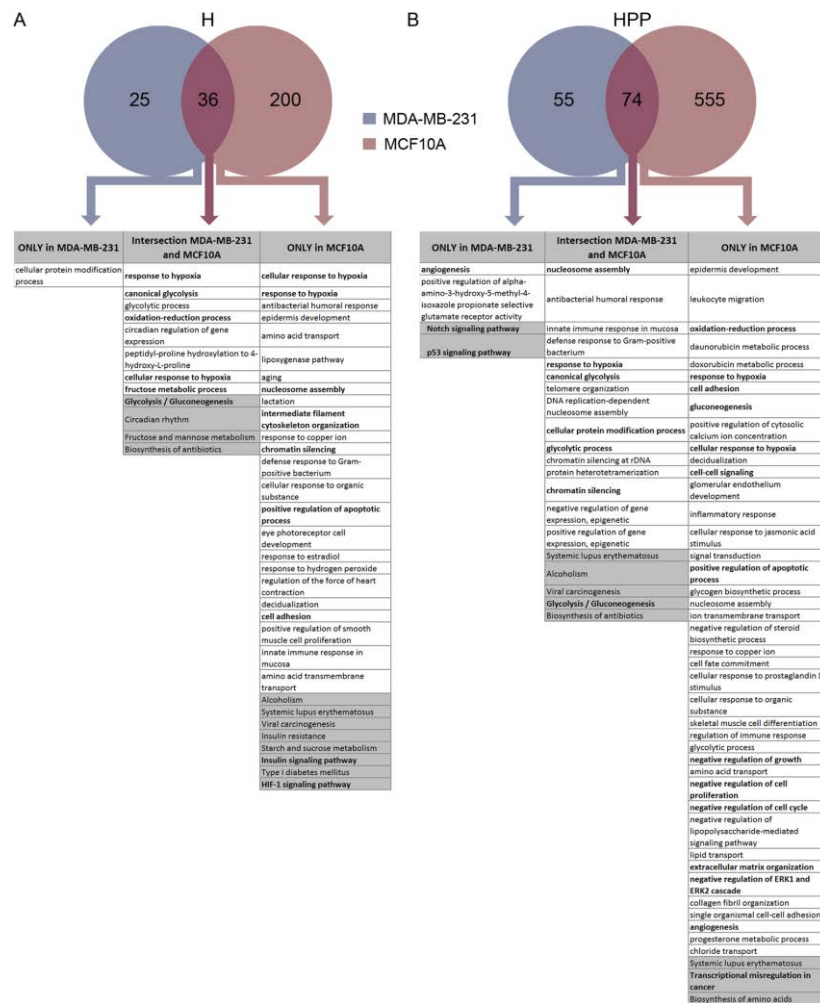


**Figure 3: Transcriptome analysis of MCF10A and MDA-MB-231 cells after hypoxia and hypoxia + PP242. (A)** Venn diagram of upregulated transcripts in hypoxia. GO (in white boxes, with  $P < 0.03$ ) and Kegg pathway analysis (in grey boxes, with  $P < 0.1$ ) of gene sets enriched only in MCF10A cells, only in MDA-MB-231 cells and in the intersection between these two cell lines. **(B)** Venn diagram of upregulated transcripts in hypoxia + PP242. GO (in white boxes, with  $P < 0.03$ ) and Kegg pathway analysis (in grey boxes, with  $P < 0.1$ ) of gene sets enriched only in MCF10A cells, only in MDA-MB-231 cells and in the intersection between these two cell lines.



were mainly translationally inactivated in HPP and NPP upon mTOR inhibitor treatment. Twice as many genes were downregulated in tumoural cells, possibly due to a highly activated mTOR pathway in this cell line, which naturally increases the number of effective PP242 targets. GO categories of activated transcripts indicated that the genes were mainly related to cell adhesion, angiogenesis and extracellular matrix organization in MCF10A cells (Figure 4B), whereas the only significant GO category in the cancer cell line was circadian regulation of gene expression.

Genes inactivated by H and HPP in both cell lines are presented in Supplementary Figure 4 and were mainly related to translation, catabolic processes and mitochondrial transport in both cell lines (Supplementary Figure 4A–4C). Genes translationally activated/inactivated in each condition are listed in Supplementary Table 1.

As a validation of our screening, most of the genes inactivated under NPP conditions, of which nearly 50% were common to the two cell lines, were cap-dependent genes containing TOP sequences. These *cis*-acting elements are found in some mRNAs that are mostly localized to polysomes in actively growing cells whose translational activation is mainly regulated by the mTOR signalling pathway [48, 49], and most were the same as those described by Thoreen and colleagues and Hsieh and colleagues after mTOR inhibition of other cell lines [36, 37] (Supplementary Figure 4D). To further validate our screening at the protein level, candidate genes that were translationally activated or inactivated in HPP were analysed by western blotting. Candidate genes with a  $T_e$  higher than 1.5 displayed an increase at the protein level under HPP conditions compared with control in both MCF10A cells (TTC30B and ITGB3) and MDA-MB-231 cells (CCDC103, ITGB3, Cx31, MMP3 and TTC30B). Although we picked these candidates from genes translationally activated by HPP, in most cases, we also observed more protein under hypoxic conditions alone. We detected reduced expression when analysing proteins from translationally inactivated genes such as RPL11, EIF3G and YBX1 (Figure 4C). As expected, we also detected increased protein expression of HIF1 $\alpha$  target genes such as CA9 in hypoxia (Figure 4C). These set of proteins activated / inactivated translationally were also validated in other breast cancer cell lines such as MCF7, MDA-MB-468 and BT-549 (Supplementary Figure 5) to ensure that this phenomena was occurring in a more general way. Importantly, we observed that ITGB3 was overexpressed in H and HPP in all cell lines analyzed.

The screening was also validated by quantitative real time RT-PCR (qRT-PCR) for some targets using the 50-gene PAM50 assay (Prosigna; NanoString Technologies, Seattle, WA) [50, 51], which is designed to identify clinically relevant molecular subtypes of breast cancer [52]. We observed a strong correlation between our RNA-Seq results and our NanoString analysis (Supplementary Figures 6 and 7).

Altogether, our RNA-Seq analysis showed that transcripts found to be transcriptionally and translationally activated in hypoxia or in hypoxia + PP242 were also found to be increased with qRT-PCR and NanoString and at the protein level by western blot, which validates our multi-level screening approach and suggests that some of the identified genes may be relevant in hypoxia, for example, by promoting survival and/or migration capabilities.

### **ITGB3 is translationally activated in hypoxia and hypoxia + PP242 and promotes cell migration *in vitro* and metastasis establishment *in vivo***

A secondary functional screening was performed using siRNA from the list of candidate genes actively translated ( $T_e > 1.5$ ) in both cell lines. Both proliferation and migration assays were conducted (Supplementary Figure 8). Of the candidates, ITGB3 silencing in MDA-MB-231 cells significantly reduced cell viability specifically in hypoxia and not in normoxia (Supplementary Figure 8A and 8B). Moreover, increased apoptosis was observed in hypoxia but not normoxia upon ITGB3 silencing (Supplementary Figure 8D). In contrast, there was a tendency for decreased cell migration (Supplementary Figure 8C).

Notably, when analysing GO categories of translationally activated genes in HPP in MCF10A cells, we observed a general activation of integrins at the protein synthesis level, particularly ITGB3, ITGB4, ITGAX and ITGA5. Based on this finding and the results of our preliminary siRNA screen, we therefore performed a more detailed analysis of ITGB3 and its regulation and role in hypoxia. Considering the important role of ITGB3 in tumorigenesis, we further studied ITGB3 in breast cancer cells under hypoxic conditions. To further validate the role of ITGB3, cells were treated with actinomycin D to avoid transcriptional changes and were subjected to hypoxia. ITGB3 protein was still induced in hypoxia in the absence of mRNA synthesis (Figure 5A), in concordance with our RNA-Seq data, suggesting that this is a translational rather than transcriptional event. As a control, we studied CA9, a well-known effector of HIF1 $\alpha$ , which was not activated in hypoxia upon treatment with actinomycin D (Figure 5A).

Having validated that ITGB3 was upregulated at the protein level in HPP and also under hypoxic conditions alone, we explored putative functional roles of ITGB3 in breast cancer progression, particularly under low-oxygen conditions. Similar to our siRNA screen (Supplementary Figure 8C), knockdown of ITGB3 using viral shRNA approaches reduced cell proliferation under both normoxic and hypoxic conditions in MCF10A and MDA-MB-231 cells (Figure 5B). Furthermore, ITGB3 depletion induced apoptosis, with more evident effects in hypoxia (Figure 5C and Supplementary Figure 8D). Knockdown of ITGB3

significantly decreased cell migration, but this was more prominent and significant under low-oxygen conditions in both cell lines (Figure 5D). This suggests that ITGB3 is important for cell migration and survival in both cancer and non-malignant cells, but particularly under hypoxic conditions.

Next, we assessed ITGB3 function *in vivo* by injecting control and ITGB3-silenced cells into the mouse tail. Our results suggested that cancer cells with silenced ITGB3 form fewer metastases and those that do appear are smaller than with control non-silenced tumour cells (Figure 6B–6D). This was reflected in the improved

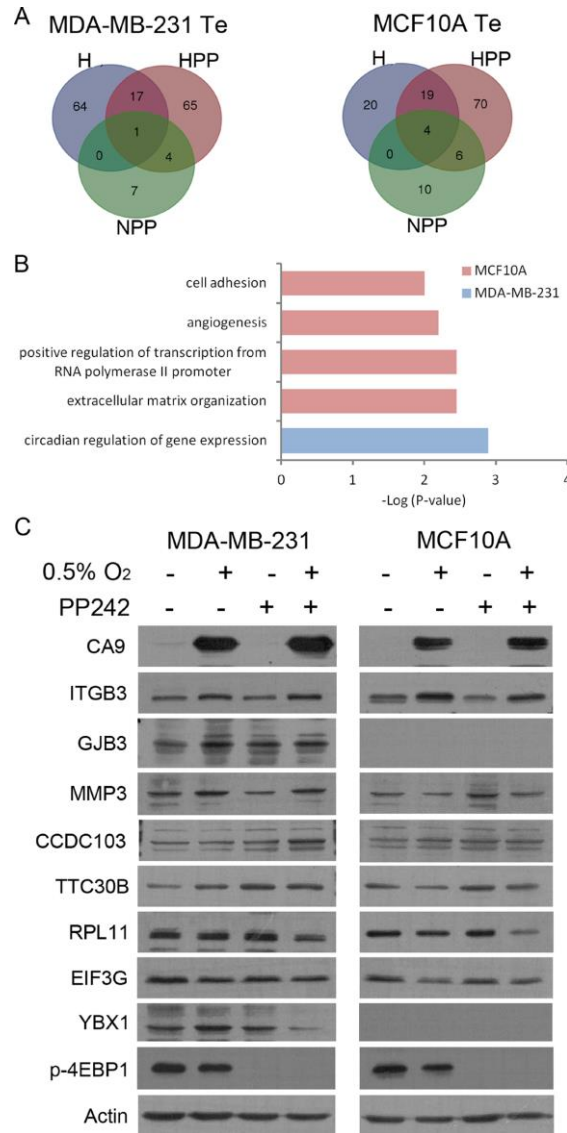


**Figure 4: Increased translational efficiency (Te) is accompanied by increased protein.** (A) Venn diagram of Te distribution of transcripts in MDA-MB-231 (left) and MCF10A (right) cells under all three experimental conditions. (B) GO analysis of Te under HPP conditions in both cell lines. (C) Immunoblots for all experimental conditions of the different translationally activated (ITGB3, GJB3, MMP3, CCDC103, TTC30B) or inactivated (RPL11, EIF3G, YBX1) targets in HPP.

overall survival of animals injected with ITGB3-silenced MDA-MB-231 cells compared with non-silenced cells (Figure 6A).

### ITGB3 amplifies TGF- $\beta$ signalling in hypoxia, enhancing the EMT and cell migration

Because ITGB3 interacts with TGF- $\beta$  receptor II in mammary epithelial cells and enhances its function through Src [53], we wondered whether the TGF- $\beta$  pathway was modulated by ITGB3 under hypoxic conditions. We measured cell migration in control and ITGB3-silenced MDA-MB-231 cells with or without treatment with TGF- $\beta$ ,

a well-known stimulator of EMT and migration in cancer cells [54]. As expected, TGF- $\beta$  increased the rate of cell migration in both normoxia and hypoxia (Figure 7A). However, when ITGB3 was silenced, TGF- $\beta$  treatment failed to induce and even partially reduced cell migration, especially under hypoxic conditions. Accordingly, TGF- $\beta$  increased ITGB3 expression in control cells but not in shITGB3 cell lines. Moreover, increased expression of the important EMT-associated transcription factor Snail was observed at the mRNA and protein levels after TGF- $\beta$  treatment in control cells but not when ITGB3 was silenced. In fact, we observed a clear downregulation of Snail expression upon ITGB3 silencing, which was especially

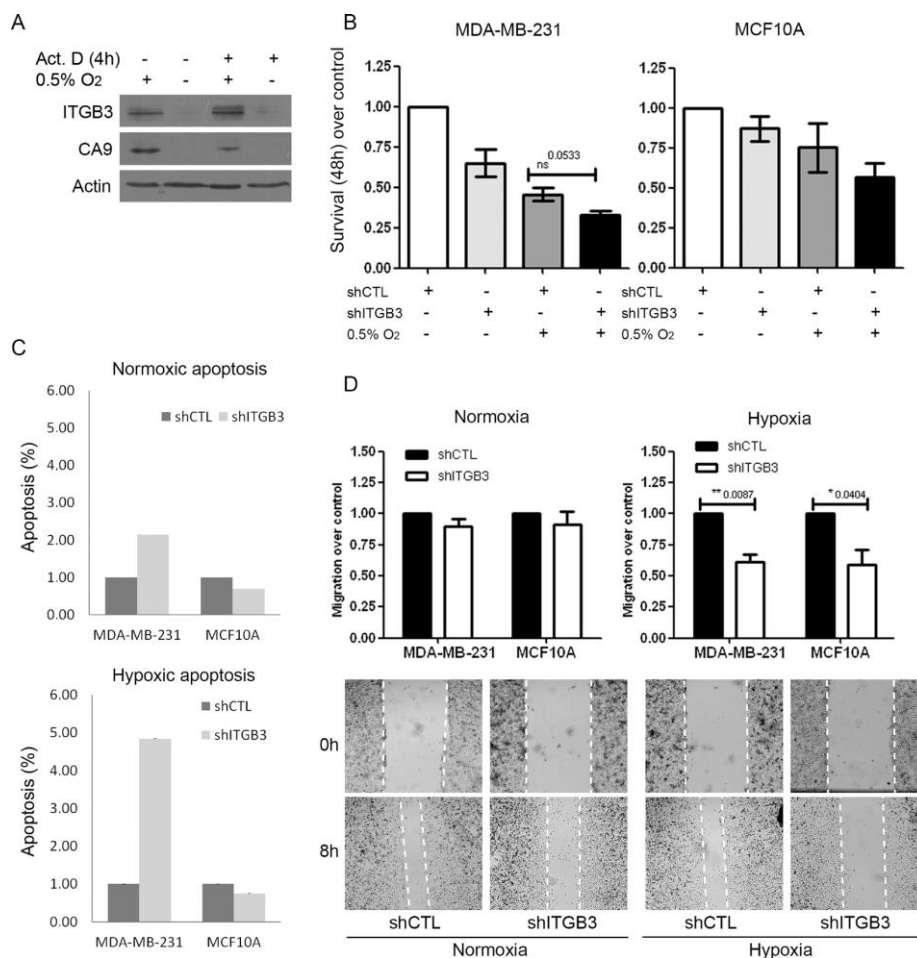


**Figure 5: ITGB3 is translationally activated under hypoxic conditions and is important for breast cell line survival and migration.** (A) Immunoblots of ITGB3 in MDA-MB-231 cells subjected to hypoxia or normoxia and treated with actinomycin D. (B–D) Phenotypes of stably shITGB3-infected cells. Effects of ITGB3 depletion on (B) survival visualized by MTT assay at 48 hours, (C) apoptosis using caspase-3/-7 activation and (D) migration in a wound healing assay in hypoxia versus normoxia.



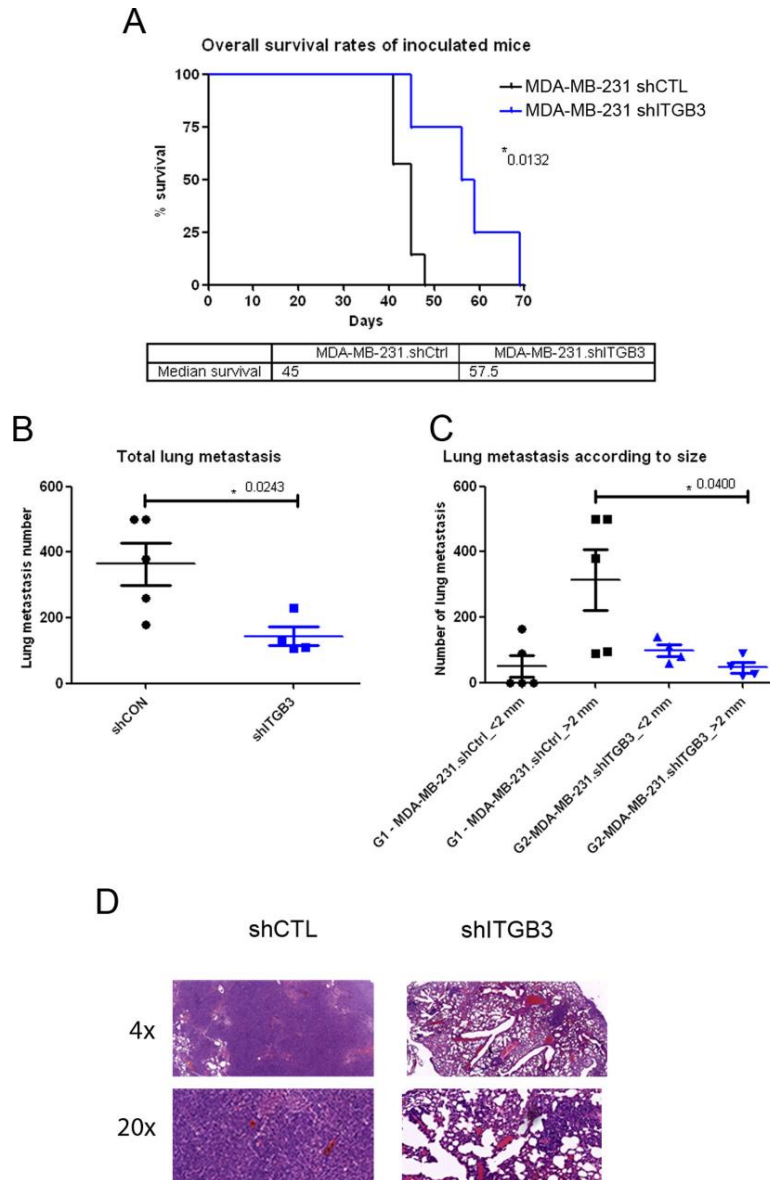


**Figure 6: Survival and lung metastasis after intravenous inoculation with ITGB3-depleted MDA-MB-231 human breast cancer cells.** (A) Overall survival rates of inoculated mice. Downregulation of ITGB3 protein significantly increased the overall survival rate of mice inoculated with the MDA-MB-231.shITGB3 cell variant. Median survival times were 45.0 days and 57.5 days for the MDA-MB-231.shCtrl- and MDA-MB-231.shITGB3-inoculated groups, respectively. Subsequently, the two Kaplan-Meier curves and estimates of survival showed them to be significantly different ( $P=0.0132$ ). (B and C) Comparative analysis of the lung metastasis number (B) and number per size (C) of MDA-MB-231.shCtrl- and MDA-MB-231.shITGB3-inoculated groups at the end time point. Lines indicate the median corresponding values of the groups. Downregulation of ITGB3 protein decreased lung metastasis growth of breast cancer with respect to control animals, with significant differences in lung total number ( $P=0.0213$ ) (B) and in number per size ( $P=0.0400$ ) (C). (D) Hematoxylin and eosin staining of mouse lung sections where tumours of shCTL and shITGB3 MDA-MB-231 cell lines are evident.

evident and significant in hypoxia (Figure 7B and 7C). The same observations were made using MCF10A cells, indicating that this integrin is required for proper TGF- $\beta$  signalling and regulation of Snail (Supplementary Figure 9). These results clearly suggest that ITGB3 is required for TGF- $\beta$ -mediated expression of Snail, particularly under low-oxygen conditions. In support, reduced TGF- $\beta$ -mediated induction of Snail-regulated EMT genes such as vimentin and N-cadherin was observed in ITGB3-silenced cells (Figure 7B and Supplementary Figure 9). Finally, we observed maximum phosphorylation of Smad2 after 1-hour treatment. At this time point, Smad was not phosphorylated when cells silenced with ITGB3 (Figure 7D). These findings suggest that ITGB3 affects the classical TGF- $\beta$  signalling pathway at an early stage, possibly by directly acting on the receptor itself, as previously suggested [53].

### EIF4E is essential for the translational activation of ITGB3 in hypoxia

Finally, we wanted to know how translation activation of ITGB3 is regulated in hypoxia. Most transcripts translated under low-oxygen conditions use the eIF4<sup>H</sup> initiation complex, especially those transcribed by the HIF transcription factor [25]. The eIF4<sup>H</sup> complex is composed of the initiation factor 4E2 (eIF4E2), eIF4A and eIF4G3. We used siRNA targeting eIF4E2 to block this mechanism of translation in hypoxic conditions. In addition, we used siRNA against HIF1 $\beta$  (ARNT1) to inhibit the HIF1 $\alpha$ -HIF1 $\beta$  complex in charge of the transcription of HIF target genes. We also treated cells with siRNA targeting eIF4E to inhibit the standard cap-dependent translation initiation complex eIF4F. In MDA-MB-231 cells, we found that ITGB3 was still activated under low-oxygen conditions when both ARNT1 and eIF4E2 were silenced, suggesting that ITGB3 is not a HIF target gene and is not translated through the eIF4<sup>H</sup> complex. As controls, expression of CA9 and EGFR were assessed, with the findings showing that CA9 was not expressed when ARNT1 was silenced and that EGFR translation was not activated with eIF4E2 siRNA, as reported [25]. However, eIF4E inhibition blocked any induction of ITGB3 protein by hypoxia, indicating that synthesis of this integrin is cap-dependent and dependent on eIF4E and the canonical translation pathway (Figure 8). The same situation was observed in MCF10A cells (Supplementary Figure 10).

## DISCUSSION

In addition to transcription, both protein stability and translation efficiency are important determinants of the protein concentration in cells, and several screens analysing and quantifying mRNA bound to ribosomes, either by ribosome or polysome profiling, have been reported [25, 31, 35–37, 55, 56]. We measured the

changes in global translation in cells subjected to hypoxia or to hypoxia plus an mTOR inhibitor, comparing non-tumoural versus tumoural human breast cancer cell lines. Although the use of polysomal fractionation combined with microarray technology has been used to identify transcripts upregulated at the protein synthesis level in tumour cells in response to hypoxia [24, 33, 34, 57, 58], our experiments allowed a comparison between non-tumoural and malignant cells using RNA-Seq technology. Our data showed that hypoxia led to transcriptional changes in 70 and 253 genes and translational changes in 94 and 65 genes in tumoural (MDA-MB-231) and non-tumoural (MCF10A) cells, respectively. When cells were treated with hypoxia + PP242, we observed 158 and 1048 transcriptionally deregulated genes and 311 and 549 genes subjected to translational regulation in the MDA-MB-231 and MCF10A cells, respectively (Supplementary Table 1). This is not simply due to an additive effect because treatment with PP242 alone only deregulated 26 and 109 genes transcriptionally and 139 and 118 transcripts at the translational level in the MDA-MB-231 and MCF10A cells, respectively. Thus, the double treatment acts synergistically at both the transcriptional and translational levels.

Another conclusion that can be drawn is that non-tumoural MCF10A cells displayed significantly more transcriptional and translational changes compared with the triple-negative MDA-MB-231 cell line. Both cell lines upregulated genes related to hypoxia and glycolysis. In hypoxia, HIF-1 $\alpha$  plays a critical role in promoting and stimulating EMT [59–62], and downstream targets of this transcription factor were transcriptionally activated in both cell lines, as expected. In particular, MCF10A cells mainly upregulated the synthesis of factors related to cell adhesion, migration, angiogenesis and EMT in general, whereas MDA-MB-231 cells did not activate transcription or translation related to these processes in hypoxia (Figures 3 and 4). This distinction suggests that the nature of the stress response, whether protective or destructive, largely depends on the cell type. A comparison of transcripts bound to polysomes clearly revealed that non-malignant cells upregulated genes related to negative regulation of cell proliferation ( $P = 2.2 \times 10^{-3}$ ) and cell death ( $P = 0.01$ ), whereas tumour cells upregulated genes related to cell migration ( $P = 4.7 \times 10^{-4}$ ) and positive regulation of cell proliferation ( $P = 9.3 \times 10^{-5}$ ). One plausible explanation for this difference may be that malignant cells have already activated many genes related to these processes (EMT, proliferation, migration and angiogenesis), reducing the extent of the activation of such genes in hypoxia. On the other hand, the control of mTORC1 activity in hypoxia influences the survival response but with different outcomes in normal versus cancer cells. Whereas mTORC1 inhibition reduces the survival of normal cells in hypoxia, it supports the emergence of tumour cells

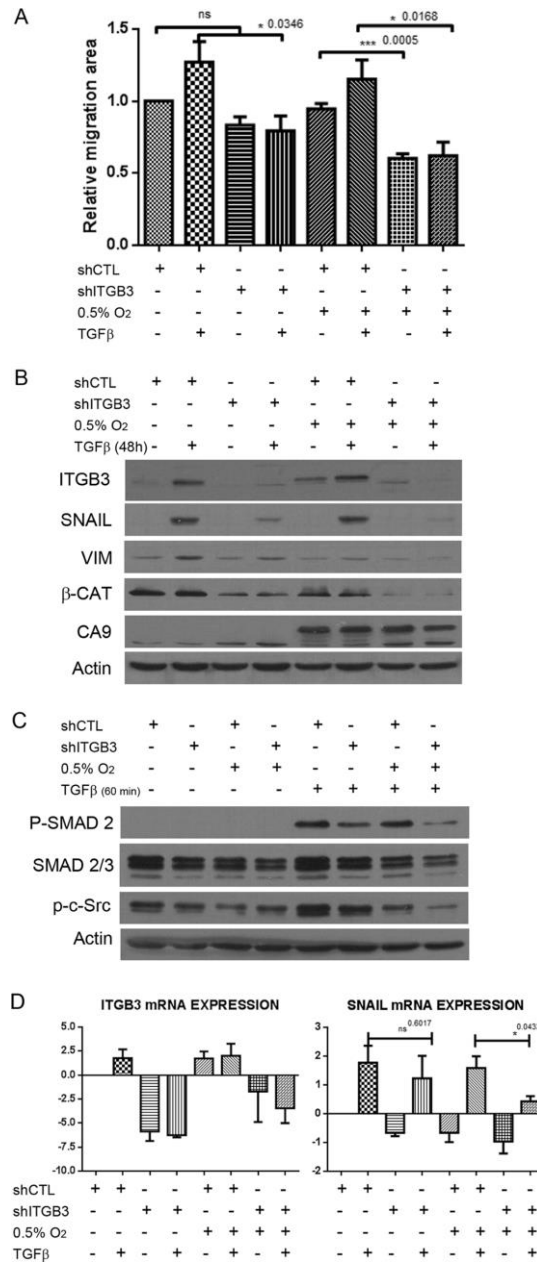


**Figure 7: ITGB3 depletion blocks TGF-β pathway activation more efficiently in hypoxia than in normoxia. (A)** Migration assays of MDA-MB-231.shITGB3 cells in hypoxia versus normoxia and treated with TGF-β. **(B)** Immunoblot of MDA-MB-231.shITGB3 and MDA-MB-231.shCTL cells treated with TGF-β and subjected to hypoxia or normoxia for 48 hours to analyse the expression of EMT factors such as Snail and vimentin. **(C)** Immunoblot analysis of Smad2 phosphorylation in MDA-MB-231 cells infected with shITGB3 or control shCTL subjected to hypoxia or normoxia for 24 hours and treated with TGF-β for 60 minutes. **(D)** qRT-PCR of cells treated with TGF-β and subjected to hypoxia or normoxia for 48 hours to analyse the expression of EMT factors such as Snail and vimentin.

that are resistant to hypoxia because, in a situation of restoration of mTOR signalling, cancer cells become sensitive to hypoxia again [31, 63]. Consistent with these results, mTOR inhibition negatively regulated GO profiles related to proliferation and growth in MCF10A cells and positively regulated apoptosis GO categories, whereas angiogenesis and tumorigenic features were identified in treated MDA-MB-231 cells (Figure 3).

In terms of translation, in hypoxia, we found similar transcriptional changes to those published by Thomas *et al.* [33] and Koritzinsky *et al.* [57] but very few translational changes compared with what was reported by Lai *et al.* [58]. This difference might be due to the use of different cell lines or more technical reasons, namely, because we isolated fractions of heavy and light polysomes, from the two ribosomes to the end, whereas Lai and colleagues isolated only the heavy polysome fractions. However, validation of our experiments revealed that the same amount and almost the same genes were translationally downregulated by mTOR inhibition compared with what has been reported and that most of these transcripts contained TOP elements [36, 37] (Supplementary Figure 4). Finally, we also validated our screening by using western blotting, showing that translationally activated transcripts in HPP correlated with an increase in protein expression in this condition (Figure 4C). More transcripts were translationally upregulated in HPP, possibly due to a synergistic effect with the hypoxia treatment. In addition to determining that transcripts activated in HPP correlated with greater protein

expression in HPP, we also found that they were activated in hypoxia, as occurred with our candidate target ITGB3 (Figure 4C). A possible explanation for this finding is that treatment with the mTOR inhibitor highlighted genes still bound to polysomes under low-oxygen conditions after cap-dependent translation inhibition in the RNA-Seq and that western blotting is more sensitive and more able to detect an increase in the real protein. In addition, some transcripts activated in HPP are also increased in hypoxia.

In this study, we showed that ITGB3 is translationally activated upon hypoxia and hypoxia + PP242 in cancer and non-tumorigenic breast epithelial cells and that this protein synthesis activation was dependent on eIF4E (Figures 4C, 5A and 8). ITGB3 has been reported to be recruited to the membrane and to regulate invasion in hypoxia in glioblastoma by interacting with type III EGF receptor (EGFRvIII) in a hypoxic microenvironment enriched with vitronectin [64, 65]. It is also transcriptionally increased in Caco-2 cells simultaneously treated with EGF and hypoxia [66]. ITGB3 activates EGFR signalling through SRC-FAK-AKT and thereby promotes invasion [65]. Phenotypes of ITGB3 siRNA are stronger in activated cells with EGFRvIII than under normal conditions, and hypoxia enhances the colocalization of these two factors, preventing degradation of this receptor. In addition, activation of  $\alpha\beta3$  is required for metastasis in a breast carcinoma model by promoting migration *in vitro* and colonization in metastasis assays [67–71]. By inhibiting ITGB3 expression in cancer cells via infection with viral

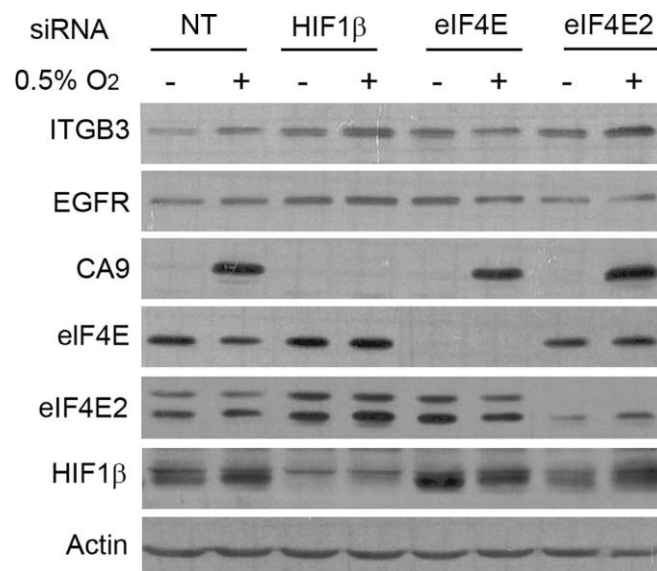


**Figure 8: eIF4E is essential for enhanced protein synthesis of ITGB3 under low-oxygen conditions.** Immunoblot showing ITGB3 expression under hypoxic conditions after eIF4E2, eIF4E or HIF1 $\beta$  silencing in the MDA-MB-231 cell line.

shRNA, we observed reduced migration, as expected, and increased apoptosis, but these effects were surprisingly more significant in hypoxia (Figure 5). In addition, silenced MDA-MB-231 cells showed fewer and smaller lung metastases in an *in vivo* mouse model, consistent with previous results [71] showing that downregulation of ITGB3 impairs spontaneous metastasis but not growth of the primary tumour and that ITGB3 is required by the tumour cell and not by the stroma surrounding the tumour. Integrins couple several growth factor receptors to regulate angiogenesis, survival and EMT. We found, as described previously [54], that ITGB3 is activated by the TGF- $\beta$  pathway (Figure 7). ITGB3 in turn enhances TGF- $\beta$  signalling by interacting physically with TGF- $\beta$  receptor (TbetaR) type II via Src-mediated phosphorylation of the receptor in mammary epithelial cells [53]. TGF- $\beta$  is involved in cancer cell invasion and migration through its participation in EMT. We observed that ITGB3 silencing blocked the effects of TGF- $\beta$  treatment, particularly under low-oxygen conditions, especially the transcription and expression of EMT markers such as SNAIL and VIM (Figure 7). The effects of ITGB3 silencing on Smad2 phosphorylation were already visible 1 hour after TGF- $\beta$  treatment and Smad2 was not phosphorylated in hypoxia when ITGB3 was silenced (Figure 7). This fits with the published data showing that the interaction between these two signalling pathways is at the receptor level, but also provides novel evidence that this pathway is particularly important under low-oxygen conditions, where ITGB3 is suggested to be more necessary [53]. This finding is consistent with the previously reported function of ITGB3 in EMT, where overexpression of ITGB3 increases motility and N-cadherin expression through binding of the FGFR1 receptor and knockdown of ITGB3 suppresses the enhancement by FGFR1 of TGF- $\beta$ 1-induced EMT in MCF10A cells [54]. Additionally, ITGB3 silencing has been reported to decrease MMP2 and MMP9 expression and reduce invasion [65, 72]. ITGB3 also increases bone metastasis [67, 73–75]. Finally, our results are consistent with data showing that genetic interference and pharmacological targeting of  $\alpha$ v integrin (the partner of ITGB3) with the non-peptide RGD antagonist GLPG0187 in different breast cancer cell lines inhibits invasion and metastasis in the zebrafish or in a mouse xenograft model. Depletion of  $\alpha$ v integrin in MDA-MB-231 cells also inhibits the expression of mesenchymal markers and the TGF- $\beta$ /Smad response [76].

ITGB3 inhibitors have shown only modest efficacy in patients with advanced solid tumours and in tumour models *in vivo*. In this respect, our results suggest that highly hypoxic tumours may be more responsive to ITGB3 therapy. Cilengitide is an antagonist of integrins and preliminary but promising results have suggested that the microenvironment plays a role in glioblastoma progression and that ITGB3 inhibitors can act in a neoadjuvant setting to prevent metastasis rather than reduce tumours once

formed [65]. Recently, other studies have used drugs to target integrin  $\alpha$ v $\beta$ 3 in glioblastoma and more recently in lung cancer [77, 78].

Finally, we demonstrated that translational activation of ITGB3 in hypoxia and hypoxia + PP242 was eIF4E dependent. During hypoxia, mTOR signalling is inhibited and translation of hypoxia-responsive genes requires alternative mechanisms, such as IRES elements [23, 79] and uORFs [80]. It is unlikely that ITGB3 is translated through an IRES-mediated mechanism because its 5'UTR is too short (21 nucleotides). Translation through HIF2a-RBM4-eIF4F<sup>H</sup>, a complex preferentially chosen by HIF target genes [25, 26], was also not implicated, because silencing of eIF4E2 (which forms part of eIF4F<sup>H</sup>) or HIF1 $\beta$  did not prevent activation of ITGB3 in hypoxia (Figure 8). Ho *et al.* [25] classify mRNAs into three classes depending on Te, with class III mRNAs, representing 15% of the transcriptome (i.e., EGFR, IGF1R), showing maintained or increased translation in hypoxia and many of the HIF target genes belonging to this class. In contrast to that study, we found that CA9 expression was independent of eIF4E2, suggesting that the eIF4F<sup>H</sup> complex is cell line dependent. Finally, we cannot discard translational regulation by microRNAs. Integrins have been shown to be downregulated by microRNAs in several studies in different types of cancer, some of which regulate ITGB3 translation, such as miR-128, which is upregulated in hypoxia [81, 82], miR-98 in hypoxia and miR-338, which inhibits migration by targeting HIF1 $\alpha$  under low-oxygen conditions [83]. Some examples in the literature are reported for other integrins, such as TGF- $\beta$ , which acts through miR-130b to increase integrin  $\alpha$ 5 expression and promote migration [84]. Several miRNAs act on ITGB3 and it is possible that one of them is expressed at a low level in hypoxia and triggers an increase in the protein under these conditions.

In summary, our findings clearly show that, under hypoxic conditions, there is a clear regulation of protein synthesis in tumourigenic and non-tumourigenic cells. ITGB3 displays enhanced translational activity in hypoxia or in hypoxia combined with mTOR inhibition. ITGB3 silencing reduced cell migration and metastasis formation, most likely by partly blocking TGF- $\beta$  pathway signalling. ITGB3 seems to play a particularly important role under hypoxic conditions and targeting of this integrin in such scenarios may provide an added therapeutic benefit

## MATERIALS AND METHODS

### Cell culture and reagents

Breast cancer and non-tumourigenic cell lines were purchased from the American Type Culture Collection (ATCC) and they were authenticated by DNA profiling using short tandem repeat (STR) (GenePrint® 10 System, Promega) at Genomics Core Facility, Instituto de Investigaciones



Biomédicas “Alberto Sols” CSIC-UAM. MDA-MB-231, MCF7, MDA-MB-468 and BT-549 cells were maintained in Dulbecco’s modified Eagle’s medium (DMEM) (Invitrogen) supplemented with 10% heat-inactivated foetal bovine serum (FBS) (Life Technologies) and antibiotics (100 U/mL penicillin, 100 µg/mL streptomycin) (Life Technologies). MCF10A cells were maintained in DMEM supplemented with 10% FBS, 20 ng/mL EGF (#E9644; Sigma), 0.5 µg/mL hydrocortisone, 100 ng/mL cholera toxin (#C9903; Sigma) and 10 µg/mL insulin (#I9278; Sigma). Cells were maintained at 37°C in a 5% CO<sub>2</sub> humidified incubator. To establish hypoxic conditions, cells were subjected to 0.5% O<sub>2</sub> in 5% CO<sub>2</sub>/95% N<sub>2</sub> and 100% humidity for 24 hours in a hypoxic chamber (INVIVO2 200; Ruskinn Technology, UK).

PP242 was purchased from Selleckchem (#S2218), reconstituted in dimethyl sulfoxide (DMSO) and used at a final concentration of 2.5 µM. Actinomycin D and TGF-β were purchased from Sigma-Aldrich and used at final concentrations of 5 µg/mL and 5 ng/mL, respectively. Cycloheximide was obtained from Sigma. Control cells were treated with the same amount of DMSO (vehicle).

#### Sucrose density gradient fractionation and polysome and total RNA purification

Polysomal mRNA was obtained by 10%–50% sucrose gradient sedimentation. Upon hypoxia or normoxia, with and without PP242 treatments, cells were washed twice with cold 1× phosphate-buffered saline (PBS) and lysed by incubation for 10 minutes on ice in polysome buffer: 1.5 mM KCl, 5 mM Tris-HCl pH 7.4, 2.5 mM MgCl<sub>2</sub>, 1% Triton X-100, 1% Na-deoxycholate, 100 µg/ml cycloheximide, 2.5 µl/mL RNAaseOut and 1× Complete Roche Protease Inhibitor. The cell lysate was centrifuged at 12,000 × g for 15 minutes at 4°C. One microgram of total protein from the supernatant was loaded onto a 10%–50% sucrose gradient, made with the BioComp Gradient Maker, and ultracentrifuged at 37,000 rpm (SW40 rotor) for 150 minutes at 4°C. The sucrose gradient was fractionated with the ISCP UV gradient fractionation system (BioComp), connected to a UV detector to monitor absorbance at 254 nm, and the polysome profile was recorded. Twelve fractions of 900 µl each were isolated and RNA was extracted using phenol:chloroform and ethanol precipitation followed by an RNeasy Mini Kit (Qiagen) for DNase treatment according to the manufacturer’s instructions. Both total RNA and polysome-bound mRNA were analysed on an Agilent Bioanalyzer to assess RNA integrity.

#### cDNA library construction, RNA sequencing (RNA-Seq) and data analysis

Total RNA was assayed for quantity and quality using Qubit® RNA HS Assay (Life Technologies) and RNA 6000 Nano Assay on a Bioanalyzer 2100 (Agilent).

The RNASeq libraries were prepared from total RNA using the TruSeq™ RNA Sample Prep Kit v2 (Illumina Inc.). Briefly, after poly-A based mRNA enrichment with oligo-dT magnetic beads from 0.5 µg of total RNA as the input material, the mRNA was fragmented (resulting RNA fragment size was 80–250 nt, with the major peak at 130 nt). After first and second strand cDNA synthesis the double stranded cDNA was end-repaired, 3’ adenylated and the Illumina barcoded adapters were ligated. The ligation product was enriched by 15 cycles of PCR.

The libraries were sequenced on HiSeq2000 (Illumina, Inc) in paired-end mode with a read length of 2 × 76 bp using the TruSeq SBS Kit v3. We generated in a mean of 37 million paired-end reads per sample, following the manufacturer’s protocol. Image analysis, base calling and quality scoring of the run were processed using the manufacturer’s software Real Time Analysis (RTA 1.13.48, HCS 1.5.15.1) and followed by generation of FASTQ sequence files by CASAVA.

The mRNA populations of each sample were converted to cDNA libraries using the TruSeq protocol and then sequenced using a HiSeq 2000 machine. Paired-end reads were mapped against the reference human genome (GRCh38) with STAR v2.5.1b (ENCODE parameters for long RNA) and GENCODE v24 annotation. Gene quantification was performed using RSEM v1.2.28 with default parameters. Only protein-coding genes were included in the analysis. Normalization of the count matrix was performed with the TMM method of the edgeR R package. Polysomal RNA (P) and RNA total (T) fold changes across conditions were calculated with edgeR. Significant genes (FDR < 5% for MCF10A cells and FDR < 10% for MDA-MB-231 cells) in polysomes were selected for translational efficiency calculation ( $\log_2(\text{FC RNA polysomes}/\log_2(\text{FC RNA total}))$ ). Genes with a z-score > 1.5 were considered to have an increased translational efficiency and genes with a z-score < -1.5 were considered to have a decreased translational efficiency. GO enrichment analysis of significant genes was performed with the DAVID database.

The data discussed in this publication have been deposited in NCBI’s Gene Expression Omnibus [85] and are accessible through GEO Series accession number GSE104193 (<https://www.ncbi.nlm.nih.gov/geo/query/acc.cgi?acc=GSE104193>).

#### qRT-PCR and NanoString

One microgram of total RNA was used to synthesize cDNA using SuperScript III Reverse Transcriptase (Life Technologies). qRT-PCR was performed on a Veriti 96-well Thermal Cycler (Applied Biosystems) using SYBR Green Technology (Applied Biosystems).

Gene	Forward 5’-3’	Reverse 5’-3’
ITGB3	CATCACCATCCA CGACCGAA	GTGCCCGGTACGTGATAT
SNAIL	CACTATGCCCGG CTCTTTC	GCTGGAAGTAACTCT GGATTAGA

VIM	CGCCAGATGCGT GAAATGG	ACCAGAGGGAGTGAATCCAGA
ECADH	CCCTCGACACCC GATTCAAA	TGGATTCCAGAAACGGAGGC
NCADH	TGTTTGACTATGAAC GCAGTGG	TCAGTCATCACCTCCACCAT
YBX1	TCGCCAAAGAC AGCCTAGAGA	TCTGCGTCGGTAATTGAAGTTG
HIFa	GAACGTCGAAAAGAA AAGTCTCG	CTTATCAAGATGCGAACTACA
Myc	TCAAGAGGGCGAA CACACAAC	GGCCTTTTCAITGTTTCCCA
MXD1	AGAAAGTTGAAGG GGCTGGTG	TCGCTGAAGCTGGTCGATT
CCND3	TGCACATGATTT CCTGGCCT	CTGTAGCACAGAGGGCCAAA
GAPDH	TGCACCACCAA CTGCTTAGC	GGCATGGACTGTGGTCATGAG
CCDN1	AGTGGAACCC ATCCGCCG	TCTGTTCTCGCAGACCTCCA
MX11	GGGTCTCAGGA GATGGAAC	TGGGAGAAGCTCTGTGCTTTCA
FLCN	AGAGTCCTCT CTCTCTCAGG	GGTCCACGTCCTCTGCTTTTC
FNIP1	CGCCTCTTCTT TGCAGITCA	GGTAGCTGTGGCACAACTT
Arde3	GCCCTCAAGG ACCACTGTT	AGGGGCAGGATGGTCTATCA
IRF9	GCTCTTCAGAA CCGCCTACTT	CCAGCAAGTATCGGGCAAAG
ADIRF	TTGCAGGACCT GAAGCAACA	TGGTTTCTGGTGGTCTTG
PTGS2	AGATCATAAGC GAGGGCCAG	GGCGCAGTTTACGCTGTCTA
DLL1	CGTGGGGAGAA AGTGTGCAA	CTCTGCACTTGCACTCCCT
BMP2	ATGGATTGCTG GTGGAGTG	GTGGAGTTCAGATGATCAGC
Actin	GCAAAGACCTGTAC GCCAAC	AGTACTTGCCTCAGGAGGA

### Knockdown analysis using siRNA transfection

Small interfering RNA (siRNA) of HOXB3, JAG2, MX11, PTGFR, RORA, ITGB3, IRF9, EGFP (esiRNA; Sigma), eIF4E, ARNT and eIF4E2 (Dharmacon Research, Inc.) were transfected at a final concentration of 10 nM using RNAi MAX Lipofectamine (Invitrogen). After 48 hours of transfection, cells were seeded for MTT assays, migration assays or western blot analysis.

### Modulation of expression using retroviral and lentiviral infection

For lentiviral shRNA of ITGB3, pLKO.1-puro-shITGB3 was constructed by annealing the oligonucleotides 5'-ccgggccaagactcatatagcattgctcga-3' and 5'-aattcaaaaagccaagactcatatagcatt-3' and cloning them into a pLKO1 vector. The shITGB3 #3 was obtained from Dharmacon. We also used pLKO1 as shCTL. MGC Human ITGB3 Sequende-Verifie cDNA (CloneId: 40128462) was

obtained from Dharmacon and was subcloned into pLPCX retroviral plasmid after annealing of the oligonucleotides 5'-CTTAGATCTA CCATGCGAGC GCGGCCGCGG CCC-3' and 5'-GGTAAGCTTT TAAGTGCCCC GGT ACGTGAT ATT-3'. Production of lentiviruses and retroviruses and their infection of target cells were performed as previously described [86]. Infected MDA-MB-231 and MCF10A cells were selected with 0.7 µg/mL or 1.5 µg/mL puromycin for 3–4 days, respectively. Viral production and infection were performed at 37°C. All of these plasmids were sequenced twice from both ends to ensure expression of the correct coding sequence.

### MTT assays

MTT (3-[4,5-dimethylthiazol-25-yl]-2,5-diphenyltetrazolium bromide; Sigma) was added to the medium to a final concentration of 0.5 mg/mL and incubated for 4 hours at 37°C. The medium was then removed and 0.2 mL DMSO was added. Absorbance was measured at 590 nm by using a Synergy spectrophotometer (Biotek). Readings were taken 0, 24, 48, 72 and 96 hours after cell treatment.

### Migration assays

Cells were plated in 24-well plates in triplicate. After 24 hours, the cells were treated overnight with mitomycin C (5 µg/mL, Santa Cruz Biotechnology). Then, a wound was made in the monolayer with a pipette tip, the medium was replaced and the cells were incubated under normoxic or hypoxic conditions. Pictures of the wounds were taken 0, 8 and 24 hours after treatment initiation, and wound closure was measured using ImageJ software.

### Caspase assays

To measure caspase-3 and -7 activity, the Caspase-Glo 3/7 Assay (Promega) was used. Five thousand cells in 200 µL were seeded in black-walled 96-well plates and subjected to normoxia or hypoxia for 48 hours. Then, 100 µL Caspase-Glo 3/7 reagent was added to each well and the cells were incubated at room temperature for 1 hour. Luminescence was measured using a Synergy Mx Monochromator-Based Multi-Mode Microplate Reader.

### Protein extraction and immunoblotting

Total protein extracts were generated using lysis buffer (50 mM Tris-HCl, pH 7.4, 150 mM NaCl, 1% Triton X-100, 1% sodium deoxycholate, 0.1% SDS, 1 mM EDTA) supplemented with PhosSTOP and Complete Phosphatase/Protease Inhibitor Cocktails (Roche Diagnostics GmbH, Mannheim, Germany). Protein extracts (20–25 µg per sample) were loaded onto SDS-PAGE gels and transferred electrophoretically to PVDF membranes and immunodetection of proteins was performed using ECL™

Western Blotting Detection Reagents (GE Healthcare, Buckinghamshire, UK). The following primary antibodies were used: anti-Myc, anti-HIF1 $\alpha$ , anti-4EBP1, anti-eIF4E, anti-YBX1, anti-Snail, anti-CA9, anti-Smad2/3, anti- $\alpha$ -catenin (Cell Signaling), anti-phospho Smad2 (Millipore), anti- $\beta$ 3 integrin, anti-MMP3, anti-N-cadherin (Abcam), anti-CycD1, anti-vimentin (Santa Cruz Biotechnology), anti-BMP2, anti-CCDC103, anti-TTC30B, anti-EIF3G, anti-RPL11 (CusaBio), anti-Cx31 (Alpha Diagnostics), anti-eIF4E2 (GeneTex), anti- $\alpha$ v integrin and anti- $\beta$ -actin (1:500; Calbiochem, Darmstadt, Germany). Anti-mouse and anti-rabbit HRP secondary antibodies were from Pierce. Bound antibodies were visualized with an enhanced chemiluminescence detection kit (Amersham Pharma-Biotech).

### Animal study

Female athymic nude mice (Harlan Interfauna Iberica, Barcelona, Spain) were kept in pathogen-free conditions and used at 7 weeks of age. Animal care was handled in accordance with the Guide for the Care and Use of Laboratory Animals of the Vall d'Hebron University Hospital Animal Facility, and the experimental procedures were approved by the Animal Experimentation Ethical Committee at the institution. All of the *in vivo* studies were performed by the ICTS 'NANBIOSIS', more specifically at the CIBER-BBN *in vivo* Experimental Platform of the Functional Validation & Preclinical Research (FVPR) area (<http://www.nanbiosis.es/portfolio/u20-in-vivo-experimental-platform/>) (Barcelona, Spain).

Mice received an intravenous injection of tumour cells (MDA-MB-231 parental cells or MDA-MB-231-shITGB3,  $2 \times 10^6$  cells per inoculum) into the left caudal tail vein. Animals' body weight and physical appearance were measured twice a week. Two set of experiments were performed. To record animal survival after inoculation, animals were kept alive until they met the established ethical criteria (in accordance with the protocol approved by the Experimental Animal Ethics Committee). In the second set of experiments, all animals were euthanized 36 days after inoculation to compare the number and extent of the lung metastases between groups. In these experiments, the lungs were collected, weighed and fixed with Bouin's solution. The number and size of lung metastases were quantified macroscopically using a stereoscopic microscope. Lungs were processed later for histopathological analyses.

### Statistics

Results are expressed as means + standard errors of the means. The two-tailed Student's *t*-test was used for statistical analysis.  $P < 0.05$  was considered significant. To analyse the distributions of qualitative variables, the Pearson coefficient was used.

### Abbreviations

CTL: Control; EGFR: Epidermal growth factor receptor; eIF4F: Eukaryotic initiation factor 4F; EMT: epithelial to mesenchymal transition; GO: Gene Ontology; H: Hypoxia; HER2: human epidermal growth factor receptor type 2; HIF1 $\alpha$ : hypoxia-inducible factor 1; HPP: Hypoxia + PP242; IRES: Internal Ribosome Entry Site; ITGB3: Integrin Beta 3; mTOR: mechanistic target of rapamycin; N: Normoxia; NPP: Normoxia + PP242; PAM50: Prediction Analysis of Microarray 50; PCA: principal component analysis; qRT-PCR: Quantitative reverse transcription PCR; RNA-Seq: high-throughput RNA sequencing; shRNA: short interfering RNA; siRNA: short hairpin RNA; TGF- $\beta$ : Transforming growth factor beta; TNBC: Triple-negative breast cancer; UTR: untranslated region.

### Author contributions

conception and design: M. Sesé, S. Ramón y Cajal, T. Aasen. Development of methodology: M. Sesé, E. Béjar, P. Fuentes, K. McGrail. Acquisition of data: M. Sesé, P. Fuentes, K. McGrail, A. Esteve-Codina, G. Thomas. Analysis and interpretation of data: M. Sesé, P. Fuentes, A. Esteve-Codina, T. Aasen. Writing: M. Sesé. Review and/or revision of manuscript: M. Sesé, T. Aasen, S. Ramón y Cajal, A. Esteve-Codina, G. Thomas, P. Fuentes. Study supervision: S. Ramón y Cajal, T. Aasen, M. Sesé.

### ACKNOWLEDGMENTS AND FUNDING

The authors thank Antonio Gentilella for his excellent technical assistance. We also thank Anna Rosell, Ibane Abasolo, Yolanda Fernández and Joan Seoane for technical advice. We appreciate the helpful comments and suggestions of Ivan Topisirovic and Javier Hernández. This work was supported by Fondo de Investigaciones Sanitarias (PI14/01320), Redes Temáticas de Investigación Cooperativa en Salud (RD12/0036/0057) and CIBERONC (CB16/12/00363). TA acknowledges support from Instituto de Salud Carlos III grants PI13/00763, PI16/00772 and CPII16/00042, co-financed by the European Regional Development Fund (ERDF). SRC acknowledges support from the Generalitat de Catalunya (2014 SGR 1131). The CNAG-CRG laboratory is a member of the Spanish National Bioinformatics Institute (INB), PRB2-ISCI and is supported by grant PT13/0001 of the PE I+D+i 2013-2016 funded by ISCI and FEDER.

### CONFLICTS OF INTEREST

The authors declare they have no competing interests.



## REFERENCES

1. Ferlay J, Autier P, Boniol M, Heanue M, Colombet M, Boyle P. Estimates of the cancer incidence and mortality in Europe in 2006. *Ann Oncol.* 2007; 18:581–92. <https://doi.org/10.1093/annonc/mdl498>.
2. Chen WY, Colditz GA. Risk factors and hormone-receptor status: epidemiology, risk-prediction models and treatment implications for breast cancer. *Nat Clin Pract Oncol.* 2007; 4:415–23. <https://doi.org/10.1038/nponc0851>.
3. Bianchini G, Balko JM, Mayer IA, Sanders ME, Gianni L. Triple-negative breast cancer: challenges and opportunities of a heterogeneous disease. *Nat Rev Clin Oncol.* 2016; 13:674–90. <https://doi.org/10.1038/nrclinonc.2016.66>.
4. Chen X, Xiopoulos D, Zhang Q, Tang Q, Greenblatt MB, Hatziapostolou M, Lim E, Tam WL, Ni M, Chen Y, Mai J, Shen H, Hu DZ, et al. XBP1 promotes triple-negative breast cancer by controlling the HIF1alpha pathway. *Nature.* 2014; 508:103–7. <https://doi.org/10.1038/nature13119>.
5. Semenza GL. Hypoxia-inducible factor 1: oxygen homeostasis and disease pathophysiology. *Trends Mol Med.* 2001; 7:345–50.
6. Muz B, de la Puente P, Azab F, Azab AK. The role of hypoxia in cancer progression, angiogenesis, metastasis, and resistance to therapy. *Hypoxia (Auckl).* 2015; 3:83–92. <https://doi.org/10.2147/HP.S93413>.
7. Wang GL, Jiang BH, Rue EA, Semenza GL. Hypoxia-inducible factor 1 is a basic-helix-loop-helix-PAS heterodimer regulated by cellular O2 tension. *Proc Natl Acad Sci U S A.* 1995; 92:5510–4.
8. Liu ZJ, Semenza GL, Zhang HF. Hypoxia-inducible factor 1 and breast cancer metastasis. *J Zhejiang Univ Sci B.* 2015; 16:32–43. <https://doi.org/10.1631/jzus.B1400221>.
9. Connolly E, Braunstein S, Formenti S, Schneider RJ. Hypoxia inhibits protein synthesis through a 4E-BP1 and elongation factor 2 kinase pathway controlled by mTOR and uncoupled in breast cancer cells. *Mol Cell Biol.* 2006; 26:3955–65. <https://doi.org/10.1128/MCB.26.10.3955-3965.2006>.
10. Liu L, Cash TP, Jones RG, Keith B, Thompson CB, Simon MC. Hypoxia-induced energy stress regulates mRNA translation and cell growth. *Mol Cell.* 2006; 21:521–31. <https://doi.org/10.1016/j.molcel.2006.01.010>.
11. Ward C, Meehan J, Mullen P, Supuran C, Dixon JM, Thomas JS, Winum JY, Lambin P, Dubois L, Pavathaneni NK, Jarman EJ, Renshaw L, Um IH, et al. Evaluation of carbonic anhydrase IX as a therapeutic target for inhibition of breast cancer invasion and metastasis using a series of *in vitro* breast cancer models. *Oncotarget.* 2015; 6:24856–70. <https://doi.org/10.18632/oncotarget.4498>.
12. Weber G, Lea MA. The molecular correlation concept of neoplasia. *Adv Enzyme Regul.* 1966; 4:115–45.
13. Bilanges B, Stokoe D. Mechanisms of translational deregulation in human tumors and therapeutic intervention strategies. *Oncogene.* 2007; 26:5973–90. <https://doi.org/10.1038/sj.onc.1210431>.
14. Stumpf CR, Ruggero D. The cancerous translation apparatus. *Curr Opin Genet Dev.* 2011; 21:474–83. <https://doi.org/10.1016/j.gde.2011.03.007>.
15. Nandagopal N, Roux PP. Regulation of global and specific mRNA translation by the mTOR signaling pathway. *Translation (Austin).* 2015; 3:e983402. <https://doi.org/10.4161/21690731.2014.983402>.
16. Sonenberg N, Hinnebusch AG. Regulation of translation initiation in eukaryotes: mechanisms and biological targets. *Cell.* 2009; 136:731–45. <https://doi.org/10.1016/j.cell.2009.01.042>.
17. Jackson RJ, Hellen CU, Pestova TV. The mechanism of eukaryotic translation initiation and principles of its regulation. *Nat Rev Mol Cell Biol.* 2010; 11:113–27. <https://doi.org/10.1038/nrm2838>.
18. Loewith R, Jacinto E, Wullschlegel S, Lorberg A, Crespo JL, Bonenfant D, Oppliger W, Jenoe P, Hall MN. Two TOR complexes, only one of which is rapamycin sensitive, have distinct roles in cell growth control. *Mol Cell.* 2002; 10:457–68.
19. Hay N, Sonenberg N. Upstream and downstream of mTOR. *Genes Dev.* 2004; 18:1926–45. <https://doi.org/10.1101/gad.1212704>.
20. Brown EJ, Beal PA, Keith CT, Chen J, Shin TB, Schreiber SL. Control of p70 s6 kinase by kinase activity of FRAP *in vivo*. *Nature.* 1995; 377:441–6. <https://doi.org/10.1038/377441a0>.
21. Gingras AC, Kennedy SG, O’Leary MA, Sonenberg N, Hay N. 4E-BP1, a repressor of mRNA translation, is phosphorylated and inactivated by the Akt(PKB) signaling pathway. *Genes Dev.* 1998; 12:502–13.
22. Pause A, Belsham GJ, Gingras AC, Donze O, Lin TA, Lawrence JC Jr, Sonenberg N. Insulin-dependent stimulation of protein synthesis by phosphorylation of a regulator of 5’-cap function. *Nature.* 1994; 371:762–7. <https://doi.org/10.1038/371762a0>.
23. Holcik M, Sonenberg N. Translational control in stress and apoptosis. *Nat Rev Mol Cell Biol.* 2005; 6:318–27. <https://doi.org/10.1038/nrm1618>.
24. Koritzinsky M, Magagnin MG, van den Beucken T, Seigneuric R, Savelkouls K, Dostie J, Pyronnet S, Kaufman RJ, Weppler SA, Voncken JW, Lambin P, Koumenis C, Sonenberg N, et al. Gene expression during acute and prolonged hypoxia is regulated by distinct mechanisms of translational control. *EMBO J.* 2006; 25:1114–25. <https://doi.org/10.1038/sj.emboj.7600998>.
25. Ho JJ, Wang M, Audas TE, Kwon D, Carlsson SK, Timpano S, Evagelou SL, Brothers S, Gonzalzo ML, Krieger JR, Chen S, Uniacke J, Lee S. Systemic Reprogramming of Translation Efficiency on Oxygen Stimulus. *Cell Rep.* 2016; 14:1293–300. <https://doi.org/10.1016/j.celrep.2016.01.036>.

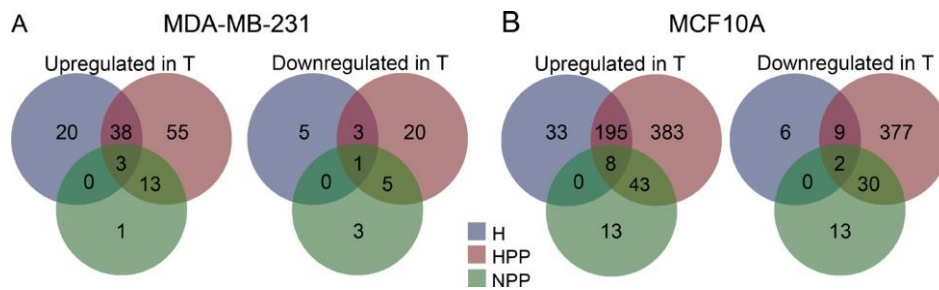
26. Uniacke J, Holterman CE, Lachance G, Franovic A, Jacob MD, Fabian MR, Payette J, Holcik M, Pause A, Lee S. An oxygen-regulated switch in the protein synthesis machinery. *Nature*. 2012; 486:126–9. <https://doi.org/10.1038/nature11055>.
27. Pawlus MR, Wang L, Ware K, Hu CJ. Upstream stimulatory factor 2 and hypoxia-inducible factor 2alpha (HIF2alpha) cooperatively activate HIF2 target genes during hypoxia. *Mol Cell Biol*. 2012; 32:4595–610. <https://doi.org/10.1128/MCB.00724-12>.
28. Braunstein S, Karpisheva K, Pola C, Goldberg J, Hochman T, Yee H, Cangiarella J, Arju R, Formenti SC, Schneider RJ. A hypoxia-controlled cap-dependent to cap-independent translation switch in breast cancer. *Mol Cell*. 2007; 28:501–12. <https://doi.org/10.1016/j.molcel.2007.10.019>.
29. Walters B, Thompson SR. Cap-Independent Translational Control of Carcinogenesis. *Front Oncol*. 2016; 6:128. <https://doi.org/10.3389/fonc.2016.00128>.
30. Komar AA, Hatzoglou M. Cellular IRES-mediated translation: the war of ITAFs in pathophysiological states. *Cell Cycle*. 2011; 10:229–40. <https://doi.org/10.4161/cc.10.2.14472>.
31. Leprivier G, Rotblat B, Khan D, Jan E, Sorensen PH. Stress-mediated translational control in cancer cells. *Biochim Biophys Acta*. 2015; 1849:845–60. <https://doi.org/10.1016/j.bbagg.2014.11.002>.
32. Faye MD, Graber TE, Holcik M. Assessment of selective mRNA translation in mammalian cells by polysome profiling. *J Vis Exp*. 2014; e52295. <https://doi.org/10.3791/52295>.
33. Thomas JD, Johannes AJ. Identification of mRNAs that continue to associate with polysomes during hypoxia. *RNA*. 2007; 13:1116–31. <https://doi.org/10.1261/rna.534807>.
34. van den Beucken T, Koritzinsky M, Wouters BG. Translational control of gene expression during hypoxia. *Cancer Biol Ther*. 2006; 5:749–55.
35. Miloslavski R, Cohen E, Avraham A, Iluz Y, Hayouka Z, Kasir J, Mudhasani R, Jones SN, Cybulski N, Ruegg MA, Larsson O, Gandin V, Rajakumar A, et al. Oxygen sufficiency controls TOP mRNA translation via the TSC-Rheb-mTOR pathway in a 4E-BP-independent manner. *J Mol Cell Biol*. 2014; 6:255–66. <https://doi.org/10.1093/jmcb/mju008>.
36. Thoreen CC, Chantranupong L, Keys HR, Wang T, Gray NS, Sabatini DM. A unifying model for mTORC1-mediated regulation of mRNA translation. *Nature*. 2012; 485:109–13. <https://doi.org/10.1038/nature11083>.
37. Hsieh AC, Liu Y, Edlind MP, Ingolia NT, Janes MR, Sher A, Shi EY, Stumpf CR, Christensen C, Bonham MJ, Wang S, Ren P, Martin M, et al. The translational landscape of mTOR signalling steers cancer initiation and metastasis. *Nature*. 2012; 485:55–61. <https://doi.org/10.1038/nature10912>.
38. Cary LA, Han DC, Guan JL. Integrin-mediated signal transduction pathways. *Histol Histopathol*. 1999; 14:1001–9.
39. Taverna D, Crowley D, Connolly M, Bronson RT, Hynes RO. A direct test of potential roles for beta3 and beta5 integrins in growth and metastasis of murine mammary carcinomas. *Cancer Res*. 2005; 65:10324–9. <https://doi.org/10.1158/0008-5472.CAN-04-4098>.
40. Brooks PC, Montgomery AM, Rosenfeld M, Reisfeld RA, Hu T, Klier G, Cheresh DA. Integrin alpha v beta 3 antagonists promote tumor regression by inducing apoptosis of angiogenic blood vessels. *Cell*. 1994; 79:1157–64.
41. Brooks PC, Clark RA, Cheresh DA. Requirement of vascular integrin alpha v beta 3 for angiogenesis. *Science*. 1994; 264:569–71.
42. Brooks PC. Role of integrins in angiogenesis. *Eur J Cancer*. 1996; 32A:2423–9.
43. Varner JA, Brooks PC, Cheresh DA. REVIEW: the integrin alpha V beta 3: angiogenesis and apoptosis. *Cell Adhes Commun*. 1995; 3:367–74.
44. Furger KA, Allan AL, Wilson SM, Hota C, Vantyghem SA, Postenka CO, Al-Katib W, Chambers AF, Tuck AB. Beta(3) integrin expression increases breast carcinoma cell responsiveness to the malignancy-enhancing effects of osteopontin. *Mol Cancer Res*. 2003; 1:810–9.
45. Lo PK, Kanojia D, Liu X, Singh UP, Berger FG, Wang Q, Chen H. CD49f and CD61 identify Her2/neu-induced mammary tumor-initiating cells that are potentially derived from luminal progenitors and maintained by the integrin-TGFbeta signaling. *Oncogene*. 2012; 31:2614–26. <https://doi.org/10.1038/onc.2011.439>.
46. Vaillant F, Asselin-Labat ML, Shackleton M, Forrest NC, Lindeman GJ, Visvader JE. The mammary progenitor marker CD61/beta3 integrin identifies cancer stem cells in mouse models of mammary tumorigenesis. *Cancer Res*. 2008; 68:7711–7. <https://doi.org/10.1158/0008-5472.CAN-08-1949>.
47. Toschi A, Lee E, Gadir N, Ohh M, Foster DA. Differential dependence of hypoxia-inducible factors 1 alpha and 2 alpha on mTORC1 and mTORC2. *J Biol Chem*. 2008; 283:34495–9. <https://doi.org/10.1074/jbc.C800170200>.
48. Dennis PB, Fumagalli S, Thomas G. Target of rapamycin (TOR): balancing the opposing forces of protein synthesis and degradation. *Curr Opin Genet Dev*. 1999; 9:49–54.
49. Ruvinsky I, Meyuhas O. Ribosomal protein S6 phosphorylation: from protein synthesis to cell size. *Trends Biochem Sci*. 2006; 31:342–8. <https://doi.org/10.1016/j.tibs.2006.04.003>.
50. Prat A, Parker JS, Fan C, Perou CM. PAM50 assay and the three-gene model for identifying the major and clinically relevant molecular subtypes of breast cancer. *Breast Cancer Res Treat*. 2012; 135:301–6. <https://doi.org/10.1007/s10549-012-2143-0>.
51. Parker JS, Mullins M, Cheang MC, Leung S, Voduc D, Vickery T, Davies S, Fauron C, He X, Hu Z, Quackenbush JF, Stijleman IJ, Palazzo J, et al. Supervised risk predictor of breast cancer based on intrinsic subtypes. *J*

- Clin Oncol. 2009; 27:1160–7. <https://doi.org/10.1200/JCO.2008.18.1370>.
52. Geiss GK, Bumgarner RE, Birditt B, Dahl T, Dowidar N, Dunaway DL, Fell HP, Ferree S, George RD, Grogan T, James JJ, Maysuria M, Mitton JD, et al. Direct multiplexed measurement of gene expression with color-coded probe pairs. *Nat Biotechnol.* 2008; 26:317–25. <https://doi.org/10.1038/nbt1385>.
  53. Galliher AJ, Schiemann WP. Beta3 integrin and Src facilitate transforming growth factor-beta mediated induction of epithelial-mesenchymal transition in mammary epithelial cells. *Breast Cancer Res.* 2006; 8:R42. <https://doi.org/10.1186/bcr1524>.
  54. Mori S, Kodaira M, Ito A, Okazaki M, Kawaguchi N, Hamada Y, Takada Y, Matsuura N. Enhanced Expression of Integrin alphavbeta3 Induced by TGF-beta Is Required for the Enhancing Effect of Fibroblast Growth Factor 1 (FGF1) in TGF-beta-Induced Epithelial-Mesenchymal Transition (EMT) in Mammary Epithelial Cells. *PLoS One.* 2015; 10:e0137486. <https://doi.org/10.1371/journal.pone.0137486>.
  55. Larsson O, Morita M, Topisirovic I, Alain T, Blouin MJ, Pollak M, Sonenberg N. Distinct perturbation of the transcriptome by the antidiabetic drug metformin. *Proc Natl Acad Sci U S A.* 2012; 109:8977–82. <https://doi.org/10.1073/pnas.1201689109>.
  56. Schwanhauser B, Busse D, Li N, Dittmar G, Schuchhardt J, Wolf J, Chen W, Selbach M. Global quantification of mammalian gene expression control. *Nature.* 2011; 473:337–42. <https://doi.org/10.1038/nature10098>.
  57. Koritzinsky M, Seigneuric R, Magagnin MG, van den Beucken T, Lambin P, Wouters BG. The hypoxic proteome is influenced by gene-specific changes in mRNA translation. *Radiother Oncol.* 2005; 76:177–86. <https://doi.org/10.1016/j.radonc.2005.06.036>.
  58. Lai MC, Chang CM, Sun HS. Hypoxia Induces Autophagy through Translational Up-Regulation of Lysosomal Proteins in Human Colon Cancer Cells. *PLoS One.* 2016; 11:e0153627. <https://doi.org/10.1371/journal.pone.0153627>.
  59. Higgins DF, Kimura K, Bernhardt WM, Shrimanker N, Akai Y, Hohenstein B, Saito Y, Johnson RS, Kretzler M, Cohen CD, Eckardt KU, Iwano M, Haase VH. Hypoxia promotes fibrogenesis *in vivo* via HIF-1 stimulation of epithelial-to-mesenchymal transition. *J Clin Invest.* 2007; 117:3810–20. <https://doi.org/10.1172/JCI30487>.
  60. Copple BL. Hypoxia stimulates hepatocyte epithelial to mesenchymal transition by hypoxia-inducible factor and transforming growth factor-beta-dependent mechanisms. *Liver Int.* 2010; 30:669–82. <https://doi.org/10.1111/j.1478-3231.2010.02205.x>.
  61. Moon JO, Welch TP, Gonzalez FJ, Copple BL. Reduced liver fibrosis in hypoxia-inducible factor-1alpha-deficient mice. *Am J Physiol Gastrointest Liver Physiol.* 2009; 296:G582–92. <https://doi.org/10.1152/ajpgi.90368.2008>.
  62. Abdul-Hafez A, Shu R, Uhal BD. JunD and HIF-1alpha mediate transcriptional activation of angiotensinogen by TGF-beta1 in human lung fibroblasts. *FASEB J.* 2009; 23:1655–62. <https://doi.org/10.1096/fj.08-114611>.
  63. Kaper F, Dornhoefer N, Giaccia AJ. Mutations in the PI3K/PTEN/TSC2 pathway contribute to mammalian target of rapamycin activity and increased translation under hypoxic conditions. *Cancer Res.* 2006; 66:1561–9. <https://doi.org/10.1158/0008-5472.CAN-05-3375>.
  64. Skuli N, Monferran S, Delmas C, Favre G, Bonnet J, Toulas C, Cohen-Jonathan Moyal E. Alphavbeta3/alphavbeta5 integrins-FAK-RhoB: a novel pathway for hypoxia regulation in glioblastoma. *Cancer Res.* 2009; 69:3308–16. <https://doi.org/10.1158/0008-5472.CAN-08-2158>.
  65. Liu Z, Han L, Dong Y, Tan Y, Li Y, Zhao M, Xie H, Ju H, Wang H, Zhao Y, Zheng Q, Wang Q, Su J, et al. EGFRvIII/integrin beta3 interaction in hypoxic and vitronectin-enriching microenvironment promote GBM progression and metastasis. *Oncotarget.* 2016; 7:4680–94. <https://doi.org/10.18632/oncotarget.6730>.
  66. Khong TL, Thairu N, Larsen H, Dawson PM, Kiriakidis S, Paleolog AE. Identification of the angiogenic gene signature induced by EGF and hypoxia in colorectal cancer. *BMC Cancer.* 2013; 13:518. <https://doi.org/10.1186/1471-2407-13-518>.
  67. Felding-Habermann B, O'Toole TE, Smith JW, Fransvea E, Ruggeri ZM, Ginsberg MH, Hughes PE, Pampori N, Shattil SJ, Saven A, Mueller BM. Integrin activation controls metastasis in human breast cancer. *Proc Natl Acad Sci U S A.* 2001; 98:1853–8. <https://doi.org/10.1073/pnas.98.4.1853>.
  68. Vellon L, Menendez JA, Lupu R. AlphaVbeta3 integrin regulates heregulin (HRG)-induced cell proliferation and survival in breast cancer. *Oncogene.* 2005; 24:3759–73. <https://doi.org/10.1038/sj.onc.1208452>.
  69. Menendez JA, Vellon L, Mehmi I, Teng PK, Griggs DW, Lupu R. A novel CYR61-triggered 'CYR61-alphavbeta3 integrin loop' regulates breast cancer cell survival and chemosensitivity through activation of ERK1/ERK2 MAPK signaling pathway. *Oncogene.* 2005; 24:761–79. <https://doi.org/10.1038/sj.onc.1208238>.
  70. Wu FH, Luo LQ, Liu Y, Zhan QX, Luo C, Luo J, Zhang GM, Feng ZH. Cyclin D1b splice variant promotes alphavbeta3-mediated adhesion and invasive migration of breast cancer cells. *Cancer Lett.* 2014; 355:159–67. <https://doi.org/10.1016/j.canlet.2014.08.044>.
  71. Carter RZ, Micocci KC, Natoli A, Redvers RP, Paquet-Fified S, Martin AC, Denoyer D, Ling X, Kim SH, Tomasin R, Selistre-de-Araujo H, Anderson RL, Pouliot N. Tumour but not stromal expression of beta3 integrin is essential, and is required early, for spontaneous dissemination of bone-metastatic breast cancer. *J Pathol.* 2015; 235:760–72. <https://doi.org/10.1002/path.4490>.

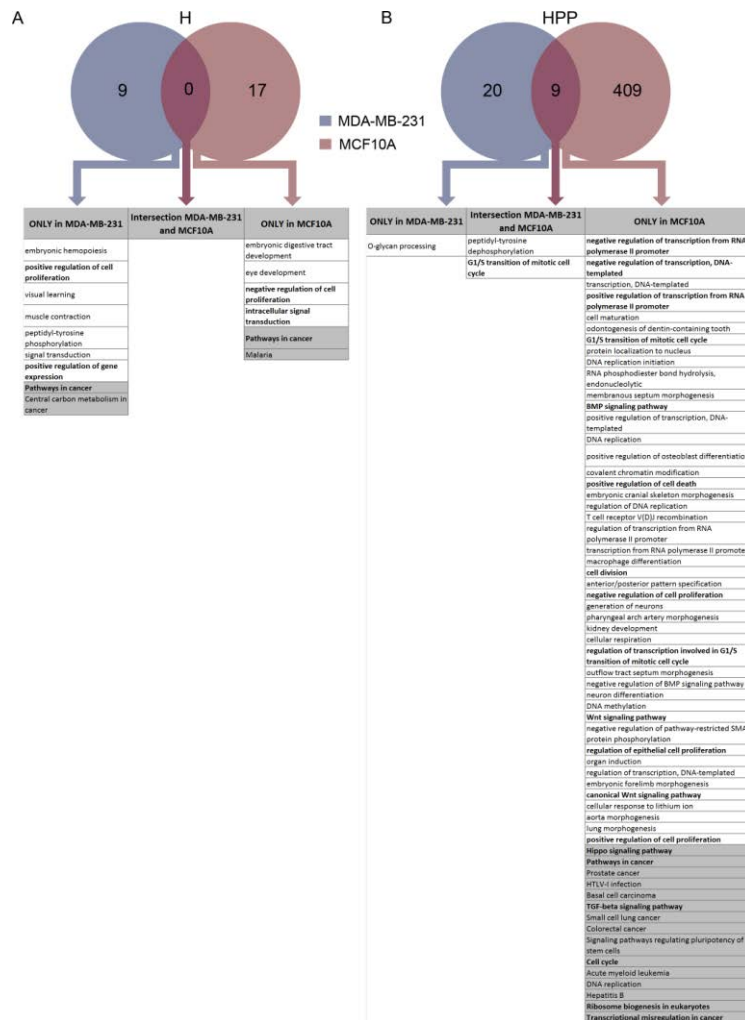
72. Parvani JG, Gujrati MD, Mack MA, Schiemann WP, Lu ZR. Silencing beta3 Integrin by Targeted ECO/siRNA Nanoparticles Inhibits EMT and Metastasis of Triple-Negative Breast Cancer. *Cancer Res.* 2015; 75:2316–25. <https://doi.org/10.1158/0008-5472.CAN-14-3485>.
73. Takayama S, Ishii S, Ikeda T, Masamura S, Doi M, Kitajima M. The relationship between bone metastasis from human breast cancer and integrin alpha(v)beta3 expression. *Anticancer Res.* 2005; 25:79–83.
74. Sloan EK, Pouliot N, Stanley KL, Chia J, Moseley JM, Hards DK, Anderson RL. Tumor-specific expression of alphavbeta3 integrin promotes spontaneous metastasis of breast cancer to bone. *Breast Cancer Res.* 2006; 8:R20. <https://doi.org/10.1186/bcr1398>.
75. Liapis H, Flath A, Kitazawa S. Integrin alpha V beta 3 expression by bone-residing breast cancer metastases. *Diagn Mol Pathol.* 1996; 5:127–35.
76. Li Y, Drabsch Y, Pujuguet P, Ren J, van Laar T, Zhang L, van Dam H, Clement-Lacroix P, Ten Dijke P. Genetic depletion and pharmacological targeting of alphav integrin in breast cancer cells impairs metastasis in zebrafish and mouse xenograft models. *Breast Cancer Res.* 2015; 17:28. <https://doi.org/10.1186/s13058-015-0537-8>.
77. Kang W, Svirskis D, Sarojini V, McGregor AL, Bevitt J, Wu Z. Cyclic-RGDyC functionalized liposomes for dual-targeting of tumor vasculature and cancer cells in glioblastoma: An *in vitro* boron neutron capture therapy study. *Oncotarget.* 2017; 8:36614–27. <https://doi.org/10.18632/oncotarget.16625>.
78. Pelaez R, Morales X, Salvo E, Garasa S, Ortiz de Solorzano C, Martinez A, Larrayoz IM, Rouzaut A. beta3 integrin expression is required for invadopodia-mediated ECM degradation in lung carcinoma cells. *PLoS One.* 2017; 12:e0181579. <https://doi.org/10.1371/journal.pone.0181579>.
79. Pelletier J, Sonenberg N. Internal initiation of translation of eukaryotic mRNA directed by a sequence derived from poliovirus RNA. *Nature.* 1988; 334:320–5. <https://doi.org/10.1038/334320a0>.
80. Blais JD, Filipenko V, Bi M, Harding HP, Ron D, Koumenis C, Wouters BG, Bell JC. Activating transcription factor 4 is translationally regulated by hypoxic stress. *Mol Cell Biol.* 2004; 24:7469–82. <https://doi.org/10.1128/MCB.24.17.7469-7482.2004>.
81. Shi ZM, Wang J, Yan Z, You YP, Li CY, Qian X, Yin Y, Zhao P, Wang YY, Wang XF, Li MN, Liu LZ, Liu N, et al. MiR-128 inhibits tumor growth and angiogenesis by targeting p70S6K1. *PLoS One.* 2012; 7:e32709. <https://doi.org/10.1371/journal.pone.0032709>.
82. Tao T, Li G, Dong Q, Liu D, Liu C, Han D, Huang Y, Chen S, Xu B, Chen M. Loss of SNAIL inhibits cellular growth and metabolism through the miR-128-mediated RPS6KB1/HIF-1alpha/PKM2 signaling pathway in prostate cancer cells. *Tumour Biol.* 2014; 35:8543–50. <https://doi.org/10.1007/s13277-014-2057-z>.
83. Shan Y, Li X, You B, Shi S, Zhang Q, You Y. MicroRNA-338 inhibits migration and proliferation by targeting hypoxia-induced factor 1alpha in nasopharyngeal carcinoma. *Oncol Rep.* 2015; 34:1943–52. <https://doi.org/10.3892/or.2015.4195>.
84. Yi R, Li Y, Wang F, Gu J, Isaji T, Li J, Qi R, Zhu X, Zhao Y. Transforming growth factor (TGF) beta1 acted through miR-130b to increase integrin alpha5 to promote migration of colorectal cancer cells. *Tumour Biol.* 2016; 37:10763–73. <https://doi.org/10.1007/s13277-016-4965-6>.
85. Edgar R, Domrachev M, Lash AE. Gene Expression Omnibus: NCBI gene expression and hybridization array data repository. *Nucleic Acids Res.* 2002; 30:207–10.
86. Pons B, Peg V, Vazquez-Sanchez MA, Lopez-Vicente L, Argelaguet E, Coch L, Martinez A, Hernandez-Losa J, Armengol G, Ramon Y Cajal S. The effect of p-4E-BP1 and p-eIF4E on cell proliferation in a breast cancer model. *Int J Oncol.* 2011; 39:1337–45. <https://doi.org/10.3892/ijo.2011.1118>.

**Hypoxia-mediated translational activation of ITGB3 in breast cancer cells enhances TGF- $\beta$  signaling and malignant features *in vitro* and *in vivo***

**SUPPLEMENTARY MATERIALS**



**Supplementary Figure 1:** Venn diagrams showing the distribution of transcriptionally deregulated genes in H, HPP and NPP in MDA-MB-231 (A) and MCF10A (B) cell lines.

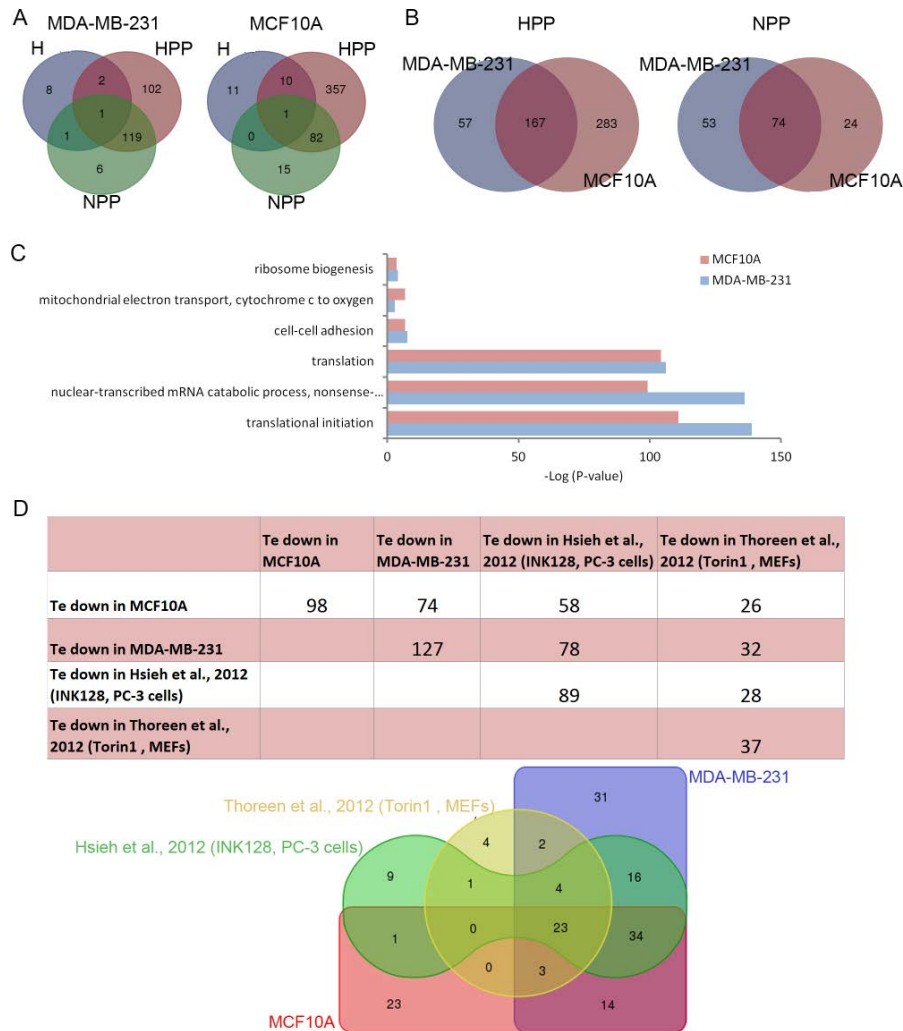


**Supplementary Figure 2: Analysis of transcriptionally downregulated genes under hypoxic and hypoxic + PP242 conditions. (A)** Venn diagram with the distribution of transcripts downregulated in hypoxia. A table showing the main GO categories (with  $P < 0.03$ ) and Kegg pathways (with  $P < 0.03$ ) associated with each cell line. **(B)** Venn diagram with the distribution of transcripts downregulated in hypoxia + PP242. A table showing the main GO categories (with  $P < 0.03$ ) and Kegg pathways (with  $P < 0.03$ ) associated with each cell line.



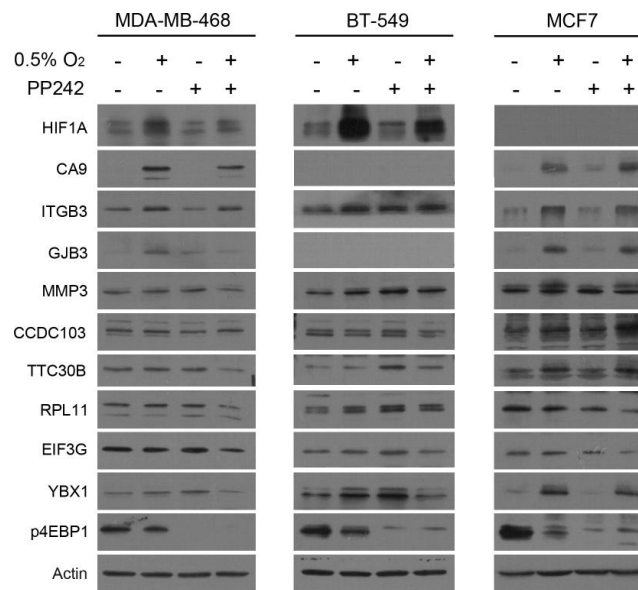


**Supplementary Figure 3: Analysis of transcriptionally deregulated genes when cells are treated with PP242. (A)** Venn diagram with the distribution of transcripts upregulated in NPP. A table showing the main GO categories (with  $P < 0.03$ ) associated with each cell line and the GO categories (with  $P < 0.03$ ) associated with genes in the intersection between the two cell lines. **(B)** Venn diagrams with the distribution of transcripts downregulated in NPP. A table showing the main GO categories (with  $P < 0.03$ ) associated with each cell line and the GO categories (with  $P < 0.03$ ) associated with genes in the intersection between the two cell lines.

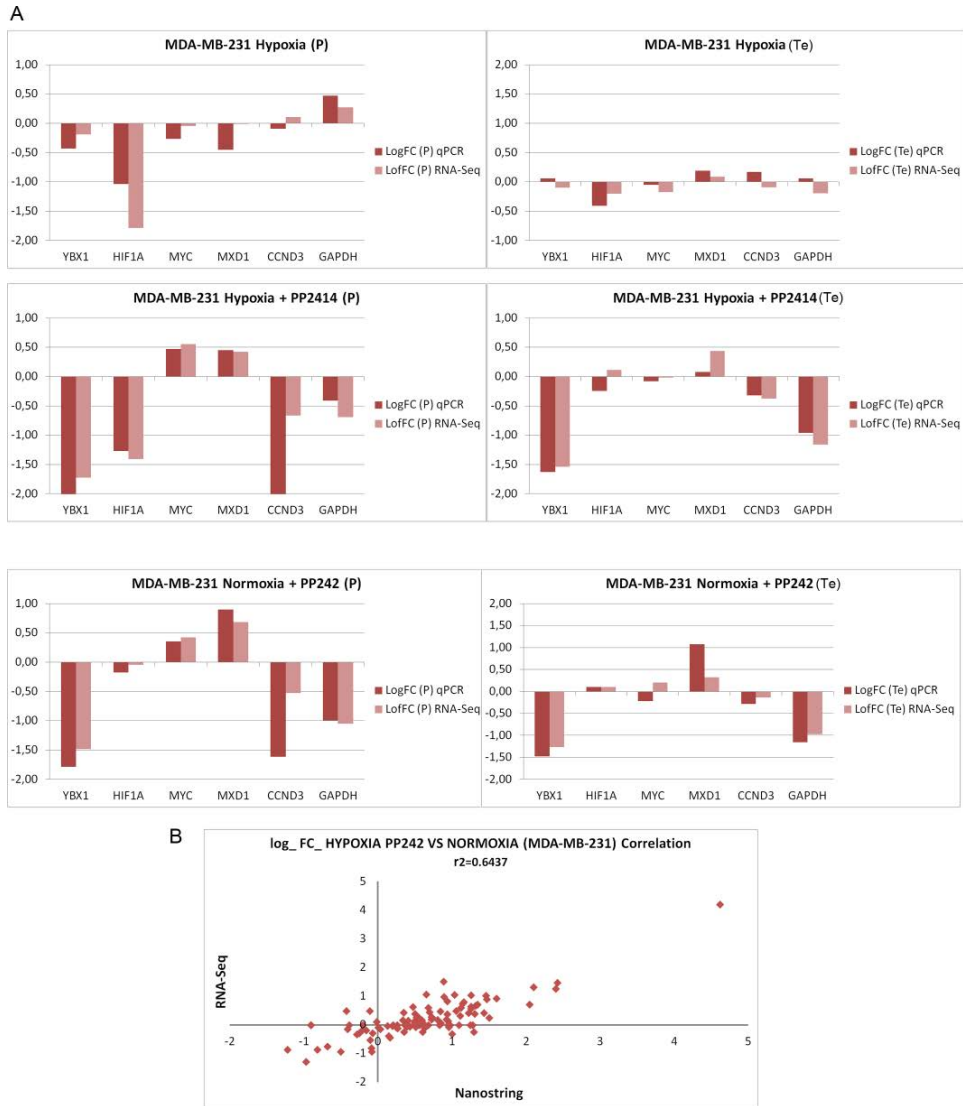


**Supplementary Figure 4: Translationally downregulated transcripts upon PP242 treatment.** (A) Venn diagrams showing the distribution of downregulated transcripts at the protein synthesis level under H, HPP and NPP conditions in each cell line. (B) Venn diagrams showing translationally downregulated transcripts in HPP and NPP highlighting genes in the intersection between the two cell lines. (C) Main GO categories associated with translationally downregulated genes in HPP in both cell lines. (D) Above: Table showing the number of genes translationally downregulated in our study and in others studies. Below: Venn diagram showing the number of genes translationally inactivated in NPP compared with the ones inactivated in other published studies.

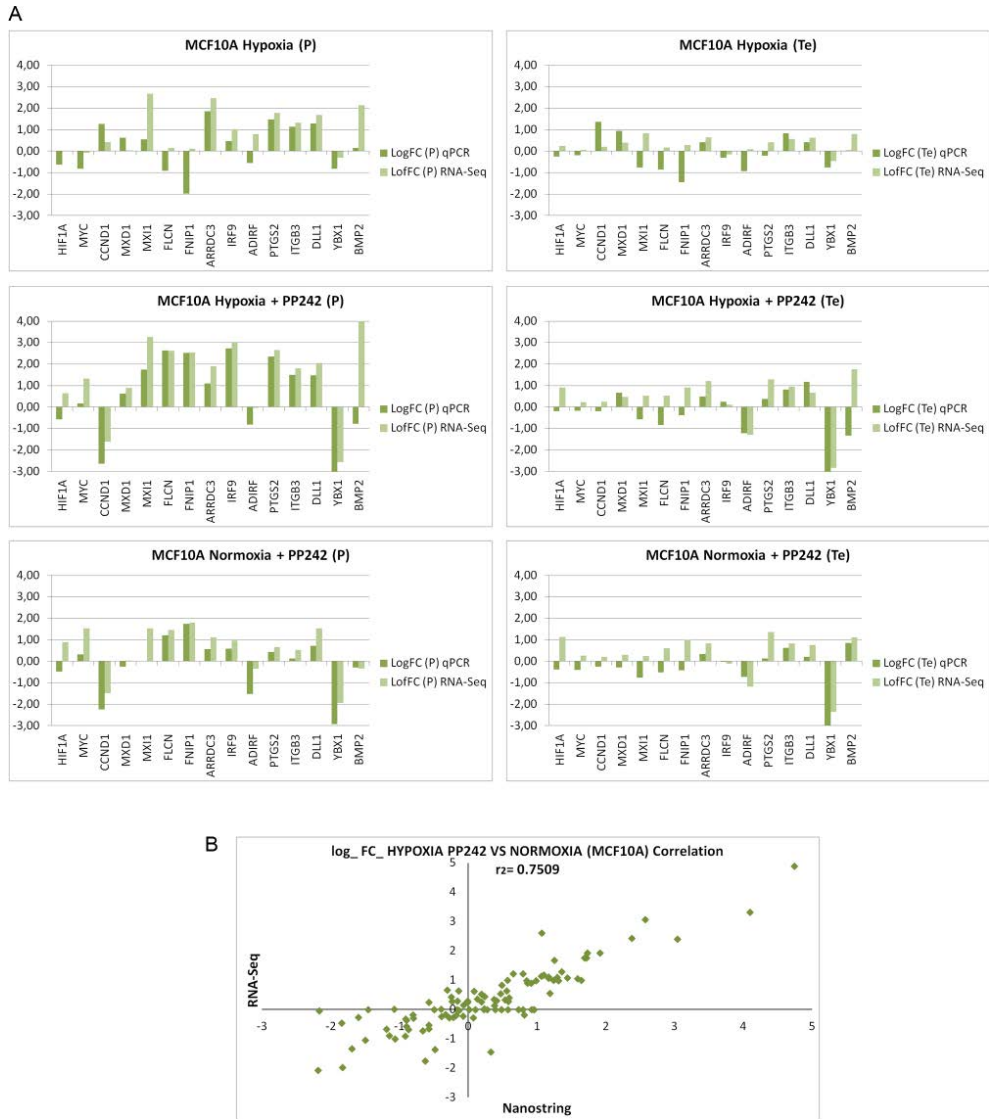




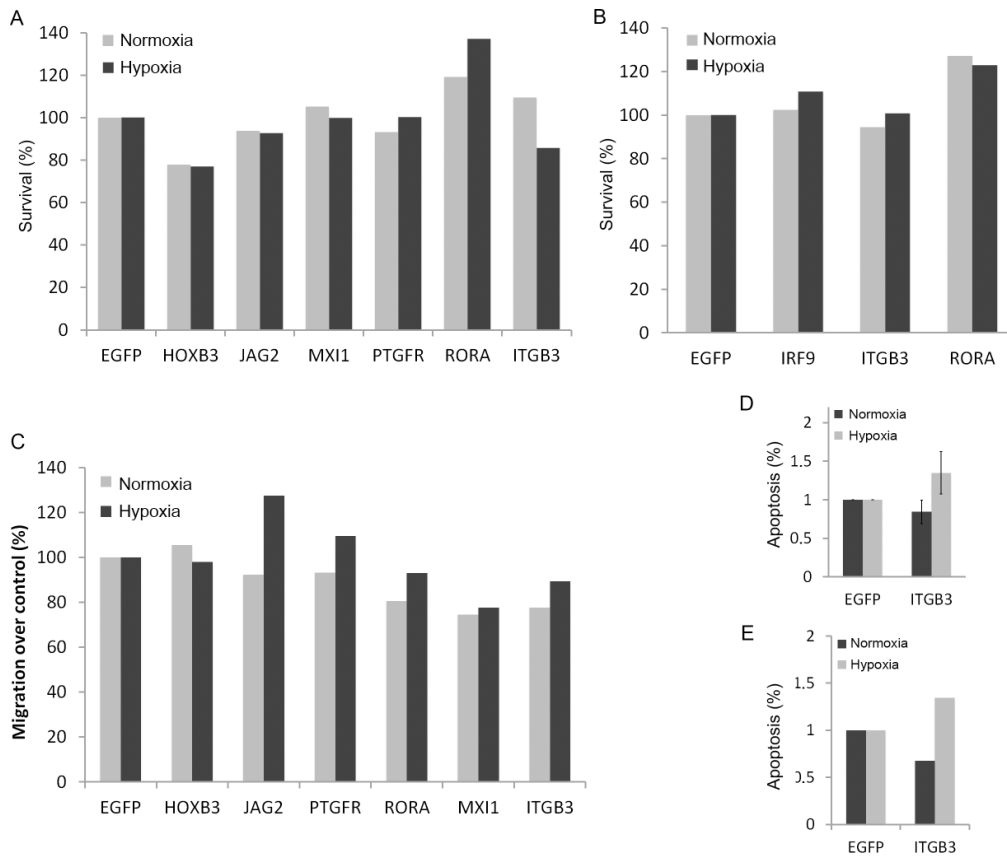
**Supplementary Figure 5: Increased translational efficiency (Te) of ITGB3 is accompanied by increased protein in other breast cancer cell lines.** Immunoblots for all experimental conditions of the different translationally activated (ITGB3, GJB3, MMP3, CCDC103, TTC30B) or inactivated (RPL11, EIF3G, YBX1) targets in HPP in MDA-MB-468, BT-549 and MCF7.



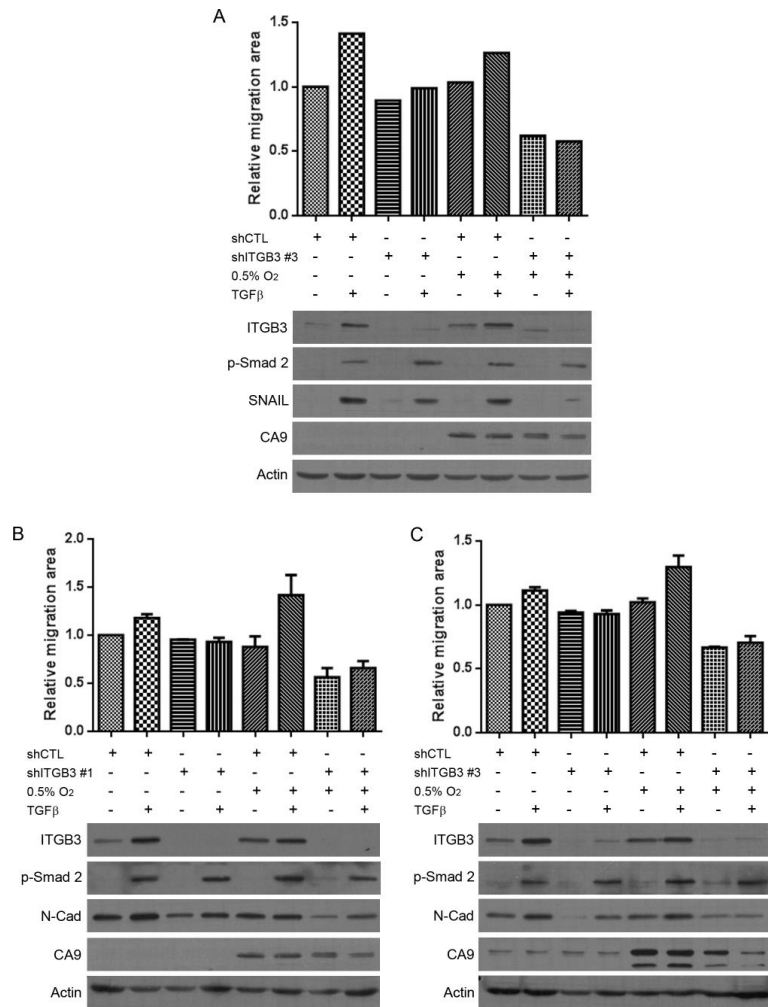
**Supplementary Figure 6: Validation of the screening by qRT-PCR and NanoString in MDA-MB-231 cells. (A)** qRT-PCR of candidate genes in polysomal mRNA (left panels) and the ratio of Log<sub>2</sub>FC P to Log<sub>2</sub>FC T (right panels) compared with the values obtained from the RNA-Seq screening under H, HPP and NPP conditions. **(B)** Correlation between the 50-gene PAM50 assay and the expression obtained in RNA-Seq for these genes from the total mRNA.



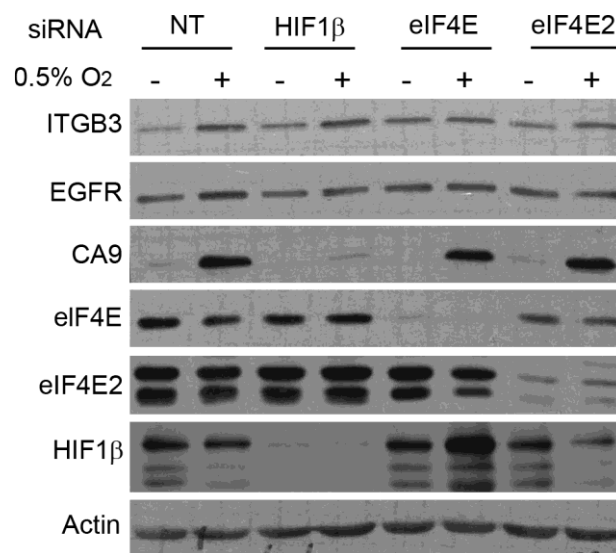
**Supplementary Figure 7: Validation of the screening by qRT-PCR and NanoString in MCF10A cells. (A)** qRT-PCR of candidate genes in polysomal mRNA (left panels) and the ratio of  $\text{Log}_2\text{FC P}$  to  $\text{Log}_2\text{FC T}$  (right panels) compared with the values obtained from the RNA-Seq screening under H, NPP and HPP conditions. **(B)** Correlation between the 50-gene PAM50 assay and the expression obtained in the RNA-Seq for these genes from the total mRNA.



**Supplementary Figure 8: Screening by siRNA of candidate translationally activated genes in hypoxia with PP242. (A)** Forty-eight hour survival rates in hypoxia compared with normoxia. **(B)** Forty-eight hour survival rates in hypoxia compared with normoxia in MCF10A cells transfected with the different siRNAs. **(C)** Migration assays in MDA-MB-231 cells transfected with the different siRNAs and subjected to hypoxia versus normoxia for 8 hours. **(D)** Apoptosis in MDA-MB-231 cells transfected with the different siRNAs. **(E)** Apoptosis in MCF10A cells transfected with the different siRNAs.



**Supplementary Figure 9: Migration assay of MDA-MB-231 and MCF10A cells with ITGB3 silencing and treated with TGF-β.** (A) Migration assay of MDA-MB-231 cells using shITGB3 #3 (above) and an immunoblot showing ITGB3 and Snail expression upon treatments (below). (B) Migration assay of MCF10A cells using shITGB3 #1 (above) and an immunoblot showing ITGB3 and N-cadherin expression upon treatments (below). (C) Migration assay of MCF10A cells using shITGB3 #3 (above) and an immunoblot showing ITGB3 and N-cadherin expression upon treatments (below).



**Supplementary Figure 10: eIF4E is essential for protein synthesis activation of ITGB3 under low-oxygen conditions.** Immunoblot showing ITGB3 expression under hypoxic conditions after eIF4E2, eIF4E or HIF1 $\beta$  silencing in the MCF10A cell line.

**Supplementary Table 1: Lists of mRNAs that are translationally regulated in MCF10A and MDA-MB-231 cells in all experimental conditions.** See Supplementary\_Table\_1



**UNPUBLISHED DATA**





In the published data of Chapter I, we performed a polysomal RNA-Seq screen to analyse the translome in hypoxia of cancer cells versus normal cells, and we identified ITGB3 as a candidate. Our data suggested that ITGB3 is translationally activated in hypoxia and regulates malignant features including EMT and cell migration through the TGF- $\beta$  pathway. Besides, downregulation of ITGB3 significantly reduced lung metastasis and improved overall survival *in vivo* revealing a novel angle to treat therapy-resistant hypoxic tumours.

After this, we were interested in expanding our knowledge in the specific role of ITGB3 in hypoxic conditions, using different *in vitro* models. Models that Professor Alan McIntyre, from the University of Nottingham, England, had a huge experience working with. That is why I had the opportunity to spend three months in the Tumour and Vascular Biology Laboratory of Professor Alan McIntyre.

Our principal goal during this stay was to study the role of ITGB3 in mammospheres formation in hypoxic conditions and the evaluation of hypoxic phenotype monitored using the spheroid model. To this end, we used two different breast cancer cell lines, MCF7 and MDA.MB.231, subjected to ITGB3 depletion using stable shRNA.

## Results

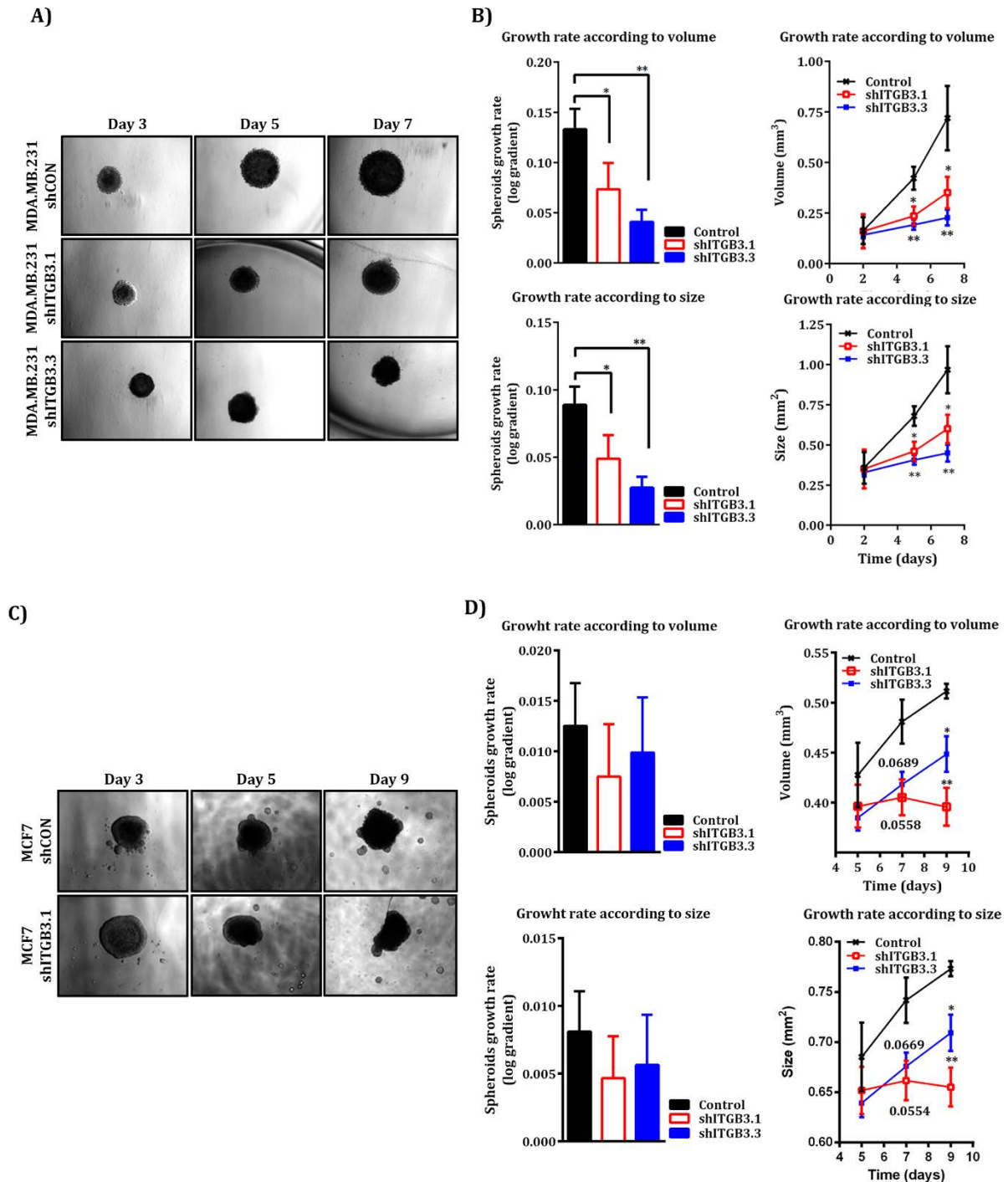
Oxygen consumption rate per volume was shown to be smaller in spheroids compared to single cells and was more similar to values measured in tumours<sup>66,212,213</sup>. Additionally, oxygen consumption was discovered to be higher in small spheroids and drops while volume increases, indicating that cells in spheroids adapt to low oxygen pressure by a shift to anaerobic metabolism or quiescence. When spheroids reach diameters of 1 mm, oxygen consumption turns out to be less dependent on size and is analogous to oxygen consumption in avascular tumour regions. Oxygen diffusion is constant regardless of spheroid size and is comparable to the diffusion detected in solid tumours<sup>212</sup>.

The stratified cellular conformation of spheroids with proliferating cells at the border and quiescent and necrotic cells within the core suggests that restriction of metabolic parameters induces cell cycle arrest and apoptosis. Concerning spheroid cell death, a correlation between the decrease of oxygen pressure and simultaneous detection of core necrosis has been found in spheroids models<sup>66,214</sup>.

### **Integrin Beta 3 increases the 3D growth rate in breast cancer cell lines**

The ability of ITGB3 to promote spheroid formation was tested in MDA.MB.231 and MCF7 breast cancer cell lines with ITGB3 depleted using stable shRNA. Reduction of ITGB3

expression significantly reduced the spheroid growth rate by 50-60% in MDA.MB.231 (Unpublished Figure 1A) cells and 30% in MCF7 (Unpublished Figure 1B) compared with shCON. It is worthy to note that MDA.MB.231 control cells showed an exponential growth rate and a compact morphology, meanwhile MCF7 cells showed more inconsistent morphology, leading to spontaneous disintegration.

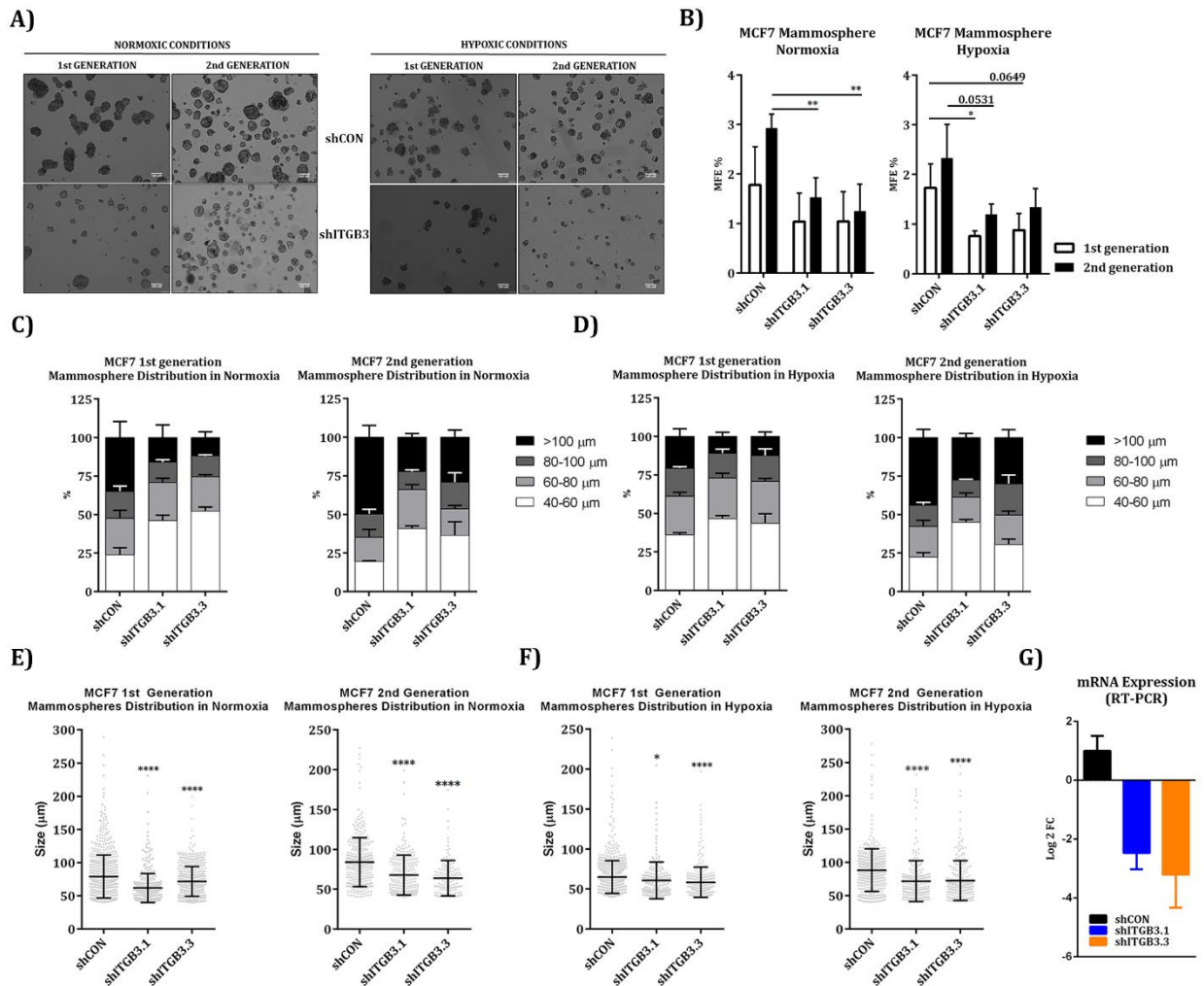


**Unpublished Figure 1.** ITGB3 depletion affects growth rate in breast cancer cell spheroids. Representative spheroid images and spheroid growth curves of (A, B) MDA.MB.231 and (C, D) MCF7 cells, (\* $p < 0.05$ , \*\* $p < 0.01$ ,  $n = 3$ ). Error bars represent standard deviation. Statistical analysis including Student's t-test and linear regression of log transformed growth data were carried out as appropriate using GraphPad Prism 6.01.

### **ITGB3 promotes mammospheres formation in both normoxic and hypoxic conditions**

The standard *in vitro* assays currently used to prove the self-renewal property of cancer stem cells are the colony-forming assays and the culture of cells in non-adherent conditions, which outcomes in the proliferation of cells as tumorspheres. This assay has exposed that only the mammary stem cells have the ability to survive in suspension and generate 3D non-adherent colonies called mammospheres. These mammospheres are enriched in mammary stem cells and are able to differentiate into all three mammary epithelial lineages as well as to clonally generate complex functional structures in reconstituted 3D culture systems<sup>215,216</sup>. Along with the ability of stem cells to form mammospheres, it has been demonstrated the ability of cells to generate secondary and subsequent generation mammospheres since this associate with better assurance the number of sphere-forming cells with the number of multipotential progenitors or stem cells<sup>217</sup>.

To investigate whether the ITGB3 knockdown cell line displays functional characteristics of cancer stem cells, we tested the ability of the population to grow as non-adherent mammospheres. Cells were grown as mammospheres for 7 days and then their secondary regeneration mammosphere capacity was tested for a total of 14 days. The analysis was done in both conditions in parallel, normoxia, and hypoxia (Unpublished Figure 2A). The results showed that the MCF7 shITGB3 cell line presented less capacity to form mammospheres as well as second generation of spheres, meaning that they present less multipotency capacity in relation to MCF7 shCON cells. This effect was observed in both conditions, normoxia and hypoxia (Unpublished Figure 2B). However, phenotypic differences were observed between groups. Wild type mammospheres were larger compared to the shITGB3 ones (Unpublished Figure 2C-F). Therefore, reduction in ITGB3 expression is translated into a reduction in cancer stem cells properties. The lack of ITGB3 affects the mammosphere formation, but equally in normoxic and hypoxic conditions. Additionally, wild type-mammospheres present bigger size.



**Unpublished Figure 2.** The lack of ITGB3 affects mammosphere formation, but similarly in Normoxia and Hypoxia in MCF7 cell line. Moreover, wild type-mammospheres are able to form bigger ones (\* $p < 0.05$ , \*\* $p < 0.01$ , \*\*\*\* $p < 0.0001$   $n = 4-6$ ). Error bars represent standard deviation. Statistical analysis was carried out as appropriate using GraphPad Prism 6.01

## Unpublished Materials and Methods

### Generation of spheroids

For the formation of tumour spheres, cells are grown in the presence of matrigel in low adherent 96 well plates (Costar). Cells cultures were trypsinised in 1X Trypsin-EDTA, neutralised with DMEM, and diluted 1:2 with Trypan Blue Solution (Sigma-Aldrich) for cell count. Stock cell suspensions of the desired cell densities were seeded using DMEM medium. Matrigel TM matrix (Corning) was added to stock cell suspensions in a 50μL:1mL ratio. 3D spheroids were formed after seeding cells: MCF7 or MDA.MB.231 at 10,000cells/well in Costar ultra-low cluster with round bottom 96-well plates. After seeding, plates were centrifuged for 10 minutes at 2,000 rpm and incubated under standard cell culture conditions in a humidified incubator at 37°C with 5% CO<sub>2</sub>. Once the spheres have reached a diameter of approximately 1000 μm they represent many features of a primary tumour, like

an external proliferation zone an inactive intern zone, caused by the limited diffusion of oxygen, nutrients, and metabolites, as well as a necrotic core, that mimics the heterogeneity features seen *in vivo*. Spheroids were visualised every two days using the Nikon Ti-E microscope with NIS-Elements AR program and analysed using Image J and GraphPad Prism v6.01 software.

### **Generation of mammospheres**

MCF7 cells were plated in 6-well ultra-low attachment surface plates (Corning) at a concentration of 40,000 cells/well. Cells were maintained in 3.0 mL MammoCult Basal Medium (StemCell Technologies), supplemented with MammoCULT Proliferation supplements (StemCell Technologies), 4,0ug/mL Heparin (StemCell Technologies), and 0,48ug/mL Hydrocortisol (StemCell Technologies). Secondary generation mammospheres were generated on day 7 by dissociating primary mammospheres with 1X Trypsin-EDTA, re-suspending in the afore-mentioned medium and plated at the same cell density in 6-well ultra-low attachment surface plates. The capacity of cells to form primary and secondary mammospheres, after 7 and 14 days in culture respectively, were visualised using the Nikon Ti – E microscope with NIS-Elements AR program and analysed using Image J and GraphPad Prism v7.00 software.

The number of primary mammospheres which are larger than 50 mm were determined using Image J (Fiji). Mammosphere forming efficiency (%) was calculated as follows: (Number of mammospheres per well / number of cells seeded per well) x 100. Assessment of self-renewal (second generation mammospheres) was calculated as done for the primary mammospheres.



## **CHAPTER 2**





## Manuscript

ITGB3 mediated extracellular vesicle uptake facilitates intercellular communication to drive breast cancer metastasis.

**Pedro Fuentes**, Marta Sesé, Pedro J. Guijarro, Marta Emperador, Sara Sánchez, Héctor Peinado, Stefan Hümmer\*, Santiago Ramón y Cajal\*

## Summary

**Introduction:** Metastasis, the spread of malignant cells from a primary tumour to distant sites causes 90% of cancer-related deaths. The integrin ITGB3 has been previously described to play an essential role in breast cancer metastasis, but the underlying mechanisms remain undefined. Tumors are complex systems where cell-cell communication between intra-tumoural and extra-tumoural cells play a crucial role. Extracellular Vesicles (EVs), membrane-limited vesicles secreted by normal and malignant cells, have been proposed to act as mediators of intercellular communication in physiological and pathological scenarios. It is now well established that integrins are constantly endocytosed and recycled back to the plasma membrane through multiple routes. Accumulating evidence clearly indicates that endocytosis and recycling of integrins plays a crucial role during cancer progression, invasion, and metastasis. Here we describe a fundamental link between endocytosis mediated integrin trafficking and the integrin-mediated uptake of exosomes.

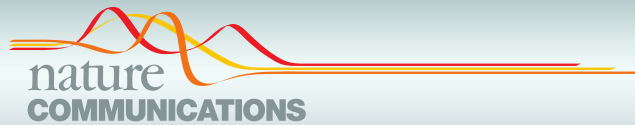
**Objectives:** As the integrins are crucial for the role of extracellular vesicles in cancer progression and particularly in metastasis together with our previous findings that ITGB3 is required for lung metastasis in MDA.MB.231 cells, we were aiming at delineating the role of ITGB3 in extracellular vesicles-mediated intercellular communication in breast cancer cell lines.

**Methodology:** Using stable shRNA of ITGB3 (shITGB3) in the triple-negative breast cancer cell line MDA.MB.231, EVs were isolated by ultracentrifugation and characterized by Western blot analysis to determine the protein composition and by NTA and CryoEM to measure the amount of EVs. An LC-MS/MS-based assay was performed to determine the differences in the protein composition of EVs after knock-down of ITGB3. Uptake of fluorescently labelled EVs into recipient cells was measured by flow cytometry. The colony-forming capacity induced by conditioned medium was used to assess the functional impact on the role of ITGB3 in intercellular communication.

**Results:** Studies of colony formation capacity, as a model for the formation of colonies within the distant organ during the metastatic process, showed that ITGB3 is required for

EVs-induced colony formation. In line with this, the uptake of fluorescently labelled EVs was strongly impaired in shITGB3 cells. In agreement with the integrin trafficking model, inhibition of FAK, HSPGs, and Dynamin proteins using chemical and genetical approaches. Furthermore, we demonstrated that this defect is linked to endocytosis of EVs. Finally, analysis of shITGB3 derived-EVs revealed a clear ITGB3-dependent alteration in the EVs secretome. On the one hand, clear defects in protein complexes required for exosome formation and on the other hand, Nanoparticle Tracking Analysis (NTA) and CryoEM showed that the overall amount of small EVs was increased upon ITGB3 inhibition.

**Conclusions:** Our work demonstrates that extracellular vesicles-stimulated clonal growth relies on ITGB3 in EVs-receiving cells and that ITGB3 plays a central and thus far unknown role in EV uptake. Our data indicate that this need for ITGB3 may be due to its dual role connecting the capture of extracellular vesicles at the cell surface by HSPG-modified proteins like syndecans to the local activation of FAK-induced Dynamin-driven endocytosis. Thus, the transmembrane protein ITGB3 is required for both extracellular recognitions of EVs by interacting with HSPGs and for intracellular FAK activation. The stimulated endocytosis of integrins results in the coordinated cellular uptake of ITGB3- and HSPG-associated EVs. Thus, the central role of ITGB3 in intracellular communication via EVs and the proposed function of EVs in cancer metastasis might explain the requirement for ITGB3 in breast cancer metastasis.









## ARTICLE


<https://doi.org/10.1038/s41467-020-18081-9>

OPEN

# ITGB3-mediated uptake of small extracellular vesicles facilitates intercellular communication in breast cancer cells

Pedro Fuentes <sup>1,2</sup>, Marta Sesé <sup>1,2</sup>, Pedro J. Guijarro<sup>1,5</sup>, Marta Emperador <sup>1,4,5</sup>, Sara Sánchez-Redondo<sup>3</sup>, Héctor Peinado <sup>3</sup>, Stefan Hümmer <sup>1,2</sup>✉ & Santiago Ramón y. Cajal <sup>1,2</sup>✉

Metastasis, the spread of malignant cells from a primary tumour to distant sites, causes 90% of cancer-related deaths. The integrin ITGB3 has been previously described to play an essential role in breast cancer metastasis, but the precise mechanisms remain undefined. We have now uncovered essential and thus far unknown roles of ITGB3 in vesicle uptake. The functional requirement for ITGB3 derives from its interactions with heparan sulfate proteoglycans (HSPGs) and the process of integrin endocytosis, allowing the capture of extracellular vesicles and their endocytosis-mediated internalization. Key for the function of ITGB3 is the interaction and activation of focal adhesion kinase (FAK), which is required for endocytosis of these vesicles. Thus, ITGB3 has a central role in intracellular communication via extracellular vesicles, proposed to be critical for cancer metastasis.

<sup>1</sup>Translational Molecular Pathology, Vall d'Hebron Research Institute (VHIR), Universitat Autònoma de Barcelona (UAB), Barcelona, Spain. <sup>2</sup>Spanish Biomedical Research Network Centre in Oncology (CIBERONC), Madrid, Spain. <sup>3</sup>Microenvironment & Metastasis Group, Molecular Oncology Program, Spanish National Cancer Research Centre (CNIO), Madrid, Spain. <sup>4</sup>Present address: Tumor Biomarkers Group, Vall d'Hebron Institute of Oncology (VHIO), Barcelona, Spain. <sup>5</sup>These authors contributed equally: Pedro J. Guijarro, Marta Emperador. ✉email: [stefan.hummer@vhir.org](mailto:stefan.hummer@vhir.org); [sramon@vhebron.net](mailto:sramon@vhebron.net)

**M**etastasis accounts for 90% of cancer deaths. It is a multistage process culminating in colonisation of a new environment<sup>1</sup>, and each step relies on the tumour cells' interactions with their microenvironment. Extracellular vesicles (EVs) secreted from primary tumours are key in this interaction<sup>2,3</sup>. EVs contain different molecular cargo (protein, RNA, or lipids) that can modify the local and distant environment, enabling primary tumours to evolve, establish pre-metastatic niches and metastasise<sup>4,5</sup>.

EVs are a heterogeneous group of secreted membranous vesicles including microvesicles, ectosomes, and exosomes<sup>6</sup>. They have become valuable biomarkers in liquid biopsies, and existing research has focused on their characterization in different cancer types<sup>7,8</sup>. However, the mechanisms underlying their biosynthesis, release from donor cells, and uptake into target cells remain poorly understood. A major difference among vesicle subtypes is their origin: while microvesicles and ectosomes bud from the plasma membrane, exosome formation begins on early endosomes<sup>9</sup>. After maturation in multivesicular bodies through the invagination of the endosomal membrane and formation of intraluminal vesicles (ILVs), exosomes are released by fusion of ILVs with the plasma membrane<sup>10</sup>. The specific proteins incorporated into ILVs are regulated mainly by the ESCRT (endosomal-sorting complex required for transport) of which there are 4: ESCRT-0, I, II, and III. Interference with protein function within these complexes has been reported to block exosome biogenesis<sup>11</sup>.

Once released from the donor cell, EVs induce cell signalling, either by interacting with target cell-surface proteins or being taken up into the receiving cell<sup>6,9</sup>. This uptake is currently the least understood step in vesicle-based intercellular communication, and proposed mechanisms range from passive membrane fusion to active uptake via macropinocytosis or endocytosis<sup>12</sup>. Interestingly, this bears similarity to the mechanisms described for virus endocytosis<sup>13</sup>, which begins when viral membrane glycoproteins bind to glycoprotein attachment factors, such as heparan sulfate proteoglycans (HSPGs), on the target cell surface. HSPGs have also been demonstrated to be essential for uptake of EVs<sup>14–16</sup>.

Integrins are multifunctional heterodimeric cell-surface receptor molecules that serve as entry receptors for a plethora of viruses. Uptake of herpes viruses has been reported to be dependent on  $\alpha v\beta 3$  integrin, and in Kaposi's sarcoma-associated herpesvirus (KSHV), binding of the virus to the cell surface via interactions with heparan sulfate results in temporary interaction between HSGPs and  $\alpha v\beta 3$ <sup>17</sup>. This activates the integrin, enabling binding and activation of focal adhesion kinase (FAK) and subsequent assembly of endocytic machinery<sup>17,18</sup>. Interplay between HSGPs, integrins, FAK and endocytosis also regulates the turnover of focal adhesion sites<sup>19–22</sup>. This turnover allows the dynamic attachment of cells to surfaces and enables cell migration. Key for this process is integrin recycling, enabling local control of FAK activity. HSPGs of the syndecan family, particularly syndecan-4, play a crucial role in this process by regulating integrin recycling.

Early integrin studies in cancer research focused on their role as cell adhesion receptors, though new roles have since been uncovered, particularly in the regulation of metastatic processes by exosomes<sup>23,24</sup>. But while the role of integrins within exosomes has been studied, little is known about their role in acceptor cells. The fundamental role of integrins in tumour progression—particularly metastasis—has long been recognised, but their exact molecular functions remain incompletely understood<sup>25</sup>. We recently identified integrin beta 3 (ITGB3) as a factor involved in tumour stress resistance and demonstrated its essential role in metastatic progression of triple-negative breast cancer (TNBC)<sup>26</sup>.

We—and others—have proposed that ITGB3 may be required for the formation of macro-metastatic foci<sup>26,27</sup>. Following on from this, we sought to investigate the mechanisms of cellular ITGB3 in exosome biogenesis and uptake in relation to tumour metastasis.

Our work now demonstrates that EV-stimulated clonal growth relies on ITGB3 in EV-receiving cells and that ITGB3 plays a central and thus far unknown role in EV uptake. The requirement for ITGB3 derives from the process of integrin endocytosis, allowing the internalisation of EVs captured by ITGB3-interacting HSPGs. This process is furthermore regulated by the ITGB3-interacting FAK, which is activated by EVs in an ITGB3-dependent manner and required for endocytosis of these vesicles. Thus, the transmembrane protein ITGB3 is required both for extracellular recognition of EVs by interacting with HSPGs and for intracellular FAK activation. The stimulated endocytosis of integrins, known from the process of focal adhesion disassembly, results in the coordinated cellular uptake of ITGB3- and HSPG-associated EVs. Thus, the central role of ITGB3 in intracellular communication via EVs and the proposed function of EVs in cancer metastasis might explain the requirement for ITGB3 in breast cancer metastasis.

## Results

**ITGB3 is required for EV-induced colony formation.** We previously demonstrated that ITGB3 is required for lung metastasis formation<sup>26</sup>, but follow-up experiments revealed no defect in the initial homing of shITGB3 cells to the lung (Supplementary Fig. 1a–c). The next step in metastasis—formation of colonies within the distant organ—involves clonal growth from a single cell<sup>28</sup>, which is dependent on factors secreted by other cells; in the laboratory, conditioned medium (CM) is generally used to generate clonal cell lines<sup>29–32</sup>. To assess the role of secreted factors on the colony-forming capacity of MDA.MB.231 cells, we measured the CM requirements for anchorage-dependent clonal growth (Fig. 1a, b). We seeded 500,000 cells, let them grow for 48 h, then collected the medium. As expected, in the presence of CM, the colony-forming capacity of MDA.MB.231 cells increased more than 2.5-fold, while shITGB3 cells had only a 1.3-fold increase (Fig. 1a, b). This difference can be attributed to the CM, since the colony-forming capacity of parental and shITGB3 MDA.MB.231 cells was not significantly altered after 7 days in normal growth medium (Fig. 1a, b). Similar results were obtained with a second shRNA construct, excluding a possible off-target effect (Supplementary Fig. 2). To test if this effect was due to soluble factors or EVs in the CM, we depleted the CM of EVs (100,000g spin)<sup>33,34</sup>, and found that this, but not the removal of large EVs only (10,000 g spin), completely negated the CM's increased colony-forming effect on the treated MDA.MB.231 cells (Fig. 1a, b; Supplementary Fig. 3a, b). Furthermore, the CM, but not the EV-depleted CM, derived from shITGB3 cells also increased the colony-forming capacity of MDA.MB.231 cells. As in the case of MDA.MB.231-derived CM, this effect was not observed in shITGB3 cells. These results therefore indicate that ITGB3 is required for increased colony-forming capacity in vesicle-receiving cells only.

During metastatic dissemination and homing within a different organ, neoplastic cells are exposed to EVs derived from a variety of cell types. In the metastatic mouse model, we previously observed that the capacity of MDA.MB.231 cells to form metastatic colonies in the lung is reduced in shITGB3<sup>26</sup>. We therefore asked if, besides MDA.MB.231-derived EVs, EVs from lung tissue cells could also stimulate colony growth of MDA.MB.231 cells. We used lung-derived IMR90 fibroblasts: CM from

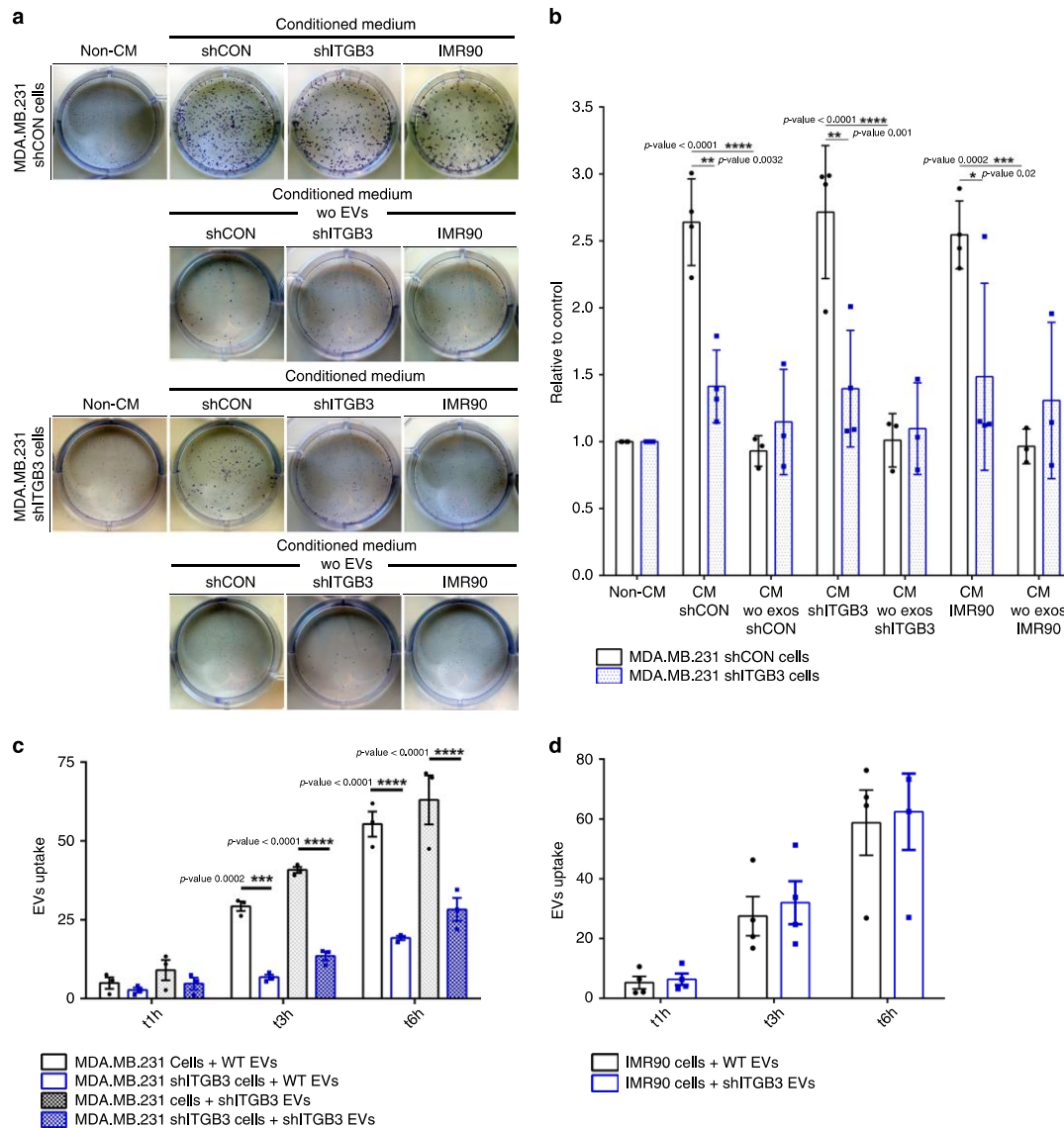


**Fig. 1** ITGB3 is required for EV-induced colony formation in MDA.MB.231 cells. **a** Representative pictures are shown for each cell population and condition. **b** Conditioned medium (CM) was collected from exponentially growing MDA.MB.231 shCON, shITGB3, or IMR90 cells. In the case of vesicle-depleted CM (CM without exosomes), the same CM was split into two parts: one was used directly and the other was depleted of vesicles by ultracentrifugation before use, to establish the clonal cell growth response to the CM. Data are normalized to the non-conditioned control medium (DMEM). **c, d** Flow cytometry analysis for MDA.MB.231 shCON, MDA.MB.231 shITGB3 cells and IMR90 cells after incubating with 2–5  $\mu\text{g mL}^{-1}$  fluorescently labelled EVs derived from both MDA.MB.231 shCON and MDA.MB.231 shITGB3 cells at different time points. Source data are provided as a Source Data file. (\* $p$  value < 0.05, \*\* $p$  value < 0.01, \*\*\* $p$  value < 0.001, \*\*\*\* $p$  value < 0.0001;  $n = 7$  for non-CM condition;  $n = 4$  for CM shCON, CM shITGB3, and CM IMR90;  $n = 3$  for CM wo EVs shCON and CM wo EVs IMR90.  $n = 3$  for panel 1c, d). Data are represented as mean  $\pm$  SD in (b–d). Statistical analysis including two-way ANOVA multiple comparisons was carried out using GraphPad Prism 6.01.

these cells, but not EV-depleted CM, stimulated colony growth in MDA.MB.231 cells in an ITGB3-dependent manner (Fig. 1a, b).

Taken together, these results show that the EV fraction of CM promotes clonal growth in MDA.MB.231 cells and indicates an essential role of ITGB3 in vesicle-receiving cells.

**ITGB3 is required for vesicle uptake.** An observed inability of shITGB3 cells to respond to the presence of EVs prompted us to speculate that these cells may have defective vesicle uptake and in turn defective delivery of the cargo molecules responsible for increased colony-forming capacity. To test this, we measured EV

uptake. EVs derived from shCON or shITGB3 cells were isolated by ultracentrifugation and fluorescently labelled with PKH26, and their uptake into both cell lines was measured by FACS at various time points after incubation. As shown in Fig. 1c, in the shCON cell line, EVs were taken up over time, and at 6 h up to 60% of cells were EV-positive. The portion of EV-positive cells (25% at 6 h) was lower in shITGB3 cells than in shCON cells. These results were confirmed by the use of an independent shRNA construct targeting ITGB3 (Supplementary Fig. 4). To exclude the possibility of a cell-line-specific function of ITGB3, we generated a stable shRNA-mediated knockdown of ITGB3 in MCF7 cells and demonstrated that EV uptake was also dependent on ITGB3 (Supplementary Fig. 5). Importantly, the origin of the vesicles—either from shCON or shITGB3 cells—did not affect their uptake into shCON and shITGB3 cells (Fig. 1c, d). These results were confirmed in IMR90 cells, which incorporated EVs from both cell lines with a similar efficiency (Fig. 1d). To further support the role of ITGB3 in EV uptake into receiving cells, we performed confocal microscopy of PKH26-labelled EVs on PFA-fixed and ITGB3 ( $\alpha v\beta 3$ )-stained cells. These experiments were carried out with shITGB3 cell-derived EVs to avoid staining of EV-localized ITGB3. Under these experimental conditions, we detected co-localisation between cellular ITGB3 and EVs at the surface of non-permeabilized cells (Supplementary Fig. 6).

These results demonstrate that the uptake of a significant portion of EVs relies on ITGB3 in the recipient cell. However, not all vesicles were dependent on ITGB3 (approximately 50%). This may have been due to incomplete knockdown of ITGB3, redundant pathways for vesicle uptake, or ITGB3 being required for the uptake of certain vesicle subtypes only. As we could not rigorously exclude any of these possibilities, we looked further at the mechanism of ITGB3-dependent EV uptake.

**ITGB3-dependent endocytosis of EVs requires HSPGs.** Having established that ITGB3 is fundamental for EV uptake in breast cancer cell lines, we explored the underlying mechanisms. First, we analysed how EVs might be captured at the cell surface. The described interactions of ITGB3 with other proteins include its selective binding to syndecans through the extracellular FERM domain<sup>35–40</sup>. Syndecans are a family of heparan sulfate-decorated cell-surface proteoglycans that recognise “heparin-binding” motifs. Treatment of different cancer cell lines with heparin, a highly sulfated glycosaminoglycan mimetic of heparan sulfate, has been shown to block EV uptake. To test if this occurred in MDA.MB.231 cells, we pretreated MDA.MB.231 shCON and MDA.MB.231 shITGB3 cells with fluorescently labelled vesicles derived from MDA.MB.231 cells. FACS analysis revealed that heparin blocked vesicle uptake to a similar degree as observed with shITGB3 knockdown. Furthermore, heparin treatment of shITGB3 cells had no additive effect on vesicle uptake, indicating that ITGB3 and HSPGs act on the same pathway (Fig. 2a). To strengthen our finding that HSPGs are required for EV uptake, cells were treated with heparinase prior to the addition of PKH26-labelled EVs. As occurred with heparin treatment, EV uptake was reduced by approximately 50% (Fig. 2b). As syndecans have been reported to directly interact with ITGB3, it is tempting to speculate that this interaction provides a physical link between exosomes and ITGB3.

Next, we asked how those captured vesicles are internalized. Previously proposed mechanisms for EV uptake and release of cargo into different target cell lines include fusion of vesicles with the plasma membrane and uptake of entire vesicles by endocytosis, phagocytosis or macropinocytosis<sup>9,10,41</sup>. We therefore began by exploring which mechanisms of vesicle uptake were used in MDA.MB.231 cells.

In line with previous reports<sup>14,42,43</sup>, EV uptake at 4 °C was also severely blocked in MDA.MB.231 cells (Supplementary Fig. 7), suggesting that the underlying mechanism may be an energy-dependent process such as endocytosis. To test this, we blocked DYNAMIN activity using Dyngo-4a<sup>44</sup> and blocked clathrin activity using Pitstop-2<sup>45</sup>. As endocytosis is an essential cell process, inhibitor treatments were reduced to 30 min, followed by incubation with fluorescently labelled vesicles. Measurements of cell fluorescence intensity after 3 h revealed that vesicle uptake in MDA.MB.231 cells was significantly reduced in Dyngo-4a but not Pitstop-2 treated cells. Depletion of DYNAMIN 2 by shRNA (shDyn2) or the overexpression of a DYNAMIN 2 dominant negative mutant (Dyn2-44K) confirmed the results obtained for Dyngo-4a treatment (Fig. 2c–e).

Interestingly, the reduction of EVs in Dyngo-4a treated cells was accompanied by an increase in the surface abundance of ITGB3 ( $\alpha v\beta 3$ ), as determined by FACS (Supplementary Fig. 8a). These results are in line with previous reports that examined recycling of integrins as a key mechanism to regulate their function at the cell surface<sup>21</sup>. In addition, we detected co-localization of ITGB3 ( $\alpha v\beta 3$ ) with EEA1 on confocal microscopy, and ITGB3 was co-localized to internalized EVs derived from shITGB3 cells (Supplementary Fig. 9). Altogether, these results imply that not solely the presence of integrin beta 3 on the cell surface, but the active internalisation of the integrin in a DYNAMIN-dependent manner appears to be crucial for EV uptake.

As described above, the uptake of a significant fraction of EVs into MDA.MB.231 cells relies on ITGB3, HSPGs and DYNAMIN. To determine whether the remaining vesicles detected by FACS analysis were taken up into the recipient cells or attached to the cell surface, we included an additional wash step with citric acid-containing buffer (CAB wash) prior to FACS analysis<sup>46</sup>. In shCON and shITGB3 cells, CAB wash only slightly reduced the EV-derived fluorescence signal (Fig. 3a), indicating that vesicles do not accumulate at the cell surface before being taken up. Supporting this, heparin treatment, which already interferes with the capture of EVs at the cell surface, resulted in a similar reduction in EVs following the CAB wash (Fig. 3b). Furthermore, interference with the DYNAMIN-dependent internalisation of EVs through Dyngo-4a treatment did not result in accumulation of EVs at the cell surface (Fig. 3b). Thus, EV recognition and uptake appear to be intimately linked, preventing the accumulation of EVs at the cell surface when uptake is impaired.

To provide further evidence for these results independent of the FACS-based measurements, we assessed EV uptake into recipient cells on confocal microscopy. Cells treated with PKH26-labelled EVs were fixed, and alpha-tubulin staining of permeabilized cells was used for 3D reconstruction (Fig. 3c, d), to discriminate between surface-bound and internalized vesicles. Analysis of fluorescently labelled particles firstly showed a strong reduction in shITGB3 and shDyn2 cells (Fig. 3e). Furthermore, the ratio of surface-bound and internalized vesicles resembled our results obtained with the CAB wash in the FACS-based measurements of EV uptake (Fig. 2a). Our data therefore suggest that ITGB3 is essential for EV uptake in recipient cells. Furthermore, analysis of the PKH26-labelled EV uptake in shDyn2 cells revealed a strong reduction in the number of fluorescent particles (Fig. 3c–e); the proportion of surface-bound and internalized vesicles was similar to control and shITGB3 cells. Thus, FACS analysis combined with CAB-wash and confocal microscopy demonstrate that, when DYNAMIN-dependent EV uptake is impaired, EVs do not accumulate at the cell surface. Therefore, the interaction of EVs with the cell surface appears to be a highly dynamic process; if attachment of EVs is not intimately linked to endocytosis, EVs may detach again from the cell surface.



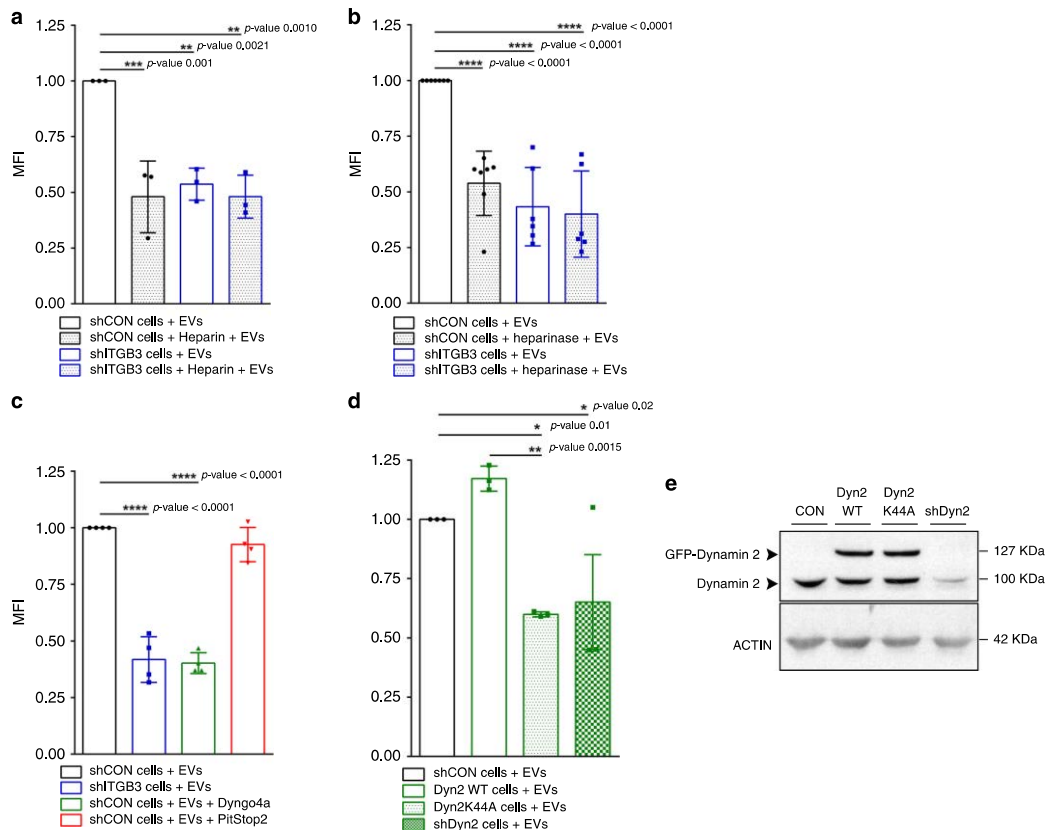


**Fig. 2 Endocytic uptake of EVs depends on ITGB3, HSPGs and DYNAMIN activity.** Internalization of 2–5  $\mu\text{g mL}^{-1}$  PKH26-labelled EVs derived from MDA.MB.231 cells by MDA.MB.231 shCON or MDA.MB.231 shITGB3 cells, measured by FACS. **a** Uptake of vesicles was measured after pretreatment with 10  $\mu\text{g mL}^{-1}$  heparin as a competitive inhibitor for cell-surface heparan-sulfated proteins for 30 min. **b** Uptake was measured in cells that were untreated or pretreated with 1.2  $\text{mIU mL}^{-1}$  heparinase I and 0.6  $\text{mIU mL}^{-1}$  heparinase III for 3 h before EV incubation. **c** Uptake of vesicles was measured after pretreatment with 20  $\mu\text{M}$  Dyngo4a or 10  $\mu\text{M}$  Pitstop 2 for 30 min in shCON cells. **d** Uptake of vesicles measured in MDA.MB.231 cells infected with Dyn2WT–Dyn2K44A– and shDyn2 constructs. **e** Representative immunoblot showing endogenous and exogenous levels of DYNAMIN 2 protein. Source data are provided as a Source Data file. (\* $p$  value < 0.05, \*\* $p$  value < 0.01, \*\*\* $p$  value < 0.001, \*\*\*\* $p$  value < 0.0001,  $n$  = 3 for panel 2a, d;  $n$  = 4 for panel 2c;  $n$  = 7 for panel 2b). Data are represented as mean  $\pm$  SD in (a–d). Statistical analysis including two-tailed unpaired Student's  $t$  test data was carried out using GraphPad Prism 6.01.

**ITGB3-dependent alterations in the EV secretome.** Having established the involvement of ITGB3 in the endocytosis-driven uptake of EVs, we wondered how this might be reflected in the secretome of shITGB3 cells. To test this, shCON and shITGB3 MDA.MB.231 cells were maintained in low-serum-containing medium (exosome-depleted 0.5% fetal bovine serum (FBS)) for 48 h and vesicles in the cell culture supernatant were isolated by differential ultracentrifugation (Fig. 4a). The vesicles were characterized by Nanosight and cryo-electron microscopy (Fig. 4) and their proteome was determined by liquid chromatography–mass spectrometry (LC–MS)/MS and Western blot (Fig. 5). The overall abundance of EVs, measured by Nanosight and normalized to the number of EV-producing cells, revealed no significant difference between shCON and shITGB3 cells (Fig. 4b–d). Similar results were obtained when the protein quantity in the EV fraction after ultracentrifugation was measured by bicinchoninic acid (BCA) protein assay (Supplementary Fig. 10c). However, we did detect clear differences in EV quantity when we analysed different

vesicle populations by size. In line with previous reports, vesicles between 150 and 200 nm comprised the peak fraction of MDA.MB.231 cells<sup>47</sup>. This vesicle population was reduced in shITGB3 cells, while those measuring 50–125 nm were significantly increased (Fig. 4b, c) (Supplementary Fig. 10a–c). We confirmed these results on cryo-electron microscopy (Fig. 4d). In summary, vesicles in the supernatant of shITGB3 displayed an altered size distribution.

To test if these changes were accompanied by alterations in the proteome of the respective EVs, we performed LC–MS/MS. We identified 3204 proteins (Supplementary Data 1), 1195 of which exhibited a statistically significant difference in abundance between EVs isolated from shCON and shITGB3 cells ( $q$  value < 0.05) (Fig. 5a, b). The fold change in protein abundance was calculated using the shCON condition as a reference, i.e.,  $\log_2(\text{shITGB3}/\text{shCON})$ . The heat map in Fig. 5a summarizes the results from the independent biological replicates and highlights the striking differences in the



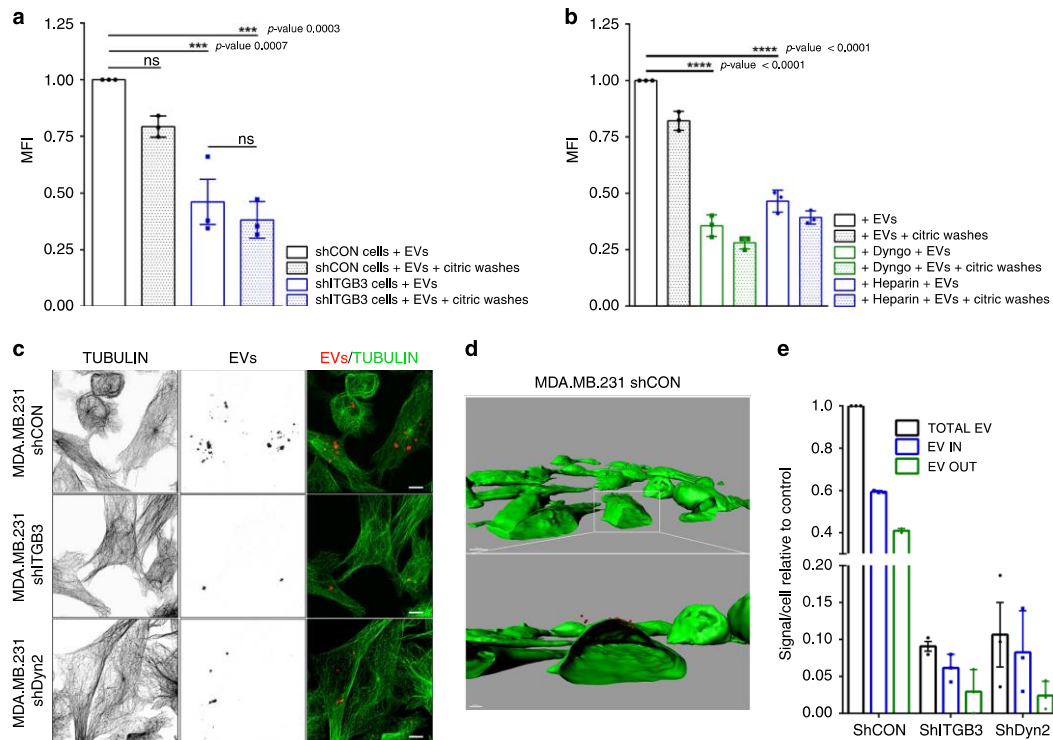


**Fig. 3** Interaction of EVs with the cell surface is a highly dynamic process. Internalization of  $2\text{-}5\ \mu\text{g mL}^{-1}$  PKH26-labelled EVs derived from MDA.MB.231 cells by MDA.MB.231 shCON or MDA.MB.231 shITGB3 cells, measured by FACS. **a** Uptake of vesicles was measured by FACS after subjecting the cells to acid washing. **b** Internalization of  $2\text{-}5\ \mu\text{g mL}^{-1}$  PKH26-labelled EVs derived from MDA.MB.231 cells by MDA.MB.231 cells, pretreated with  $20\ \mu\text{M}$  Dyngo4a and pre-treated with  $10\ \mu\text{g mL}^{-1}$  heparin, with or without subjecting the cells to acid washing. **c** Representative confocal pictures used for 3D reconstruction. **d** Representative 3D reconstruction picture of MDA.MB.231 shCON cells. Bar represents  $5\ \mu\text{m}$ . **e** Analysis of EV internalization in MDA.MB.231 shCON, shITGB3 and shDyn2 cells after 3D reconstruction. Source data are provided as a Source Data file. (\*\*\*)  $p$  value  $< 0.001$ , (\*\*\*\*)  $p$  value  $< 0.0001$ ,  $n = 3$ ). Data are represented as mean  $\pm$  SD in (**a**, **b**, **e**). Statistical analysis including two-way ANOVA multiple comparisons was carried out using GraphPad Prism 6.01.

proteome of vesicles derived from shCON and shITGB3 cells. These differences were furthermore supported by GO-term and KEGG pathway analysis (Supplementary Fig. 11).

To validate our findings, we performed Western blot analysis on proteins from the EV fractions derived from shCON and shITGB3 cells (Fig. 5c). This confirmed the knockdown of ITGB3 in EVs from the shITGB3 cell line, accompanied by a reduction in ITGAV, the alpha subunit of the  $\alpha\text{v}\beta 3$  heterodimer of ITGB3. However, the levels of ITGB1, also described to be present in EVs, were almost indistinguishable between vesicle fractions derived from shCON and shITGB3 cells. These results not only confirm the specificity of our knockdown, but also indicate that different integrins might be associated with different types of EV. In line with our proteomic analysis, we also confirmed a strong reduction in TSG101, a member of the ESCRT family, and the tetraspanin CD81, a bona fide exosome marker. Importantly, this defect appears to be specific to exosomes, as general EV marker proteins such as flotillin-1 or actin were not affected by the knockdown of ITGB3. In contrast, certain proteins, such as EIF4E, were exclusively associated with vesicles derived from shITGB3 cells. These results were confirmed with another shRNA construct, excluding the possibility of an off-target effect (Supplementary Fig. 4). Furthermore, we obtained the same results in MCF7 cells (Supplementary Fig. 12), excluding a cell-

line-specific phenomenon. Finally, we performed iodixanol gradient purification of EVs isolated by ultracentrifugation from shCON and shITGB3 cells. Western blot analysis confirmed that while flotillin and actin were equally present in the EV fractions (fraction 6/7) from shCON and shITGB3 cells, CD81 and TSG101 were strongly reduced in those fractions from shITGB3 cells (Fig. 5d, e).

As described above, EVs from both MDA.MB231 shCON and shITGB3 cells were equally capable of promoting colony growth of recipient MDA.MB231 cells in an ITGB3-dependent manner. However, the striking differences in the EV secretome of shCON and shITGB3 cells prompted us to speculate that other cellular processes might be altered. To test this, we used an indirect coculture system<sup>48</sup> to measure the migratory capacity of IMR90 cells in the presence of MDA.MB.231 shCON or shITGB3 cells. In line with the reported pro-migratory effect of MDA.MB231-derived exosomes<sup>49</sup>, IMR90 cells cocultured with MDA.MB.231 cells displayed an increased migratory capacity. Such migration was not induced in IMR90 cells cocultured with shITGB3 cells (Supplementary Fig. 13a, b). These results were not due to impaired uptake of vesicles derived from shITGB3 cells, since isolated vesicles from both shCON and shITGB3 cells were incorporated into IMR90 cells with similar kinetics (Fig. 1d). Thus, while secreted factors from shITGB3 cells did not promote

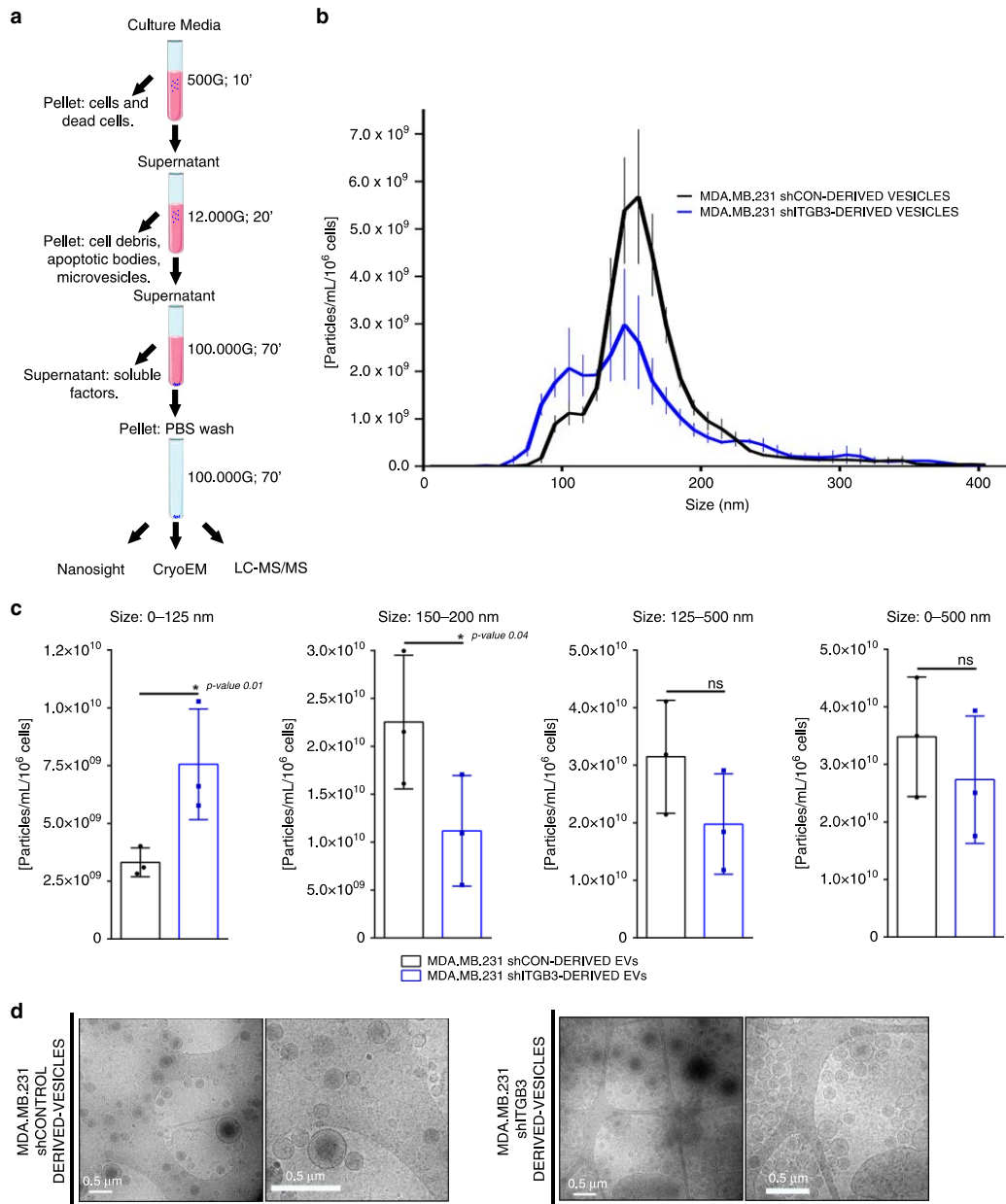


**Fig. 4** Characterization of EVs isolated from shCON and shITGB3 cells. **a** Schematic workflow for the preparation of EV samples for LC-MS/MS analysis. **b** Vesicle size distribution based on NTA data. **c** Particle concentration of isolated vesicle fractions normalized per million cells. **d** Representative CryoEM images of EV isolated from cultured MDA.MB.231 shCON and MDA.MB.231 shITGB3 cells. Source data are provided as a Source Data file. Scheme created with BioRender (<https://biorender.com/>). (\* $p$  value < 0.05,  $n = 3$ ). Data are represented as mean  $\pm$  SD in (**b**, **c**). Statistical analysis including two-tailed unpaired Student's  $t$  test data was carried out using GraphPad Prism 6.01.

cell migration in IMR90 cells, MDA.MB231 colony growth was stimulated similarly by EVs from shCON and shITGB3 cells, indicating functional diversity within the heterogeneous population of EVs.

In summary, the overall number of vesicles was not significantly altered between shCON and shITGB3 cells but the EVs isolated from the cell culture supernatant differed in size and protein composition. Particularly exosomes, defined as

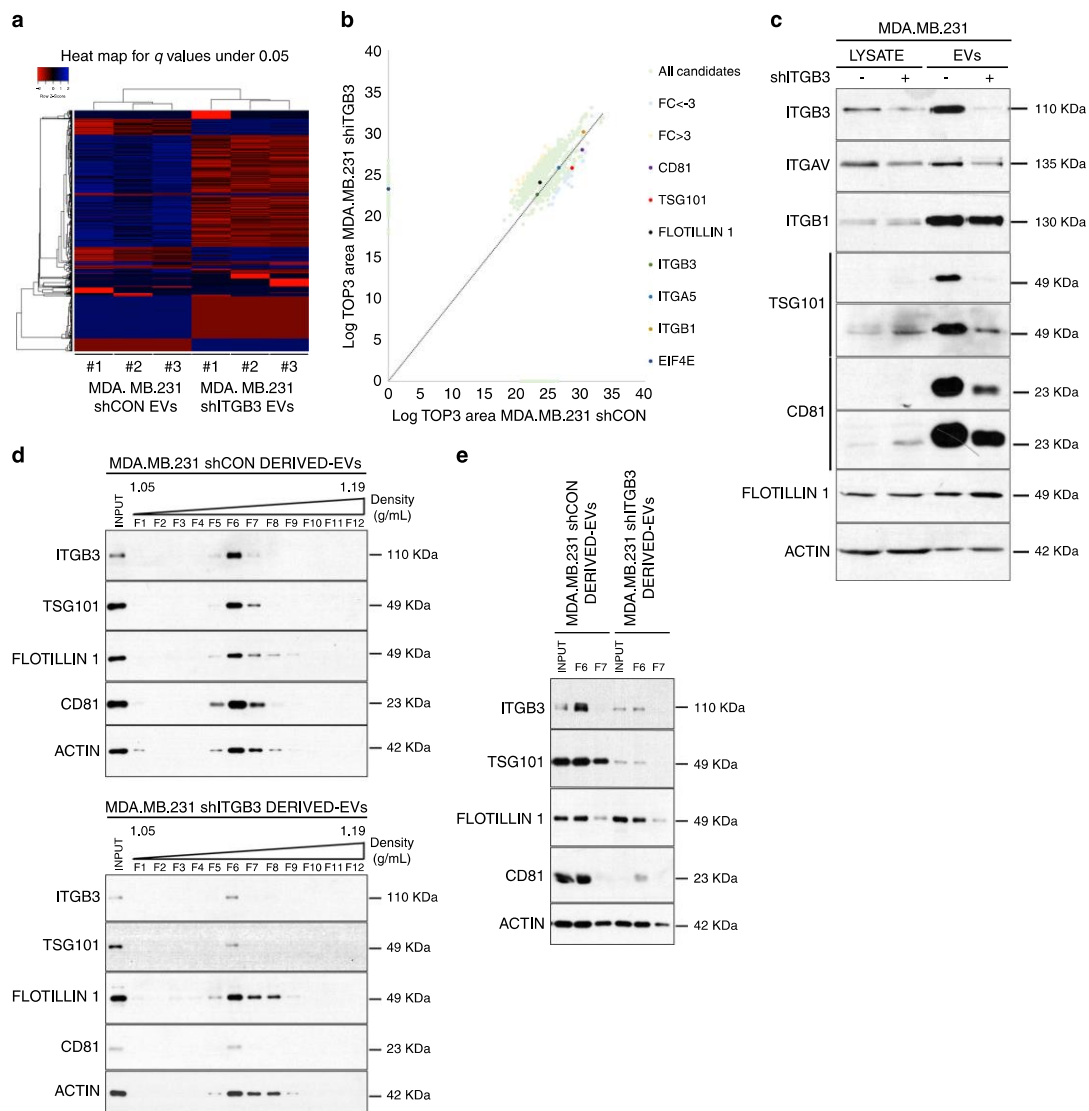


**Fig. 5** Alterations in the proteome of shITGB3-derived EVs. **a** Heat map representation of the normalized protein abundance (Log TOP3 area) ( $q$ -value  $< 0.05$ ) for the comparison of experimental replicates. **b** Scatter plot comparison of the abundance (Log TOP3 area) of proteins in the LC-MS/MS analysis of MDA.MB.231 shCON- and MDA.MB.231 shITGB3-derived EVs. The proteins validated by Western blot are highlighted. **c** Representative immunoblot analysis of candidate proteins identified in the proteomic survey. **d** Representative immunoblots after separation of vesicles in an iodixanol gradient for both MDA.MB.231 shCON (upper panel) and MDA.MB.231 shITGB3 (lower panel). **e** Representative immunoblot analysis of input and fractions 6 and 7. Source data are provided as a Source Data file.

CD81/TSG101-positive vesicles, appear strongly diminished in the case of shITGB3. The cause of this phenotype might be due to defective exosome biogenesis in shITGB3 cells or linked to the role of ITGB3 in vesicle uptake. Regarding a putative role in exosome biogenesis, it is important to mention that the ITGB3-interacting protein SRC has previously been shown to be required for exosome biogenesis<sup>34</sup>. Linking the described alterations in the EV secretome of shITGB3 cells to the role of ITGB3 in EV uptake, the abundance of small vesicles (50–125 nm) indicates

that their uptake is particularly dependent on ITGB3. As we could not rigorously rule out if defects in exosome biogenesis or EV uptake were responsible for the alterations in the EV secretome of shCON and shITGB3 cells, we looked further at the mechanism of ITGB3-dependent EV uptake.

**Uptake of EVs by MDA.MB.231 cells is dependent on FAK.** As described above, DYNAMIN-dependent endocytic recycling is integral to the regulation of integrin function<sup>50</sup>. In the case of

ITGB3, this recycling enables the assembly and disassembly of focal adhesions to allow cell migration. A key regulator of this process is FAK, which binds to and regulates the function of both proteins: DYNAMIN and ITGB3<sup>51–53</sup>.

To elaborate a putative link between FAK and ITGB3 in EV-related functions, we first monitored the activity of FAK in cells in different growth conditions. We prepared protein extracts from cells grown as colonies in the absence or presence of CM and normally growing cells, and monitored FAK activity by Western blot using the Y397 autophosphorylation as readout. In comparison to normal growth conditions, FAK activity was strongly increased when cells were grown as individual clones, particularly under CM-stimulated conditions (Fig. 6a). This FAK activity correlates with its described role in clonogenic growth<sup>54,55</sup>. However, FAK as a multifunctional protein kinase is required for clonogenic growth under basal conditions, complicating further analysis to establish a link to the ITGB3-dependent function in CM-stimulated colony formation.

Nevertheless, the described interaction between FAK and ITGB3 prompted us to examine in more detail if FAK activity is also required for EV uptake. To test this, cells were pre-treated with the small-molecule inhibitor FAK14 for 16 h to inactivate the kinase, then incubated with fluorescently labelled EVs. After 3 h, FACS analysis of internalized vesicles revealed a reduction in fluorescent intensity of approximately 60% compared to cells treated with DMSO as solvent control (Fig. 6b). Knockdown of FAK by siRNA confirmed these results (Fig. 6b, c). These data suggest that FAK activity is required for EV uptake into recipient cells. To test if FAK activity alone was sufficient for EV uptake in the absence of ITGB3, we transiently expressed FAK-GFP or the pCDNA3-GFP vector as a negative control in shCON and shITGB3 cells. Cells were treated with PKH26-labelled EVs for 3 h and the uptake into GFP-positive cells was determined by FACS. While we did observe a slight increase in EV uptake in shCON cells expressing FAK-GFP, the defect in vesicle uptake in shITGB3 cells was similar to the vector control (Fig. 6d). The activity of the overexpressed FAK-GFP was confirmed by Western blot, using the autophosphorylation of FAK on Y397 as readout (Fig. 6e). These results therefore suggest that, while FAK is required for EV uptake, ITGB3 interaction with HSPGs is required to link vesicle recognition at the cell surface to FAK activation in the cytoplasm.

As described above for the knockdown of ITGB3, a significant portion of vesicles were still taken up following FAK14 treatment or knockdown of FAK by siRNA. We therefore wondered if FAK inhibition would result in the same alterations in EVs in the cell culture supernatant as we observed in shITGB3 cells. To test this, control and FAK-14-treated MDA.MB.231 cells were maintained in low-serum-containing medium (exosome-depleted 0.5% FBS) for 48 h, and vesicles in the cell culture supernatant were isolated by differential ultracentrifugation (Fig. 4a). Western blot analysis of the obtained EVs revealed that CD81 and TSG101 were significantly reduced, while flotillin-1 and actin remained unaffected (Fig. 6f).

Considering these parallelisms in the EV-related functions of ITGB3 and FAK, we next wondered if ITGB3-mediated recognition of EVs was directly linked to the activation of FAK. To demonstrate this, we first serum-starved cells for 24 h to eliminate residual FAK activity<sup>19,52</sup>, then added purified EVs. As shown in Fig. 6g, the purified vesicles resulted in FAK activation, as demonstrated by autophosphorylation at Y397. The specificity of this phosphorylation event was confirmed by FAK-14 treatment. Importantly, this activation was strongly reduced in shITGB3 cells, pointing towards an ITGB3-dependent activation of FAK. Moreover, FAK activation was

blocked when DYNAMIN-dependent endocytosis was inhibited (Dyngo), but not when clathrin-dependent endocytosis was inhibited (Pitstop) (Fig. 6g). Notably, among all tested signalling pathways reported to be downstream of ITGB3, only FAK activity was stimulated by EVs (Supplementary Fig. 14). Together with our previous observation that vesicle uptake relies on DYNAMIN-dependent endocytosis (Fig. 2b, c), these results suggest that DYNAMIN and FAK are mutually dependent and together regulate EV uptake in an ITGB3-dependent manner. Notably, DYNAMIN and FAK have been shown to be interdependent for regulating focal adhesion turnover<sup>51,52</sup>, a scenario reminiscent of our observations.

In summary, we postulate that the transmembrane cell-surface protein ITGB3 plays a central role in the uptake of a subset of EVs. In this function, ITGB3 does not act as an EV receptor but is critical for mediating the link between EV capture at the cell surface and their uptake by endocytosis. Through the critical position of ITGB3 at the interface of extracellular and cellular interactions, the recognition of EVs at the cell surface by ITGB3-interacting HSPGs can be transmitted to the cytoplasm to trigger the interplay between DYNAMIN and FAK which ultimately allows the endocytic uptake of EVs (Fig. 6h).

## Discussion

Building on the findings<sup>26,27,56</sup> that ITGB3 is required for lung metastasis in MDA.MB.231 cells, we have demonstrated that the underlying mechanism may relate to the role ITGB3 plays in EV uptake and exosome biogenesis. In light of the preserved lung-homing capacity of shITGB3 cells in animal models, we focused on the next step in metastasis—clonal growth—and found that it was largely dependent on secreted factors in the cellular environment; shITGB3 cells had reduced EV uptake, rendering them insensitive to these factors. Our data indicate that this need for ITGB3 may be due to its dual role in connecting the capture of vesicles at the cell surface by HSPG-modified proteins like syndecans to the local activation of FAK-induced DYNAMIN-driven endocytosis (Fig. 6h).

As depicted in our model, endocytosis of EVs is linked to integrin internalisation. Integrins are established key players in the interaction between cells and their environment. This interaction must be tightly regulated for normal cell development; the deregulated expression of various integrins correlates with disease progression in several cancers. As transmembrane cell-surface receptors, integrins are critically positioned for cellular–extracellular interactions. Together with other scaffold proteins and signalling molecules they form focal adhesion complexes that link the actin cytoskeleton to the extracellular environment. These complexes form following integrin clustering induced by interactions with the extracellular matrix. The attachment of EVs to integrin-linked cell-surface receptors may induce a similar effect. The existence of such “endocytic hotspots<sup>57</sup>” for EV uptake on filopodia has been described previously. Cell spreading and motility requires active turnover of cell adhesion complexes, achieved mainly through endocytic recycling of integrins, a process that has been studied in detail in recent years<sup>21,58</sup>. Many common molecular players are involved, and certain specific integrin variations have been described, mainly relating to the highly variable C-terminal tail of beta integrins<sup>59,60</sup>. These sequence motifs define specific interactions with proteins, determining whether the uptake will be dependent upon caveolae, clathrin, neither, or both. In the case of ITGB3, endocytosis has been reported to rely solely on DYNAMIN<sup>49</sup>—our findings support this. Finally it is important to mention that the accurate localisation of individual EVs and the discrimination between different vesicle types among the heterogeneous population



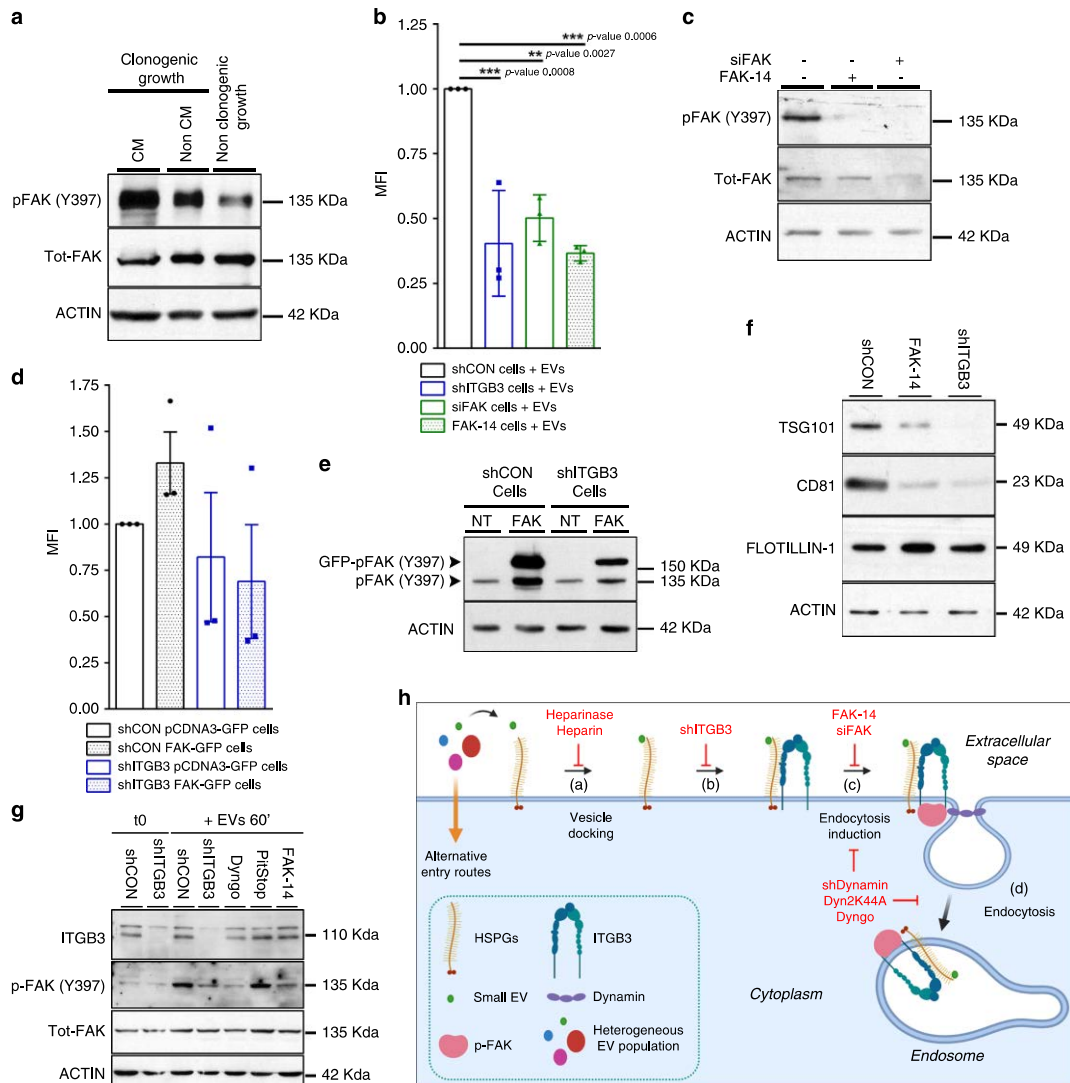


**Fig. 6 EV-induced activation of FAK is required for ITGB3-dependent EV uptake.** **a** Representative immunoblot analysis of pFAK activity either in normal conditions or clonogenic growth conditions with and without conditional medium (CM). **b** Internalization of 2–5  $\mu\text{g mL}^{-1}$  PKH26-labelled exosomes derived from MDA.MB.231 cells by MDA.MB.231 shCON, shITGB3, siFAK or shCON pretreated with 15  $\mu\text{M}$  FAK 14 for 14–16 h, measured by FACS. **c** Representative immunoblot analysis confirming FAK knockdown and pFAK activity reduction after FAK-14 treatment. **d** Internalization of 2–5  $\mu\text{g mL}^{-1}$  PKH26-labelled exosomes derived from MDA.MB.231 cells by MDA.MB.231 shCON pCDNA3-GFP, shCON FAK-GFP, shITGB3 pCDNA3-GFP, and shITGB3 FAK-GFP, in GFP-positive cells measured by FACS. **e** Representative immunoblot analysis of pFAK activity in shCON pCDNA3-GFP, shCON FAK-GFP, shITGB3 pCDNA3-GFP, and shITGB3 FAK-GFP. **f** Representative immunoblot analysis of TSG101, CD81 and flotillin-1 on EVs derived from untreated MDA.MB.231 shCON or MDA.MB.231 shITGB3 cells or from control or FAK-14 inhibitor (15  $\mu\text{M}$ ) treated MDA.MB.231 shCON cells. **g** Representative immunoblot analysis of the autophosphorylation of FAK at Y397 as readout for its kinase activity. MDA.MB.231 shCON or shITGB3 serum-starved cells were pretreated with 20  $\mu\text{M}$  Dyngo4a, 10  $\mu\text{M}$  Pitstop 2 or 10  $\mu\text{g mL}^{-1}$  heparin for 30 min or with 15  $\mu\text{M}$  FAK-14 for 14–16 h followed by addition of EVs for 60 min. **h** Model for the proposed role of ITGB3 in vesicle uptake and exosome biogenesis. (a) EV-HSPG interaction; (b)  $\alpha\text{v}\beta 3$  recruitment; (c) pFAK-DYNAMIN recruitment to endocytosis complex; (d) Dynamin-mediated internalization of EVs and EE formation. Source data are provided as a Source Data file. Model created with BioRender (<https://biorender.com/>). (\*\**p* value < 0.01, \*\*\**p* value < 0.001 *n* = 3). Data are represented as mean  $\pm$  SD in (b) and (d). Statistical analysis including two-way ANOVA multiple comparisons was carried out using GraphPad Prism 6.01.

of EVs is still hindered by the current limitations of the applied microscopy techniques<sup>10</sup>. This is particularly important, when considering the role ITGB3 in the selective uptake of small EVs. While NTA can readily discriminate those different sized EV populations, the resolution limit of conventional confocal microscopy does not permit visualisation of those vesicles and to discriminate among EV subpopulations at reliable resolution *in vivo*. Current advancements of FACS (asymmetric-flow field-flow fractionation technology) and microscope-based techniques will complement the NTA based technologies in the future, which will allow the precise determination of vesicle size and localisation *in vivo*<sup>10,61</sup>.

As described above, FAK and DYNAMIN are key players in the ITGB3-dependent endocytosis of EVs. Supporting this, the interaction between FAK and the C-terminal tail of ITGB3 is well established<sup>60,62</sup>. FAK-dependent phosphorylation and regulation of the effector protein DYNAMIN is required for the turnover of focal adhesions<sup>19,51,52</sup>. Interestingly, our studies indicate that FAK and DYNAMIN are mutually dependent on each other for the ITGB3-dependent uptake of EVs. This interdependency might be due to the reported direct interaction between the two proteins for the endocytic uptake of ITGB1. However, given the marked differences in the cytoplasmic tail of ITGB3 and ITGB1, detailed molecular analysis exploring the involvement of other adapter proteins or the reported interaction with signalling molecules like SRC will be required to delineate the exact molecular mechanisms. As for ITGB3, we cannot rigorously exclude the possibility that FAK might also be required for exosome biogenesis. While our data strongly support a role of FAK in the ITGB3-dependent uptake of EVs, a closer examination of the potential role of FAK in exosome biogenesis might present an interesting focus for future investigation.

Interestingly, our proposed model for ITGB3-dependent EV uptake closely resembles the uptake of herpes viruses. Viral endocytosis begins with the viral capsid binding to integrin-associated HSPGs at the cell surface. Following attachment and receptor clustering, activation of receptor tyrosine kinases (FAK, SRC) drive specific signalling pathways that activate membrane fission and fusion factors. To date, a variety of mechanisms have been described for EV uptake. A similar variety has been described for the uptake of different viruses (20–300 nm) into specific cell types. Drawing a further comparison between the cell-specificity of viruses and that of EVs, we demonstrated that a specific fraction of EVs (approximately 50% of the total vesicles) were taken up in an ITGB3-dependent manner. Since this effect was not increased by combining treatments (shITGB3 + heparin), we conclude that a certain type of EVs are taken up via this route. Analysis of the EVs in cell culture supernatant revealed a significant increase in vesicles with a diameter between 50 and 100 nm in shITGB3 cells, which might indicate that the uptake of those vesicles is particularly dependent on ITGB3. Interestingly, vesicles of this size (termed exomeres or P200 exosomes) are described to contain less CD81 than other EVs<sup>63,64</sup>, which might explain why the relative increase in these vesicles in the total isolated EVs results in a reduction of CD81 in the cell culture supernatant of shITGB3 cells. However, detailed molecular analysis using recently developed techniques like asymmetric flow field-flow fractionation of EVs are required to determine the exact molecular identity of those vesicles<sup>61</sup>. Although we cannot rigorously exclude that the differences in the EV secretome of shITGB3 cells might be caused by alterations in exosome biogenesis, the data presented here on the role of ITGB3 in vesicle uptake and the parallelism in the phenotype with the ITGB3-interacting protein FAK rather suggest a selective defect in the uptake of small vesicles devoid of CD81. The recently discovered variety in EV size and molecular composition is reminiscent of the variety seen in viruses, for which different uptake mechanisms

have been described. Finally, certain receptor cell-specific adaptations to this mechanism may also occur, such as the use of different integrin receptors. The most likely candidates would be integrins that can interact with heparinised cell-surface receptors and contain a  $\beta$ -subunit capable of binding and activating FAK.

We found that ITGB3 knockdown rendered breast cancer cells insensitive to secreted factors in their environment, reducing their clonal growth capacity. Intercellular communication represents an important target for future cancer treatment strategies. Current approaches target cancer cells, yet the past decade of research has demonstrated the importance of the cell environment and intercellular communication in disease progression and treatment resistance: blocking these interactions seems a sensible strategy to improve current treatments.

## Methods

**Cell culture and reagents.** Breast cancer cell lines were purchased from the American Type Culture Collection (ATCC) and authenticated by DNA profiling using short tandem repeat (GenePrint® 10 System, Promega) at Genomics Core Facility, Instituto de Investigaciones Biomédicas Alberto Sols CSIC-UAM. MDA.MB.231 and MCF7 cells were maintained in Dulbecco's modified Eagle's medium (DMEM) (Invitrogen) supplemented with 10% heat-inactivated FBS (Life Technologies) and antibiotics (100 U mL<sup>-1</sup> penicillin, 100  $\mu$ g mL<sup>-1</sup> streptomycin) (Life Technologies). Cells were maintained at 37 °C in a 5% CO<sub>2</sub> humidified incubator. The FBS used for exosome purification experiments was depleted of EVs by centrifugation at 100,000g for 1 h 10 min at 4 °C. For the preparation of medium with EV-depleted 0.5% FBS, EV-depleted FBS was added to DMEM to a final concentration of 0.5% v/v.

**Cell culture migration assays in co-culture.** Cells were cultured in a double chamber coculture system allowing cell types to grow in close proximity to one another without mixing (TC insert for 24-well plate, PET membrane bottom, translucent, pore size 0.4  $\mu$ m, sterile, non-pyrogenic/endotoxin-free, non-cytotoxic, 1 pc/blister (Sarstedt)). The upper part is a transwell comprised of 24 cell culture inserts with a 0.4- $\mu$ m pore size to avoid mixing the two cell types. The lower part is a well of the 24-well plate. IMR90 cells were plated in the lower culture 24-well plate area in triplicate. Either MDA.MB.231 shCONTROL or MDA.MB.231 shITGB3 cells were plated in triplicate in the upper inserts. After 48 h growing in shared medium, IMR90 reached a monolayer and were treated overnight with mitomycin C (5  $\mu$ g mL<sup>-1</sup>, Santa Cruz Biotechnology). Then, a wound was made in the monolayer with a pipette tip, the medium was replaced, and the cells were incubated in normal conditions. Pictures of the wounds were taken after 24 h, and wound closure was measured using ImageJ software.

**Cell-surface flow cytometry staining protocol.** For cell-surface levels, after 1 h treatment with heparin (Sigma Aldrich), Dyngo-4a (Abcam) or Pitstop-2 (Abcam) or after an overnight treatment in the case of FAK-14 inhibitor, cells were detached using enzyme-free phosphate-buffered saline (PBS)-based Cell Dissociation Buffer (Gibco). Cells were washed in PBS solution and incubated with the FITC-conjugated ITGB3 antibody at room temperature for 1 h in non-permeabilized conditions. Cells were washed in PBS solution, suspended in FACS buffer (EDTA 2.5 mM, 1% bovine serum albumin (BSA) in PBS), and analysed on a FACSCalibur instrument with integrated FACSDiva (BD Biosciences) v8.0.1 Software.

**Clonal cell growth assay.** Cells were seeded in six-well plates (500 cells/well) and cultured for 7–9 days at 37 °C and 5% CO<sub>2</sub>. The supernatant was discarded and the cells were gently washed with 1 mL of PBS. Clonal cell growth was assessed following staining with 0.5% crystal violet in ddH<sub>2</sub>O. The crystal violet staining of cells from each well was solubilized using 15% acetic acid and the optical density of the solution was measured.

**Cryogenic electron microscopy (CryoEM).** EVs collected by ultracentrifugation were analysed at similar dilutions on electron cryomicroscopy (CryoEM) in the microscopy facility at the Universitat Autònoma de Barcelona. Vitrified specimens were prepared by placing 3  $\mu$ L of a sample on a holey carbon TEM grid, blotted to a thin film and plunged into liquid ethane-N<sub>2</sub>(l) in the Leica EM GP cryoworkstation. The grids were transferred to a 626 Gatan cryoholder and maintained at –179 °C. The grids were analysed with a Jeol JEM 2011 transmission electron microscope operating at an accelerating voltage of 200 kV. Images were recorded on a Gatan Ultrascan 2000 cooled charge-coupled device (CCD) camera with the Digital Micrograph software package (Gatan).

**Enzymatic treatments.** The protocol followed for heparan sulfate enzymatic digestion experiments was described in Christianson et al.<sup>14</sup>. Briefly, cells were cultured in digestion buffer (DMEM supplemented with 0.5% [wt vol<sup>-1</sup>] BSA and

20 mM Hepes-HCl, pH 7.4) and either untreated or treated with 1.2 mIU mL<sup>-1</sup> heparinase I and 0.6 mIU mL<sup>-1</sup> heparinase III (Sigma-Aldrich) for 3 h at 37 °C. Then, EVs were added and incubated for 3 h, followed by flow cytometry analysis (as described later).

**EV labelling.** For EV-uptake experiments, purified EVs were fluorescently labelled using PKH26 Red Fluorescent Cell Linker Midi Kit (Sigma-Aldrich). EVs isolated by ultracentrifugation and resuspended in 1 mL of PBS were labelled with the PKH26 dye (2 µM final concentration) according to the manufacturer's instructions.

**EV purification.** For all experiments, EVs were isolated by ultracentrifugation. Cells were cultured in media supplemented with 10% exosome-depleted FBS and after 48 h were changed to media supplemented with 0.5% exosome-depleted FBS. Equivalent amounts of supernatant fractions collected after 48–72 h cell culture were pelleted by centrifugation at 500 g for 10 min, to remove cells. The supernatant was centrifuged at 12,000 g for 20 min, to remove cell debris and dead cells, and finally, EVs were collected by centrifugation at 100,000 g for 70 min (Thermo Scientific, mx ultra-series centrifuge). The EV pellet was resuspended in 20 mL of phosphate-buffered saline (PBS) and collected by ultracentrifugation at 100,000 g for 70 min (Thermo Scientific, mx ultra-series centrifuge), and the final pellet was resuspended in 100 µL of PBS. Protein concentration in the final EV pellet was measured by BCA (Pierce, Thermo Fisher Scientific) according to the manufacturer's instructions. A detailed protocol for EV preparation is available at Protocol Exchange (Nature Research, <https://doi.org/10.21203/rs.3.pex-1044/v1>).

**EV gradient separation.** A discontinuous iodixanol gradient was prepared by diluting a stock solution of OptiPrep™ (60% w/v) with 0.25 M sucrose/10 mM Tris, pH 7.5, to generate 40, 20, 10, and 5% w/v iodixanol solutions. The discontinuous iodixanol gradient was generated by sequentially layering 3 mL each of 40, 20, and 10% (w/v) iodixanol solutions, followed by 2.5 mL of the 5% iodixanol solution. EVs, previously purified by ultracentrifugation, were loaded on the discontinuous iodixanol gradient and centrifuged for 16 h at 100,000 g at 4 °C. Fractions of 1 mL were collected from the top of the gradient, and recentrifuged at 100,000 g for 2 h at 4 °C. The resulting pellets were resuspended in 25 µL Laemmli buffer 1× and analysed by Western blot.

**FAK activity.** Starved cells were treated with Dyngo-4a or Pitstop-2 30 min prior to adding EVs; FAK 14 inhibitor was added the night before the EVs. Acceptor cells were incubated with EVs (10–25 µg mL<sup>-1</sup>) for 1 h, then washed with cold PBS and collected on ice for immunoblotting.

**Flow cytometry.** For EV uptake studies, acceptor cells were incubated with PKH-labelled EVs (1–5 µg mL<sup>-1</sup>) for 1–6 h. Cells were detached using enzyme-free PBS-based Cell Dissociation Buffer (Gibco). Cells were washed in PBS solution, suspended in FACS buffer (EDTA 2.5 mM, 1% BSA in PBS), and analysed on a FACSCalibur instrument with integrated FACSDiva (BD Biosciences) v8.0.1. FCS Express 4 Flow Research was used to perform Flow cytometry analysis. In blocking experiments, heparin, Dyngo-4a or Pitstop-2 were added 30 min prior to EVs; FAK 14 inhibitor was added the night before the EVs.

**Homing of MDA.MB.231 cells to lung.** Female athymic nude mice (Harlan Interfauna Iberica, Barcelona, Spain) were kept in pathogen-free conditions and used at 7 weeks of age. Temperature and relative humidity is continuously recorded in the animal housing. The temperature ranged from 23 to 25 °C. Relative humidity ranged between 45 and 65%. Lighting was artificial, from an automatic controlled supply. The cycle gradually simulates twilight and sunset from 7:30 to 8:00 a.m. and from 19:30 to 20:00 p.m., respectively, giving 12 h of light with an intensity of 300 Lux and 12 h of darkness for each 24 h period. Animal care was handled in accordance with the Guide for the Care and Use of Laboratory Animals of the Vall d'Hebron University Hospital Animal Facility, and the experimental procedures were approved by the Animal Experimentation Ethical Committee of the institution (76/17 CEEA).

For the homing assays, we used shCON and shITGB3 MDA.MB.231 cells that were labelled with DiIC18 (D7757; Molecular Probes) according to the manufacturer instructions; 100,000 cells were injected intravenously into the left caudal tail vein of each mouse. Mice were sacrificed 12 h later for lung harvest. The whole lungs were minced with scalpels and incubated in 2 mL of freshly prepared DMEM containing 0.8 mg mL<sup>-1</sup> dispase (Gibco) and 1.5 mg mL<sup>-1</sup> collagenase P (Roche) at 37 °C in agitation for 15 min. After incubation, 10 mL of DMEM was added, and tissue fragments and cell suspensions were spun at 500 g for 5 min. Pellets were incubated with 0.05% trypsin-EDTA at 37 °C for 2 min. Single-cell suspensions were filtered through 70-µm nylon filter and washed in PBS with 2 mM EDTA and 1% BSA. Cells were blocked and stained with CD45 Monoclonal Antibody (30-F11) (1:200), FITC (eBioscience) for flow cytometry, and absolute counts of CD45-negative DiIC18-positive cells were obtained and analysed on a FACSCalibur instrument with integrated FACSDiva (BD Biosciences) v8.0.1.

**Immunofluorescence.** Cells were grown on cover glasses for 1 day, rinsed with TBS at room temperature and fixed for 10 min with 4% paraformaldehyde. After rinsing with TBS, in the case of permeabilized conditions, cells were incubated with 0.1% Triton X-100 in TBS for 30 min followed by 30 min in blocking buffer (BSA 2% in TBS-T 0.1% Triton X-100) at room temperature. For non-permeabilized conditions, cells were directly incubated in blocking buffer (BSA 2% in TBS) for 1 h at room temperature. Next, cells were incubated in the suitable primary antibodies for 1 h at room temperature and rinsed repeatedly with TBS before incubating in the appropriate fluorescein-labelled secondary antibody for 1 h at room temperature. Cells were then washed extensively with TBS and mounted on a glass slide in Prolong Diamond Antifade mountant with DAPI (Pierce, Thermo Fisher Scientific). The following primary antibodies were used: anti-EEA1 (1:1000) (Cell Signalling), anti-LAMP-1 (1:1000) (Santa Cruz), anti-avb3 (1:50) clone LM609 (Merck) and anti-tubulin (1:1000) (DM1a-FITC, Sigma). The following secondary antibodies were used: goat anti-mouse IgG (H + L) Alexa Fluor Plus 488 and goat anti-rabbit IgG (H + L) Alexa Fluor 633 (Thermo Fisher Scientific) (1:1000).

**Microscopy and image analysis.** Cells were observed under a confocal laser scanning microscope LSM980 (Carl Zeiss, Germany) with a 63× 1.4 NA oil immersion lens. Images for EV location analysis were captured with a pixel size of 0.07 × 0.07 × 0.31 px µm<sup>-1</sup> (xyz, respectively). Images for co-localization analysis were optimally sampled (Nyquist–Shannon theorem) at 0.03 × 0.03 × 0.16 px µm<sup>-1</sup> (xyz, respectively). Images were firstly deconvoluted using Zeiss Zen 3.0 program. EV location and counting was done using Imaris software (7.2.3) through 3D cell reconstruction. Co-localization was done using Zeiss Zen 3.0 program.

**Modulation of expression using plasmid transient transfection.** Wild-pGFP FAK was a gift from Kenneth Yamada (Addgene plasmid # 50515; <http://n2t.net/addgene:50515>; RRID:Addgene\_50515)<sup>65</sup>. Transfections using TransIT-BrcA (Mirrus) were performed according to the manufacturer's protocol, at a final concentration of 3 µg of plasmid DNA in a single well of a 6-well plate. Western blotting with anti-phospho-FAK (Y397) antibody was used to confirm plasmids were expressing the wild type.

**Expression modulation by retroviral and lentiviral infection.** For lentiviral shRNA of ITGB3, pLKO.1-puro-shITGB3 was constructed by annealing the oligonucleotides 5'-CCGGGCCAAGACTCATATAGCATTGCTCGA-3' and 5'-AAT TCAAAAAGCCAAAGACTCATATAGCATT-3' and cloning them into a pLKO1 vector. The shITGB3 #3 was obtained from Dharmacon. We also used pLKO1 as shCTL. Sigma Mission shRNA clone TRCN000006649 plasmid was used for targeting DYNAMIN 2. WT DYNAMIN 2 pEGFP (Addgene plasmid # 34686; <http://n2t.net/addgene:34686>; RRID:Addgene\_34686) and K44A DYNAMIN 2 pEGFP (Addgene plasmid # 34687; <http://n2t.net/addgene:34687>; RRID:Addgene\_34687), a gift from Sandra Schmid, were used for subcloning (HindIII/NotI) into pLPCX retroviral plasmid. Cell monolayers were incubated with virus containing cell culture supernatant in the presence of 4 µg/ml polybrene (Sigma-Aldrich) for 24 h. Infected MDA.MB.231 and MCF7 cells were selected with 0.7 or 1.5 µg mL<sup>-1</sup> puromycin, respectively, for 3–4 days. Viral production and infection were performed at 37 °C. All plasmids were sequenced twice from both ends to ensure expression of the correct coding sequence.

**Expression modulation by small interfering RNA knockdown.** siRNA transfections were performed in Opti-MEM medium (Life Technologies) using Lipofectamine RNA-iMAX (Life Technologies), following manufacturer's instructions. Unless otherwise indicated, transfections were performed for 48 h, with 50 nM siRNA. The following siRNAs were used: non-silencing control siRNA (D-001810-01-05) from Dharmacon and siFAK from Sigma-Aldrich (SASI\_Hs01\_00035697).

**Nanoparticle tracking analysis (NTA).** EVs collected by ultracentrifugation were analysed at similar dilutions in a Nanosight NS-300 instrument (Malvern Instruments) for real-time characterization of the vesicles. Using the Automatic Syringe Pump (Malvern) at a pump speed of 40, three videos of 60 s were recorded for each sample at 20 °C and a concentration of 10–55 particles per frame and used to calculate mean particle concentration and size. The measurements were analysed using a detection threshold of 5. For all analyses, NTA version 3.1 Build 3.1.45 was used.

All NTA and CryoEM studies were performed at the CIBER-BBN (Bioingeniería, Biomateriales y Nanomedicina), Institut de Ciència de Materials de Barcelona (ICMAB-CSIC, Barcelona, Spain) (<http://www.nanbiosis.es/ue-e04-nanosight-lm-20-for-nanoparticle-tracking-analysis/>).

**Preparation of EVs and cell lysates.** EV pellets prepared by differential high-speed centrifugation were resuspended in PBS and a known concentration was loaded on SDS-polyacrylamide gels in Laemmli buffer. The corresponding cell layers were washed in cold PBS and scraped on ice in lysis buffer (50 mM Tris-HCl, pH 7.4, 150 mM NaCl, 1% Triton X-100, 1% sodium deoxycholate, 0.1% SDS, 1 mM EDTA) supplemented with PhosSTOP and Complete Phosphatase/Protease Inhibitor Cocktails (Roche Diagnostics GmbH, Mannheim, Germany). The whole



cellular lysate was centrifuged at 16,000 g for 15 min to clear cell debris then stored at  $-20^{\circ}\text{C}$ . Protein concentration in the cellular extracts was determined using the BCA method (Pierce, Thermo Fisher Scientific) according to the manufacturer's instructions. Protein extracts (40–50  $\mu\text{g}$  per sample) were loaded onto sodium dodecyl sulfate-polyacrylamide gel electrophoresis gels and transferred electrophoretically to PVDF membranes, and immunodetection of proteins was performed using ECL<sup>™</sup> Western Blotting Detection Reagents (GE Healthcare, Buckinghamshire, UK). The following primary antibodies were used: anti-CD81 (1:5000), anti-pFAK (1:1000) and anti-FAK (1:1000), anti-DYNAMIN 2 (1:500), anti-LAMP1 (1:500) and anti-ERK (1:1000) (Santa Cruz Biotechnology); anti-Vinculin (1:1000) (Sigma-Aldrich) anti-TSG101 (1:2500), anti- $\alpha\text{v}$  integrin (1:2000) and anti- $\beta\text{1}$  (1:5000) integrin (Abcam); anti- $\beta\text{3}$  integrin (1:500), anti-pERK (1:1000), anti-pSrc (1:500), anti-Src (1:500), anti-pAKT (1:1000), anti-AKT (1:1000), anti-EEA1 (1:2500) and anti-EIF4E (1:1000) (Cell Signalling); anti-flotillin-1 (1:1500) (Novus Biologicals) and anti- $\beta$ -actin (1:500; Sigma-Aldrich). Anti-mouse and anti-rabbit HRP secondary antibodies were from Pierce (1:10000). Bound antibodies were visualized with an enhanced chemiluminescence detection kit (Amersham Pharma-Biotech).

**Proteomics sample preparation.** Eluted proteins were reduced, alkylated and digested to peptide mixes according to the filter-aided sample preparation<sup>66</sup> method using LysC 1:10 ratio (w:w; enzyme:substrate) at  $37^{\circ}\text{C}$  overnight, followed by trypsin 1:10 ratio (w:w; enzyme:substrate) at  $37^{\circ}\text{C}$  for 8 h. Tryptic peptide mixtures were desalted using a C18 UltraMicroSpin column<sup>67</sup>. Protein extracts (15  $\mu\text{g}$ ) were reduced with dithiothreitol (30 nmol,  $37^{\circ}\text{C}$ , 60 min) and alkylated in the dark with iodoacetamide (60 nmol,  $25^{\circ}\text{C}$ , 30 min). Samples were first diluted to 2 M urea with 200 mM  $\text{NH}_4\text{HCO}_3$  for digestion with endoproteinase LysC (1:10 w-w,  $37^{\circ}\text{C}$ , o/n, Wako), and then diluted 2-fold with 200 mM  $\text{NH}_4\text{HCO}_3$  for trypsin digestion (1:10 w-w,  $37^{\circ}\text{C}$ , 8 h, Promega). After digestion, peptide mix was acidified with formic acid and desalted with a MicroSpin C18 column (The Nest Group, Inc) prior to LC-MS/MS analysis.

**Chromatographic and mass spectrometric analysis.** Samples were analysed using an LTQ-Orbitrap Velos Pro mass spectrometer (Thermo Fisher Scientific, San Jose, CA, USA) coupled to an EASY-nLC 1000 (Thermo Fisher Scientific [Proxeon], Odense, Denmark). Peptides were loaded onto the 2-cm Nano Trap column with an inner diameter of 100  $\mu\text{m}$  packed with C18 particles of 5  $\mu\text{m}$  particle size (Thermo Fisher Scientific) and were separated by reversed-phase chromatography using a 25-cm column with an inner diameter of 75  $\mu\text{m}$ , packed with 1.9  $\mu\text{m}$  C18 particles (Nikkoyo Technos Co., Ltd. Japan). Chromatographic gradients started at 93% buffer A and 7% buffer B with a flow rate of 250  $\text{nL min}^{-1}$  for 5 min and were gradually adjusted to 65% buffer A and 35% buffer B over 120 min. After each analysis, the column was washed for 15 min with 10% buffer A and 90% buffer B. Buffer A: 0.1% formic acid in water. Buffer B: 0.1% formic acid in acetonitrile. The mass spectrometer was operated in positive ionization mode with nanospray voltage set at 2.1 kV and source temperature at  $300^{\circ}\text{C}$ . Ultramark 1621 was used for external calibration of the FT mass analyser before the analyses, and an internal calibration was performed using the background polysiloxane ion signal at  $m/z$  445.1200. The acquisition was performed in data-dependent acquisition (DDA) mode, and full MS scans with 1 micro scans at a resolution of 60,000 were used over a mass range of  $m/z$  350–2000 with detection in the Orbitrap. Auto gain control (AGC) was set to 1E6, dynamic exclusion (60 s), and charge state filtering disqualifying singly charged peptides was activated. In each cycle of DDA analysis, following each survey scan, the 20 most intense ions with multiple charged ions above a threshold ion count of 5000 were selected for fragmentation. Fragment ion spectra were produced via collision-induced dissociation (CID) at normalized collision energy of 35% and acquired in the ion trap mass analyser. AGC was set to 1E4, with an isolation window of 2.0  $m/z$ , an activation time of 10 ms and a maximum injection time of 100 ms. All data were acquired with Xcalibur software v2.2. Digested bovine serum albumin (New England Biolabs cat # P8108S) was analysed between each sample to avoid sample carryover and to assure stability of the instrument, and QCloud<sup>66</sup> was used to control instrument longitudinal performance during the project.

**Data analysis.** Acquired spectra were analysed using the Proteome Discoverer software suite (v1.4, Thermo Fisher Scientific) and the Mascot search engine (v2.5, Matrix Science<sup>67</sup>). The data were searched against a Swiss-Prot human database plus a list<sup>68</sup> of common contaminants and all the corresponding decoy entries. For peptide identification a precursor ion mass tolerance of 7 ppm was used for MS1 level; trypsin was chosen as the enzyme and up to three missed cleavages were allowed. The fragment ion mass tolerance was set to 0.5 Da for MS2 spectra. Oxidation of methionine and N-terminal protein acetylation were used as variable modifications whereas carbamidomethylation on cysteines was set as a fixed modification. False discovery rate in peptide identification was set to a maximum of 5%. Protein abundance was estimated using the area under the chromatographic peak of the three most intense peptides per protein. Data were log transformed and normalized by equalizing the median of the total protein abundance per sample. Fold changes,  $p$  values and  $q$ -values were calculated to assess protein relative

quantification. Proteins observed in all replicates of one condition and in none of the other conditions were considered significantly different (presence/absence).

**Statistics.** Results are expressed as means + standard errors of the means. Two-tailed Student's  $t$  test and two-way ANOVA multiple comparisons were carried out as appropriate, both using GraphPad Prism 6.01.  $p < 0.05$  was considered significant.

**Reporting summary.** Further information on research design is available in the Nature Research Reporting Summary linked to this article.

### Data availability

The mass spectrometry raw data have been deposited into the PRIDE<sup>69</sup> repository with the dataset identifier PXD013489. All the data supporting the findings of this study are available within the article and its supplementary information files and from the corresponding author upon reasonable request. A reporting summary for this article is available as a Supplementary Information file. Source data are provided with this paper.

Received: 25 April 2019; Accepted: 31 July 2020;

Published online: 26 August 2020

### References

1. Massagué, J. & Obenauf, A. C. Metastatic colonization. *Nature* **529**, 298–306 (2016).
2. Wan, Z. et al. Exosome-mediated cell-cell communication in tumor progression. *Am. J. Cancer Res.* **8**, 1661–1673 (2018).
3. Peinado, H. et al. Pre-metastatic niches: organ-specific homes for metastases. *Nat. Rev. Cancer* **17**, 302–317 (2017).
4. Costa-Silva, B. et al. Pancreatic cancer exosomes initiate pre-metastatic niche formation in the liver. *Nat. Cell Biol.* **17**, 816–826 (2015).
5. Becker, A. et al. Extracellular vesicles in cancer: cell-to-cell mediators of metastasis. *Cancer Cell* **30**, 836–848 (2016).
6. Mathieu, M., Martin-Jaular, L., Lavieu, G. & Théry, C. Specificities of secretion and uptake of exosomes and other extracellular vesicles for cell-to-cell communication. *Nat. Cell Biol.* **21**, 9–17 (2019).
7. Choi, D. S., Kim, D. K., Kim, Y. K. & Gho, Y. S. Proteomics, transcriptomics and lipidomics of exosomes and ectosomes. *Proteomics* **13**, 1554–1571 (2013).
8. Green, T. M., Alpaugh, M. L., Barsky, S. H., Rappa, G. & Lorico, A. Breast cancer-derived extracellular vesicles: Characterization and contribution to the metastatic phenotype. *Biomed. Res. Int.* **2015**, 6977–6994 (2015).
9. Van Niel, G., D'Angelo, G. & Raposo, G. Shedding light on the cell biology of extracellular vesicles. *Nat. Rev. Mol. Cell Biol.* **19**, 213–228 (2018).
10. Kalluri, R. & LeBleu, V. S. The biology, function, and biomedical applications of exosomes. *Science* **367**, 640–655 (2020).
11. Colombo, M. et al. Analysis of ESCRT functions in exosome biogenesis, composition and secretion highlights the heterogeneity of extracellular vesicles. *J. Cell Sci.* **126**, 5553–5565 (2013).
12. Mulcahy, L. A., Pink, R. C. & Carter, D. R. F. Routes and mechanisms of extracellular vesicle uptake. *J. Extracell. Vesicles* **3**, 24641–24656 (2014).
13. Yamauchi, Y. & Helenius, A. Virus entry at a glance. *J. Cell Sci.* **126**, 1289–1295 (2013).
14. Christianson, H. C., Svensson, K. J., van Kuppevelt, T. H., Li, J.-P. & Belting, M. Cancer cell exosomes depend on cell-surface heparan sulfate proteoglycans for their internalization and functional activity. *Proc. Natl Acad. Sci. USA* **110**, 17380–17385 (2013).
15. Friand, V., David, G. & Zimmermann, P. Syntenin and syndecan in the biogenesis of exosomes. *Biol. Cell* **107**, 331–341 (2015).
16. Christianson, H. C. & Belting, M. Heparan sulfate proteoglycan as a cell-surface endocytosis receptor. *Matrix Biol.* **35**, 51–55 (2014).
17. Kumar, B. & Chandran, B. KSHV entry and trafficking in target cells—hijacking of cell signal pathways, actin and membrane dynamics. *Viruses* **8**, 305–328 (2016).
18. Cynthia, Y. A. & Patricio, I. M. Usage of heparan sulfate, integrins, and FAK in HPV16 infection. *Virology* **403**, 1–16 (2010).
19. Burridge, K. Foot in mouth: do focal adhesions disassemble by endocytosis? *Nat. Cell Biol.* **7**, 545–547 (2005).
20. Woods, A. J., White, D. P., Caswell, P. T. & Norman, J. C. PKD1/PKC?? promotes??v??3 integrin recycling and delivery to nascent focal adhesions. *EMBO J.* **23**, 2531–2543 (2004).
21. Moreno-Layseca, P., Icha, J., Hamidi, H. & Ivaska, J. Integrin trafficking in cells and tissues. *Nat. Cell Biol.* <https://doi.org/10.1038/s41556-018-0223-z> (2019).
22. Roper, J. A., Williamson, R. C. & Bass, M. D. Syndecan and integrin interactomes: large complexes in small spaces. *Curr. Opin. Struct. Biol.* **22**, 583–590 (2012).



23. Hamidi, H. & Ivaska, J. Every step of the way: integrins in cancer progression and metastasis. *Nat. Rev. Cancer* <https://doi.org/10.1038/s41568-018-0038-z> (2018).
24. Paolillo, M. & Schinelli, S. Integrins and exosomes, a dangerous liaison in cancer progression. *Cancers* **9**, 95–103 (2017).
25. Jay, S. D. & Cherech, D. A. Integrins in cancer: biological implications in therapeutic opportunities. *Cancer Nat. Rev.* **10**, 9–22 (2015).
26. Sesé, M. et al. Hypoxia-mediated translational activation of ITGB3 in breast cancer cells enhances TGF- $\beta$  signaling and malignant features in vitro and in vivo. *Oncotarget* **8**, 114856–114876 (2017).
27. Silencing  $\beta 3$  Integrin by Targeted ECO\_siRNA Nanoparticles Inhibits EMT and Metastasis of Triple Negative Breast Cancer.pdf.
28. Lambert, A. W., Pattabiraman, D. R. & Weinberg, R. A. Emerging biological principles of metastasis. *Cell* **168**, 670–691 (2017).
29. Tóth, L., Pásti, G., Sárvary, A., Balázs, M. & Ádány, R. Effect of tumor-conditioned medium on intercellular communication and proliferation of Balb/c 3T3 cells. *Cancer Lett.* **151**, 57–61 (2000).
30. Cellular, I. V. Effects of various conditioned media on proliferation of an isolated single cell from insect cell lines author(s): Toshinori Itoh and Jun Mitsuhashi Source: In Vitro Cellular & Developmental Biology. *Animal* **31**, 814–816 (2016). (Dec., 1995), pp.
31. Chen, Y. H. & Pruetz-Miller, S. M. Improving single-cell cloning workflow for gene editing in human pluripotent stem cells. *Stem Cell Res.* **31**, 186–192 (2018).
32. Zitzmann, J. et al. Single-cell cloning enables the selection of more productive *Drosophila melanogaster* S2 cells for recombinant protein expression. *Biotechnol. Rep.* **19**, e00272 (2018).
33. Takahashi, A. et al. Small extracellular vesicles secreted from senescent cells promote cancer cell proliferation through EphA2. *Nat. Commun.* **8**, 15729 (2017).
34. Imjeti, N. S. et al. Syntenin mediates SRC function in exosomal cell-to-cell communication. *Proc. Natl Acad. Sci. USA* **114**, 201713433 (2017).
35. Beauvais, D. M., Ell, B. J., McWhorter, A. R. & Rappraeger, A. C. Syndecan-1 regulates  $\text{I}\alpha\text{v}\text{I}^23$  and  $\text{I}\alpha\text{v}\text{I}^25$  integrin activation during angiogenesis and is blocked by synstatin, a novel peptide inhibitor. *J. Exp. Med.* **206**, 691–705 (2009).
36. Rappraeger, A. C. Synstatin: a selective inhibitor of the syndecan-1-coupled IGF1R- $\alpha\text{v}\beta 3$  integrin complex in tumorigenesis and angiogenesis. *FEBS J.* **280**, 2207–2215 (2013).
37. Yang, N. & Friedl, A. Syndecan-1-induced ECM fiber alignment requires integrin  $\alpha\text{v}\beta 3$  and syndecan-1 ectodomain and heparan sulfate chains. *PLoS ONE* **11**, e015032–57 (2016).
38. Gharbaran, R. Advances in the molecular functions of syndecan-1 (SDC1/CD138) in the pathogenesis of malignancies. *Crit. Rev. Oncol. Hematol.* **94**, 1–17 (2015).
39. Beauvais, D. M., Burbach, B. J. & Rappraeger, A. C. The syndecan-1 ectodomain regulates  $\alpha\text{v}\beta 3$  integrin activity in human mammary carcinoma cells. *J. Cell Biol.* **167**, 171–181 (2004).
40. Afratis, N. A. et al. Syndecans—key regulators of cell signaling and biological functions. *FEBS J.* **284**, 27–41 (2017).
41. Colombo, M., Raposo, G. & Théry, C. Biogenesis, secretion, and intercellular interactions of exosomes and other extracellular vesicles. *Annu. Rev. Cell Dev. Biol.* **30**, 255–289 (2014).
42. Emam, S. E. et al. Liposome co-incubation with cancer cells secreted exosomes (extracellular vesicles) with different proteins expressions and different uptake pathways. *Sci. Rep.* **8**, 1–11 (2018).
43. Schneider, D. J. et al. Mechanisms and modulation of microvesicle uptake in a model of alveolar cell communication. *J. Biol. Chem.* **292**, 20897–20910 (2017).
44. McCluskey, A. et al. Building a better dynasore: the dyngo compounds potentially inhibit dynamin and endocytosis. *Traffic* **14**, 1272–1289 (2013).
45. Caswell, P. T., Vadrevu, S. & Norman, J. C. Integrins: masters and slaves of endocytic transport. *Nat. Rev. Mol. Cell Biol.* **10**, 843–853 (2009).
46. Feng, D. et al. Cellular internalization of exosomes occurs through phagocytosis. *Traffic* **11**, 675–687 (2010).
47. Yoshioka, Y. et al. Comparative marker analysis of extracellular vesicles in different human cancer types. *J. Extracell. Vesicles* **2**, 1–9 (2013).
48. Knol, J. C. et al. Sensing of latent EBV infection through exosomal transfer of 5'pppRNA. *Proc. Natl Acad. Sci. USA* **113**, E587–E596 (2016).
49. Westbroek, W. et al. Exosomes released from breast cancer carcinomas stimulate cell movement. *PLoS ONE* **10**, e0117495 (2015).
50. Lee, M. Y. et al. Dynamin 2 regulation of integrin endocytosis, but not VEGF signaling, is crucial for developmental angiogenesis. *Development* **141**, 1465–1472 (2014).
51. Wang, Y., Cao, H., Chen, J. & McNiven, M. A. A direct interaction between the large GTPase dynamin-2 and FAK regulates focal adhesion dynamics in response to active Src. *Mol. Biol. Cell* **22**, 1529–1538 (2011).
52. Ezratty, E. J., Partridge, M. A. & Gundersen, G. G. Microtubule-induced focal adhesion disassembly is mediated by dynamin and focal adhesion kinase. *Nat. Cell Biol.* **7**, 581–590 (2005).
53. Alanko, J. et al. Integrin endosomal signalling suppresses anoikis. *Nat. Cell Biol.* **17**, 1412–1421 (2015).
54. Johnson, T. R. et al. Focal adhesion kinase controls aggressive phenotype of androgen-independent prostate cancer. *Mol. Cancer Res.* **6**, 1639–1648 (2008).
55. Begum, A. et al. The extracellular matrix and focal adhesion kinase signaling regulate cancer stem cell function in pancreatic ductal adenocarcinoma. *PLoS ONE* **12**, 1–21 (2017).
56. Liu, Z. et al. EGFRvIII/integrin  $\beta 3$  interaction in hypoxic and vitronectin-enriching microenvironment promote GBM progression and metastasis. *Oncotarget* **7**, 4680–4694 (2016).
57. Heusermann, W. et al. Exosomes surf on filopodia to enter cells at endocytic hot spots, traffic within endosomes, and are targeted to the ER. *J. Cell Biol.* **213**, 173–184 (2016).
58. Schmid, S. L. Reciprocal regulation of signaling and endocytosis: implications for the evolving cancer cell. *J. Cell Biol.* **216**, 2623–2632 (2017).
59. Arias-Salgado, E. G. et al. Src kinase activation by direct interaction with the integrin  $\beta$  cytoplasmic domain. *Proc. Natl Acad. Sci. USA* **100**, 13298–13302 (2003).
60. Wang, R., Shattil, S. J., Ambruso, D. R. & Newman, P. J. Truncation of the cytoplasmic domain of  $\beta 3$  in a variant form of glanzmann thrombasthenia abrogates signaling through the integrin  $\alpha(\text{IIb})\beta 3$  complex. *J. Clin. Invest.* **100**, 2393–2403 (1997).
61. Zhang, H. et al. Identification of distinct nanoparticles and subsets of extracellular vesicles by asymmetric flow field-flow fractionation. *Nat. Cell Biol.* **20**, 332–343 (2018).
62. Schaffner-Reckinger, E., Gouon, V., Melchior, C., Plançon, S. & Kieffer, N. Distinct involvement of  $\beta 3$  integrin cytoplasmic domain tyrosine residues 747 and 759 in integrin-mediated cytoskeletal assembly and phosphotyrosine signaling. *J. Biol. Chem.* **273**, 12623–12632 (1998).
63. Zhang, Q. et al. Transfer of functional cargo in exosomes article transfer of functional cargo in exosomes. *Cell Rep.* **27**, 1–15 (2019).
64. Lee, S.-S. et al. A novel population of extracellular vesicles smaller than exosomes promotes cell proliferation. *Cell Commun. Signal* **17**, 1–15 (2019).
65. Gu, J. et al. Modulated by PTEN. *Cell* **146**, 389–403 (1999).
66. Chiva, C. et al. QCloud: a cloud-based quality control system for mass spectrometry-based proteomics laboratories. *PLoS ONE* **13**, 1–14 (2018).
67. Pappin, D. J. C., Creasy, D. M., Cottrell, J. S. & Perkins, D. N. Probability-based protein identification by searching sequence databases using mass spectrometry data. *Electrophoresis* **20**, 3551–3567 (1999).
68. Beer, L. A., Liu, P., Ky, B., Barnhart, K. T. & Speicher, D. W. Serum/plasma. *Proteomics* **728**, 339–352 (2011).
69. Vizcaino, J. A. et al. 2016 update of the PRIDE database and its related tools. *Nucleic Acids Res.* **44**, D447–D456 (2016).

### Acknowledgements

The authors thank Hector Peinado and his laboratory team (Microenvironment & Metastasis Group, Molecular Oncology Program, Spanish National Cancer Research Centre (CNIO)). The authors thank Dr. Manel Bosch for helpful discussion and assistance with confocal microscopy. The authors thank Dr. Anne Spang and Dr Jordi Berenguer for helpful suggestions and discussion on the paper, and Jane Marshall for language review and editing support. This work was supported by Fondo de Investigaciones Sanitarias (PI14/01320), Redes Temáticas de Investigación Cooperativa en Salud (RD12/0036/0057) and CIBERONC (CB16/12/00363). SRC acknowledges support from the Generalitat de Catalunya (2014 SGR 1131). The CRG/UPF Proteomics Unit is part of the Spanish Infrastructure for Omics Technologies (ICTS OmicsTech) and it is a member of the ProteoRed PRB3 consortium which is supported by grant PT17/0019 of the PE I + D + i 2013–2016 from the Instituto de Salud Carlos III (ISCIII) and ERDF.

### Author contributions

Concept and design: P. Fuentes, S. Hümmer, M. Sesé, S. Ramón y Cajal. Development of methodology: P. Fuentes, S. Hümmer, M. Sesé, H. Peinado. Data acquisition: P. Fuentes, P. J. Guíjarro, M. Emperador, S. Sánchez-Redondo, H. Peinado. Data analysis and interpretation: P. Fuentes, S. Hümmer, M. Sesé, H. Peinado. Writing: P. Fuentes, S. Hümmer. Review of paper: P. Fuentes, S. Hümmer, M. Sesé, H. Peinado, S. Ramón y Cajal. Study supervision: S. Ramón y Cajal, M. Sesé, S. Hümmer.

### Competing interests

The authors declare no competing interests.

**Additional information**

**Supplementary information** is available for this paper at <https://doi.org/10.1038/s41467-020-18081-9>.

**Correspondence** and requests for materials should be addressed to S.H.üm. or S.R.ön.y.C.

**Peer review information** *Nature Communications* thanks the anonymous reviewer(s) for their contribution to the peer review of this work. Peer reviewer reports are available.

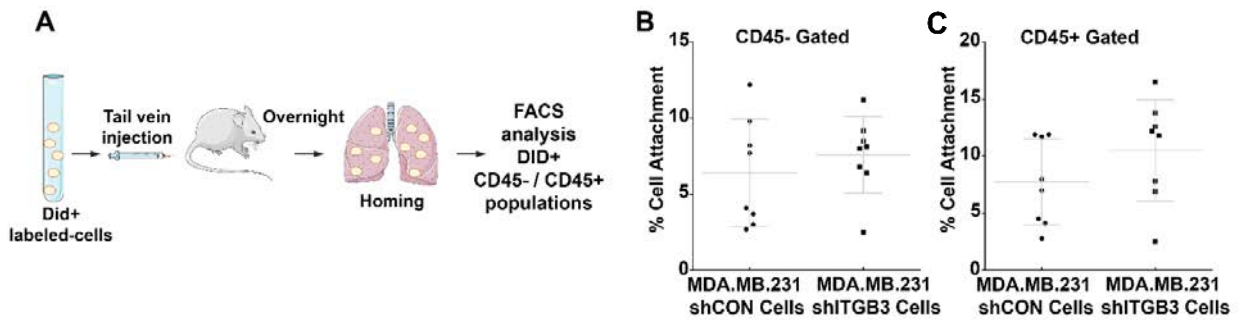
**Reprints and permission information** is available at <http://www.nature.com/reprints>

**Publisher's note** Springer Nature remains neutral with regard to jurisdictional claims in published maps and institutional affiliations.



**Open Access** This article is licensed under a Creative Commons Attribution 4.0 International License, which permits use, sharing, adaptation, distribution and reproduction in any medium or format, as long as you give appropriate credit to the original author(s) and the source, provide a link to the Creative Commons license, and indicate if changes were made. The images or other third party material in this article are included in the article's Creative Commons license, unless indicated otherwise in a credit line to the material. If material is not included in the article's Creative Commons license and your intended use is not permitted by statutory regulation or exceeds the permitted use, you will need to obtain permission directly from the copyright holder. To view a copy of this license, visit <http://creativecommons.org/licenses/by/4.0/>.

© The Author(s) 2020



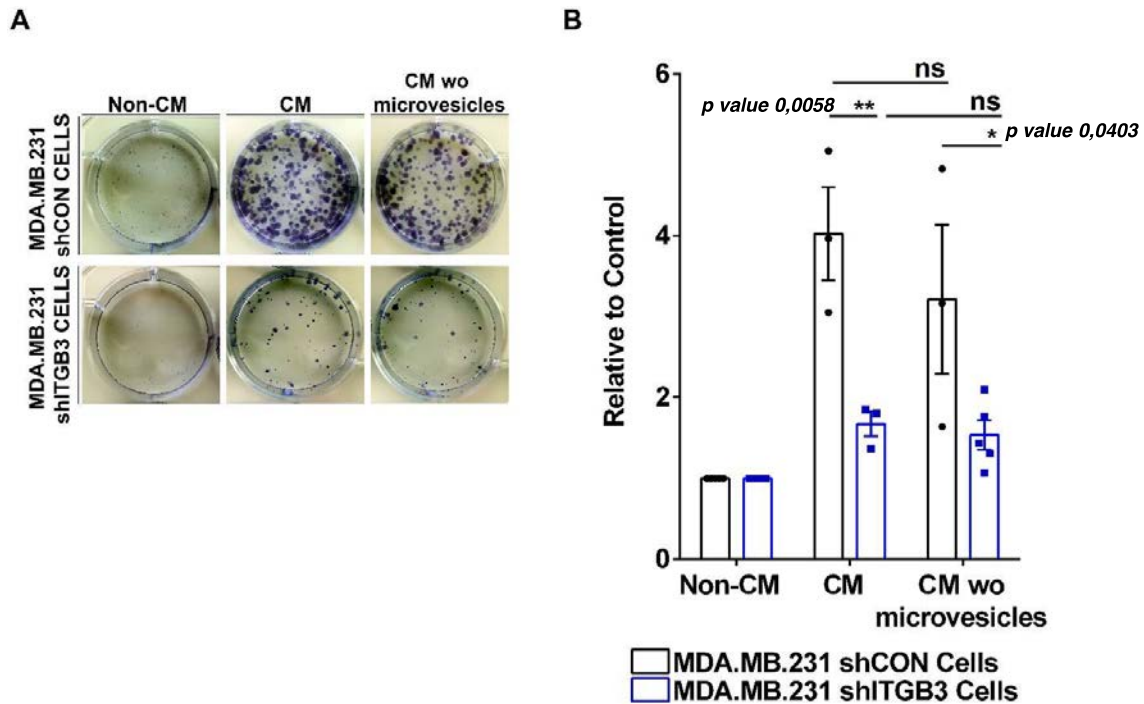
**Supplementary Figure 1. shITGB3 MDA.MB.231 cells are capable of homing in the lung.**

A) Schematic workflow for lung homing tumour cells analysis. B-C) Flow cytometry analysis for DID+ labelled shITGB3 and shCON MDA.MB.231 cells gated for CD45- (left panel) and CD45+ (right panel). Source data are provided as a Source Data file.

(n= 8 animals). Data are represented as mean ± SD in b-c. Scheme created with BioRender.

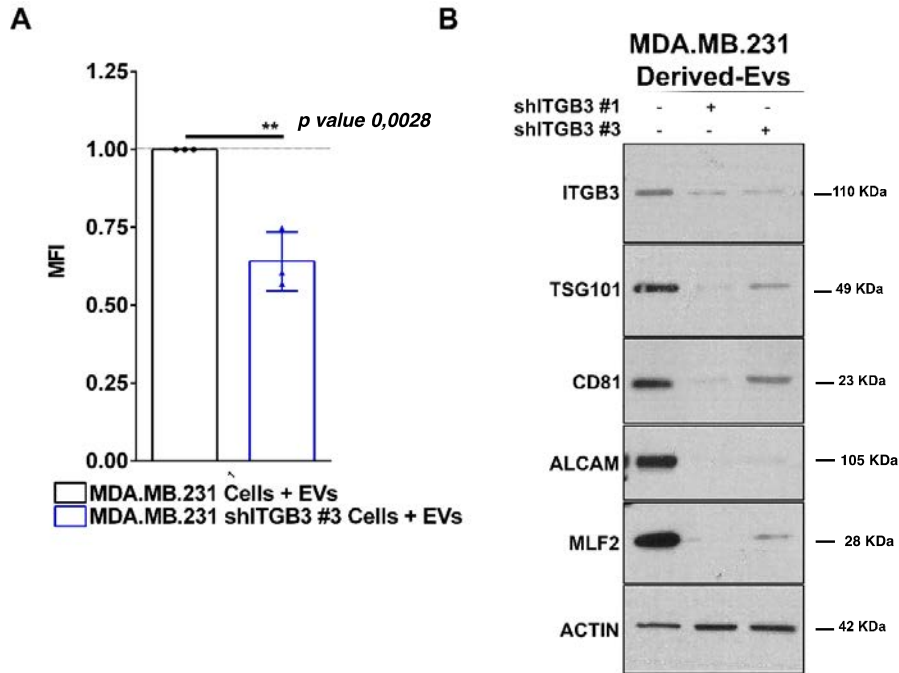
**SUMMARY.** A) Clonogenic cell growth analysis using shITGB3 #3. Source data are provided as a Source Data file.

(\*\*\*\*p value<0.0001, n=6). Data are represented as mean ± SD. Statistical analysis including two-tailed unpaired Student’s t-test data was carried out using GraphPad Prism 6.01.



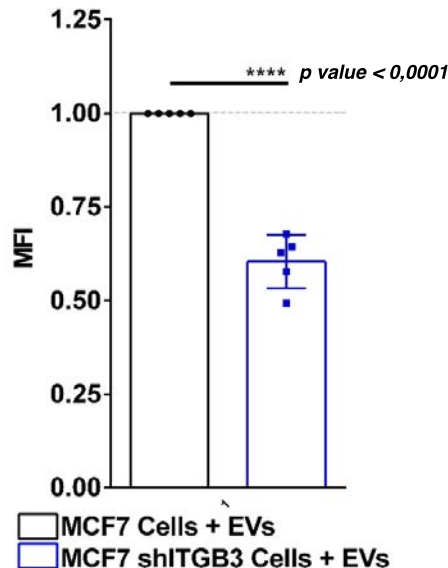
**Supplementary Figure 3. Microvesicles are not able to sustain the clonogenic growth capacity.** A) Representative pictures are shown for each cell population and condition. B) Conditioned medium (CM) was collected from exponentially growing MDA.MB.231 shCON cells. In the case of CM wo microvesicles, the same CM was split into two parts: one was used directly and the other was depleted of microvesicles by centrifugation at 10,000 g before use, to establish the response in clonal cell growth to the CM. Data are normalized to the non-conditioned control medium (DMEM). Source data are provided as a Source Data file.

(\**p* value<0.05, \*\**p* value<0.01, n=5). Data are represented as mean ± SD in b. Statistical analysis including two-way ANOVA multiple comparisons was carried out using GraphPad Prism 6.01.



**Supplementary Figure 4. Phenotype confirmation using a different ITGB3-targeting shRNA.** A) Flow cytometry analysis for MDA.MB.231 shCON and MDA.MB.231 shITGB3 #3 cells after incubating with 2-5  $\mu\text{g}/\text{mL}$  fluorescently-labelled EVs derived from MDA.MB.231 shCONTROL cells. B) Representative immunoblot analysis in two cell lines stably expressing different ITGB3-targeting shRNAs #1, #3. Source data are provided as a Source Data file.

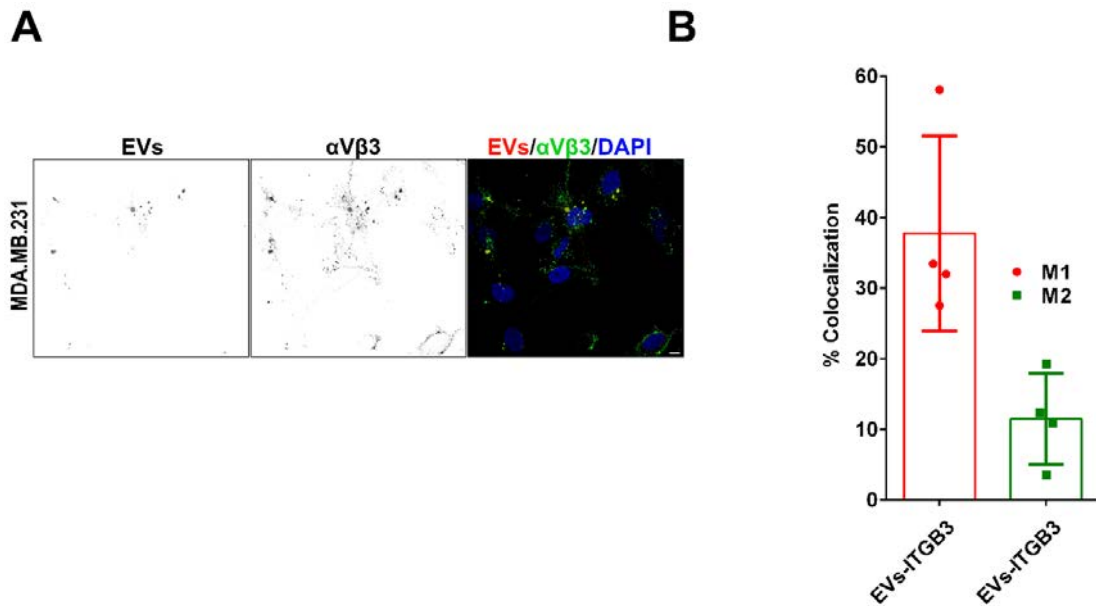
(\*\* $p$  value $<0.01$ ,  $n=3$ ). Data are represented as mean  $\pm$  SD in a. Statistical analysis including two-tailed unpaired Student's t-test data was carried out using GraphPad Prism 6.01.



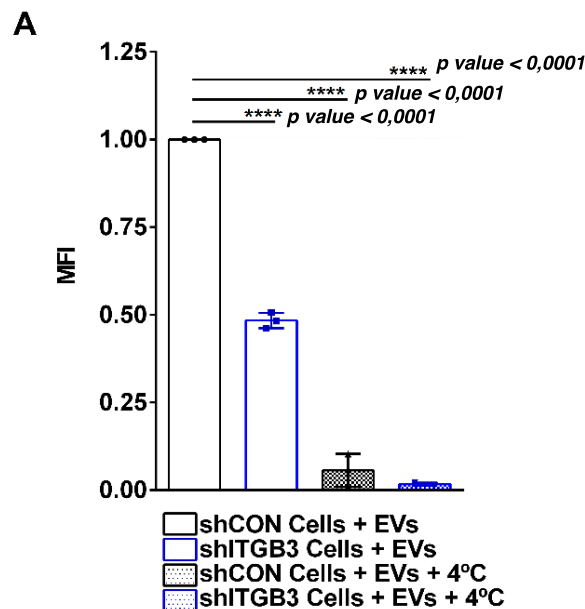
**Supplementary Figure 5. Phenotype confirmation using a different breast cancer cell line.**

A) Flow cytometry analysis for MCF7 shCON and MCF7 shITGB3 cells after incubating with 2-5  $\mu\text{g}/\text{mL}$  fluorescently-labelled EVs. Source data are provided as a Source Data file.

(\*\*\*\* $p$  value $<0.0001$ ,  $n=5$ ). Data are represented as mean  $\pm$  SD. Statistical analysis including two-tailed unpaired Student's t-test data was carried out using GraphPad Prism 6.01.

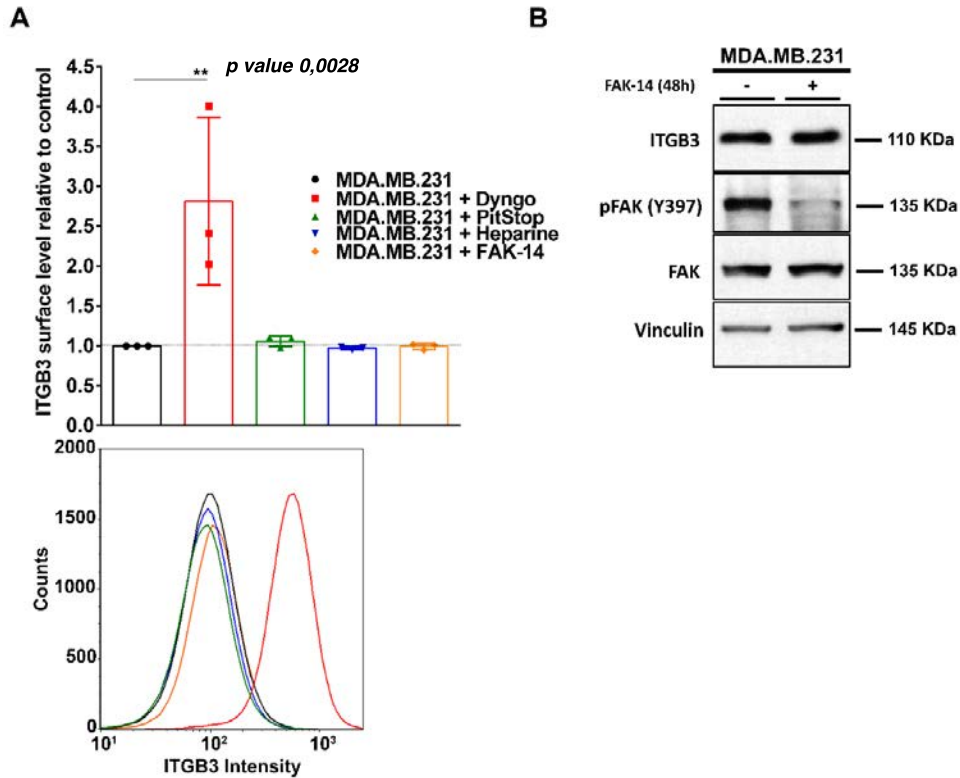


**Supplementary Figure 6. Co-localization between EVs and ITGB3 at cellular membrane** A) Representative confocal pictures of non-permeabilized MDA.MB.231 cells treated for 1h with PKH26-labelled shITGB3-derived EVs, fixed, and stained for  $\alpha$ V $\beta$ 3. B) Graphical representation of the Mander's coefficient values for determining co-localization between the different markers. (n=111 cells/condition). Bar represents 5 $\mu$ m. Source data are provided as a Source Data file.



**Supplementary Figure 7. EV uptake is an energy-dependent process.** Flow cytometry analysis for MDA.MB.231 shCON and MDA.MB.231 shITGB3 cells after incubating with 2-5  $\mu$ g/mL fluorescently-labelled EVs derived from MDA.MB.231 shCON cells at 37°C and 4°C. Source data are provided as a Source Data file.

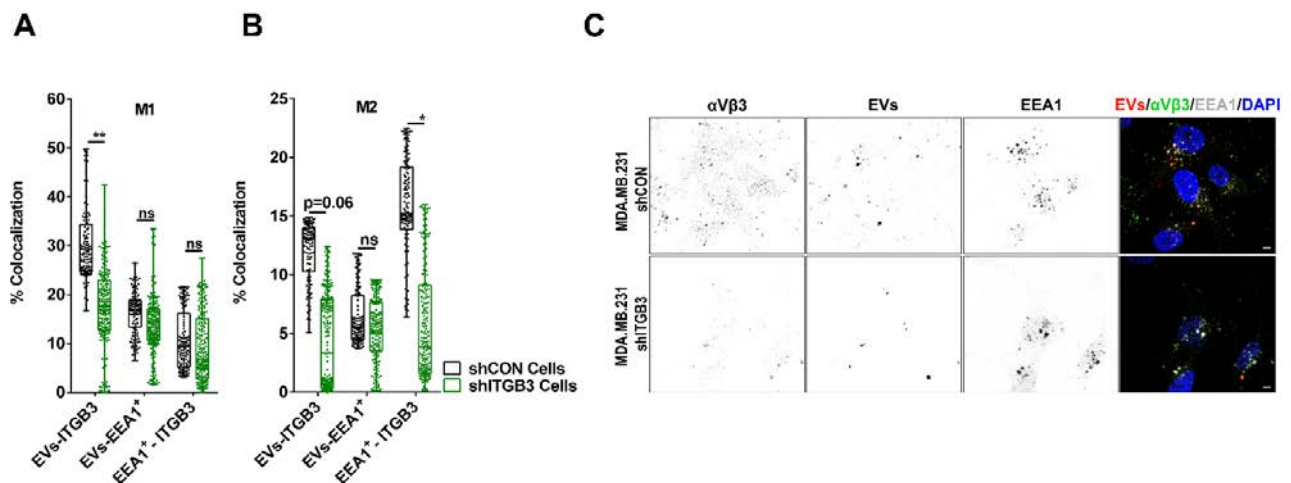
(\*\*\*\* $p$  value<0.0001, n=3). Data are represented as mean  $\pm$  SD. Statistical analysis including two-way ANOVA multiple comparisons was carried out using GraphPad Prism 6.01.



**Supplementary Figure 8. Dynamin regulates ITGB3 localization.** A) ITGB3 cell-surface level measured by FACS after 20  $\mu$ M Dyngo4a, 10  $\mu$ M Pitstop 2 or 10  $\mu$ g/mL heparin for 30 minutes or with 15  $\mu$ M FAK-14 for 14-16 hours. B) Representative immunoblot analysis of ITGB3 levels after 14-16 h of FAK-14 treatment. Source data are provided as a Source Data file.

(\*\*p value<0.01, n=3). Data are represented as mean  $\pm$  SD in a. Statistical analysis including two-tailed unpaired Student's t-test data was carried out using GraphPad Prism 6.01.

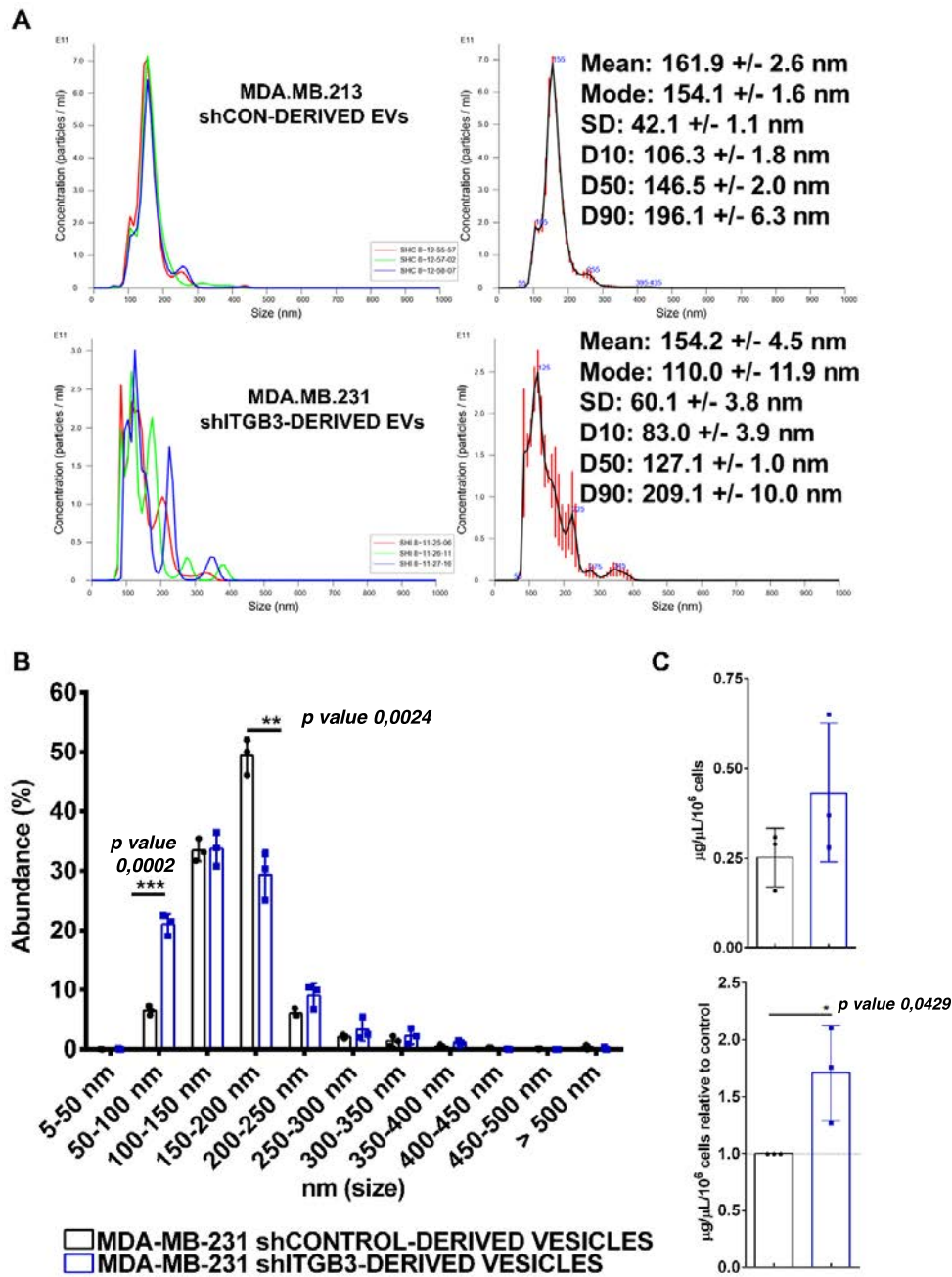
## Supplementary Figure 9



**Supplementary Figure 9. Extracellular vesicles co-localizes with ITGB3 in endocytic-pathway structures.** MDA.MB.231 shCON and MDA.MB.231 shITGB3 cells were treated for 1h with PKH26-labelled EVs, fixed, and stained for EEA1 and  $\alpha$ V $\beta$ 3 and EEA1 and LAMP1 respectively. A-B) Graphical representation of the Mander's coefficient values for determining co-localization between the different markers. (n= 75 cells/condition). C) Representative confocal pictures of MDA.MB.231 shCON and MDA.MB.231 shITGB3 cells. Bar represents 5 $\mu$ m.

(\*p value<0.05, \*\*p value<0.01). In a-b data are represented as boxplots using the MIN to MAX method. The middle line is the median, the lower and upper hinges correspond to the 25th to 75th percentiles. The upper whisker extends from the hinge to the largest value and the lower whisker extends from the hinge to the smallest value. Statistical analysis including two-way ANOVA multiple comparisons was carried out using GraphPad Prism 6.01.

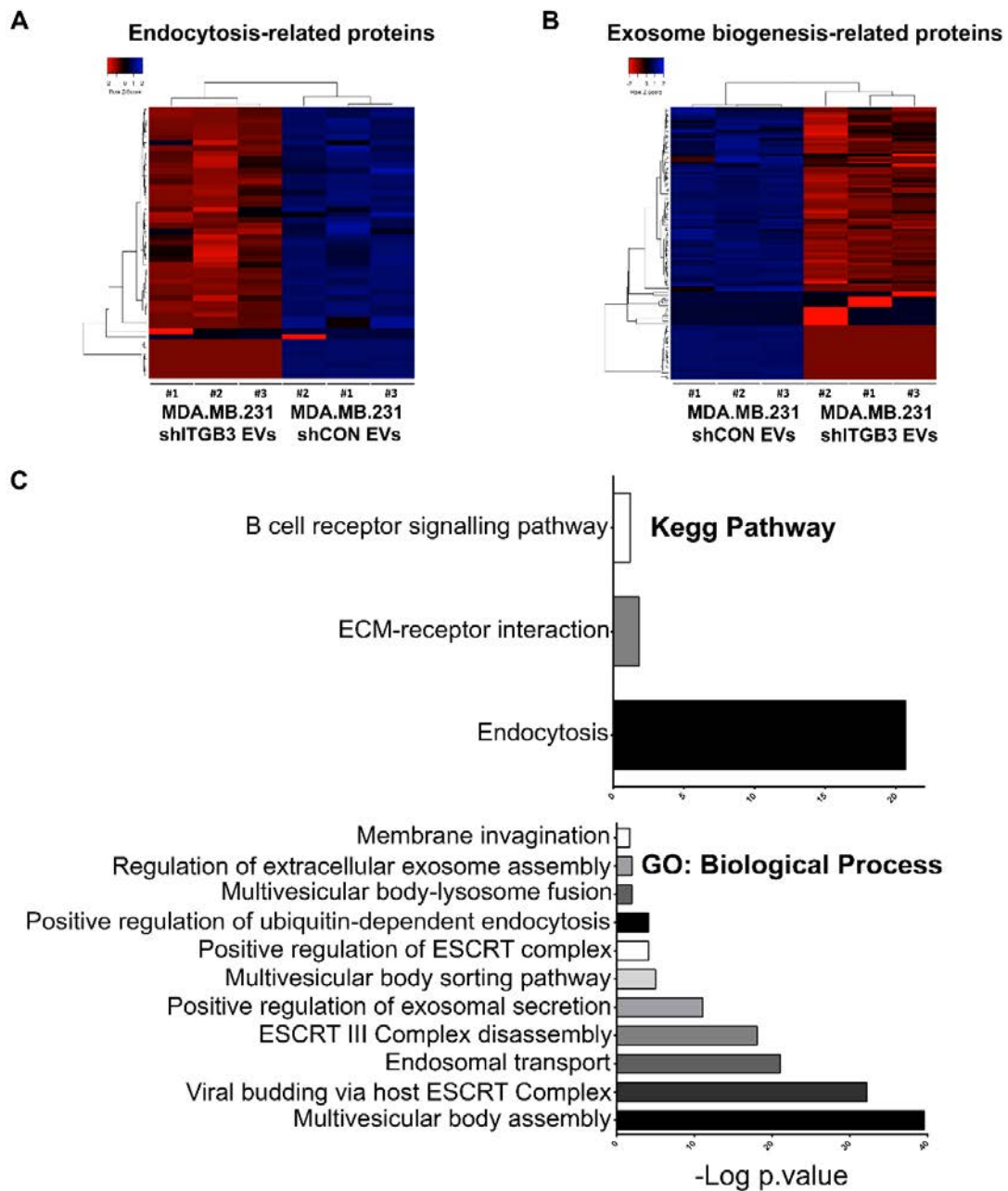




**Supplementary Figure 10. Characterization of EVs isolated from MDA.MB.231 shCON and MDA.MB.231 shITGB3 cells.** A) Nanosight Tracking Analysis (NTA) of MDA.MB.231 shCON- (upper) and MDA.MB.231 shITGB3-derived vesicles (lower). Average FTLA concentration/size (right). Error bars indicate +/-1 standard error of the mean. B) Vesicle size distribution based on NTA data. C) Protein concentration of isolated vesicle fractions normalized per million cells (upper) and normalized to shCON cells (lower). Source data are provided as a Source Data file.

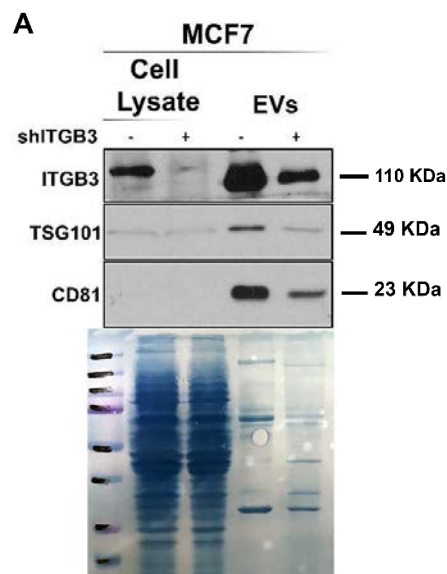
(\**p* value<0.05, \*\**p* value<0.01, \*\*\**p* value<0.001, n=3). Data are represented as mean ± SD in b-c. Statistical analysis including two-tailed unpaired Student's t-test was carried out using GraphPad Prism 6.01.

## Supplementary Figure 11

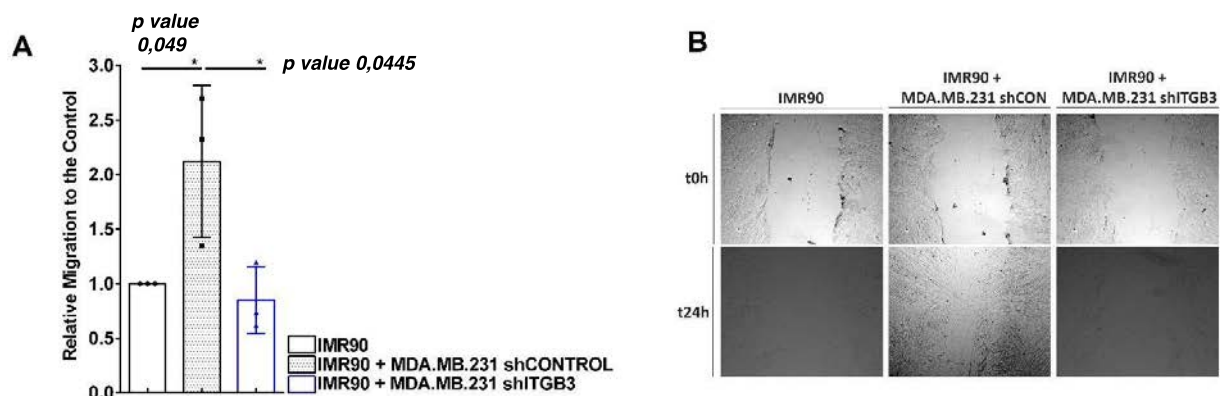


**Supplementary Figure 11.** Heat map representation showing the difference in the abundance of proteins with a described role in endocytosis (A) and exosome biogenesis (B). C) Gene ontology enrichment analysis of proteins with a  $\log_2$  FC of -1 and a  $q$ .value  $< 0.05$  in the comparison of proteins identified in the vesicle fraction of MDA.MB.231 shCON and MDA.MB.231 shITGB3 cells. In addition, proteins uniquely identified under either of the two conditions we included in the analysis. Pie charts are arranged by the mean  $-\log_{10}$  p.values for the individual categories. Source data are provided as a Source Data file.

## Supplementary Figure 12



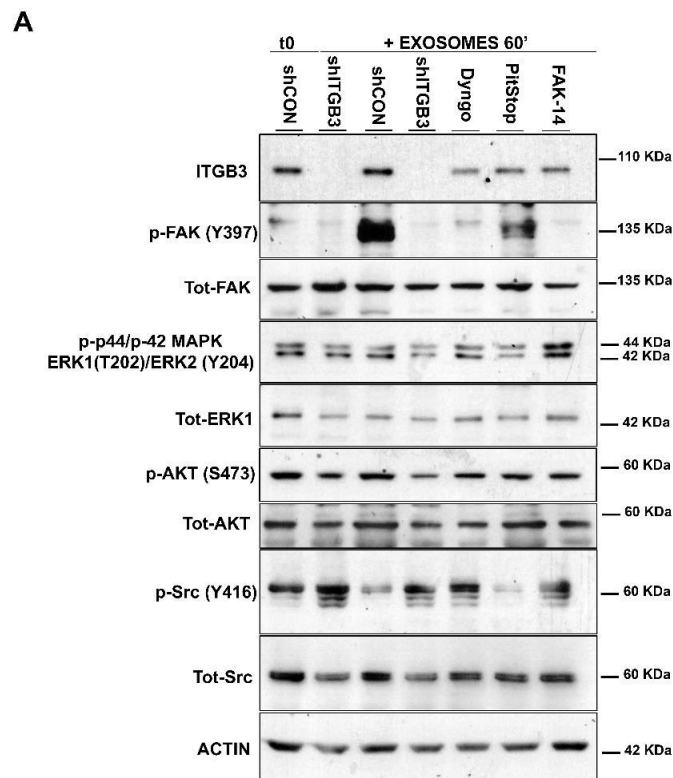
**Supplementary Figure 12. Phenotype confirmation using a different breast cancer cell line.**  
 A) Representative immunoblot showing ITGB3, TSG101 and CD81 expression in MCF7 and MCF7 shITGB3 cells. Amido black staining (lower). Source data are provided as a Source Data file. Three independent experiments were performed with similar results.



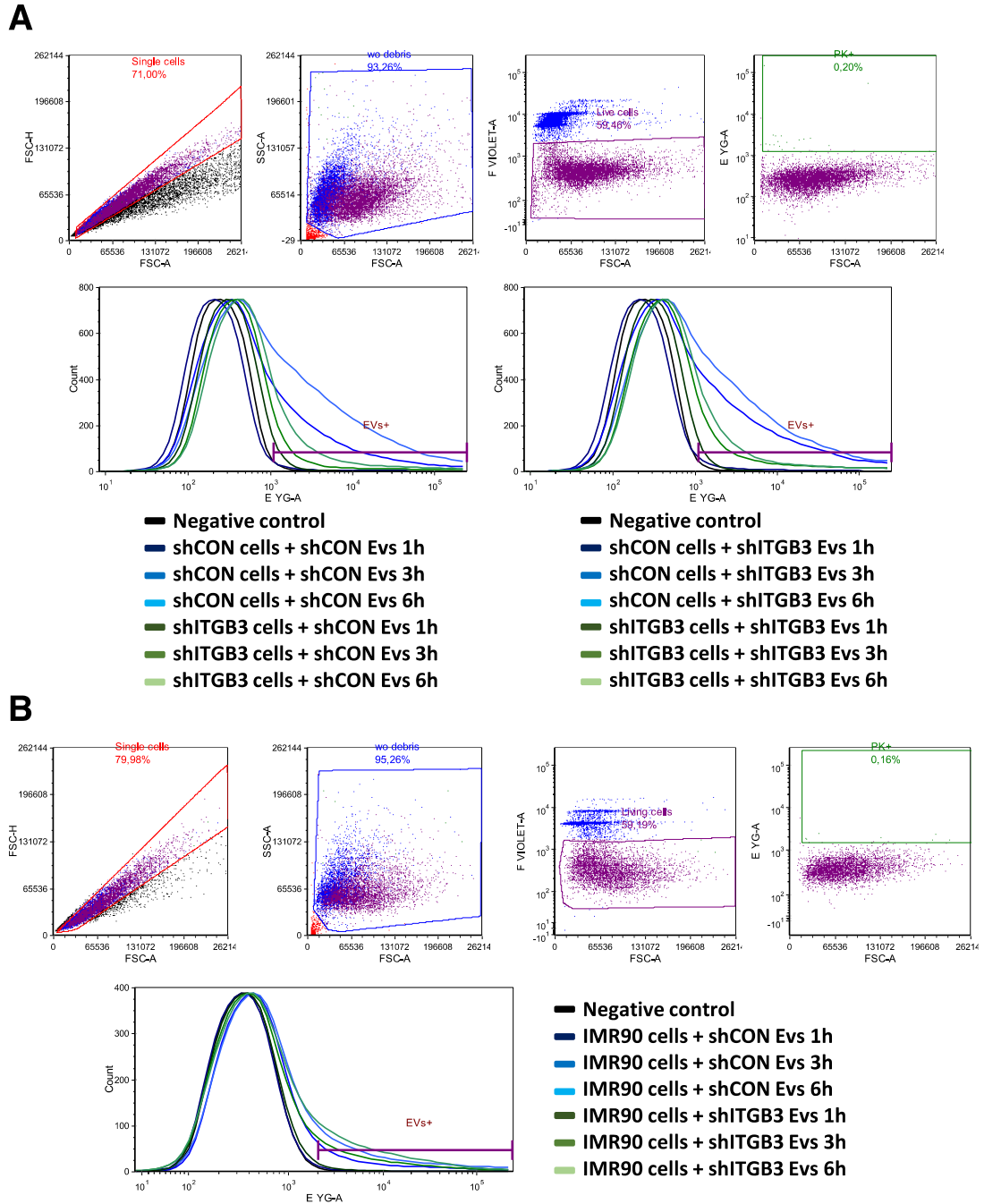
**Supplementary Figure 13. IMR90 cells displayed an increased migratory capacity when co-cultured with MDA.MB.231 cells, but not when co-cultured with shITGB3 cells.** A) Cell migration of IMR90 cell line using wound healing assay in a double chamber co-culture system. B) Representative pictures of wound healing assay at different time points and conditions. Source data are provided as a Source Data file.

(\**p* value<0.05, n=3). Data are represented as mean  $\pm$  SD in a. Statistical analysis including two-tailed unpaired Student's *t*-test data was carried out using GraphPad Prism 6.01.

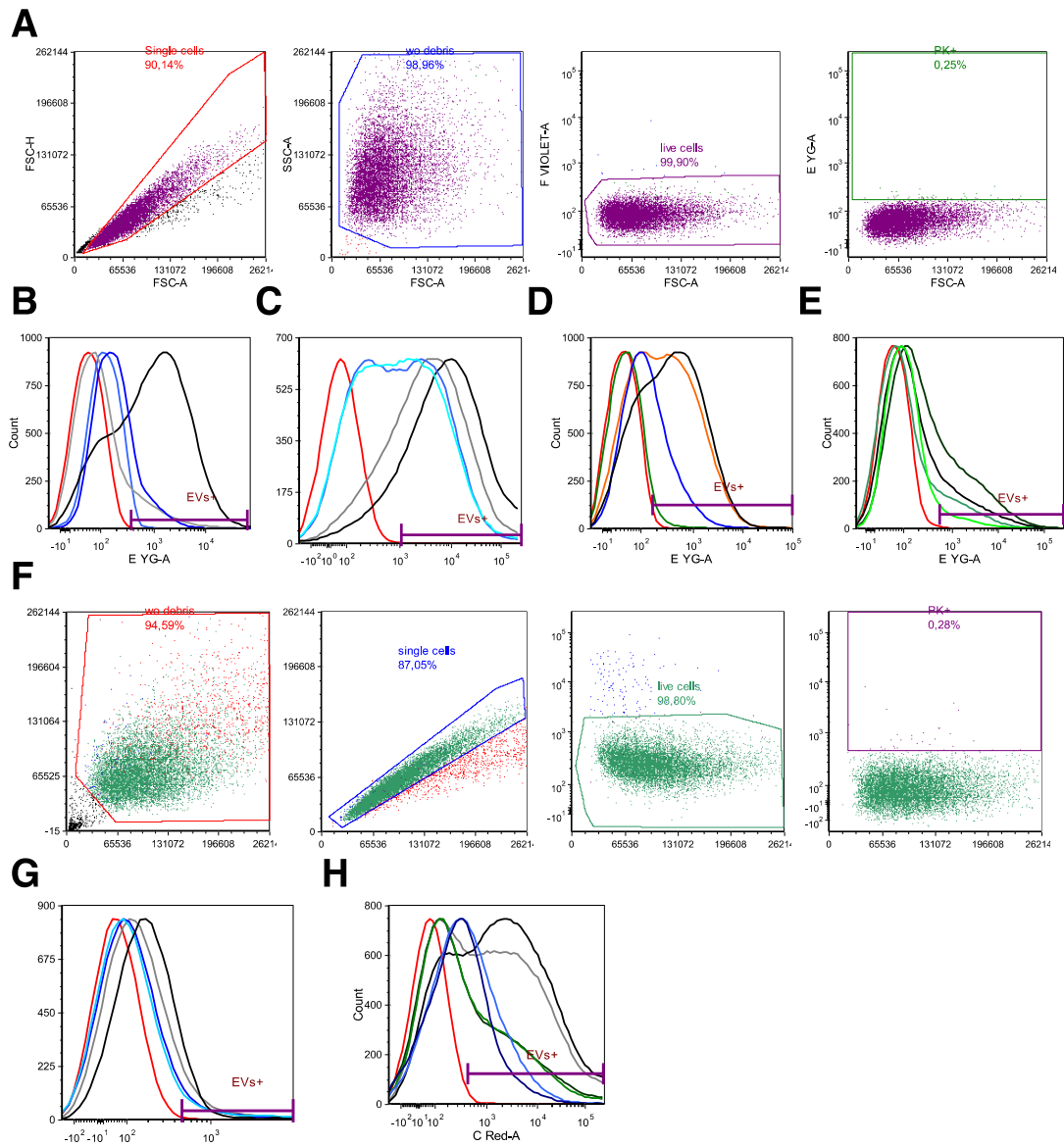
## Supplementary Figure 14



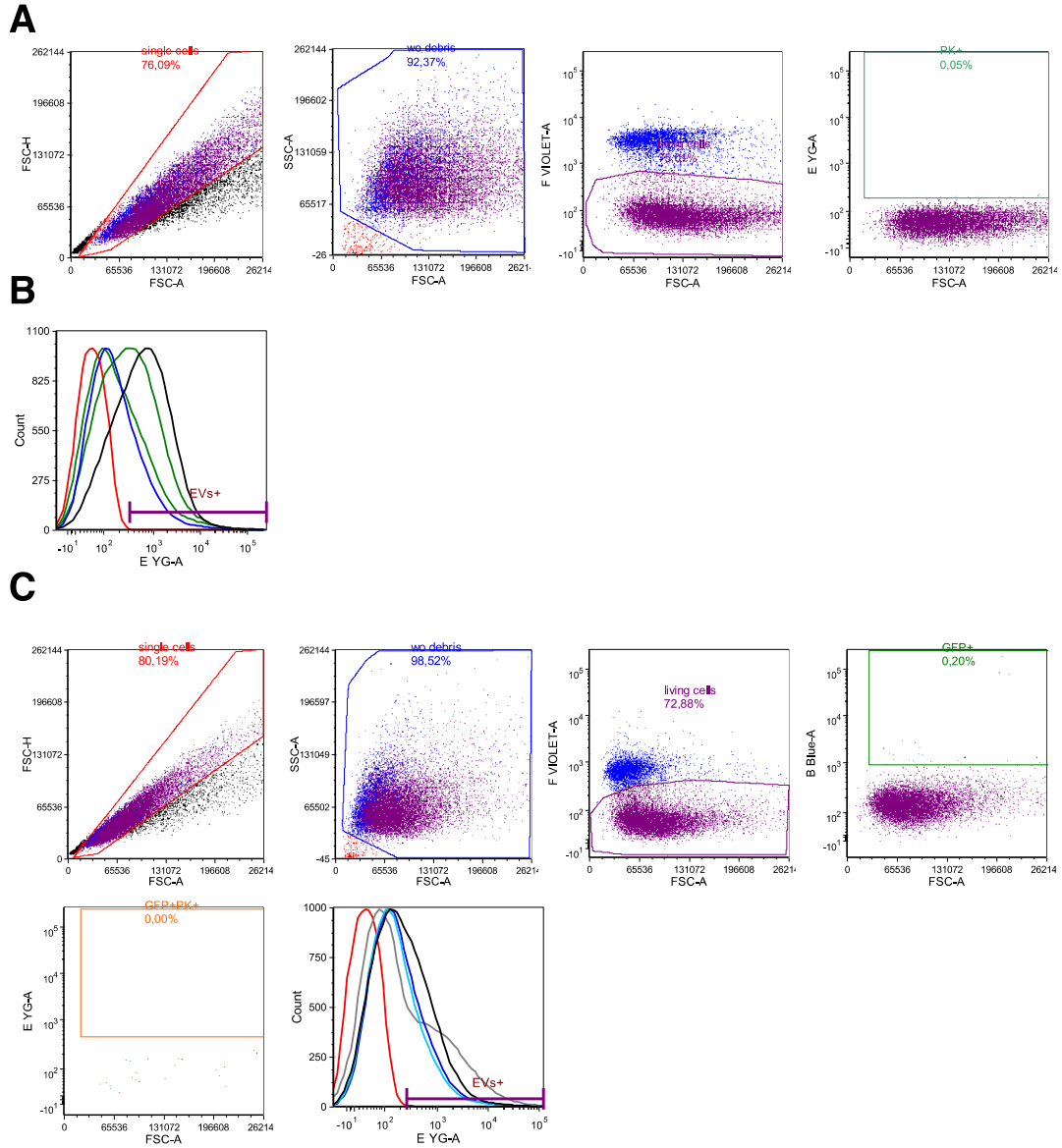
**Supplementary Figure 14. Only FAK activity was stimulated by EV treatment among all tested signalling pathways reported to be downstream of ITGB3.** A) Representative Western blot analysis. Source data are provided as a Source Data file. Three independent experiments were performed with similar results.



**Supplementary Figure 15.** FACS gating strategy and histogram intensity from which the bar charts for EVs internalization in A) Figure 1C, and B) Figure 1D were generated.

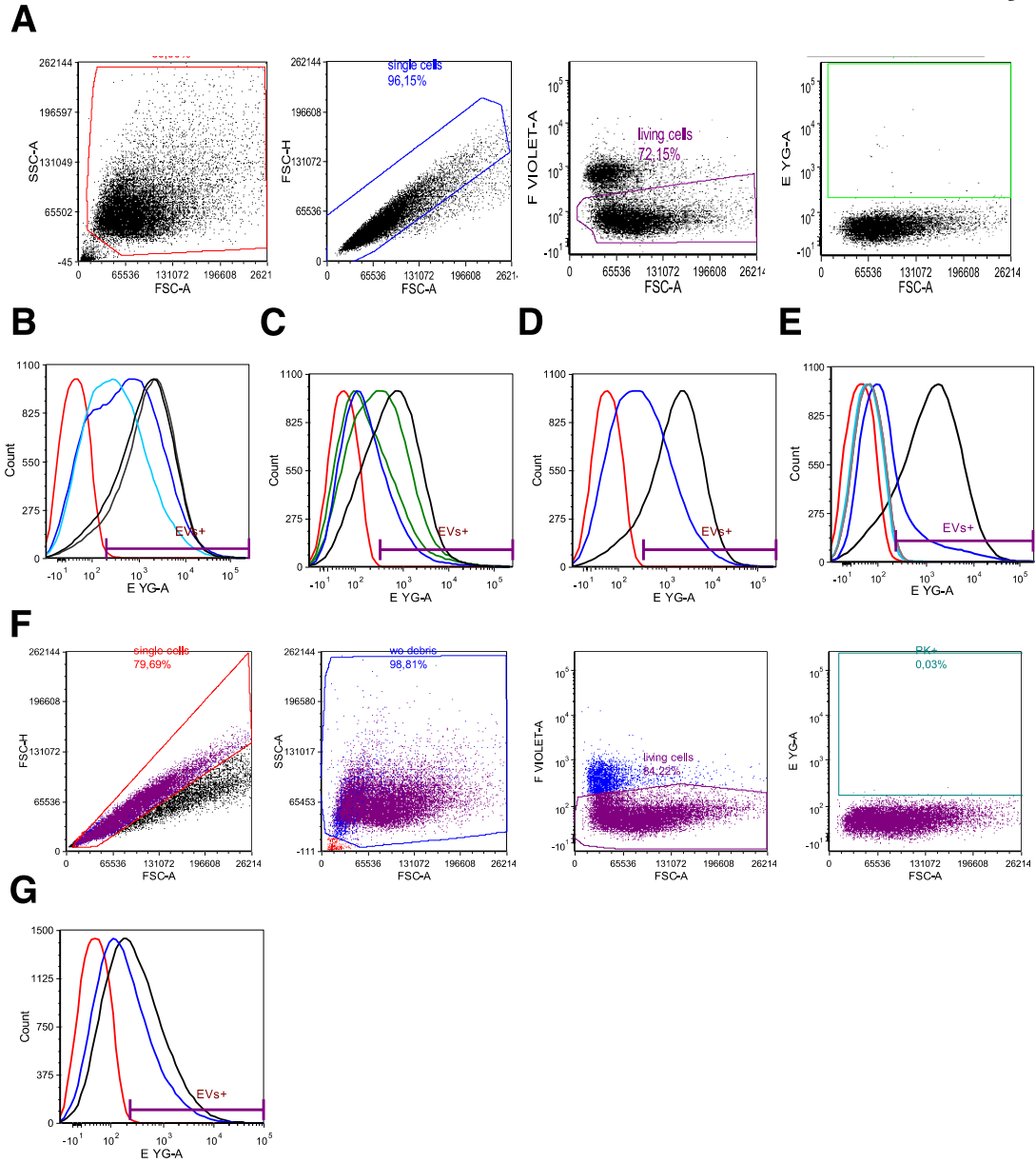


**Supplementary Figure 16.** FACS gating strategy and histogram intensity from which the bar charts for EVs internalization in A-E) Figure 2, and F-H) Figure 3A-B were generated.



**Supplementary Figure 17.** FACS gating strategy and histogram intensity from which the bar charts for EVs internalization in A-B) Figure 6B, and C) Figure 6D were generated.





**Supplementary Figure 18.** FACS gating strategy and histogram intensity from which the bar charts for EVs internalization in A-D) Supplementary Figure 4, E) Supplementary Figure 5, and F-G) Supplementary Figure 7 were generated.





## **DISCUSSION**



Although cancer cells are subject to constant cellular stresses, such as hypoxia, low nutrient levels and oxidative conditions, they are still able to proliferate, survive and develop malignant characteristics. The mechanisms and factors that help tumour cells to overcome cellular stress are not fully understood. The present thesis focused on the identification of new players required for the adaptation of tumour cells to hypoxic stress. To do so, we performed high-throughput RNA-Seq analysis of both the transcriptome and the translome of a malignant and a benign BrCa cell line subjected to low-oxygen conditions. This screening approach led to the identification of several transcripts that are translationally activated by hypoxia in an mTOR-dependent or -independent manner. Of these transcripts, we selected ITGB3 for further functional studies.

### **Rationale and reliability of high-throughput polysomal mRNA-Seq screening**

Even though mRNA transcription is still widely studied in the post-genomic era as the basis of gene expression, it is important to note that the mere presence of an mRNA is not a guarantee that the encoded protein is translated. Thus, the study of translationally active transcripts appears to be essential for determination of the response at the protein level<sup>30,31</sup>. While the direct assessment of protein levels at a genome-wide scale remains limited by the capacity of the applied mass spectrometry, the readout of translational activity by ribosome profiling provides a valuable tool to predict the cellular abundance of a protein. Under physiological conditions, normal and cancerous tissues are often only transiently exposed to hypoxia, which does not allow a sufficiently rapid cellular response based on the activation of mRNA transcription. Therefore, gene expression requires additional layers of regulation, such as protein translation, to allow a swift response to changes in the microenvironment. Ultimately, the ability of a cell to rapidly respond to cellular stress is essential for cellular adaptation and survival. However, in the case of hypoxic stress, mRNA translation is severely, although reversibly, inhibited under hypoxic conditions after only a few minutes of oxygen deprivation<sup>218</sup>. Nonetheless, the precise control of protein synthesis is required for cell growth, and deregulation of this process promotes tumour progression and the development of resistance to therapy and cellular stress. In this respect, tumour cells use alternative modes of translational regulation to express fundamental survival factors for their maintenance. In this regard, the capacity of tumour cells to survive under cellular stress conditions is achieved through their ability to stimulate non-canonical translation pathways, which promote tumour progression. This mechanism is used to compensate for the reduction in the canonical protein synthesis pathway and the inactivation of the mTOR pathway under hypoxic conditions<sup>59,86</sup>.

The ability of translational control to regulate the expression of individual genes has been poorly investigated on a genome-wide scale. Previous studies assessed the contribution of translational regulation during hypoxia on a genome-wide scale through the use of microarray technology. Our study was based on the use of RNA-Seq technology to detect translationally active transcripts. In addition, the use of differentiated polysomal and total mRNA fractions allowed us to compare translational efficiency (TE) with transcriptional changes.

We performed RNA-Seq screening to determine the translational activation of mRNAs under hypoxic stress alone and in combination with inhibition of the canonical protein synthesis pathway. To do so, the established mTORC1/mTORC2 inhibitor PP242 was used to block mTOR-dependent protein synthesis. We isolated cytosolic mRNA and translationally active mRNA (polysome-associated) via a 10–50% sucrose gradient sedimentation. This procedure was carried out in parallel for breast epithelial cells (MCF10A) and BrCa cells (MDA.MB.231) under several conditions: 1) normoxia, 2) hypoxia, 3) normoxia + PP242 treatment, and 4) hypoxia + PP242 treatment (Figure 1, Paper I). Using these different combinations, we aimed to identify candidate mRNAs subjected to non-canonical control mechanisms of protein translation. In this regard, IRES-mediated protein translation has been suggested to be sustained under hypoxic conditions. However, only a few candidates with IRES-mediated protein translation were identified. Thus, alternative and parallel pathways of non-canonical translation must co-exist to ensure protein synthesis under hypoxic conditions. A detailed analysis of the mRNAs efficiently translated under hypoxic conditions might therefore reveal novel mechanisms of non-canonical protein translation.

In relation to other studies that investigated protein translation under hypoxic conditions, we found comparable changes to those published by Thomas *et al.*<sup>219</sup> and Koritzinsky *et al.*<sup>76,220</sup>, but only a small overlap with the translational changes reported by Lai *et al.*<sup>221</sup>. These differences might be explained by the use of different cell lines, the duration of exposure to hypoxia (20 and 16 hours of hypoxia exposure instead of 24 hours) and the different O<sub>2</sub> conditions (0.02% instead of 0.05%). All of these experimental criteria have previously been shown to affect the cellular response to hypoxia. Therefore, different results could be expected.

For future studies, it would be of interest to further evaluate the regulation of mRNA translation at a range of oxygen concentrations typically seen in tumours (i.e., 0.02–5% O<sub>2</sub>), as well as at different time points (acute vs sustained effects). Moreover, it would be

interesting to also focus on early time points because translational regulation can result in an immediate response while transcriptional regulation might be required for the subsequent adaptation phase. Moreover, it suggests its involvement in transient changes in oxygenation *in vivo*. These different response “waves” might provide the basis for the acute and sustained adaptation to hypoxia and explain the differences in the TE of different groups of genes at different times as a result of changes in molecular mechanisms. Another option would be that some mRNAs could be transcriptionally induced but translationally repressed under normal conditions. In response to stress, protein synthesis would be restored to allow the cell to resist the adverse situation.

To confirm the results obtained after mTOR inhibition, we compared our results with additional studies. Similar changes were also observed in other studies, where almost the same genes were translationally downregulated by mTOR inhibition<sup>222,223</sup>. Moreover, most of these transcripts contained TOP elements, *cis*-acting elements found in mRNAs localised to polysomes in actively growing cells whose translational activation is mainly regulated by the mTOR signalling pathway<sup>224</sup> (Supplementary Figure 4, Paper I). The mRNA encoding RPL11 (ribosomal protein L11) is an example of a TOP motif-containing mRNA that is reduced in the polysomal fraction of PP242-treated cells (Figure 4C, Paper I). These results validate the sufficient inhibition of the canonical pathway in the screening procedure and therefore provide a solid base for the detection of mRNAs translated by non-canonical pathways.

Through this innovative approach, this thesis revealed several changes in gene expression at both transcriptional and translational levels that might have been overlooked in previous studies. Differences between tumour and non-tumour cells, particularly in terms of ITGB3, the candidate gene chosen for further studies, will be discussed below.

### **The MCF10A and MDA.MB.231 transcriptome and translome in hypoxia and hypoxia + PP242**

The results of the screening highlight marked differences in the mechanisms of the stress response between tumour and non-tumour cells. We analysed these transcriptional differences between the two cell lines under hypoxic and hypoxic + PP242 conditions. Under hypoxic conditions, 236 overexpressed and 17 downregulated genes were detected in non-tumour cells. In contrast, only 61 overexpressed and 9 downregulated genes were regulated in tumour cells. Interestingly, 23 genes showed a response pattern in both cell types. Analysis of the biological significance of these 23 genes revealed that most belonged to Gene Ontology (GO) categories related to response to hypoxia, glycolysis and oxidation-

reduction processes, as expected. In the case of MDA.MB.231 cells, no other significantly differentiated categories were found, likely due to the low number of genes differentially expressed. Instead, MCF10A cells demonstrated categories such as apoptosis, angiogenesis and proliferation. The first conclusion is that non-tumour cells promote greater transcriptional changes than tumour cells in response to hypoxic stress. This may be because tumour cells present a high basal activation threshold of related genes, whereas non-tumour cells need the activation of these genes as an adaptation mechanism to the new scenario.

The observed changes in MCF10A cells were even more evident when the cells were subjected to double treatment comprising hypoxia + mTOR inhibition. A total of 631 mRNAs were upregulated in non-tumour cells compared with the 130 genes found to be upregulated in tumour cells; 74 of the genes were the same. GO analysis revealed that the 74 shared genes were part of the following functional categories: response to hypoxia, glycolysis and nucleosome assembly. GO analysis of the transcriptional changes in the tumour cells under hypoxia + PP242 revealed upregulated genes in the functional categories of angiogenesis and Notch and p53 signalling pathways. In contrast, MCF10A cells showed a greater variety in their response. We found that they promoted changes related to a global attempt to escape the stressful situation. These changes were mainly related to cell adhesion, cell-cell signalling, apoptosis, cell growth, proliferation and the cell cycle.

Although many of the genes transcriptionally upregulated upon hypoxia + PP242 treatment were important for cell survival, we focused on those genes activated at the protein synthesis level, a less well-understood and more unknown field. Significantly regulated mRNAs with significantly altered levels in the polysomal fraction upon hypoxia and/or PP242 (FDR < 5% for MCF10A cells and FDR < 10% for MDA.MB.231 cells) were selected for TE calculation ( $\log_2\text{FC polysomal RNA}/\log_2\text{FC total RNA}$ ). Genes with a z-score > 1.5 were considered more efficient in terms of translation, whereas genes with a z-score < -1.5 were considered to have decreased TE.

Bioinformatics analysis revealed that 65 (43 upregulated and 22 downregulated) and 94 (82 upregulated and 12 downregulated) mRNAs were differentially expressed in MCF10A and MDA.MB.231 cell lines, respectively, under hypoxic conditions. The GO categories were related to cell death and negative regulation of cell proliferation in MCF10A cells and to migration and proliferation in MDA.MB.231 cells. In contrast, with hypoxia + PP242 treatment, the number of affected genes considerably increased to 549 (99

upregulated and 450 downregulated) for MCF10A cells and 311 (81 upregulated and 224 downregulated) for MDA.MB.231 cells. The GO categories obtained from activated transcripts upon double treatment were related to cell adhesion, angiogenesis and extracellular matrix organisation in MCF10A cells (Figure 4B, Paper I), whereas the only significant GO category in the cancer cell line was circadian regulation of the gene. This differential response between the two cell lines indicates that non-tumour cells respond to stress through the control of proliferation and the activation of death mechanisms, whereas tumour cells have a more aggressive response, evading death through the activation of migration, invasion and proliferation. This behaviour highlights the cell type-dependent response to stress adaptation and the importance of translational regulation and efficiency in handling these kinds of situations.

In summary, translational control is essential for the regulation of mRNAs related to invasion and metastasis during tumorigenesis, especially when cells are subjected to stress situations. Cancer cells, in order to metastasise to secondary organs, must preserve a high capacity for migration and invasion to bypass tissue fences, intravasate into the blood flow and extravasate at distant secondary sites. This multistep process requires fast and particular modulation of gene expression. In this context, efficient control of protein translation is key.

### **Adaptive protein synthesis in hypoxia and translational activation of ITGB3**

The translational activation of certain mRNAs during hypoxia can have crucial effects on gene expression because the proteins encoded by these mRNAs will continue to be synthesised when mTOR-dependent protein synthesis is compromised.

Several articles have suggested that hypoxia can disturb the formation of the eIF4F complex through a reduction in mTOR activity and a consequent decrease in the phosphorylation of 4E-BP1. Non-phosphorylated 4EBP1 binds to and sequesters eIF4E away from the eIF4F complex, which results in inhibition of the canonical mRNA translation pathway. Even under these conditions, where protein synthesis is globally inhibited, translation of certain transcripts is maintained or even increased. Clarification is required of the exact mechanisms through which these mRNAs are translated during hypoxia. Elucidation of the underlying molecular mechanisms will be a challenging task but is essential for the design and improvement of anti-tumour treatments. IRES-mediated translation may be one of the mechanisms to ensure the synthesis of certain proteins during hypoxia, but our data did not support this hypothesis. Therefore, alternative routes must exist to ensure mRNA translation in response to stressful conditions. Several mechanisms



have been proposed to contribute to this process in hypoxia, including CITE, TISU elements, uORF-mediated mRNA regulation, the presence of an rHRE in the mRNA recognised by the hypoxic translation machinery and other trans-elements such as miRNA and lncRNAs (Figure 3). However, it remains incompletely understood how these elements can prevent the translational inhibition of the mRNA by the non-canonical protein synthesis pathway and/or promote alternative translation mechanisms. Many authors have proposed that the answer lies mostly within the 5' and 3' UTRs of the protein transcripts. In response to stressful inputs, TE would be influenced, both positively and negatively, by the binding of regulatory elements to the UTRs.

We found enhanced integrin beta-3 protein synthesis in cell lines under both hypoxic conditions and hypoxia + PP242 treatment, confirming that this activation is not dependent on the mTOR pathway. Furthermore, translation of the ITGB3 mRNA under stress conditions was dependent on eIF4E because ITGB3 levels were not increased upon eIF4E depletion under hypoxic conditions (Figure 8, Paper I), demonstrating that ITGB3 may be an example of an mRNA that harbours regulatory elements that allow protein synthesis in a non-canonical fashion. Bioinformatics analysis revealed that the 5' UTR of ITGB3 is particularly short (21 nucleotides). Because IRES elements are longer and more complex, it is highly unlikely that the short UTR harbours an IRES element and that ITGB3 is translated through an IRES-mediated mechanism. We also excluded translation through HIF-2 $\alpha$ -RBM4-eIF4FH, a complex preferentially chosen by HIF target genes, because eIF4E2 (uniquely found in the eIF4FH complex) or HIF-1 $\beta$  silencing did not prevent the increased expression of ITGB3 in hypoxia (Figure 8, Paper I).

Although the mechanism involved in the translational control of ITGB3 under hypoxic conditions has not been studied in detail during this thesis, its further analysis would be interesting. We hypothesise that the most likely non-canonical mechanism governing ITGB3 translation would be the presence of TISU elements. On the one hand, short 5' UTR mRNAs are enriched in TISU, a 12-nucleotide element directing efficient translation. On the other hand, TISU activity requires the presence of an mRNA cap but does not rely on scanning. Moreover, efficient AUG recognition of TISU is intrinsic to the basal translation machinery, including eIF4E, but does not require specific additional factors. Interestingly, Hadar Sinvani *et al.*<sup>44,45</sup> showed that TISU confers translational resistance to global inhibition of translation in response to energy stress.

In summary, several studies exploring dysregulated translation in cancer have highlighted the critical significance of translational control in the fast response of cancer cells to numerous stresses existing at different stages of tumour development and

progression. Crucial translationally regulated targets have been recognised, and technologies that enable genome-wide translational analysis are opening up new roads for research and for the establishment of innovative therapeutic strategies.

### **Metastasis and ITGB3: enhancement of migratory phenotypes through the TGF- $\beta$ pathway under hypoxic conditions**

Focusing on genes actively translated under stress conditions ( $TE > 1.5$ ), a secondary siRNAs screen was performed to identify functionally relevant genes required for the response to cellular stress. Both proliferation and migration assays were conducted (Supplementary Figure 8, Paper I). Interestingly, ITGB3 was the most promising of the tested candidates because ITGB3 silencing in MDA.MB.231 cells reduced cell viability, specifically under hypoxic conditions (Supplementary Figure 8A and 8B, Paper I). Moreover, increased apoptosis was observed upon ITGB3 silencing in hypoxia but not in normoxia (Supplementary Figure 8D, Paper I). On the other hand, cell migration appeared to be diminished upon ITGB3 depletion (Supplementary Figure 8C, Paper I). Interestingly, besides ITGB3, activation of the mRNA translation of other integrins such as ITGB4, ITGAX and ITGA5 was also observed under hypoxic conditions, which may suggest a key role for integrins in the response to hypoxic stress. Finally, we validated the importance of translational control mechanisms for the expression of ITGB3 through the use of the transcriptional inhibitor actinomycin D. Based on all of these findings and the established role of ITGB3 in tumourigenesis<sup>164,179,184,211</sup>, we focused our further studies on the role of ITGB3 in BrCa cells, as well as its regulation and specific role in hypoxia.

Our data confirmed that stable inhibition of ITGB3 using three different shRNAs reduced migration and increased apoptosis, especially under hypoxic conditions (Figure 5, Paper I). These results, together with the fact that shITGB3 inhibits TGF- $\beta$  induction and, consequently, TGF- $\beta$ -induced migration, indicate that ITGB3 is necessary for the regulation of TGF- $\beta$  and its downstream effectors (Figure 7, Paper I). This finding was supported by additional studies demonstrating that ITGB3 regulates the invasion of glioblastoma cells in hypoxic and vitronectin-enriched environments through interaction with EGFRvIII<sup>184</sup>. This regulation was dependent on SRC; however, we observed that SRC protein was not activated under low-oxygen conditions (Figure 7, Paper I).

Remarkably, ITGB3, which is expressed at low levels in normal epithelial tissues, has been demonstrated to be an EMT biomarker in several carcinomas, including BrCa<sup>225,226</sup>. Our study provides additional evidence regarding the role of ITGB3 in this process. ITGB3 is upregulated at the transcriptional level upon TGF- $\beta$  stimulation. We confirmed that its

silencing blocked the effects of TGF- $\beta$ , particularly under low-oxygen conditions. This was observed through a decrease in the expression of EMT markers downstream of TGF- $\beta$ , such as SNAIL and VIM (Figure 7, Paper I), as well as inhibition of Smad2 phosphorylation in hypoxia when ITGB3 was silenced (Figure 7, Paper I). In addition, ITGB3 downregulation significantly reduced lung metastasis and improved overall survival in mice, consistent with previous results.

Collectively, these data suggest that ITGB3, which is translationally activated in hypoxia, regulates malignant features, including EMT and cell migration, in a TGF- $\beta$ -dependent manner. This association is in line with the findings of several studies<sup>197-227</sup> and reveals that ITGB3 targeting might ultimately serve as a novel therapeutic approach to therapy-resistant hypoxic tumours. Moreover, it further supports the idea of ITGB3 involvement in EMT regulation through a positive feedback loop: TGF- $\beta$  upregulates ITGB3 expression at a transcriptional level and induces ITGB3-TGF- $\beta$ RII binding, which triggers the auto-phosphorylation of TGF- $\beta$ RII and thereby mediates EMT progression<sup>164</sup> (Figure Dis. 1). Therefore, ITGB3 overexpression might facilitate EMT through hyperactivation of the TGF- $\beta$  signalling pathway. Consequently, inhibition of ITGB3 would result in a decrease in metastasis, as reported for inhibition of the TGF- $\beta$  pathway and as observed after knockdown of ITGB3 *in vivo*.

From a more phenotypic point of view regarding cell spreading, several studies have shown that eIF4E is associated with the Golgi apparatus and membrane microdomains such as the perinuclear region and lamellipodia, which are essential for cell motility<sup>30</sup>. Most significantly, a fraction of these initiation factors is localised to sites of active translation near the leading edge of migrating cells, which would be relevant in the process of cancer cell migration from the primary tumour to secondary locations<sup>30,228</sup>. Mechanistically, eIF4E regulates the translation of mRNAs encoding key players in cancer metastasis, such as ITGB3<sup>30</sup>. Accordingly, it is not unexpected that the extracellular matrix, which is vital for the growth and survival of cells, is also involved in translational control. Integrins are essential for the communication between cells and the extracellular matrix. Moreover, the complexity of integrin signalling regulation, including heterodimer formation and localisation, can also be exploited by the translational machinery<sup>229</sup>. Therefore, eIF4E-dependent modulation of translation is important for the regulation of the expression of certain factors (e.g., ITGB3) that allow cancer cells to communicate with the extracellular environment, permitting an adequate response to the various stresses encountered along the path of tumorigenesis and allowing the cancer cells to spread throughout the body.

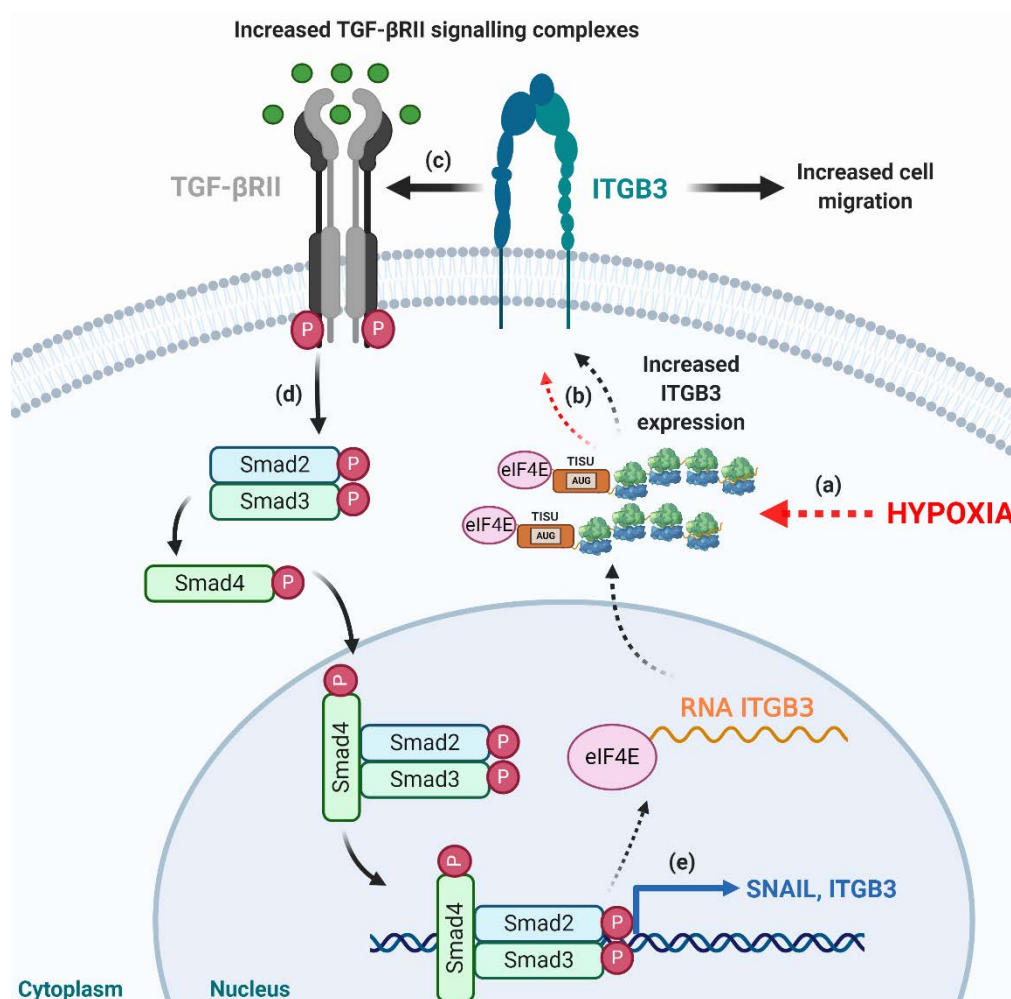


**Figure Dis. 1.** Schematic of ITGB3-TGF- $\beta$  signaling pathway. a) Hypoxia activation of ITGB3 translation in an eIF4E-dependent manner. b) Increased ITGB3 expression. c) Increased number of TGF- $\beta$ -ITGB3 complexes. d) Activation of the SMAD2-dependent TGF- $\beta$  pathway. e) Transcriptional activation of TGF- $\beta$  targets genes, such as SNAIL and ITGB3.

### Metastasis and ITGB3: role in exosome internalisation and intercellular communication

The fundamental role of integrins in tumour progression, particularly in metastasis, has long been recognised, but the exact underlying molecular mechanisms remain incompletely understood. As we and others have demonstrated, ITGB3 is required for the formation of macro-metastatic foci in BrCa, particularly in the TNBC subtype<sup>230,231</sup>. Knockdown of ITGB3 by shRNA strongly reduces the metastasis-forming capacity of the TNBC cell line MDA.MB.231 after its tail vein injection into nude mice. Importantly, this phenotype appears to be independent of the initial homing of the cells to the lung (Supplementary Figure 1, Paper II). Thus, we ruled out the potential role of ITGB3 in the initial cell homing step (Supplementary Figure 1, Paper II). In Chapter 2, we centred our analysis on the next metastasis step, the formation of colonies within the distant organ, which involves clonal growth from a single cell. This process is dependent on factors

secreted by neighbouring cells or, in others words, on cell-to-cell communication<sup>87,88,232,233</sup>. Our data revealed that clonogenic growth largely depends on secreted factors in the cellular environment, with the reduced capacity of ITGB3 knockdown cells to take up EVs from the environment rendering them insensitive to these factors (Figure 1, Paper II).

Follow-up studies based on mass spectrometry analysis of EV composition revealed a significant reduction in vesicle-located proteins derived from shITGB3 cells. This population, containing 92 proteins, was subjected to bioinformatic analysis. Firstly, we confirmed the reduction in exosomes among the EV fraction (34 of the 92 proteins were common to the exosome database <http://exocarta.org/>) and, secondly, we found an association with metastatic disease progression in the literature for 24 of the 92 proteins (HCMDDB [Human Cancer Metastasis Database]).

We mechanistically demonstrated how ITGB3 cooperates with other adhesion molecules such as HSPGs in EV-dependent cell-to-cell communication, supporting its role in exosome uptake through dynamin-dependent endocytosis together with FAK recruitment.

Previous studies revealed the role of EVs in intercellular communication and describe how this cellular communication, a hallmark feature of several cancers<sup>65</sup>, triggers biological changes in the target cell. Among the described tumorigenic processes, exosomes influence neoplasia, tumour growth, metastasis, paraneoplastic syndromes and therapeutic resistance. The regulation of these processes is dynamic and depends on cancer type, genotype and disease stage<sup>121</sup>. Although many advances have been made in the field, little is known about one of the key steps of their biology: the uptake of EVs into the target cell. Many mechanistic pathways are involved and can be active at the same time, with endocytosis the most important one. In parallel to our proposal, where ITGB3 acts as a central player between vesicle-recognising surface receptors, such as HSPG proteins, and the local activation of dynamin-driven endocytosis by FAK, additional mechanisms must exist. This is supported by the fact that a significant proportion of EVs is still taken up under ITGB3 knockdown conditions.

### **Biological parallelisms: uptake of exosomes, integrin trafficking and uptake of viruses**

Our proposed model for ITGB3-dependent EV uptake (Figure Dis. 2) is based on the integrin trafficking mechanism, which closely resembles the well-described virus uptake process. Both processes share many mechanistic similarities, including interplay among integrin-coupled receptors, ITGB3, FAK and dynamin, which is essential to connect extracellular and intracellular components. Dynamin and FAK are interdependent on each

other for the mediation of integrin endocytosis and adhesion control during cell migration<sup>204</sup>. In the case of viruses, after the attachment of the virus to HSPGs (integrin-coupled receptors), specific tyrosine kinases (FAK, SRC) are recruited that trigger certain signalling pathways needed for the activation of membrane fission and fusion factors that enable endocytosis. In the specific case of KSHV virus, binding to HSPGs leads to interaction of the complex with  $\alpha v\beta 3$ <sup>234</sup>. This interaction, in turn, results in an intermediate activation of the integrin that enables the binding and activation of FAK and the subsequent assembly of the endocytic machinery, as described above.

As occurs with virus internalisation, EV recognition by cells is dependent on HSPGs, which mediate the interaction of cancer cell-derived exosomes with the plasma membrane of the target cell<sup>235</sup>.

The integrin trafficking model provides another well-established process for the ITGB3-mediated uptake of EVs. Notably, not only EVs, but also ITGB3-associated proteins such as TGF- $\beta$  (see Chapter 1) are internalised together with ITGB3. The direct interaction between ITGB3 and TGF- $\beta$  receptor has already been demonstrated. In addition, the joint uptake of ITGB3 and an associated receptor, TGF- $\beta$  in this case, might be used by the cell to regulate the presence of different receptors at the cell surface.

### **Exosome subpopulations have a distinct protein composition**

Exosome biology is a recently emerging field and several basic mechanisms remain largely unknown. Initial work on EVs led to the proposal that exosomes were required for the maintenance of cellular homeostasis due to their function in removing unnecessary or damaged material from cells. In contrast, many recent studies indicate the accumulation of specific cellular components within exosomes and propose the functional involvement of these factors in intercellular communication.

Exosome composition may not be homogeneous. The idea of exosome heterogeneity has in part been demonstrated by others and was further validated within this thesis. EVs largely differ in size and in their protein, lipid and RNA molecule composition. This heterogeneity of EVs must be due to the different paths to EV production, which permits different biological functions and allows us to discriminate among different EV populations for uptake into the target cell according to the origin. To confirm this hypothesis, in Chapter 2, we demonstrated how cells with ITGB3 knockdown have an altered exosomal profile compared with wild-type cells, both qualitatively and quantitatively. Similar results were suggested by Quaglia *et al.*<sup>236</sup>, who demonstrated that upregulation of  $\alpha v\beta 3$  in donor cells alters the cargo composition of the secreted exosomes.

Analysis of the EV composition of the cell culture supernatant revealed an enrichment in vesicles ranging from 50 to 100 nm in size in shITGB3 cells, indicating that regulation of the uptake of these vesicles seems to be particularly dependent on ITGB3. Moreover, we observed that ITGB3-depleted exosomes exhibit a dramatic decrease in some classical exosome markers, such as CD81 and TSG101, whereas others, such as flotillin-1, remain unaffected. Similar results were obtained by Imjeti *et al.*<sup>237</sup>, where a significant decrease in syntenin, ALIX, syndecan-1 and CD63, but not CD9, was found after inhibition of SRC. Along this line, Bart Roucourt *et al.*<sup>140</sup> revealed that heparanase stimulates the exosomal secretion of syntenin-1, syndecan and other exosomal proteins, such as CD63. In contrast, exosomal CD9, CD81 and flotillin-1 were not affected. Interestingly, vesicles within this range of size, from 50 to 100 nm, also called P200 exomers or exosomes<sup>120</sup>, have been reported to contain less CD81 than other EVs, which could explain why the relative increase in these vesicles in the total EV population results in a reduction in CD81 in shITGB3 cell culture supernatant.

Finally, it is important to point out that the proposed mechanism of EV uptake might be subject to cell type-specific modifications and, in particular, that the cell type-specific expression of integrins might result in the use of alternative integrins within receptor cells for EVs. The most likely candidates would be integrins that can interact with HSPG proteins at the cell membrane and at the same time contain a  $\beta$  subunit for the binding and activation of FAK.

### **Is the HSPG-ITGB3-FAK-DYN complex a potential base complex for exosome biogenesis?**

Although these data seem to indicate that a specific defect in EV uptake alters the secretome of shITGB3 cells, we cannot exclude the possibility that these differences might not be due to alterations in exosome biogenesis, or even between both mechanisms. After LC-MS/MS measurements, GO analysis was performed to further analyse the differences in EV composition. Strikingly, the GO terms that were markedly reduced upon analysis of the proteome of shITGB3 cell-derived vesicles were linked to two major cellular processes: endocytosis and exosome biogenesis. In particular, the ESCRT complex, including TSG101, appeared to be affected. Moreover, proteins of the syndecan-syntenin-ALIX pathway, such as SDC4 (log<sub>2</sub>FC -1.32), SDC1 (log<sub>2</sub>FC -1.68), syntenin-1 (log<sub>2</sub>FC -2.14) and ALIX (log<sub>2</sub>FC > -2.46), as well as SDC2 and syntenin-2 (present only in shCON-derived EVs), were strongly reduced in EVs derived from shITGB3 cells. Both complexes are required for the formation of endosomal intraluminal vesicles that are later released as exosomes<sup>139,140,238-240</sup>. While the putative role of ITGB3 in exosome biogenesis requires future study, it is

interesting to speculate that ITGB3 might play a central role in connecting EV uptake and exosome biogenesis, with ITGB3-dependent uptake of EVs the first step in exosome biogenesis.

Along these lines, it would be exciting to explore if the endosomal structures formed after the HSPG-ITGB3-FAK-DYN complex-dependent endocytosis of EVs defines their starting point as precursors of exosome biogenesis. ITGB3 may play a central role in coordinating both processes, acting as a possible link between vesicle endocytosis and exosome biogenesis. Taken together, the ITGB3-regulated interplay between the selective endocytosis of EVs and exosome biogenesis will be a stimulating area of future research.

We have demonstrated that a key regulator of endocytosis is FAK, which binds to and regulates the function of both dynamin and ITGB3 proteins. Moreover, knockdown of FAK or pharmacological inhibition of its activity mimicked the phenotypes observed after shITGB3 knockdown: impaired clonogenic growth, defective EV uptake and alterations in the protein composition of EVs in the cell culture supernatant. In this case, proteins of the exosome biogenesis pathway were mainly affected. Thus, we cannot conclusively exclude the possibility that FAK might also play a key role in exosome biogenesis. Structurally, the interaction between FAK and the C-terminal tail of ITGB3 has been well-established in the literature<sup>241-243</sup>. On the one hand, FAK-dependent phosphorylation and regulation of SRC and dynamin are required to orchestrate the turnover of focal adhesions. On the other hand, SRC and dynamin have previously been described to be required for exosome biogenesis and EV uptake<sup>237,244,245</sup>. However, the specific role of FAK in exosome biogenesis remains unknown. As in the case of ITGB3, FAK might also play a role in exosome biogenesis. Future investigation of a possible function of FAK in exosome biogenesis will be interesting. Based on our current results, it is already now tempting to speculate that the signalling platform regulating exosome biogenesis comprises endosomes formed by the uptake of EVs and containing ITGB3, SRC and FAK kinases. This hypothesis is based on the fact that a) internalised ITGB3 is found in early endosomal structures, b) the cytoplasmic tail of the integrin can act as a molecular hub for the recruitment of these kinases, and c) endosomes have recently been described as emerging platforms for integrin-mediated FAK signaling<sup>153,246</sup>. The putative targets of endosomal FAK with a direct role in exosome biogenesis have not yet been described; however, given the established role of FAK as a cytoskeleton regulator, it is reasonable to assume that the target proteins may be involved in the transport of MVB via microtubules or actin fibres. This step might be particularly critical for directing MVBs to the cell surface rather than to lysosomes and thus ensuring the release of exosomes into the extracellular space. Moreover, endosomal fractionation



experiments gave the first hints that a sequential recruitment of FAK and SRC to endosomes in an ITGB3-dependent manner might regulate different steps of exosome biogenesis.

The field of EV research is still emerging and it can sometimes be challenging to find a consensus among studies. The main reasons for these discrepancies are methodological challenges, such as the use of different methods for exosome isolation and quantification, as well as the difficulties in detecting EVs at a reliable resolution *in vivo*. However, future research in the field will surely help to overcome these limitations and will ultimately open up new therapeutic avenues for the treatment of metastasised tumours. Given the role of exosomes in physiological and pathological conditions, strategies that interfere with the uptake/release of exosomes and impair exosome-mediated cell-to-cell communication could potentially be therapeutically exploited.

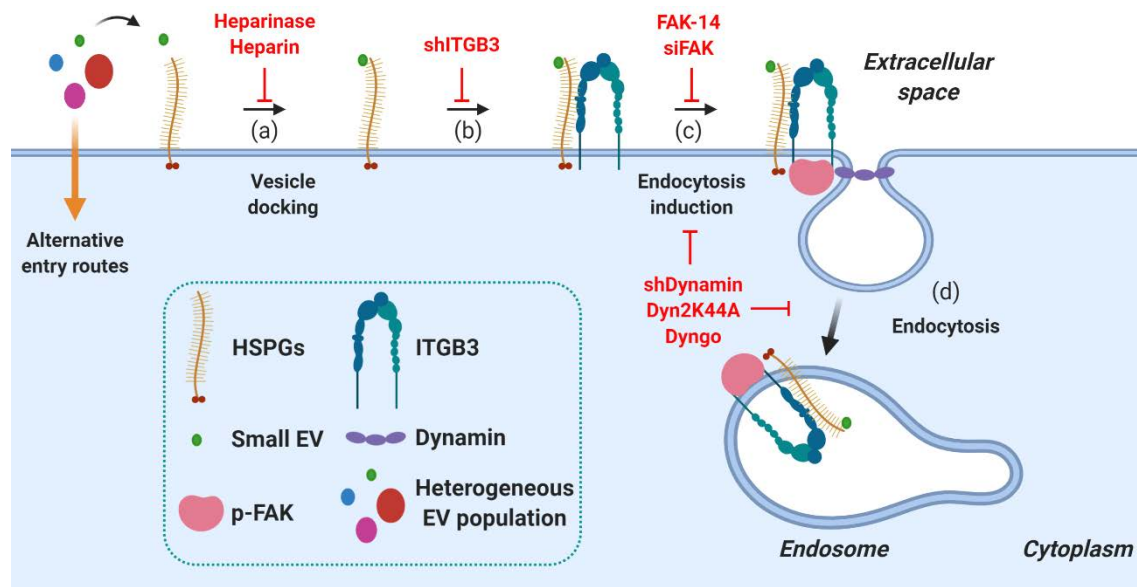


**Figure Dis. 2.** Model for the proposed role of ITGB3 in EV uptake. (a) EV-HSPG interaction; (b)  $\alpha\beta3$  recruitment; (c) pFAK-dynamamin recruitment to an endocytosis complex; (d) Dynamamin-mediated internalisation of EVs and EE formation.

### ITGB3 targeting as a novel therapeutic opportunity in BrCa

BrCa is the most common malignancy in women and the second most common cause of cancer-related deaths, with metastasis the major reason for morbidity and mortality in BrCa patients. Despite improvements in systemic therapies, there are still no approaches with proven efficacy against metastatic tumours<sup>20</sup>. Therapeutic interventions are complicated and survival rates worsened by the emergence of micrometastasis before clinically evident metastasis. Taking into account the results presented in this thesis, we propose an alternative and complementary approach for BrCa treatments, namely, the use of integrin inhibitors for the prevention of metastatic spreading, which is the ultimate cause of 90% of cancer-associated death.

Our results demonstrate the potential use of ITGB3 as a therapeutic target in the context of metastatic BrCa. Importantly, tail vein injection of ITGB3 knockdown cells revealed an essential role for ITGB3 in metastatic disease progression. ITGB3 targeting could be used to modulate EMT, which is a major cause of metastasis. This might be of special interest due to the poor druggability of EMT-associated proteins.

The described roles of ITGB3 could be the basis for various interventional strategies that might provide an added therapeutic benefit. Moreover, ITGB3 seems to play a particularly important role under hypoxic conditions, which occur in the vast majority of TNBCs<sup>25,247</sup>. In this regard, our results suggest that highly hypoxic tumours may be more responsive to ITGB3 therapy.

Regarding exosome uptake, we have determined that BrCa cells with knockdown of ITGB3 are insensitive to secreted factors in the environment and exhibit reduced clonal growth capacity. Targeting of intercellular communication might be a valuable strategy for future clinical approaches to the treatment of cancer. Current anticancer treatments are based on targeted strategies to eliminate tumour cells. However, research over the last decade has demonstrated that the tumour environment is crucial for disease progression. Intercellular communication between tumour cells and neighbouring cells might promote tumour progression and drug resistance<sup>103,107,248</sup>. Thus, blockage of these connections might be a promising strategy for improving current anti-tumour therapies.

Several drugs targeting ITGB3 in both described integrin complexes— $\alpha v\beta 3$  and/or  $\alpha II\beta 3$ —have been developed and subjected to clinical trials (Table 1). These drugs are either chemical compounds or synthetic monoclonal antibodies.

In our laboratory, we have tested several chemical inhibitors, such as eptifibatide, tirofiban, cyclo(-RGDfk) and cilengitide, and compared the results with the known phenotypes after ITGB3 knockdown by shRNA. Although we detected mild impairment in cell migration with cilengitide and cyclo(-RGDfk), the same phenotype as after ITGB3 knockdown could not be achieved even with the maximum applicable doses. It remains to be addressed if this might be due to the limited potency of those inhibitors or the phenotypic difference between knockdown and inhibition of activity by a small molecule.

Cilengitide was the first anti-angiogenic small molecule targeting the integrins  $\alpha v\beta 3$ ,  $\alpha v\beta 5$  and  $\alpha 5\beta 1$ . When tested in clinical studies in combination with radiotherapy and with the chemotherapeutic temozolomide, it demonstrated excellent drug safety profiles. Nevertheless, cilengitide failed in the CENTRIC EORTC 26071-22072 phase III study and in the CORE phase II trial due to low response rates and its development as a therapy was thus

discontinued. Several *in vitro* and *in vivo* results, including those presented in this thesis, support further studies with cilengitide in an attempt to improve its clinical effects. Our preliminary studies indicate that cilengitide is the only tested commercially available drug able to partially phenocopy the results obtained through genetic inhibition of ITGB3 (data not shown).

**Table Dis. 1.** Summary of ITGB3 inhibitors currently being tested or soon to be tested in clinical trials.

Inhibitor	Mechanism	Clinical trial	Reference
<b>Cilengitide</b>	Selectively binds to the ligand of $\alpha\beta3$	NCT01118676: Phase I NSCLC NCT00121238: Phase II prostate cancer NCT01044225: Phase II glioblastoma NCT00689221: Phase III glioblastoma NCT00082875: Randomised phase II metastatic melanoma	PMID: 21269250 PMID: 21049281 PMID: 25163906 PMID: 22668797
<b>MK-0429</b>	Selectively inhibits binding of the ligand to integrin $\beta3$	NCT00302471: Phase I hormone-refractory prostate cancer and metastatic bone disease	PMID: 20398037
<b>Vitaxin</b>	Integrin $\alpha\beta3$ -specific monoclonal antibody	NCT00066196: Phase II metastatic melanoma NCT00072930: Phase II metastatic androgen-independent prostate cancer	PMID: 9600913
<b>Luteolin</b>	Inhibits the integrin $\beta3$ -FAK signalling pathway	-	PMID: 22983392
<b>Methylseleninic acid (MSA)</b>	Downregulates the integrin $\beta3$ signalling pathway	-	PMID: 28842587
<b>Phoyunnanin E</b>	Downregulates the integrins $\alpha\text{v}$ and $\beta3$	-	PMID: 29284478
<b>Pinocembrin</b>	Inactivates the integrin $\beta3$ -FAK-p38 $\alpha$ signalling pathway	-	PMID: 25949790

Table adapted from Zhu *et al.*<sup>164</sup>

We have tested alternative ITGB3 inhibitors in collaboration with the laboratory of Professor Horst Kessler (Munich), who has developed a series of cilengitide peptide mimetics that have greater activity towards individual integrins. We obtained a reduction in exosome uptake, similar to that seen under shITGB3 conditions. This opens a door to the promising future applicability of this drug in the targeting of ITGB3-dependent cell-to-cell communication.

Despite compelling experimental results demonstrating that integrins contribute to cancer progression and that their inhibition has therapeutic effects, clinical trials with

integrin inhibitors have not shown overall therapeutic benefits, and no inhibitors have been registered as anticancer drugs. However, therapeutic strategies have only focused on the role of integrins in tumour and vascular cells. Our results suggest that integrin targeting might provide a novel way to interfere with intercellular communication.

Collectively, ITGB3 regulates cell behaviour at different levels. Understanding of the multiple roles of ITGB3 in the tumour and in the tumour microenvironment is necessary to improve current strategies and to maximise the clinical effects of  $\alpha v\beta 3$  inhibitors.



## **CONCLUSIONS**



1. Polysome profiling combined with RNA-Seq permits the detection of alterations in protein Translational efficiency and has been successfully applied to the identification of gene-specific alterations in protein translation under stress conditions.
2. Hypoxia and the simultaneous inhibition of mTOR with PP242 (hypoxia + PP242) causes the most significant changes at both transcriptional and translational levels.
3. Non-tumour cells need greater adaptive changes compared with tumour cells under both hypoxic conditions and hypoxic conditions plus PP242 treatment, as stronger alterations at the transcriptional level has been observed.
4. In contrast to the transcriptional changes, the response to hypoxia results in stronger alterations at the translational level in tumour cell lines compared with non-tumour cell lines.
5. The combination of hypoxia and mTOR inhibitor treatment identifies a unique subset of genes activated only at translationally level (Te).
6. ITGB3 is translationally activated in hypoxia and hypoxia + PP242 in a HIF-independent manner and is not translated through the hypoxia-specific eIF4F<sup>H</sup> complex. However, eIF4E is needed for the translational activation of ITGB3 in hypoxia
7. ITGB3 is essential for cell migration and survival in both cancer cells and non-malignant cells, particularly under hypoxic conditions.
8. ITGB3 is required for TGF- $\beta$ -mediated expression of SNAIL, mostly under low-oxygen conditions.
9. ITGB3 downregulation significantly reduces lung metastasis and improves overall survival in mice.
10. ITGB3 sustains the growth rate in BrCa cell spheroids, promotes mammosphere formation, but to a similar extent under normoxia and hypoxia in the MCF7 cell line.
11. ITGB3 is dispensable for the homing step of lung metastasis.
12. EVs increase colony formation.
13. ITGB3 is required for EV-induced colony formation (growth).
14. ITGB3 is required for EV uptake.
15. ITGB3-dependent vesicle uptake is an energy-dependent process mediated via a dynamin-dependent endocytic mechanism.
16. ITGB3-dependent endocytosis of EVs requires HSPG.
17. Uptake of EVs by MDA.MB.231 cells is dependent on FAK.
18. ITGB3 knockdown causes alterations in the heterogeneous pool of EVs: small vesicles are enriched while the overall amount of EVs is not altered.





## **REFERENCES**



1. Siegel, R. L., Miller, K. D. & Jemal, A. Cancer Statistics, 2017. *CA. Cancer J. Clin.* **67**, 7–30 (2017).
2. Smalley, M., Piggott, L. & Clarkson, R. Breast cancer stem cells: Obstacles to therapy. *Cancer Lett.* **338**, 57–62 (2013).
3. Dai, X. *et al.* Breast cancer intrinsic subtype classification, clinical use and future trends. *Am. J. Cancer Res.* **5**, 2929–2943 (2015).
4. Badve, S. Tumor heterogeneity in breast cancer. *Mol. Pathol. Breast Cancer* **4**, 121–132 (2016).
5. Dai, X., Xiang, L., Li, T. & Bai, Z. Cancer hallmarks, biomarkers and breast cancer molecular subtypes. *J. Cancer* **7**, 1281–1294 (2016).
6. Fisusi, F. A. & Akala, E. O. Drug Combinations in Breast Cancer Therapy. *Pharm. Nanotechnol.* **7**, 3–23 (2019).
7. Waks, A. G. & Winer, E. P. Breast Cancer Treatment: A Review. *JAMA - J. Am. Med. Assoc.* **321**, 288–300 (2019).
8. Bianchini, G., Balko, J. M., Mayer, I. A., Sanders, M. E. & Gianni, L. HHS Public Access. *Triple-negative breast cancer challenges Oppor. a Heterog. Dis.* **13**, 674–690 (2017).
9. Xiao, W. *et al.* Breast cancer subtypes and the risk of distant metastasis at initial diagnosis: a population-based study. *Cancer Manag. Res.* **Volume 10**, 5329–5338 (2018).
10. Lehmann, B. D. *et al.* Identification of human triple-negative breast cancer subtypes and preclinical models for selection of targeted therapies. *J. Clin. Invest.* **121**, 2750–2767 (2011).
11. Ruddy, K. J. & Ganz, P. A. Treatment of Nonmetastatic Breast Cancer. *JAMA - J. Am. Med. Assoc.* 4–5 (2019). doi:10.1001/jama.2019.3927
12. Kronblad, Å., Jirström, K., Rydén, L., Nordenskjöld, B. & Landberg, G. Hypoxia inducible factor-1 $\alpha$  is a prognostic marker in premenopausal patients with intermediate to highly differentiated breast cancer but not a predictive marker for tamoxifen response. *Int. J. Cancer* **118**, 2609–2616 (2006).
13. Schindl, M. *et al.* Overexpression of hypoxia-inducible factor 1 $\alpha$  is associated with an unfavorable prognosis in lymph node-positive breast cancer. *Clin. Cancer Res.* **8**, 1831–1837 (2002).
14. Dales, J. P. *et al.* Overexpression of hypoxia-inducible factor HIF-1 $\alpha$  predicts early relapse in breast cancer: Retrospective study in a series of 745 patients. *Int. J. Cancer* **116**, 734–739 (2005).
15. Liu, Z., Semenza, G. L. & Zhang, H. Hypoxia-inducible factor 1 and breast cancer metastasis. *J. Zhejiang Univ. B* **16**, 32–43 (2015).
16. Chen, X. *et al.* XBP1 promotes triple-negative breast cancer by controlling the HIF1 $\alpha$  pathway. *Nature* **508**, 103–107 (2014).
17. Dales, J. P. *et al.* Hypoxia inducible factor 1 $\alpha$  gene (HIF-1 $\alpha$ ) splice variants: Potential prognostic biomarkers in breast cancer. *BMC Medicine* **8**, (2010).
18. Zhao, Z. *et al.* Clinicopathological and prognostic value of hypoxia-inducible factor-1 $\alpha$  in breast cancer: a meta-analysis including 5177 patients. *Clin. Transl. Oncol.* (2020). doi:10.1007/s12094-020-02332-8
19. Yan, M., Rayoo, M., Takano, E. A., Thorne, H. & Fox, S. B. BRCA1 tumours correlate with a HIF-1 $\alpha$  phenotype and have a poor prognosis through modulation of hydroxylase enzyme profile expression. *Br. J. Cancer* **101**, 1168–1174 (2009).
20. Khosravi-Shahi, P., Cabezón-Gutiérrez, L. & Custodio-Cabello, S. Metastatic triple negative breast cancer: Optimizing treatment options, new and emerging targeted therapies. *Asia. Pac. J. Clin. Oncol.* **14**, 32–39 (2018).
21. Ahmad, A. Pathways to Breast Cancer Recurrence. *ISRN Oncol.* **2013**, 1–16 (2013).
22. Cardoso, F. *et al.* Research needs in breast cancer. *Ann. Oncol.* **28**, 208–217 (2017).
23. Masoud, V. & Pagès, G. Targeted therapies in breast cancer: New challenges to fight against resistance. *World J. Clin. Oncol.* **8**, 120 (2017).
24. Estadual, C. U. *et al.* Challenges in the treatment of triple-negative breast cancer: chemoresistance and identification of molecular targets. (2016).
25. O'Reilly, E. A. *et al.* The fate of chemoresistance in triple negative breast cancer (TNBC). *BBA Clin.* **3**, 257–275 (2015).
26. Tahmasebi, S., Khoutorsky, A., Mathews, M. B. & Sonenberg, N. Translation deregulation in human disease. *Nat. Rev. Mol. Cell Biol.* **19**, 791–807 (2018).
27. Robichaud, N. & Sonenberg, N. Translational control and the cancer cell response to stress. *Curr. Opin. Cell Biol.* **45**, 102–109 (2017).
28. Gnanasundram, S. V. & Fåhræus, R. Translation stress regulates ribosome synthesis and cell proliferation. *Int. J. Mol. Sci.* **19**, (2018).

## References

29. Pavitt, G. D. Regulation of translation initiation factor eIF2B at the hub of the integrated stress response. *Wiley Interdiscip. Rev. RNA* **9**, 1–22 (2018).
30. Robichaud, N., Sonenberg, N., Ruggero, D. & Schneider, R. J. Translational control in cancer. *Cold Spring Harb. Perspect. Biol.* **11**, 1–27 (2019).
31. Hsieh, A. C. *et al.* NIH Public Access. **485**, 55–61 (2013).
32. Laplante, M. & Sabatini, D. M. mTOR signaling in growth control and disease. *Cell* **149**, 274–293 (2012).
33. Loewith, R. *et al.* Two TOR complexes, only one of which is rapamycin sensitive, have distinct roles in cell growth control. *Mol. Cell* **10**, 457–468 (2002).
34. Thoreen, C. C. *et al.* translation. **485**, 109–113 (2012).
35. Yang, Y. & Wang, Z. IRES-mediated cap-independent translation, a path leading to hidden proteome. *J. Mol. Cell Biol.* **11**, 911–919 (2019).
36. Sriram, A., Bohlen, J. & Teleman, A. A. Translation acrobatics: how cancer cells exploit alternate modes of translational initiation. *EMBO Rep.* **19**, (2018).
37. Shatsky, I. N., Terenin, I. M., Smirnova, V. V. & Andreev, D. E. Cap-Independent Translation: What's in a Name? *Trends Biochem. Sci.* **43**, 882–895 (2018).
38. Leppek, K., Das, R. & Barna, M. Functional 5' UTR mRNA structures in eukaryotic translation regulation and how to find them. *Nature Reviews Molecular Cell Biology* **19**, 158–174 (2018).
39. Shi, Y. *et al.* Therapeutic potential of targeting IRES-dependent c-myc translation in multiple myeloma cells during ER stress. *Oncogene* **35**, 1015–1024 (2016).
40. Le Quesne, J. P. C., Stoneley, M., Fraser, G. A. & Willis, A. E. Derivation of a structural model for the c-myc IRES. *J. Mol. Biol.* **310**, 111–126 (2001).
41. Jaud, M. *et al.* Translational Regulations in Response to Endoplasmic Reticulum Stress in Cancers. *Cells* **9**, 540 (2020).
42. Kwok, C. K., Marsico, G. & Balasubramanian, S. Detecting RNA G-quadruplexes (rG4s) in the transcriptome. *Cold Spring Harb. Perspect. Biol.* **10**, 1–14 (2018).
43. Terenin, I. M., Andreev, D. E., Dmitriev, S. E. & Shatsky, I. N. A novel mechanism of eukaryotic translation initiation that is neither m7G-cap-, nor IRES-dependent. *Nucleic Acids Res.* **41**, 1807–1816 (2013).
44. Haimov, O., Sinvani, H. & Dikstein, R. Cap-dependent, scanning-free translation initiation mechanisms. *Biochim. Biophys. Acta - Gene Regul. Mech.* **1849**, 1313–1318 (2015).
45. Elfakess, R. *et al.* Unique translation initiation of mRNAs-containing TISU element. *Nucleic Acids Res.* **39**, 7598–7609 (2011).
46. Baker, K. E. & Collier, J. The many routes to regulating mRNA translation. *Genome Biol.* **7**, (2006).
47. Rissland, O. S. The organization and regulation of mRNA–protein complexes. *Wiley Interdiscip. Rev. RNA* **8**, 1–17 (2017).
48. Fukao, A., Aoyama, T. & Fujiwara, T. The molecular mechanism of translational control via the communication between the microRNA pathway and RNA-binding proteins. *RNA Biol.* **12**, 922–926 (2015).
49. Oliveto, S., Mancino, M., Manfrini, N. & Biffo, S. Role of microRNAs in translation regulation and cancer. *World J. Biol. Chem.* **8**, 45 (2017).
50. Chassé, H., Boulben, S., Costache, V., Cormier, P. & Morales, J. Analysis of translation using polysome profiling. *Nucleic Acids Res.* **45**, e15 (2017).
51. Faye, M. D., Graber, T. E. & Holcik, M. Assessment of selective mRNA translation in mammalian cells by polysome profiling. *J. Vis. Exp.* 1–8 (2014). doi:10.3791/52295
52. Obrig, T. G., Culp, W. J., McKeenan, W. L. & Hardesty, B. The mechanism by which cycloheximide and related glutarimide antibiotics inhibit peptide synthesis on reticulocyte ribosomes. *J. Biol. Chem.* **246**, 174–181 (1971).
53. Tscherner, J. S. & Pestka, S. Inhibition of protein synthesis in intact HeLa cells. *Antimicrob. Agents Chemother.* **8**, 479–487 (1975).
54. Hajizadeh, F. *et al.* Hypoxia inducible factors in the tumor microenvironment as therapeutic targets of cancer stem cells. *Life Sci.* **237**, 116952 (2019).
55. Wilson, W. R. & Hay, M. P. Targeting hypoxia in cancer therapy. *Nat. Rev. Cancer* **11**, 393–410 (2011).
56. Chipurupalli, S., Kannan, E., Tergaonkar, V., D'andrea, R. & Robinson, N. Hypoxia induced ER stress response as an adaptive mechanism in cancer. *Int. J. Mol. Sci.* **20**, (2019).
57. Majmundar, A. J., Wong, W. J. & Simon, M. C. Hypoxia-Inducible Factors and the Response to Hypoxic Stress. *Mol. Cell* **40**, 294–309 (2010).

58. Sridharan, S., Varghese, R., Venkatraj, V. & Datta, A. Hypoxia Stress Response Pathways: Modeling and Targeted Therapy. *IEEE J. Biomed. Heal. Informatics* **21**, 875–885 (2017).
59. Simon, M. C. Cellular adaptation to hypoxia through hypoxia inducible factors and beyond. *Nat. Rev. Mol. Cell Biol.* doi:10.1038/s41580-020-0227-y
60. Davalli, P., Marverti, G., Lauriola, A. & D'Arca, D. Targeting oxidatively induced DNA damage response in cancer: Opportunities for novel cancer therapies. *Oxid. Med. Cell. Longev.* **2018**, (2018).
61. Wang, H., Jiang, H., Van De Gucht, M. & De Ridder, M. Hypoxic radioresistance: Can ROS be the key to overcome it? *Cancers (Basel)*. **11**, (2019).
62. Al-Hajj, M., Wicha, M. S., Benito-Hernandez, A., Morrison, S. J. & Clarke, M. F. Prospective identification of tumorigenic breast cancer cells. *Proc. Natl. Acad. Sci. U. S. A.* **100**, 3983–3988 (2003).
63. Lorico, A. & Rappa, G. Phenotypic heterogeneity of breast cancer stem cells. *J. Oncol.* **2011**, (2011).
64. Yang, F. *et al.* Evaluation of breast cancer stem cells and intratumor stemness heterogeneity in triple-negative breast cancer as prognostic factors. *Int. J. Biol. Sci.* **12**, 1568–1577 (2016).
65. Hanahan, D. & Weinberg, R. A. Hallmarks of cancer: The next generation. *Cell* **144**, 646–674 (2011).
66. Jensen, C. & Teng, Y. Is It Time to Start Transitioning From 2D to 3D Cell Culture? *Front. Mol. Biosci.* **7**, 1–15 (2020).
67. Rao, S. *et al.* Three dimensional culture models to study drug resistance in breast cancer. 0–1 doi:10.1002/bit.27356
68. Semenza, G. L. Hypoxia-inducible factors in physiology and medicine. *Cell* **148**, 399–408 (2012).
69. Wang, G. L., Jiang, B.-H., Rue, E. A. & Semenza, G. L. Hypoxia-inducible factor 1 is a basic-helix-loop-helix-PAS heterodimer regulated by cellular O<sub>2</sub> tension (dioxin receptor/erythropoietin/hypoxia/transcription). *Genetics* **92**, 5510–5514 (1995).
70. Jiang, B. H., Rue, E., Wang, G. L., Roe, R. & Semenza, G. L. Dimerization, DNA binding, and transactivation properties of hypoxia-inducible factor 1. *J. Biol. Chem.* **271**, 17771–17778 (1996).
71. Yang, J. *et al.* Functions of the Per/ARNT/Sim domains of the hypoxia-inducible factor. *J. Biol. Chem.* **280**, 36047–36054 (2005).
72. Koh, M. Y., Darnay, B. G. & Powis, G. Hypoxia-Associated Factor, a Novel E3-Ubiquitin Ligase, Binds and Ubiquitinates Hypoxia-Inducible Factor 1, Leading to Its Oxygen-Independent Degradation. *Molecular and Cellular Biology* **28**, 7081–7095 (2008).
73. Yamashita, K., Discher, D. J., Hu, J., Bishopric, N. H. & Webster, K. A. Molecular regulation of the endothelin-1 gene by hypoxia. Contributions of hypoxia-inducible factor-1, activator protein-1, GATA-2, and p300/CBP. *J. Biol. Chem.* **276**, 12645–12653 (2001).
74. Khong, T. L. *et al.* Identification of the angiogenic gene signature induced by EGF and hypoxia in colorectal cancer. *BMC Cancer* **13**, 1 (2013).
75. Uniacke, J. *et al.* An oxygen-regulated switch in the protein synthesis machinery. *Nature* **486**, 126–129 (2012).
76. Van Den Beucken, T., Koritzinsky, M. & Wouters, B. G. Translational control of gene expression during hypoxia. *Cancer Biol. Ther.* **5**, 749–755 (2006).
77. Hardie, D. G. New roles for the LKB1→AMPK pathway. *Curr. Opin. Cell Biol.* **17**, 167–173 (2005).
78. Reiling, J. H. & Hafen, E. The hypoxia-induced paralogs Scylla and Charybdis inhibit growth by down-regulating S6K activity upstream of TSC in *Drosophila*. *Genes Dev.* **18**, 2879–2892 (2004).
79. Brugarolas, J. *et al.* Regulation of mTOR function in response to hypoxia by REDD1 and the TSC1/TSC2 tumor suppressor complex. *Genes Dev.* **18**, 2893–2904 (2004).
80. Pouyssegur, J., Dayan, F. & Mazure, N. M. Hypoxia signalling in cancer and approaches to enforce tumour regression. *Nature* **441**, 437–443 (2006).
81. Komar, A. A. & Hatzoglou, M. Cellular IRES-mediated translation: The war of ITAFs in pathophysiological states. *Cell Cycle* **10**, 229–240 (2011).
82. Koumenis, C. & Wouters, B. G. 'Translating' tumor hypoxia: Unfolded protein response (UPR)-dependent and UPR-independent pathways. *Mol. Cancer Res.* **4**, 423–436 (2006).
83. Braunstein, S. *et al.* A Hypoxia-Controlled Cap-Dependent to Cap-Independent Translation Switch in Breast Cancer. *Mol. Cell* **28**, 501–512 (2007).

## References

84. Föhling, M. Surviving hypoxia by modulation of mRNA translation rate. *J. Cell. Mol. Med.* **13**, 2770–2779 (2009).
85. Leprivier, G., Rotblat, B., Khan, D., Jan, E. & Sorensen, P. H. Stress-mediated translational control in cancer cells. *Biochim. Biophys. Acta - Gene Regul. Mech.* **1849**, 845–860 (2015).
86. Chee, N. T., Lohse, I. & Brothers, S. P. mRNA-to-protein translation in hypoxia. *Mol. Cancer* **18**, 1–13 (2019).
87. Massagué, J., Batlle, E. & Gomis, R. R. Understanding the molecular mechanisms driving metastasis. *Mol. Oncol.* **11**, 3–4 (2017).
88. Massagué, J. & Obenaus, A. C. Metastatic Colonization. *Nature* **529**, 298–306 (2016).
89. Go, L., Tracey, N., Ma, R., Qian, B. & Brunton, V. G. Mouse models of metastasis : progress and prospects. 1061–1074 (2017). doi:10.1242/dmm.030403
90. Lambert, A. W., Pattabiraman, D. R. & Weinberg, R. A. Emerging Biological Principles of Metastasis. *Cell* **168**, 670–691 (2017).
91. Tseng, L. M. *et al.* Distant metastasis in triple-negative breast cancer. 290–294 (2013). doi:10.4149/neo
92. Nakaya, Y. & Sheng, G. EMT in developmental morphogenesis. *CANCER Lett.* **3132**, (2013).
93. Ingthorsson, S., Briem, E., Bergthorsson, J. T. & Gudjonsson, T. Epithelial Plasticity During Human Breast Morphogenesis and Cancer Progression. *J. Mammary Gland Biol. Neoplasia* 139–148 (2016). doi:10.1007/s10911-016-9366-3
94. Nieto, M. A. Epithelial plasticity: A common theme in embryonic and cancer cells. *Science (80-. )*. **342**, (2013).
95. Nieto, M. A., Huang, R. Y., Jackson, R. A. & Thiery, J. P. Review EMT : 2016. 21–45 (2016). doi:10.1016/j.cell.2016.06.028
96. Brabletz, T. *et al.* Variable -catenin expression in colorectal cancers indicates tumor progression driven by the tumor environment. *Proceedings of the National Academy of Sciences* **98**, 10356–10361 (2001).
97. Huang, R. Y. J. *et al.* An EMT spectrum defines an anoikis-resistant and spheroidogenic intermediate mesenchymal state that is sensitive to e-cadherin restoration by a src-kinase inhibitor, saracatinib (AZD0530). *Cell Death Dis.* **4**, (2013).
98. Massagué, J. TGF $\beta$  in Cancer. *Cell* **134**, 215–230 (2008).
99. Syed, V. TGF- $\beta$  Signaling in Cancer. *J. Cell. Biochem.* **1287**, 1279–1287 (2016).
100. The dynamic roles of TGF- $\beta$  in cancer.pdf.
101. Screening of circulating TGF- $\beta$  levels and its clinicopathological significance in human breast cancer..pdf.
102. Zarzynska, J. M. Two Faces of TGF-Beta1 in Breast Cancer. *Mediators Inflamm.* **2014**, 1–16 (2014).
103. Herst, P. M., Dawson, R. H. & Berridge, M. V. Intercellular communication in tumor biology: A role for mitochondrial transfer. *Front. Oncol.* **8**, (2018).
104. Eiro, N., Gonzalez, L. O., Cid, S., Schneider, J. & Vizoso, F. J. Breast Cancer Tumor Stroma : Cellular Components , Therapeutic Opportunities. *Cancers (Basel)*. **664**, 1–26 (2019).
105. Bian, X. *et al.* Microvesicles and chemokines in tumor microenvironment: Mediators of intercellular communications in tumor progression. *Mol. Cancer* **18**, 1–13 (2019).
106. Sullivan, R. *et al.* The emerging roles of extracellular vesicles as communication vehicles within the tumor microenvironment and beyond. *Front. Endocrinol. (Lausanne)*. **8**, 1–11 (2017).
107. Wan, Z. *et al.* Exosome-mediated cell-cell communication in tumor progression. *Am. J. Cancer Res.* **8**, 1661–1673 (2018).
108. Peinado, H. *et al.* Melanoma exosomes educate bone marrow progenitor cells toward a pro-metastatic phenotype through MET. *Nat. Med.* **18**, 883–891 (2012).
109. Costa-Silva, B. *et al.* Pancreatic cancer exosomes initiate pre-metastatic niche formation in the liver. *Nat. Cell Biol.* **17**, 816–826 (2015).
110. Peinado, H. *et al.* Pre-metastatic niches: Organ-specific homes for metastases. *Nat. Rev. Cancer* **17**, 302–317 (2017).
111. Choi, D. S., Kim, D. K., Kim, Y. K. & Ghos, Y. S. Proteomics, transcriptomics and lipidomics of exosomes and ectosomes. *Proteomics* **13**, 1554–1571 (2013).
112. Green, T. M., Alpaugh, M. L., Barsky, S. H., Rappa, G. & Lorico, A. Breast cancer-derived extracellular vesicles: Characterization and contribution to the metastatic phenotype. *Biomed Res. Int.* **2015**, (2015).
113. Jossion, S. *et al.* Stromal fibroblast-derived miR-409 promotes epithelial-to-mesenchymal

- transition and prostate tumorigenesis. *Oncogene* **34**, 2690–2699 (2015).
114. Goulet, C. R. *et al.* Exosomes induce fibroblast differentiation into cancer-associated fibroblasts through TGF $\beta$  signaling. *Molecular Cancer Research* **16**, 1196–1204 (2018).
  115. Yang, X., Li, Y., Zou, L. & Zhu, Z. Role of exosomes in crosstalk between cancer-associated fibroblasts and cancer cells. *Front. Oncol.* **9**, 1–6 (2019).
  116. Xabier Osteikoetxea, thesis. Improved Extracellular Vesicle Detection and Characterization. (2016).
  117. Abusamra, A. J. *et al.* Tumor exosomes expressing Fas ligand mediate CD8<sup>+</sup> T-cell apoptosis. *Blood Cells, Mol. Dis.* **35**, 169–173 (2005).
  118. Anel, A., Gallego-Lleyda, A., de Miguel, D., Naval, J. & Martínez-Lostao, L. Role of Exosomes in the Regulation of T-cell Mediated Immune Responses and in Autoimmune Disease. *Cells* **8**, 154 (2019).
  119. Mathieu, M., Martin-Jaular, L., Lavieu, G. & Théry, C. Specificities of secretion and uptake of exosomes and other extracellular vesicles for cell-to-cell communication. *Nat. Cell Biol.* **21**, 9–17 (2019).
  120. Zhang, H. *et al.* Identification of distinct nanoparticles and subsets of extracellular vesicles by asymmetric flow field-flow fractionation. *Nat. Cell Biol.* **20**, 332–343 (2018).
  121. Kalluri, R. & LeBleu, V. S. The biology, function, and biomedical applications of exosomes. *Science* **367**, (2020).
  122. Van Niel, G., D'Angelo, G. & Raposo, G. Shedding light on the cell biology of extracellular vesicles. *Nat. Rev. Mol. Cell Biol.* **19**, 213–228 (2018).
  123. McKelvey, K. J., Powell, K. L., Ashton, A. W., Morris, J. M. & McCracken, S. A. Exosomes: Mechanisms of Uptake. *J. Circ. Biomarkers* **1** (2015). doi:10.5772/61186
  124. Feng, D. *et al.* Cellular internalization of exosomes occurs through phagocytosis. *Traffic* **11**, 675–687 (2010).
  125. Svensson, K. J. *et al.* Exosome uptake depends on ERK1/2-heat shock protein 27 signaling and lipid raft-mediated endocytosis negatively regulated by caveolin-1. *J. Biol. Chem.* **288**, 17713–17724 (2013).
  126. Al-Nedawi, K. *et al.* Intercellular transfer of the oncogenic receptor EGFRvIII by microvesicles derived from tumour cells. *Nat. Cell Biol.* **10**, 619–624 (2008).
  127. Mulcahy, L. A., Pink, R. C. & Carter, D. R. F. Routes and mechanisms of extracellular vesicle uptake. *J. Extracell. Vesicles* **3**, (2014).
  128. Gonda, A., Kabagwira, J., Senthil, G. N. & Wall, N. R. Internalization of exosomes through receptor-mediated endocytosis. *Mol. Cancer Res.* **17**, 337–347 (2019).
  129. Wall, N. R., Gonda, A., Kabagwira, J. & Senthil, G. N. Internalization of Exosomes through Receptor-Mediated Endocytosis. *Mol. Cancer Res.* molcanres.0891.2018 (2018). doi:10.1158/1541-7786.MCR-18-0891
  130. Franzen, C. A. *et al.* Characterization of uptake and internalization of exosomes by bladder cancer cells. *Biomed Res. Int.* **2014**, (2014).
  131. Christianson, H. C., Svensson, K. J., van Kuppevelt, T. H., Li, J.-P. & Belting, M. Cancer cell exosomes depend on cell-surface heparan sulfate proteoglycans for their internalization and functional activity. *Proc. Natl. Acad. Sci.* **110**, 17380–17385 (2013).
  132. Christianson, H. C. & Belting, M. Heparan sulfate proteoglycan as a cell-surface endocytosis receptor. *Matrix Biol.* **35**, 51–55 (2014).
  133. Yamauchi, Y. & Helenius, A. Virus entry at a glance. *J. Cell Sci.* **126**, 1289–1295 (2013).
  134. Grove, J. & Marsh, M. The cell biology of receptor-mediated virus entry. *J. Cell Biol.* **195**, 1071–1082 (2011).
  135. McAndrews, K. M. & Kalluri, R. Mechanisms associated with biogenesis of exosomes in cancer. *Mol. Cancer* **18**, 1–11 (2019).
  136. Colombo, M. *et al.* Analysis of ESCRT functions in exosome biogenesis, composition and secretion highlights the heterogeneity of extracellular vesicles. *J. Cell Sci.* **126**, 5553–5565 (2013).
  137. Stoorvogel, W. Resolving sorting mechanisms into exosomes. *Cell Res.* **25**, 531–532 (2015).
  138. Hessvik, N. P. & Llorente, A. Current knowledge on exosome biogenesis and release. *Cell. Mol. Life Sci.* **75**, 193–208 (2018).
  139. Fares, J., Kashyap, R. & Zimmermann, P. Syntenin: Key player in cancer exosome biogenesis and uptake? *Cell Adhes. Migr.* **11**, 124–126 (2017).
  140. Roucourt, B., Meeussen, S., Bao, J., Zimmermann, P. & David, G. Heparanase activates the syndecan-syntenin-ALIX exosome pathway. *Cell Res.* **25**, 412–428 (2015).



## References

141. Kechagia, J. Z., Ivaska, J. & Roca-Cusachs, P. Integrins as biomechanical sensors of the microenvironment. *Nat. Rev. Mol. Cell Biol.* **20**, 457–473 (2019).
142. Campbell, I. D. & Humphries, M. J. Integrin structure, activation, and interactions. *Cold Spring Harb. Perspect. Biol.* **3**, 1–14 (2011).
143. Holmes, R. S. & Rout, U. K. Comparative studies of vertebrate beta integrin genes and proteins: Ancient genes in vertebrate evolution. *Biomolecules* **1**, 3–31 (2011).
144. Moreno-Layseca, P., Icha, J., Hamidi, H. & Ivaska, J. Integrin trafficking in cells and tissues. *Nat. Cell Biol.* **1** (2019). doi:10.1038/s41556-018-0223-z
145. Hamidi, H. & Ivaska, J. Every step of the way: integrins in cancer progression and metastasis. *Nat. Rev. Cancer* 1–16 (2018). doi:10.1038/s41568-018-0038-z
146. Subramani, D. & Alahari, S. K. Integrin-mediated function of Rab GTPases in cancer progression. *Mol. Cancer* **9**, 312 (2010).
147. Caswell, P. T., Vadrevu, S. & Norman, J. C. Integrins: Masters and slaves of endocytic transport. *Nat. Rev. Mol. Cell Biol.* **10**, 843–853 (2009).
148. Ivaska, J. & Heino, J. Cooperation Between Integrins and Growth Factor Receptors in Signaling and Endocytosis. *Annu. Rev. Cell Dev. Biol.* **27**, 291–320 (2011).
149. Cooper, J. & Giancotti, F. G. Integrin Signaling in Cancer: Mechanotransduction, Stemness, Epithelial Plasticity, and Therapeutic Resistance. *Cancer Cell* **35**, 347–367 (2019).
150. Wickström, S. A. & Fässler, R. Regulation of membrane traffic by integrin signaling. *Trends Cell Biol.* **21**, 266–273 (2011).
151. Ezratty, E. J., Bertaux, C., Marcantonio, E. E. & Gundersen, G. G. Clathrin mediates integrin endocytosis for focal adhesion disassembly in migrating cells. *J. Cell Biol.* **187**, 733–747 (2009).
152. Ezratty, E. J., Partridge, M. A. & Gundersen, G. G. Microtubule-induced focal adhesion disassembly is mediated by dynamin and focal adhesion kinase. *Nat. Cell Biol.* **7**, 581–590 (2005).
153. Alanko, J. *et al.* Integrin endosomal signalling suppresses anoikis. *Nat. Cell Biol.* **17**, 1412–1421 (2015).
154. Nader, Ezratty, Gundersen - 2016 - FAK, talin and PIPKIγ regulate endocytosed integrin activation to polarize focal adhesion assembly.pdf.
155. Barrow-McGee, R. *et al.* Beta 1-integrin-c-Met cooperation reveals an inside-in survival signalling on autophagy-related endomembranes. *Nat. Commun.* **7**, (2016).
156. Bass, M. D. *et al.* A Syndecan-4 Hair Trigger Initiates Wound Healing through Caveolin- and RhoG-Regulated Integrin Endocytosis. *Dev. Cell* **21**, 681–693 (2011).
157. Aoudjit, F. & Vuori, K. Integrin signaling inhibits paclitaxel-induced apoptosis in breast cancer cells. *Oncogene* **20**, 4995–5004 (2001).
158. Scatena, M. *et al.* NF-kappaB mediates alphavbeta3 integrin-induced endothelial cell survival. *J. Cell Biol.* **141**, 1083–1093 (1998).
159. Courter, D. L., Lomas, L., Scatena, M. & Giachelli, C. M. Src kinase activity is required for integrin αβ 3-mediated activation of nuclear factor-κB. *J. Biol. Chem.* **280**, 12145–12151 (2005).
160. Bao, W. & Strömblad, S. Integrin αv-mediated inactivation of p53 controls a MEK1-dependent melanoma cell survival pathway in three-dimensional collagen. *J. Cell Biol.* **167**, 745–756 (2004).
161. Arjonen, A. *Integrins on the move.* (2013).
162. Jay S. Desgrosellier & Cherech, D. A. Integrins in cancer: biological implications in therapeutic opportunities. *Cancer, Nat Rev* **10**, 9–22 (2015).
163. Alday-Parejo, B., Stupp, R. & Rüegg, C. Are integrins still practicable targets for anti-cancer therapy? *Cancers (Basel)*. **11**, 1–30 (2019).
164. Zhu, C. *et al.* ITGB3/CD61: A hub modulator and target in the tumor microenvironment. *Am. J. Transl. Res.* **11**, 7195–7208 (2019).
165. J., S. S., Chung0ho, K. & H, G. M. The final steps of integrin activation: the end game. *Nat. Rev. Mol. cell Biol.* **11**, 288–300 (2014).
166. Desgrosellier, J. S. & Cheresch, D. A. Integrins in cancer: Biological implications and therapeutic opportunities. *Nat. Rev. Cancer* **10**, 9–22 (2010).
167. Ahmedah, H. T. A. Correlation between the expression of integrins and their role in cancer progression. (2012).
168. Nurden, A. T. *et al.* Expanding the Mutation Spectrum Affecting αIIbβ3 Integrin in Glanzmann Thrombasthenia: Screening of the ITGA2B and ITGB3 Genes in a Large International Cohort.

- Hum. Mutat.* **36**, 548–561 (2015).
169. Eisman, R., Vilaire, O. G., Schwartz, E., Bennett, U. J. S. & Poncz, M. Structure of Platelet Glycoprotein IIb/IIIa. *Blood* **81**, 1470–1475 (1988).
  170. Nurden, A. T. & Nurden, P. Congenital platelet disorders and understanding of platelet function. *Br. J. Haematol.* **165**, 165–178 (2014).
  171. Nurden, A. T., Fiore, M., Nurden, P. & Pillois, X. Glanzmann thrombasthenia: A review of ITGA2B and ITGB3 defects with emphasis on variants, phenotypic variability, and mouse models. *Blood* **118**, 5996–6005 (2011).
  172. Gu, R. *et al.* Integrin  $\beta 3$ /Akt signaling contributes to platelet-induced hemangioendothelioma growth. *Sci. Rep.* **7**, 1–14 (2017).
  173. Xu, X. R. *et al.* Apolipoprotein A-IV binds  $\alpha$ IIb $\beta$ 3 integrin and inhibits thrombosis. *Nat. Commun.* **9**, (2018).
  174. Zhang, N. *et al.* Insufficient radiofrequency ablation treated hepatocellular carcinoma cells promote metastasis by up-regulation ITGB3. *J. Cancer* **8**, 3742–3754 (2017).
  175. Miyazaki, Y. J. *et al.* HOXD3 enhances motility and invasiveness through the TGF- $\beta$ -dependent and -independent pathways in A549 cells. *Oncogene* **21**, 798–808 (2002).
  176. Cordes, N., Hansmeier, B., Beinke, C., Meineke, V. & Van Beuningen, D. Irradiation differentially affects substratum-dependent survival, adhesion, and invasion of glioblastoma cell lines. *Br. J. Cancer* **89**, 2122–2132 (2003).
  177. Roth, P. *et al.* Integrin control of the transforming growth factor- $\beta$  pathway in glioblastoma. *Brain* **136**, 564–576 (2013).
  178. Desgrosellier, J. S. *et al.* Using finite difference modeling to understand direct-SV illumination produced by P sources Donald Wagner and Bob Hardage \*, Bureau of Economic Geology, The University of Texas at Austin. **15**, 5167–5171 (2017).
  179. Noh, K. W. *et al.* Integrin B3 inhibition enhances the antitumor activity of ALK inhibitor in ALK-rearranged NSCLC. *Clin. Cancer Res.* **24**, 4162–4174 (2018).
  180. Taherian, A., Li, X., Liu, Y. & Haas, T. A. Differences in integrin expression and signaling within human breast cancer cells. *BMC Cancer* **11**, 293 (2011).
  181. Gruber, G. *et al.* Correlation between the tumoral expression of  $\beta 3$ -integrin and outcome in cervical cancer patients who had undergone radiotherapy. *Br. J. Cancer* **92**, 41–46 (2005).
  182. Hosotani, R. *et al.* Expression of integrin  $\alpha v\beta 3$  in pancreatic carcinoma: Relation to mmp-2 activation and lymph node metastasis. *Nursing (Lond)*. **25**, 30–35 (1995).
  183. Skuli, N. *et al.*  $\alpha v\beta 3/\alpha v\beta 5$  integrins-fak-rho: A novel pathway for hypoxia regulation in glioblastoma. *Cancer Res.* **69**, 3308–3316 (2009).
  184. Liu, Z. *et al.* EGFRvIII/integrin  $\beta 3$  interaction in hypoxic and vitronectin-enriching microenvironment promote GBM progression and metastasis. *Oncotarget* **7**, 4680–4694 (2016).
  185. Mori, S. *et al.* Enhanced expression of integrin  $\alpha v\beta 3$  induced by TGF- $\beta$  is required for the enhancing effect of fibroblast growth factor 1 (FGF1) in TGF- $\beta$ -induced epithelial-mesenchymal transition (EMT) in mammary epithelial cells. *PLoS One* **10**, 1–18 (2015).
  186. Wang, W. *et al.* Integrin  $\beta 3$  mediates the endothelial-to-mesenchymal transition via the notch pathway. *Cellular Physiology and Biochemistry* **49**, 985–997 (2018).
  187. Seguin, L., Desgrosellier, J. S., Weis, S. M. & Cheres, D. A. HHS Public Access. **25**, 234–240 (2016).
  188. Elliott, K. C., Yebra, M., Mielgo, A. & Lowy, A. M. resistance to EGFR inhibition. **16**, 457–468 (2014).
  189. Cai, H. *et al.* Nogo-B promotes tumor angiogenesis and provides a potential therapeutic target in hepatocellular carcinoma. *Mol. Oncol.* **12**, 2042–2054 (2018).
  190. Felcht, M. *et al.* Angiopoietin-2 differentially regulates angiogenesis through TIE2 and integrin signaling. *J. Clin. Invest.* **122**, 1991–2005 (2012).
  191. Tóth, B. *et al.* Over-expression of integrin  $\beta 3$  can partially overcome the defect of integrin  $\beta 3$  signaling in transglutaminase 2 null macrophages. *Immunol. Lett.* **126**, 22–28 (2009).
  192. Luo, D., McGettrick, H. M., Stone, P. C., Rainger, G. E. & Nash, G. B. The roles of integrins in function of human neutrophils after their migration through endothelium into interstitial matrix. *PLoS One* **10**, 1–24 (2015).
  193. Heichler, C. *et al.* STAT3 activation through IL-6/IL-11 in cancer-associated fibroblasts promotes colorectal tumour development and correlates with poor prognosis. *Gut* 1–14 (2019). doi:10.1136/gutjnl-2019-319200
  194. Wen, S. *et al.* Cancer-associated fibroblast (CAF)-derived IL32 promotes breast cancer cell

- invasion and metastasis via integrin  $\beta 3$ -p38 MAPK signalling. *Cancer Letters* **442**, 320–332 (2019).
195. Attieh, Y. *et al.* Cancer-associated fibroblasts lead tumor invasion through integrin- $\beta 3$ -dependent fibronectin asse. *Journal of Cell Biology* **216**, 3509–3520 (2017).
  196. Cruet-Hennequart, S. *et al.*  $\alpha v$  integrins regulate cell proliferation through integrin-linked kinase (ILK) in ovarian cancer cells. *Oncogene* **22**, 1688–1702 (2003).
  197. Galliher, A. J. & Schiemann, W. P.  $\beta 3$  Integrin and Src facilitate transforming growth factor- $\beta$  mediated induction of epithelial-mesenchymal transition in mammary epithelial cells. *Breast Cancer Res.* **8**, 1–16 (2006).
  198. Desgrosellier, J. S. *et al.* Integrin  $\alpha v \beta 3$  drives slug activation and stemness in the pregnant and neoplastic mammary gland. *Developmental Cell* **30**, 295–308 (2014).
  199. Somanath, P. R., Ciocea, A. & Byzova, T. V. Integrin and growth factor receptor alliance in angiogenesis. *Cell Biochem. Biophys.* **53**, 53–64 (2009).
  200. De, S. *et al.* VEGF - Integrin interplay controls tumor growth and vascularization. *Proc. Natl. Acad. Sci. U. S. A.* **102**, 7589–7594 (2005).
  201. Desgrosellier, J. S. *et al.* An integrin  $\alpha v \beta 3$ -Src oncogenic unit promotes anchorage-independence and tumor progression. *Nat. Med.* **15**, 1163–1169 (2009).
  202. Zhang, W. *et al.* Rab34 regulates adhesion, migration, and invasion of breast cancer cells. *Oncogene* **37**, 3698–3714 (2018).
  203. Morgan, M. R. *et al.* Syndecan-4 Phosphorylation Is a Control Point for Integrin Recycling. *Dev. Cell* **24**, 472–485 (2013).
  204. Paul, N. R., Jacquemet, G. & Caswell, P. T. Endocytic Trafficking of Integrins in Cell Migration. *Curr. Biol.* **25**, R1092–R1105 (2015).
  205. Roberts, M., Barry, S., Woods, A., Van der Sluijs, P. & Norman, J. PDGF-regulated rab4-dependent recycling of  $\alpha v \beta 3$  integrin from early endosomes is necessary for cell adhesion and spreading. *Curr. Biol.* **11**, 1392–1402 (2001).
  206. Woods, A. J., White, D. P., Caswell, P. T. & Norman, J. C. PKD1/PKC $\delta$  promotes  $\alpha v \beta 3$  integrin recycling and delivery to nascent focal adhesions. *EMBO J.* **23**, 2531–2543 (2004).
  207. Onodera, Y., Nam, J. M. & Sabe, H. Intracellular trafficking of integrins in cancer cells. *Pharmacol. Ther.* **140**, 1–9 (2013).
  208. Wang, L. *et al.* Bone sialoprotein- $\alpha v \beta 3$  integrin axis promotes breast cancer metastasis to the bone. *Cancer Science* **110**, 3157–3172 (2019).
  209. Felding-Habermann, B. *et al.* Integrin activation controls metastasis in human breast cancer. *Proc. Natl. Acad. Sci.* **98**, 1853–1858 (2001).
  210. Liu, H. *et al.* MYC suppresses cancer metastasis by direct transcriptional silencing of  $\alpha v \beta 3$  integrin subunits. *Nature Cell Biology* **14**, 567–574 (2012).
  211. Parvani, J. G., Gujrati, M. D., Mack, M. A., Schiemann, W. P. & Lu, Z. R. Silencing  $\beta 3$  integrin by targeted ECO/siRNA nanoparticles inhibits EMT and metastasis of triple-negative breast cancer. *Cancer Research* **75**, 2316–2325 (2015).
  212. For, M., Determination, T. H. E. & Oxygen, O. F. Consumption rates and diffusion coefficients. *Biophys. J.* 343–348 (1982).
  213. Hamilton, G. Multicellular spheroids as an in vitro tumor model. *Cancer Lett.* **131**, 29–34 (1998).
  214. Mueller-Klieser, W. Tumor biology and experimental therapeutics. *Crit. Rev. Oncol. Hematol.* **36**, 123–139 (2000).
  215. Dontu, G. *et al.* In vitro propagation and transcriptional profiling of human mammary stem/progenitor cells. *Genes Dev.* **17**, 1253–1270 (2003).
  216. Yousefnia, S., Ghaedi, K., Seyed Forootan, F. & Nasr Esfahani, M. H. Characterization of the stemness potency of mammospheres isolated from the breast cancer cell lines. *Tumor Biol.* **41**, 1–14 (2019).
  217. Rota, L. M., Lazzarino, D. A., Ziegler, A. N., LeRoith, D. & Wood, T. L. Determining mammosphere-forming potential: Application of the limiting dilution analysis. *J. Mammary Gland Biol. Neoplasia* **17**, 119–123 (2012).
  218. Koritzinsky, M. *et al.* Gene expression during acute and prolonged hypoxia is regulated by distinct mechanisms of translational control. *EMBO J.* **25**, 1114–1125 (2006).
  219. Johannes, G. J. & Thomas, J. D. Identification of mRNAs that continue to associate with polysomes during hypoxia. *Rna* **13**, 1116–1131 (2007).
  220. Koritzinsky, M. *et al.* The hypoxic proteome is influenced by gene-specific changes in mRNA translation. *Radiother. Oncol.* **76**, 177–186 (2005).

221. Lai, M. C., Chang, C. M. & Sun, H. S. S. Hypoxia Induces Autophagy through Translational Up-Regulation of Lysosomal Proteins in Human Colon Cancer Cells. *PLoS One* **11**, 1–21 (2016).
222. Miloslavski, R. *et al.* Oxygen sufficiency controls TOP mRNA translation via the TSC-Rheb-mTOR pathway in a 4E-BP-independent manner. *J. Mol. Cell Biol.* **6**, 255–266 (2014).
223. Nandagopal, N. & Roux, P. P. Regulation of global and specific mRNA translation by the mTOR signaling pathway. *Translation* **3**, e983402 (2015).
224. Gentilella, A. *et al.* Autogenous Control of 5'TOP mRNA Stability by 40S Ribosomes. *Mol. Cell* **67**, (2017).
225. Lei, Y. *et al.* Proteomics identification of ITGB3 as a key regulator in reactive oxygen species-induced migration and invasion of colorectal cancer cells. *Mol. Cell. Proteomics* **10**, 1–16 (2011).
226. Deep, G. *et al.* SNAI1 is critical for the aggressiveness of prostate cancer cells with low E-cadherin. *Mol. Cancer* **13**, 1–15 (2014).
227. Pechkovsky, D. V. *et al.* Transforming growth factor  $\beta$ 1 induces  $\alpha$  $\beta$ 3 integrin expression in human lung fibroblasts via a  $\beta$ 3 integrin-, c-Src-, and p38 MAPK-dependent pathway. *J. Biol. Chem.* **283**, 12898–12908 (2008).
228. Willett, M., Brocard, M., Davide, A. & Morley, S. J. Translation initiation factors and active sites of protein synthesis co-localize at the leading edge of migrating fibroblasts. *Biochem. J.* **438**, 217–227 (2011).
229. Gorrini, C. *et al.* Fibronectin controls cap-dependent translation through  $\beta$ 1 integrin and eukaryotic initiation factors 4 and 2 coordinated pathways. *Proceedings of the National Academy of Sciences of the United States of America* **102**, 9200–9205 (2005).
230. Sesé, M. *et al.* Hypoxia-mediated translational activation of ITGB3 in breast cancer cells enhances TGF- $\beta$  signaling and malignant features *in vivo* and *in vitro*. *Oncotarget* **8**, (2017).
231. Silencing  $\beta$ 3 Integrin by Targeted ECO\_siRNA Nanoparticles Inhibits EMT and Metastasis of Triple Negative Breast Cancer.pdf.
232. Becker, A. *et al.* Extracellular Vesicles in Cancer: Cell-to-Cell Mediators of Metastasis. *Cancer Cell* **30**, 836–848 (2016).
233. Celià-terrassa, T. & Kang, Y. Distinctive properties of metastasis- initiating cells. 892–908 (2016). doi:10.1101/gad.277681.116.892
234. Kumar, B. & Chandran, B. KSHV entry and trafficking in target cells—Hijacking of cell signal pathways, actin and membrane dynamics. *Viruses* **8**, (2016).
235. Christianson, H. C., Svensson, K. J., van Kuppevelt, T. H., Li, J.-P. J. P. & Belting, M. Cancer cell exosomes depend on cell-surface heparan sulfate proteoglycans for their internalization and functional activity. *Proc. Natl. Acad. Sci. U. S. A.* **110**, 17380–17385 (2013).
236. Quaglia, F. *et al.* Small extracellular vesicles modulated by  $\alpha$ V $\beta$ 3 integrin induce neuroendocrine differentiation in recipient cancer cells. *Journal of Extracellular Vesicles* **9**, (2020).
237. Imjeti, N. S. *et al.* Syntenin mediates SRC function in exosomal cell-to-cell communication. *Proc. Natl. Acad. Sci.* **114**, 201713433 (2017).
238. Baietti, M. F. *et al.* Syndecan-syntenin-ALIX regulates the biogenesis of exosomes. *Nat. Cell Biol.* **14**, 677–685 (2012).
239. Bissig, C. & Gruenberg, J. ALIX and the multivesicular endosome: ALIX in Wonderland. *Trends Cell Biol.* **24**, 19–25 (2014).
240. Friand, V., David, G. & Zimmermann, P. Syntenin and syndecan in the biogenesis of exosomes. *Biol. Cell* **107**, 331–341 (2015).
241. Wang, R., Shattil, S. J., Ambruso, D. R. & Newman, P. J. Truncation of the cytoplasmic domain of  $\beta$ 3 in a variant form of glanzmann thrombasthenia abrogates signaling through the integrin  $\alpha$ (IIb) $\beta$ 3 complex. *J. Clin. Invest.* **100**, 2393–2403 (1997).
242. Schmid, S. L. Reciprocal regulation of signaling and endocytosis: Implications for the evolving cancer cell. *J. Cell Biol.* **216**, 2623–2632 (2017).
243. Schaffner-Reckinger, E., Gouon, V., Melchior, C., Plançon, S. & Kieffer, N. Distinct involvement of  $\beta$ 3 integrin cytoplasmic domain tyrosine residues 747 and 759 in integrin-mediated cytoskeletal assembly and phosphotyrosine signaling. *Journal of Biological Chemistry* **273**, 12623–12632 (1998).
244. Wang, R. *et al.* Exosome adherence and internalization by hepatic stellate cells triggers sphingosine 1-phosphate-dependent migration. *J. Biol. Chem.* **290**, 30684–30696 (2015).
245. Schneider, D. J. *et al.* Mechanisms and modulation of microvesicle uptake in a model of

## References

- alveolar cell communication. *J. Biol. Chem.* **292**, 20897–20910 (2017).
246. Alanko, J. & Ivaska, J. Endosomes: Emerging Platforms for Integrin-Mediated FAK Signalling. *Trends Cell Biol.* **26**, 391–398 (2016).
247. Bernardi, R. & Gianni, L. Hallmarks of triple negative breast cancer emerging at last? *Cell Res.* **24**, 904–905 (2014).
248. Shender, V. O. *et al.* The Role of Intercellular Communication in Cancer Progression. *Russ. J. Bioorganic Chem.* **44**, 473–480 (2018).
249. Schaaf, M. B., Garg, A. D. & Agostinis, P. Defining the role of the tumor vasculature in antitumor immunity and immunotherapy article. *Cell Death Dis.* **9**, (2018).
250. Costanza, B., Umelo, I., Bellier, J., Castronovo, V. & Turtoi, A. Stromal Modulators of TGF- $\beta$  in Cancer. *J. Clin. Med.* **6**, 7 (2017).



There must be some kind of way outta here  
Said the joker to the thief  
There's too much confusion  
I can't get no relief

Business men, they drink my wine  
Plowmen dig my earth  
None will level on the line  
Nobody offered his word  
Hey, hey

No reason to get excited  
The thief, he kindly spoke  
There are many here among us  
Who feel that life is but a joke  
But, uh, but you and I, we've been through that  
And this is not our fate  
So let us stop talkin' falsely now  
The hour's getting late, hey

Hey

All along the watchtower  
Princes kept the view  
While all the women came and went  
Barefoot servants, too  
Well, uh, outside in the cold distance  
A wildcat did growl  
Two riders were approaching  
And the wind began to howl, hey

All along the watchtower

("All Along the Watchtower" Lyrics: Bob Dylan, John Wesley Harding, 1967  
Covered by Jimi Hendrix with the Jimi Hendrix Experience, Electric Ladyland, 1968)